Functional characterization of the cell polarity proteins Bazooka and LKB1

DISSERTATION ZUR ERLANGUNG DES DOKTORGRADES DER NATURWISSENSCHAFTEN (DR.RER. NAT.) DER FAKULTÄT FÜR BIOLOGIE UND VORKLINISCHE MEDIZIN DER UNIVERSITÄT REGENSBURG

vorgelegt von

Lars Kullmann

aus

Flensburg

im Jahr 2017

Das Promotionsgesuch wurde eingereicht am:
16.11.2017

Die Arbeit wurde angeleitet von:

Prof. Dr.vet. med. Dr. rer. nat. Michael Krahn

Unterschrift:

Declaration of publications

Parts of this dissertation were published in the following articles:

1. Giada Dogliotti[#], **Lars Kullmann[#]**, Pratibha Dhumale, Christian Thiele, Olga Panichkina, Gudrun Mendl, Roland Houben, Sebastian Haferkamp, Andraes W. Püschel and Michael P. Krahn (2017). Membrane-binding and activation of LKB1 by phosphatidic acid is essential for development and tumour suppression. Nature Communications 8:15747 DOI: 10.1038/ncomms15747 (# indicates equal contribution)

2. **Lars Kullmann** and Michael P. Krahn. Controlling the master – upstream regulation of the tumour suppressor LKB1. Oncogene 37, 3045 – 3057, DOI: 10.1007/s00018-018-2792-1

3. **Lars Kullmann** and Michael P. Krahn. Redundant regulation of localization and protein stability of DmPar3. Cellular and Molecular Life Science, Volume 75, Issue 17, 3269 – 3282, DOI: 10.1038/s41388-018-0145-z

4. Fabian A. Renschler, Susanne R. Bruekner, Paulin L. Salomon, Amrita Mukherjee, **Lars Kullmann**, Mira C. Schütz-Stoffregen, Christine Henzler, Tony Pawson, Michael P. Krahn and Silke Wiesner. Structural basis for the interaction between the cell polarity proteins Par3 and Par6. Science Signalig, Volume 11, Issue 517, DOI: 10.1126/scisignal.aam9899

Table of contents

Acknowledgement

Ich möchte mich zuerst herzlich bei meinem Betreuer Prof. Dr. Dr. Michael Krahn für die Möglichkeit dieser Dissertation bedanken. Darüber hinaus möchte ich mich für die gute Anleitung meiner Projekte, aber auch die Chance eigene Projekte zu entwickeln und durchzuführen bedanken.

Ich möchte mich zudem bei Prof. Dr. Ralph Witzgall für die Rückmeldungen zu meinen Projekten bedanke. Darüber hinaus gilt mein Dank seinem gesamten Lehrstuhl, insbesondere während des letzten halben Jahres meiner Arbeit.

An dieser Stelle möchte ich mich bei Prof. Dr. Stephan Schneuwly und Dr. Juan Antonio Navarro für die Möglichkeit bedanken in den letzten Monaten meiner Arbeit Versuche bei ihnen im Labor durchführen zu dürfen.

Mein ganz besonderer Dank gilt meinen ehemaligen und aktuellen Kollegen, mit denen ich die letzten drei Jahre teilen durfte. Liebe Sabine, Rui, Olga, Giada, Ina, Barbara, Daniela, Vroni, Lucia, Arnab, Florian und Gudrun unsere gemeinsame Zeit war einfach klasse und ich werde euch nie vergessen!

Vielen Dank auch an meine Eltern und meinen Bruder, die mich immer unterstützt haben und halfen wo sie nur konnten. Bei meinem Bruder Björn möchte ich mich zudem für das Korrekturlesen dieser Arbeit bedanken.

Ramona, bei dir möchte ich mich für deine ständige Unterstützung und dein Verständnis bedanken.

Summary

Cell polarity is a highly conserved characteristic of epithelia. Baz and LKB1 are two key players in the establishment of a cellular polarity and the role of their membrane localization and organization were the subjects of this study.

The liver kinase B1 (LKB1) is an essential kinase that regulates various cellular processes by modulating the activity of several downstream kinases. Its loss or inactivation is closely linked to tumorigenesis. Understanding the regulation of this tumour suppressor will help to better understand the process of tumorigenesis itself. The C-terminus of LKB1 beard a polybasic motif (lysine and arginine residues), which mediates its membrane localization together with a farnesylation site. The polybasic motif acts as a lipid binding (LB) domain that directly binds to phosphoinsotides. Deletions of the LB domain and farnesylation site cause embryonic lethality and phenocopies a null allele. LKB1 preferentially binds to phosphatidic acid (PA), which in turn significantly enhances its catalytic activity. Furthermore, also human LKB1 (hLKB1) localizes at the plasmamembrane of epithelial cells, which requires its conserved LB domain. Lipid binding is important for hLKB1 to counteract mTORC1 in order to suppress cell proliferation in human cancer cell lines. Finally, in specimen of melanoma patients, an association of downregulated LKB1 with elevated levels of PLD2 (which produces PA that activates LKB1 and mTOR) and activated mTORC1 targets has been found. Taken together, membrane binding of LKB1 is essential to fully activate it in order to counteract cell proliferation and promote development.

The oligomerization domain (OD) of Bazooka (Baz) has been reported to be important for viability of the *Drosophila* embryo and the cortical localization of the protein. This study found a functional redundancy of the OD and the lipid binding (LB) motif that is essential for the cortical localization of Baz. Thus, it has been confirmed that the OD contributes to the membrane localization of Baz. Nevertheless, in contrast to previous studies oligomerization was dispensable for viability of embryos, but a yet undescribed function of the OD to stabilize Baz has been observed.

In the end, a novel basis for the interaction between Baz and Par6 has been determined. A so far unrecognized PDZ binding motif (PBM) at the C-terminus of Par6 directly binds to the first and the third PDZ domains of Baz. The previously assumed PDZ-PDZ domain interaction could not be confirmed *in vitro*. However, *in vivo* a functional redundancy of the PDZ domain and the PBM of Par6 promotes its apical localization in the epithelium of *Drosophila* embryos.

Introduction

Cell polarity

Many cell types, such as epithelial cells and stem cells, have a characteristic apical-basal or planar polarization. A polarization is established by the asymmetric distribution of cellular components, such as proteins or lipids. Polarization might either be a transient or permanent feature of cells. Migrating cells are transiently polarized along their migratory direction, whereas the oocytes of the worm *Caenorhabditis elegans* and the fruit fly *Drosophila melanogaster* are polarized from their anterior to posterior pole. Epithelial cells display a permanent apical-basal polarization. The apical region of these cells faces towards the outer environment or a lumen and the basal region contacts the basement membrane (Wodarz, 2002). The apical-basal axis is further separated into subdomains with specific functions. These subdomains are characterized by different protein complexes that surround the apical domain. In *Drosophila*, the most apical region is the subapical region (SAR), which includes the Crumbs (Crb) and Par complexes. The Crb complex consists of the transmembrane protein Crb, the scaffold protein Stardust (Sdt), the adaptor protein Lin7 and the scaffold protein Pals1 associated tight junction protein (PATJ). Beneath the Crb complex localizes the ternary Par complex, which is formed by the scaffold protein Bazooka (Baz), the atypical protein kinase C (aPKC) and the scaffold protein Par6 (Tepass, 2012).

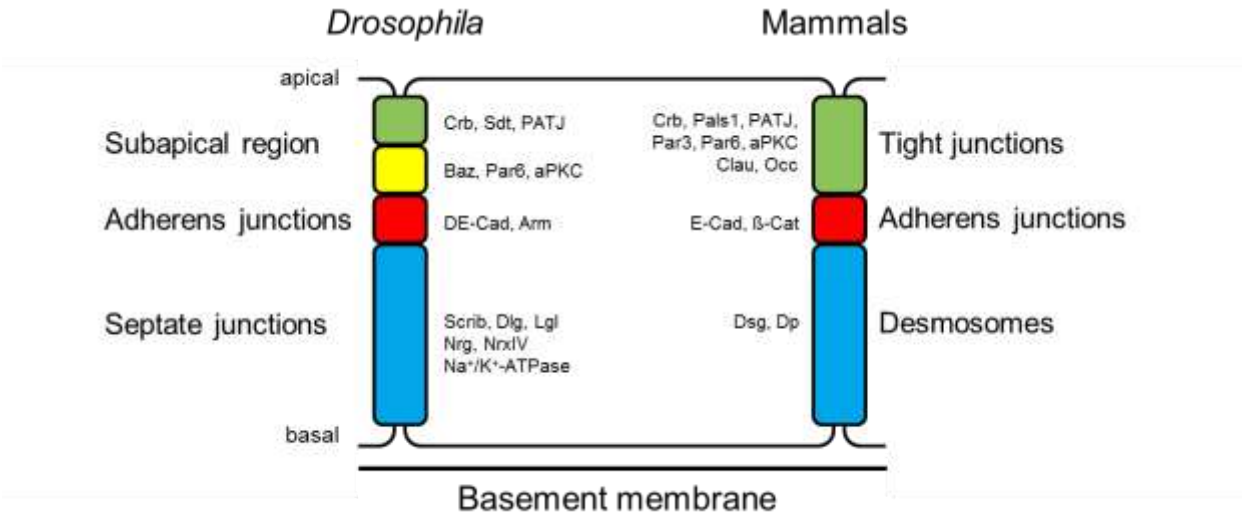

Fig. 1.1: Simplified scheme of the apical-basal polarity of epithelial cells in *Drosophila* and mammals. The different functional domains are highlighted in different colors and characteristic proteins are mentioned.

The adherens junctions (AJ), which are essential to mediate adhesive cell-cell contacts, are the subjacent region. The AJ are mainly characterized by the transmembrane protein DE-Cadherin (DE-Cad), which forms extracellular homophilic interactions and thereby generates cellular adhesion. Moreover, DE-Cad connects the cell cortex with the Actin cytoskeleton via p120-Catenin, Armadillo (Arm) and α-Catenin (Harris, 2012).

In the baso-lateral domain localize the septate junctions (SJ), which act as a para cellular diffusion barrier. The diffusion barrier is mediated among others by Yurt (Yrt), Coracle (Cor), Neurexin IV (NrxIV), Neuroglian (Nrg) and Na^+/K^+-ATPase (Fehon *et al.*, 1994; Baumgartner *et al.*, 1996; Genova and Fehon, 2003; Laprise *et al.*, 2009). In addition, the Scribble (Scrib) complex, which contains the proteins Scrib, Lethal 2 giant larvae (Lgl) and Disc large (Dlg) is required to establish the basolateral identity by antagonizing the formation of apically localized protein complexes (Bilder *et al.*, 2000; Bilder *et al.*, 2003).

Although the epithelial cell polarity is highly conserved among animals and most proteins are conserved from fly to human, its molecular organization varies. In mammals, the most apical region is characterized by the tight junctions (TJ). The TJ are the functional equivalent to the SJ in *Drosophila* and act as a para cellular diffusion barrier. Within the apical TJ localize the Crb and Par complexes similar to invertebrates. Moreover, the TJ harbor additional proteins, such as Occludin and Claudins, that mediate the barrier function (Anderson and van Itallie, 2009). The AJs are comparable within animals, but the vertebrate baso-lateral domain is characterized by desmosomes that connect the intermediate filaments with the plasma-membrane and form cell-cell contacts with neighboring cells (Fig. 1.1) (Getsios *et al.*, 2004).

The Par Complex

The Par complex is a ternary complex that is formed by the scaffolding proteins Baz/Par3, Par6 and the kinase aPKC (Suzuki and Ohno, 2006). The name Par originates from an initial studies in *C. elegans*, where "partitioning-defective" genes were identified that affect the anterior posterior polarity of the early embryo (Kemphues *et al.*, 1988; Watts *et al.*, 1996). Six Par proteins have been identified: Par1/MARK, Par2 (*C. elegans* specific), Par3/Baz, Par4/LKB1, Par5/14-3-3 and Par6. The Par complex itself and its functions in cell polarity are highly conserved among animals (Goldstein and Macara, 2007; Salinas-Saavedra *et al.*, 2015).In *Drosophila*, the Par complex localizes in the SAR and in mammalian cells at the TJ (Izumi *et al.*, 1998; Lin *et al.*, 1999; Suzuki *et al.*, 2001; Suzuki and Ohno, 2006; Goldstein and Macara, 2007). The Par complex is a key player in the establishment of an apical-basal cell polarity in epithelial cells and loss of either of the Par complex proteins results in severe

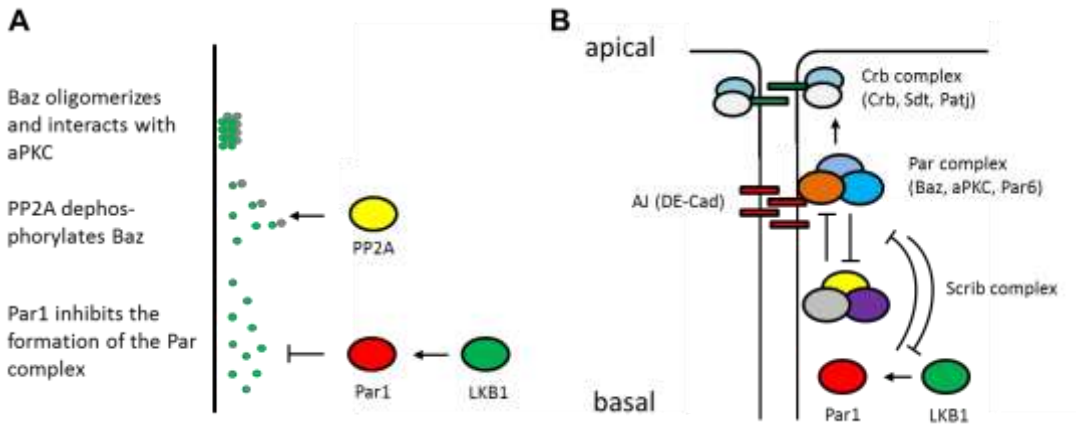

Fig. 1.2: Scheme of the apical-basal regulatory network. (A) The formation of the Par complex is mainly regulated by the Par1 dependent phosphorylation of Baz (green). Phosphorylated Baz fails to form oligomers and cannot interact with aPKC (gray). The dephosphorylation of Baz by PP2A in the apical region mediates the maturation of the Par complex. (B) Different polarity complexes mutually inhibit each other and thereby create an apical-lateral boundary. Par1 (activated by LKB1) counteracts the Par complex formation, as well as the Scrib complex. By contrast, the Par complex promotes the formation of the Crb complex and the AJ, whereas it represses basolateral cues.

polarity defects. The initial exclusion of Baz/Par3 from the baso-lateral region by Par1 promotes its apical accumulation (Benton and St Johnston, 2003a). In the apical domain of the cell, aPKC and Par6 bind to Baz/Par3 in order to give rise to the mature Par complex, which in turn promotes the formation of the Crb complex, the TJ and the AJ (Wodarz *et al.*, 2000b; Petronczki and Knoblich, 2001; Hirose *et al.*, 2002; Bilder *et al.*, 2003; Sotillos *et al.*, 2004; Harris and Peifer, 2004)

Basolateral proteins (such as Par1 and the Scrib complex) and the Par complex mutually antagonize each other to create a boundary between the lateral and the apical domain (Fig. 1.2). At the lateral membrane, the Par1 mediated phosphorylation of Baz inhibits the formation of the Par complex (Benton and St Johnston, 2003a). Moreover, Lgl (a component of the Scrib complex) outcompetes Baz/Par3 for binding Par6 and aPKC and thus, prevents the ectopic formation of the Par complex (Yamanaka *et al.*, 2003; Yamanaka *et al.*, 2006; Wirtz-Peitz *et al.*, 2008). By contrast, at the apical domain, the Par complex counteracts the Par1 and Lgl mediated inhibitions. In human cells, aPKCζ phosphorylates Par1b, which decreases its kinase activity and membrane association (Hurov *et al.*, 2004). In addition, aPKC phosphorylates Lgl in *Drosophila*, which excludes Lgl from the apical cortex and causes the dissociation from Par6 and aPKC (Betschinger *et al.*, 2003; Hutterer *et al.*, 2004; Betschinger *et al.*, 2005). Thus, the reciprocal inhibition of lateral and apical cues creates

distinct domains along the apical-basal axis (Fig. 1.2B). Thereupon, these domains further specify their identity and form a functional epithelium.

Beyond the polarization of epithelial cells the Par complex is also involved in the polarization of neurons. In mammalian neurons the Par complex displays a polarized distribution at the tip of the future axon and mediates the axon formation (Shi *et al.*, 2003; Insolera *et al.*, 2011), whereas the Par complex is not required for axon and dendrite specification in *Drosophila* (Rolls and Doe, 2004). Hence, although the Par complex and its general functions in polarized epithelial cells are conserved among animals, the process of axon specification might underlie fundamental different processes in *Drosophila* and mammals. However, in contrast to adult neurons in *Drosophila* neuroblasts (NBs), which are neuronal stem cells, the Par complex is required for their apical-basal polarization. NBs have a characteristic asymmetric cell division where the Par complex defines the apical cortex that maintains its stem cell identity after cell division. In response to aPKC phosphorylation of Miranda and Numb, both proteins become restricted to the basal domain of the NB and recruit the cell fate determinants Prospero and Brat. The basal domain will give rise to a ganglion mother cell, which gives rise to either glia cells or neurons (Homem and Knoblich, 2012).

The assembly of the Par complex is mediated by multiple interactions of different functional protein domains among Par complex members. The scaffolding protein Baz/Par3 has three

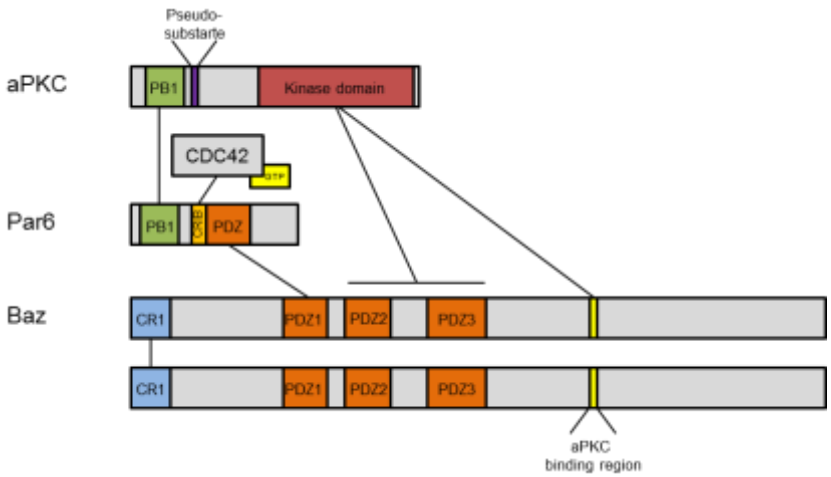

Fig. 1.3: Scheme of the molecular interactions among the members of the Par complex. The assembly of the Par complex is mediated by several protein interaction modules. Par6 and aPKC bind each other via their N-terminal PB1 domains. Moreover, aPKC bids directly to the PDZ domains two and three or to the aPKC binding region of Baz. Par6 also binds directly to the first PDZ domain of Baz and interacts with the GTPase CDC42 via its CRIB domain. Finally, Baz self-associates with its N-terminal oligomerization domain. Modified from McCaffrey and Macara (2012).

PDZ (Postsynaptic density protein 95, Disc large, Zonula occludens 1) domains and a C-terminal aPKC binding domain (Kuchinke *et al.*, 1998b; Morais-de-Sá *et al.*, 2010). Par6 also bears a single PDZ domain that binds to the first PDZ domain of Baz/Par3 (Lin *et al.*, 2000; Joberty *et al.*, 2000). Moreover, Par 6 binds with its N-terminal PB1 (Phox and Bem1) domain the PB1 domain of aPKC (Noda *et al.*, 2003; Hirano *et al.*, 2005). In addition, aPKC binds directly to the PDZ domains two and three as well as the aPKC binding region of Baz/Par3 (Wodarz *et al.*, 2000b; Morais-de-Sá *et al.*, 2010). Taken together, the assembly of the Par complex depends on the interaction of multiple protein interaction domains of the complex members (Fig. 1.3).

The activity of the Par complex is regulated by itself, because Par6 inhibits the kinase activity of aPKC. This inhibition is reversed upon binding of the GTPase CDC42 to the CRIM domain of Par6, which induces a conformational change of Par6 and consequently activates aPKC (Yamanaka *et al.*, 2001). In contrast, more recent studies demonstrate that Par6 activates aPKC by replacing its intramolecular pseudosubstrate (Graybill *et al.*, 2012), whereas the aPKC binding domain of Baz inhibits the kinase activity of aPKC (Soriano *et al.*, 2016). Thus, Baz and Par6 act as regulators of the aPKC kinase activity.

Nevertheless, the Par complex is not a permanent complex, but rather dissociates or rearranges during development. In *Drosophila*, Baz localizes beneath Par6 and aPKC at the AJ (Nam and Choi, 2003; Vogelmann and Nelson, 2004; Harris and Peifer, 2005; Martin-Belmonte *et al.*, 2007; Morais-de-Sá *et al.*, 2010; Doerflinger *et al.*, 2010). Baz has been reported to interact with aPKC and Par6 (Wodarz *et al.*, 2000b; Petronczki and Knoblich, 2001; Hutterer *et al.*, 2004), however in polarized epithelial cells it seems that the Par complex assembles only transiently and afterwards Baz segregates towards the AJ (Harris and Peifer, 2005). The aPKC dependent phosphorylation of Baz at S980 induces the dissociation of the Par6 and aPKC from Baz (Morais-de-Sá *et al.*, 2010). Par6 and aPKC might either be retained in the SAR in complex with the Crb-Sdt complex or with CDC42, which have been reported to bind Par6 and aPKC and mediate their cortical localization (Lin *et al.*, 2000; Joberty *et al.*, 2000; Hurd *et al.*, 2003b; Wang *et al.*, 2004; Kempkens *et al.*, 2006; Atwood *et al.*, 2007; Fletcher *et al.*, 2012; Whitney *et al.*, 2016). Moreover, Baz forms an additional complex with Sdt, which binds to the aPKC binding region of Baz with its PDZ domain. Upon S980 phosphorylation of Baz by aPKC, Baz and Sdt dissociate to give rise to the Crb-Sdt complex (Krahn *et al.*, 2010a). In summary, the phosphorylation of S980 of Baz by aPKC initiates the segregation of Baz to the AJ, the disassembly of the Par complex and the formation of the Crb complex, most likely together with Par6 and aPKC.

The scaffold protein Bazooka/Par3

The scaffold protein Baz/Par3 is a key player in the establishment of cell polarity. Loss of *baz* prevents the formation of polarized epithelia and causes embryonic lethality. The embryonic epidermis of *baz* mutants displays holes, from which its name originates. Likewise, mice that are homozygous mutant for the mammalian orthologue *Par3* die during early embryogenesis (around E12.5) (Hirose *et al.*, 2006). In *Drosophila*, Baz is already maternally provided to initiate the early epithelial polarization. During cellularization (the formation of the cellular blastoderm) Baz is transported in a Dynein-dependent manner to the apical region (Harris and Peifer, 2005). To ensure the lateral inhibition of Baz the serine/threonine kinase Par1 phosphorylates Baz at two conserved residues (S151 and S1085) (Benton and St Johnston, 2003a). Binding of 14-3-3 proteins to theses phosphorylated residues prevents Baz from oligomerization and binding to aPKC (Benton and St Johnston, 2003a; Hurd *et al.*, 2003a). In the apical domain of the cell the protein phosphatase PP2A antagonizes the Par1 mediated phosphorylation to promote the maturation of the Par complex (Fig. 1.2A) (Krahn *et al.*, 2009). By contrast, in *Drosophila* follicle cells (the epithelium around the egg chamber, FCs) Baz is dispensable for the formation of a polarized epithelium (Shahab *et al.*, 2015). Thus, in FCs redundant mechanisms contribute to the cellular polarization.

In mice, Par3 has been reported to act as an exocyst receptor at the AJs (Ahmed and Macara, 2017). The exocyst is an octameric protein complex that mediates directed vesicle trafficking to deliver proteins (e.g. E-Cadherin) to the plasmamembrane. However, in *Drosophila* NBs the exocyst complex is dispensable for cell apical-basal polarity (Halbsgut *et al.*, 2011), thus Baz's function as an exocyst receptor might be restricted to epithelial cells.

In mouse mammary glands, Par3 antagonizes tumorigenesis by counteracting metastasis formation by inhibiting aPKC (McCaffrey *et al.*, 2012; Guyer and Macara, 2015). Nevertheless, loss of Par3 alone does not promote the formation of tumors, however, loss of Par3 associates with a decreased survival rate of breast cancer patients (McCaffrey *et al.*, 2012). Similar, in *baz* mutant clones of the *Drosophila* wing disc the loss of Baz does not enhace the levels of Cycline-E (personal unpublished observation).

In mammals, another isoform of Par3, namely Par3-like (Par3L), has been identified (Fig. 1.4). In contrast to Par3, Par3L lacks the critical aPKC binding domain (Gao *et al.*, 2002). A Par3L specific function is the inhibition of LKB1 in order to maintain mammary stem cell identity (Huo and Macara, 2014). Although *Drosophila* encodes only a single Par3 isoform, this isoform fails to bind LKB1 and hence, cannot compensate the function of Par3L (personal unpublished observation).

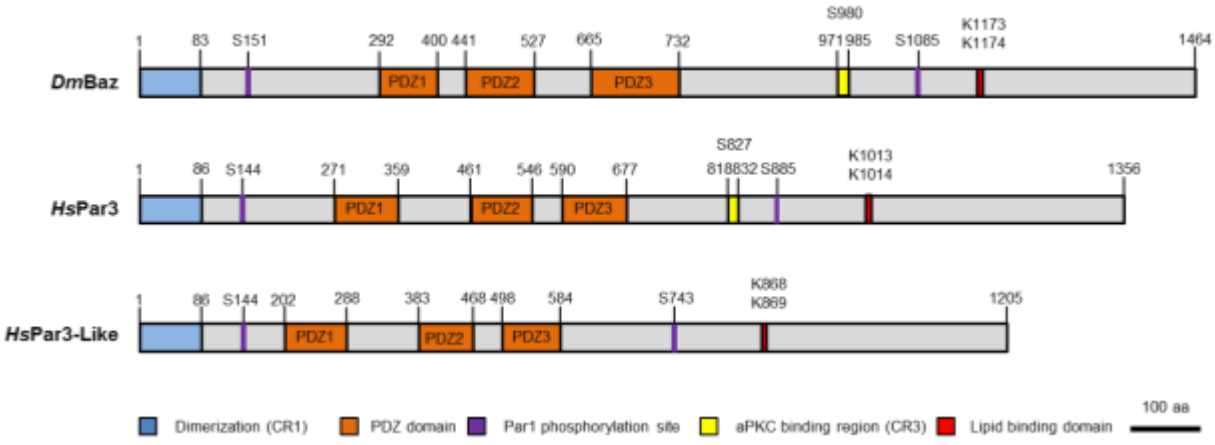

Fig. 1.4: Comparison of *Drosophila* and human Par3 homologs. The N-terminal oligomerization domain (blue) of Baz is followed by three PDZ domains (orange) that mediate protein-protein interactions. At the C-terminus Baz has a lipid binding domain (red). The two Par1 phosphorylation sites (S151 and S 1085, purple) are important for its lateral exclusion. The aPKC phosphorylation site (S980 in *Drosophila* and S827 in human) is essential for the interaction of Baz and aPKC. The numbers represent amino acid positions.

At the structural level, Baz/Par3 has a conserved N-terminal oligomerization domain (OD) that mediates self-association of Baz monomers in a front-to-back manner, which are further assembled into a filament-like oligomer (Mizuno *et al.*, 2003; Benton and St. Johnston, 2003b; Feng *et al.*, 2007; Zhang *et al.*, 2013a). Additionally, Baz contains three PDZ domains, which mediate protein interaction (Fig. 1.4). By interacting with the cell adhesion molecule Echinoid, the tight-junction-associated protein junctional adhesion molecule (JAM) and Armadillo (Arm)/ß-Catenin redundant mechanisms target Baz to the apical junctions (Itoh *et al.*, 2001; Ebnet *et al.*, 2001; Takekuni *et al.*, 2003; Wei *et al.*, 2005). In *Drosophila* photoreceptor cells, the phosphorylation of Arm by the P21-activated kinase (Pak4) is required to retain Baz at the AJs (Walther *et al.*, 2016). The conserved region 3 (CR3) around Ser980 binds aPKC and negatively regulates its kinase activity. However, upon phosphorylation of Ser980 by aPKC the two proteins dissociate and Baz becomes excluded from the SAR and accumulates at AJs. A C-terminal lipid binding motif (K1173-74) directly binds to $PtdIns_{(4,5)}P_2$ (PIP2) and $PtdIns_{(3,4,5)}P_3$ (PIP3) to target Baz to the plasmamembrane (Krahn *et al.*, 2010b). Furthermore, the second PDZ domain of rat Par3 has been reported to bind directly to phosphatidylinositol lipids (Wu *et al.*, 2007) and the three *Drosophila* Baz PDZ domains bind *in vitro* to phosphatidic acid (Yu and Harris, 2012). Hence, several different direct interactions between Par3 and the plasmamembrane contribute to its cortical localization.

The Liver Kinase B1

The liver kinase B1 (LKB1 or STK11) has initially been identified in patients suffering from Peutz-Jeghers syndrome (PJS) (Hemminki *et al.*, 1998). PJS is a cancer prone rare genetic disorder and will be described later. LKB1 is a highly conserved serine/threonine kinase that is involved in many different cellular processes, such as cell metabolism, cell proliferation and cell polarity. In mice, the *LKB1* gene gives rise to three different LKB1 isoforms (LKB1 long ($LKB1_L$), LKB1 short ($LKB1_S$) and ΔN-LKB1) as a result of alternative splicing or internal initiation of translation (Fig. 1.5). The expression of $LKB1_S$ is restricted to testis and ΔN-LKB1 lacks catalytic activity, but promotes $LKB1_L$ (hereafter LKB1) mediated AMPK activation, however, inhibits the LKB1 dependent cell polarization of a lung cancer cell line (Towler *et al.*, 2008; Denison *et al.*, 2009; Dahmani *et al.*, 2015).

LKB1 is essential for development, because *LKB1*$^{-/-}$ mice die during embryonic development (E8.5 – E11) with vascular and neural tube defects (Ylikorkala *et al.*, 2001; Jishage *et al.*, 2002). Similar, *Drosophila lkb1* mutants do not develop further than mid-pupal stage (Lee *et al.*, 2006).

LKB1 is a tumour suppressor that regulates cell proliferation in response to the cellular energy level. LKB1 has been reported to regulate mTOR signaling, p53 and the Hippo pathway (Shaw *et al.*, 2004a; Jones *et al.*, 2005; Mohseni *et al.*, 2014). The role of LKB1 in mTOR signaling and the Hippo pathway will be discussed later, as their regulation depends on downstream kinases of LKB1. Although p53 has been reported to be phosphorylated by AMP-activated protein kinase (AMPK) (Jones *et al.*, 2005), which stabilizes and activates p53, LKB1 has also been reported to interact with p53 (Karuman *et al.*, 2001a). Moreover, this interaction takes place in the nucleus where p53 and LKB1 together bind to the promoter of the *p21/WAF1* gene, which is essential to induce its transcription and consequently G1 cell cycle arrest (Zeng and Berger, 2006).

LKB1 forms a ternary complex with the pseudokinase STRADα and the scaffold protein Mo25 (Boudeau *et al.*, 2003a; Baas *et al.*, 2003). LKB1 has up to five N-terminal nuclear localization sequences, which mediates its nuclear transport upon binding of Importin-α (Smith *et al.*, 1999b; Dogliotti and Krahn, unpublished data). STRADα promotes the cytoplasmic shuttling of LKB1 by binding to Exportin7 and CRM1 in complex with LKB1. In the cytoplasm, STRADα outcompetes Importin-α for binding LKB1 (Dorfman and Macara, 2008). In addition, binding of STRADα to LKB1 induces a conformational change of LKB1, which drastically enhances its catalytic activity. Binding of Mo25 to the LKB1/STRADα complex stabilizes the active conformation of LKB1 (Zeqiraj *et al.*, 2009). In the cytoplasm

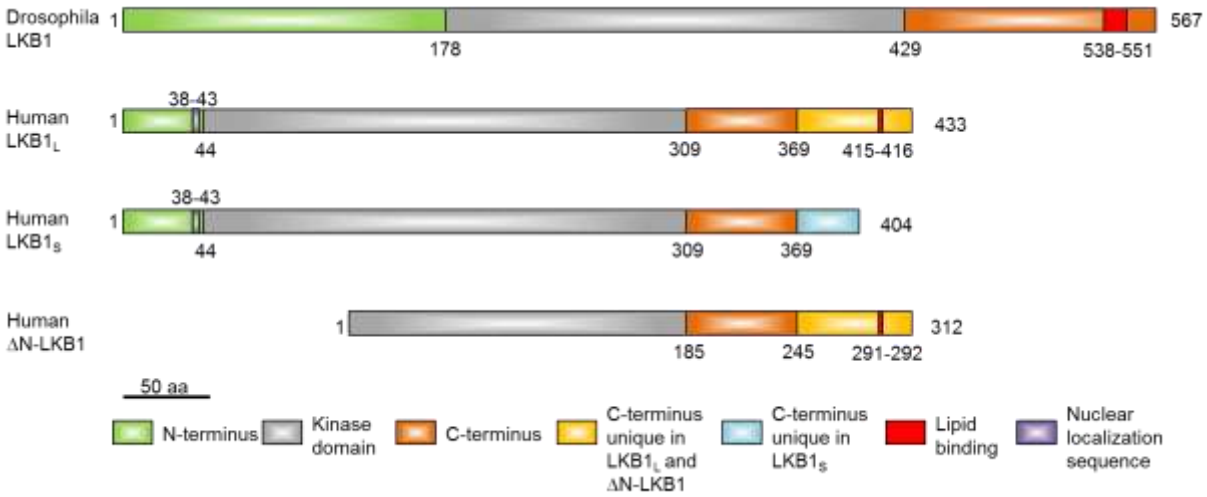

Fig. 1.5: Scheme of the *Drosophila* and human LKB1 variants. The large N-terminal domain of the *Drosophila* LKB1 is not conserved in the human proteins. The two human LKB1 variants LKB1-long ($LKB1_L$) and LKB1-short ($LKB1_S$) result from alternative splincing and are identical with the exception of their C-terminus. An alternative translation initiation gives rise to the human ΔN-LKB1 variant. Conserved domains are indicated and the numbers correspond to amino acid positions.

the active LKB1/STRADα/Mo25 complex baers the potential to localize at the cell cortex as well (Collins *et al.*, 2000; Sapkota *et al.*, 2001; Sebbagh *et al.*, 2009). Thus, the diversity of LKB1's cellular localizations highlights its potential to regulate cellular processes on many different levels.

The LKB1/AMPK signalling pathway

The ternary LKB1/STRADα/Mo25 complex acts together with AMPK as a cellular energy sensor. Under energy deprivation LKB1 phosphorylates AMPK to inhibit mTOR activity (Fig. 1.6) (Shackelford and Shaw, 2009). Additionally, LKB1 phosphorylates 12 AMPK related kinases in their activation loop: SAD-A/B (BRSK2 and BRSK1), NUAK1/2 (ARK5 and SNARK), SIK1/2/3, MARK1/2/3/4 and SNRK (Lizcano *et al.*, 2004; Jaleel *et al.*, 2005). Therefore, LKB1 acts as a master kinase to control cellular processes, such as cell metabolism, cell proliferation and cell polarity.

Under energetic stress the amount of cellular AMP increases, which is bound by AMPKγ. Upon binding of a second AMP molecule the AMPK holoenzyme becomes active (Scott *et al.*, 2004), but requires a critically phosphorylation in the activation loop on Thr172 of AMPKα by LKB1 (Hawley *et al.*, 1996; Lizcano *et al.*, 2004). Fully activated AMPK in turn phosphorylates and activates TSC2 (also known as Tuberin) (Inoki *et al.*, 2003b). The GTPase activating enzyme TSC2 forms a complex with TSC1 (also known as Hamartin) and

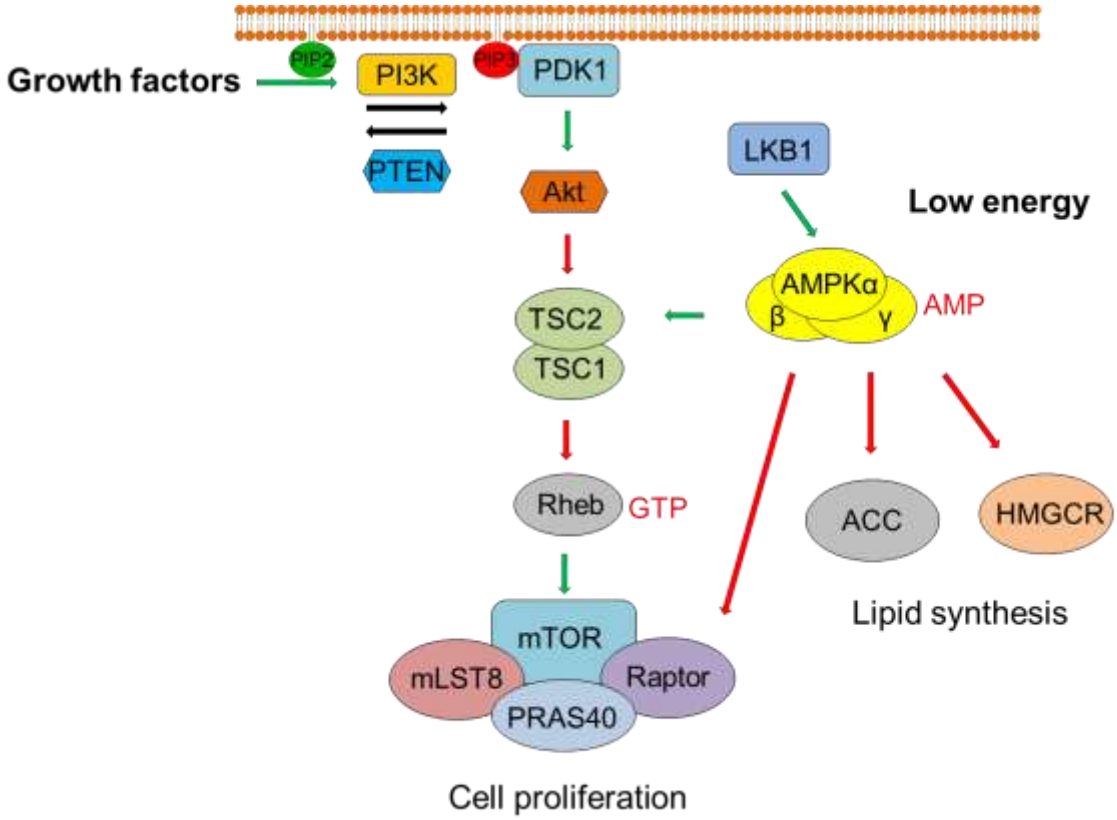

Fig. 1.6: Scheme of the interplay between the PI3K/Akt/mTOR and LKB1/AMPK signalling pathways. The stimulation of growth factors leads to a receptor mediated activation of PI3K, which in turn phosphorylates PIP2 to produce PIP3. PIP3 is bound by PDK1 and Akt causing the phosphorylation an activation of Akt by PDK1. Activated Akt phosphorylates and inhibits the GTPase activating enzyme TSC2. The GTPase Rheb stimulates in its GTP bound active form mTORC1, which promotes protein translation by activating S6K and eIF4E-BP. Upon low energy conditions, AMPK detects the increasing amount of AMP molecules and binds to LKB1, which triggers its phosphorylation and activation. AMPK phosphorylates TSC2, such as Akt, however, thereby activating it. Stimulating the GTPase activity of Rheb inactivates it and consequently decreases the activity mTOR. Moreover, AMPK phosphorylates Raptor to create a binding site for 14-3-3 proteins to prevent Raptor from joining the mTORC1. In addition, AMPK inactivates Acety-CoA carboxylase (ACC) and HMG-CoA-Reductase (HMGCR) to inhibit lipid synthesis. Green arrows indicate activation and red arrows inhibition.

stimulates the GTPase activity of Rheb, which becomes inactive after GTP hydrolysis (Inoki *et al.*, 2003a). In contrast, active Rheb promotes the activity of the kinase mTOR (Tee *et al.*, 2003). The activation of mTOR causes an elevated protein translation, which is mediated by phosphorylation of eIF4E-BP and S6K by mTOR (Carrera, 2004). The mTOR complex1 (mTORC1) requires binding of the scaffold protein Raptor, which recruits eIF4E-BP and S6K for phosphorylation (Kim *et al.*, 2002; Hara *et al.*, 2002). However, phosphorylation of Raptor (on Ser722 and Ser792 in humans) by AMPK causes its sequestration by 14-3-3

proteins and consequently an inhibition of mTORC1 (Gwinn *et al.*, 2008). Thus, LKB1 mediates the metabolic switch from anabolism towards catabolism under energetic stress. Therefore, AMPK also inhibits Acety-CoA carboxylase and HMG-CoA-Reductase to antagonize lipid synthesis (Fig. 1.6) (Carling *et al.*, 1987; Winder and Hardie, 1996).

In addition to the well-studied activation of the LKB1/AMPK pathway by AMP, recently the a fructose-1,6-bisphosphate (FBP) dependent mechanism to activate the LKB1/AMPK pathway has been described. Under energy deprivation the amount of FBP decreases and unoccupied Aldolase, which splits FBP into dihydroxyacetone phosphate (DHAP) and glyceraldehyde 3-phosphate (G3P), promotes the formation of a complex consisting of LKB1, AMPK, v-ATPase, Ragulator and AXIN (Zhang *et al.*, 2017a). This complex localizes on endosomes and is essential to activate the LKB1-AMPK pathway. The knockout of either *AXIN* or *LAMTOR1* (a component of the Ragulator complex) in mice prevents the LKB1 dependent activation of AMPK (Zhang *et al.*, 2013b; Zhang *et al.*, 2014).

Moreover, the LKB1/AMPK signaling pathway is implicated in cell polarity. In *C. elegens* and *Drosophila*, LKB1 is required for the anterior-posterior polarization of the embryo and oocyte, respectively (Watts *et al.*, 2000; Martin and St Johnston, 2003). In *Drosophila*, AMPK has been reported to phosphorylate Myosin regulatory light chain (MRLC), which is essential for proper apical-basal polarization of the embryonic epithelium. Loss of either LKB1 or AMPK results in severe polarity defects (Lee *et al.*, 2007). However, the phosphorylation of MRLC is not due to AMPK, but rather to other kinases, that act downstream of AMPK (Bultot *et al.*, 2009). In contrast to *Drosophila*, LKB1 is dispensable for the early polarization of the eight-cell stage mouse embryo (Krawchuk *et al.*, 2015). In addition to AMPK, LKB1 phosphorylates and activates the AMPK-related kinase Par1 (MARK1-4 in vertebrates), which regulates microtubule dynamics and counteracts the formation of the Par complex (as previously described) (Benton and St Johnston, 2003a; Lizcano *et al.*, 2004; Wang *et al.*, 2007; Granot *et al.*, 2009; Amin *et al.*, 2009).

Taken together, the regulation of cell proliferation, metabolism and cell polarity are tightly connected to the LKB1/AMPK signaling axis. Loss of either LKB1 or AMPK causes severe defects that result in embryonic lethality. The significance of the LKB1 dependent regulations with respect to human pathologies will be described in the next section.

The role of LKB1 in human pathologies

The regulation of cell proliferation, energy metabolism and cell polarity are essential processes that have to be precisely controlled. In response to energy deprivation or ionizing radiation LKB1 becomes active to induce a metabolic switch from anabolism towards catabolism. Germline mutations in the *STK11* gene (encoding LKB1), which localizes on chromosome 19p13.3 cause the Peutz-Jeghers syndrome (PJS). The PJS is a rare autosomal dominant genetic disease with an incident varying from 1:50.000 to 1:200.000 individuals. The PJS is characterized by cutaneous mispigmentation, gastro intestinal polyps and a high risk of cancer (Jansen *et al.*, 2009). The risk of PJS patients to develop cancer is highest in the gastro intestinal tract, however female patients bear also an increased risk to develop breast cancer (Hearle *et al.*, 2006). In mice, loss of heterozygosity (LOH) of *LKB1* has been reported by several groups to induce polyposis as well, suggesting that polyps develop due to a *LKB1* haploinsufficiency (Bardeesy *et al.*, 2002; Miyoshi *et al.*, 2002; Jishage *et al.*, 2002).

Mutations or loss of LKB1 have also been found in cancer patients without PJS, such as non-small cell lung cancer (NSCLC), cervical cancer, ovarian cancer, breast cancer, pancreatic cancer and malignant melanoma (Rowan *et al.*, 1999; Guldberg *et al.*, 1999; Sanchez-Cespedes *et al.*, 2002; Carretero *et al.*, 2004; Matsumoto *et al.*, 2007; Wingo *et al.*, 2009; Morton *et al.*, 2010; Gill *et al.*, 2011; Tanwar *et al.*, 2014; George *et al.*, 2016). Moreover, loss of LKB1 is associated with a poor survival rate of breast cancer patients (Sengupta *et al.*, 2017). The majority of mutations that have been reported from PJS and cancer patients affect the catalytic domain, but some affect the less characterized C-terminus as well (Boudeau *et al.*, 2003c).

Lung cancer is worldwide the most diagnosed cancer with 1.82 million new cases and 1.59 million deaths in 2012 (Ferlay *et al.*, 2015). In lung adenocarcinoma, *LKB1* is the third most frequently mutated gene (Ding *et al.*, 2008) and 60 – 70 % of lung adenocarcinoma are affected by LOH of *LKB1* (Sanchez-Cespedes *et al.*, 2002; Gill *et al.*, 2011). Generally in NSCLC, which are with 85 % the most common lung cancer, 39 - 41 % of the tumours display genomic alterations of the *LKB1* locus (Matsumoto *et al.*, 2007; Gill *et al.*, 2011; Calles *et al.*, 2015). In lung adenocarcinoma, LKB1 counteracts enhanced cell migration independent of AMPK. Thereby LKB1 activates MARK1/4, which in turn phosphorylates the scaffold protein DIXDC1, which leads to a decreased activation of the FAK/MEK/ERK mediated *Snail* expression. *DIXDC1* is frequently mutated in various tumours and thus, fails to convey the LKB1/MARK mediated tumour suppression (Goodwin *et al.*, 2014). Similar, LKB1 has also been reported to repress *Snail* expression by activating Salt-inducible kinase 1

(SIK1) to maintain E-Cadherin levels (Eneling *et al.*, 2012).

Furthermore, LKB1 suppresses cell proliferation also by counteracting the activity of the co-transcriptional activator YAP. The phosphorylation of MARK1/4 by LKB1 recruits the SCRIB complex to the lateral plasmamembrane of epithelial cells, which is essential for the core Hippo kinases MST1/2 and LATS1/2 to phosphorylate and inhibit YAP (Mohseni *et al.*, 2014). Taken together, beyond the canonical LKB1/AMPK tumour suppressor pathway a redundant LKB1/MARK axis antagonizes tumorigenesis.

In addition to mutations and LOH, the promotor of the *LKB1* gene is targeted by an aberrant methylation status in some types of cancer, such as colorectal cancer, melanoma and adenocarcinoma (Trojan *et al.*, 2000; Sanchez-Cespedes *et al.*, 2002; Zhang *et al.*, 2017b). The methylation of CpG-islands in the promotor region of *LKB1* reduces its gene expression and therefore reduces the tumour suppressive capacity of the affected cell. Nevertheless, CpG hypermethylation is not a frequent aberration and affects only a minor number of tumours.

Until now there are no pharmaceuticals that directly target LKB1 in order to elevate its activity or expression. However, with respect to data from cell culture and mice the polyphenol Honokiol (HNK) from *Magnolia grandiflora* enhances the protein level and activity of LKB1 (Nagalingam *et al.*, 2012; Avtanski *et al.*, 2015; Seo *et al.*, 2015; Sengupta *et al.*, 2017). A xenograft breast cancer mouse model that is treated with HNK displays a reduced tumour growth depending on LKB1 (Sengupta *et al.*, 2017). The activation of LKB1 results from the HNK mediated activation of the deacetylase SIRT1, which deacetylates and thereby activates LKB1 (Nagalingam *et al.*, 2012; Avtanski *et al.*, 2015; Seo *et al.*, 2015).

Although HNK treatment might become a promising anti-cancer therapy, the challenge will be to target cancers that are deprived of LKB1. The former anti-diabetic drug Phenformin bears the potential to specifically target tumours that lack LKB1 (Shackelford *et al.*, 2013). Phenformin inhibits the mitochondrial complex I, causing energetic stress. Treatment of a *LKB1*$^{-/-}$ NSCLC mouse model with Phenformin specifically induces apoptosis in *LKB1* null tumours and prolongs survival (Shackelford *et al.*, 2013).

In summary, the loss of active LKB1 leads to the PJS and is a predisposition for cancer. Under energetic stress LKB1 is essential to promote a catabolic switch. Nevertheless, with respect to a potential treatment of cancer patients with Phenformin the loss of LKB1 might bear the advantage that cells cannot respond via the LKB1/AMPK axis and undergo apoptosis.

Aims of the study

For development and homeostasis the polarization of epithelia is an essential process. The serine/threonine kinase LKB1 and the scaffold protein Bazooka (Baz) are key mediators of a celllar polarity. However, the regulation of both proteins is only poorly understood in the epithelium.

LKB1 is an important regulator of cell proliferation, metabolism and cell polarity. Mutations or loss of LKB1 have frequently been reported from various tumours. Therefore, it is essential to better understand the regulation of this enzyme. The subcellular localization of LKB1 varies strongly from nuclear to cytoplasmic and even cortical. Several functions of the nuclear and cytoplasmic LKB1 have already been described, however, the function and the mechanism by which LKB1 is targeted to the plasmamembrane remain elusive. Thus, this study aims to analyze the cortical localization of LKB1 and its function during development and tumour suppression.

Moreover, in *Drosophila*, the scaffold protein Baz is an essential cue for the establishment of an apical-basal cell polarity in epithelial cells and neuroblasts (NBs). Baz is the core component of the heterotrimeric Par complex, which also includes scaffold protein Par6 and the atypical protein kinase C (aPKC). The N-terminal oligomerization domain (OD) and the C-terminal lipid binding motif of Baz are involved in the membrane localization of Baz. Nevertheless, the function of the Baz OD beyond its contribution to the cortical localization is not clear, yet. Given that the OD largely contributes to the viability of embryos, it is another objective of this study to further characterize the role of the OD during the development of *Drosophila*.

Finally, although the formation and function of the Par complex in epithelial polarization are a dogma, the *in vivo* relevance of the Baz-Par6 interaction is unclear. Both proteins have *in vitro* been reported to interact via their PDZ domains, this is why this study clarifies the molecular basis of this interaction using *in vitro* structural approaches and *Drosophila* as an *in vivo* model. The goal of these experiments will be to understand the relevance of the *in vitro* obtained results.

Chapter 1: Membrane-binding and activation of LKB1

Membrane-binding and activation of LKB1 by phosphatidic acid is essential for development and tumour suppression

Authors: Giada Dogliotti[#], **Lars Kullmann**[#], Pratibha Dhumale, Christian Thiele, Olga Panichkina, Gudrun Mendl, Roland Houben, Sebastian Haferkamp, Andraes W. Püschel and Michael P. Krahn (# indicates equal contribution)

Personal contributions: preparation and analysis of some *Drosophila* embryos and S2R cells by immunofluorescence, liposome flotation assays, some Western blots of embryonic lysates, *in vitro* kinase assays, data analysis and discussion of results

The serine/threonine kinase LKB1 regulates various cellular processes such as cell proliferation, energy homeostasis and cell polarity and is frequently downregulated in various tumours. Many downstream pathways controlled by LKB1 have been described but little is known about the upstream regulatory mechanisms. Here we show that targeting of the kinase to the membrane by a direct binding of LKB1 to phosphatidic acid is essential to fully activate its kinase activity. Consequently, LKB1 mutants that are deficient for membrane binding fail to activate the downstream target AMPK to control mTOR signalling. Furthermore, the *in vivo* function of LKB1 during development of *Drosophila* depends on its capacity to associate with membranes. Strikingly, we find LKB1 to be downregulated in malignant melanoma, which exhibit aberrant activation of Akt and overexpress phosphatidic acid generating Phospholipase D. These results provide evidence for a fundamental mechanism of LKB1 activation and its implication *in vivo* and during carcinogenesis.

Introduction

The serine/threonine kinase LKB1 is ubiquitously expressed and highly conserved throughout evolution. It has been demonstrated to function as a 'master kinase' potentially activating several downstream kinases (Lizcano *et al.*, 2004). Apart from its implication in carcinogenesis LKB1 plays a role in various cellular signalling pathways such as Wnt-, TGFβ-signalling or the mTOR-pathway reviewed by Vaahtomeri and Makela (Vaahtomeri and Mäkelä, 2011). The latter one is controlled by LKB1-mediated activation of AMP-dependent kinase (AMPK), which is essential for cell survival and polarity in *Drosophila* and vertebrates, in particular under energetic stress (Hawley *et al.*, 2003; Woods *et al.*, 2003; Shaw *et al.*, 2004b; Lee *et al.*, 2007; van der Velden *et al.*, 2011). Mechanistically, AMPK phosphorylates (among others) Raptor (a core component of mTOR complex 1) and TSC2 (an mTOR inhibitor), resulting in reduced mTOR activity (Arsham *et al.*, 2003; Kimura *et al.*, 2003; Inoki *et al.*, 2003b; Corradetti *et al.*, 2004; Shaw *et al.*, 2004a; Shaw *et al.*, 2005; Gwinn *et al.*, 2008; Shackelford *et al.*, 2009). Consequently, the LKB1-AMPK-axis is believed to be a key modulator in carcinogenesis and cell polarity (Hardie and Alessi, 2013).

Apart from its function in cell proliferation and tumour suppression, LKB1 is directly implicated in the establishment and maintenance of cell polarity in different cell types and organisms (Nakano and Takashima, 2012).

Although many downstream pathways mediating the function of LKB1 have been described, little is known about the upstream mechanisms regulating LKB1 activity. Two pseudokinases tightly control the localization and kinase activity of LKB1: STRADα (Ste20-like kinase (Stlk) in *Drosophila*) and Mo25 form a stable ternary complex with LKB1 (Boudeau *et al.*, 2003a). Both proteins enhance the export of LKB1 from the nucleus into the cytoplasm and increase its kinase activity (Boudeau *et al.*, 2003a; Dorfman and Macara, 2008). Secondly, the conserved C-terminus of LKB1 is farnesylated *in vivo* and thereby might directly interact with the plasma membrane to attach the protein to the cell cortex. Although the majority of the protein accumulates at the plasma membrane of polarized (epithelial) cells, farnesylation has been reported to be not essential for the (tumour suppressor) function of LKB1 in mammalian cells or mice but might be essential for oogenesis in *Drosophila* (Sapkota *et al.*, 2001; Martin and St Johnston, 2003; Houde *et al.*, 2014). Therefore the question remains, whether membrane association of LKB1 is essential for the kinase activity and function of the protein during development and tumour suppression.

Here we report that binding of LKB1 to membranes by direct interaction with phospholipids, in particular to phosphatidic acid, is essential for its function *in vivo* during development of *Drosophila*. Membrane association of LKB1 is required for its kinase activity and for efficient activation of AMPK in cultured mammalian cells, thus contributing to the tumour suppressor function of LKB1. Strikingly, we reveal a strong correlation between overexpression of Phospholipase D (PLD), which increases cellular levels of phosphatidic acid, downregulation of LKB1 and enhanced activity of mTOR in malignant melanoma, thus likely contributing to the pathogenesis of malignant melanoma.

Methods

Fly stocks and genetics

UASt::GFP-LKB1 and *lkb1*::GFP-LKB1 transgenes were generated using phiC31-mediated germ line transformation on attp40. For rescue experiments of different LKB1 variants, we used the $lkb1^{x5}$ null allele. Lethality tests were performed in three independent experiments with n=100 in each experiment. For rescue experiments using the UAS/GAL4 system, we used UAS::GFP-LKB1 and actin5C::GAL4 instead of *lkb1*::GFP-LKB1.

DNA and constructs

Cloning of the cDNA of wild-type LKB1 into pENTR was performed using standard PCR on a full length EST clone (*Drosophila* Genomics Resources Center, DGRC) as template using the following primers: LKB1-F: 5′- CACCATGCAATGTTCTAGCTCTCGG-3′, LKB1-R: 5′-CTACGAAGTTCGGCAGTGG-3′. Similar, truncated fragments of LKB1 were cloned with the following oligonucleotides: $LKB1_{512}$-F: 5′-CACCATGCACACCTACGAACCGCC-3′, $LKB1_{536}$-F: 5′-CACCATGGCGCCCGTCAAGAAG-3′, $LKB1_{552}$ -F: 5′-CACCATGCTGACGTCCTGCATCTCCG-3′. For expression of LKB1 from its endogenous promoter we inserted a genomic fragment (from 2.8 kbp upstream of the translation start to 1 kbp downstream of the stop codon) into pENTR using the following primers: $LKB1_{gen}$-F: 5′- CACC CACTAGCGTAATTTGACGG-3′, $LKB1_{gen}$-R: 5′- CTC GAG CAGCAGTACGGTCATCTC-3′. An XbaI-cutting site was introduced replacing the start codon using mutagenesis PCR and the following primer: $LKB1_{gen}$-XbaI-F: 5′-GGCTCCGCGGAGGTTTTCTAGACAATGTTCTAGCTCTC-3′. Subsequently, GFP was inserted into the XbaI site by PCR and standard ligation. Mutagenesis PCR was used to generate defined point mutations with full length or genomic LKB1 cDNA in pENTR as template. The following oligonucleotides were used for mutagenesis (mutation underlined): $LKB1_{\Delta LB}$: Combination of 1. $LKB1_{K546A\ R547A\ R548A\ K550A\ K551A}$-F: 5′-TCGGCACTGGCGGCGGCCGCCGCGGCGCTGACGTCCTGC-3′ and 2.$LKB1_{K539A\ K540A\ K541A}$-F: 5′-GAGGAGGCGCCCGTCGCCGCGGCGGGATCGGCACTG-3′, $LKB1_{C564A}$-F: 5′-GTGCGCAAGCTTAGCCACGCCCGAACTTCGTAG, $LKB1_{D317A}$-F: 5′-CAAACGCTGAAGATTTCCGCCTTCGGTGTGGCG.

To express $LKB1_{\Delta LBC564A\ PH(PLD)}$ and $LKB1_{\Delta LBC564A\ PH(Akt)}$, the PH domain of PLCδ and Akt was amplified by PCR and ligated via an endogenous Bpu1101-I site into lkb1::LKB1 pENTR using the following primers:

PH(PLCδ)-F: 5′- GCTGAGCCACGCCCGAACT TCGgatgaggatctacaggcgct-3′,
PH(PLCδ)-R: 5′- GCTGAGCTAGATCTTGTGCAGCCCCAG-3′,
PH(Akt)-F: 5′-GCTGAGCCACGCCCGAACTTCGGTCGTAAAGGAGGGGTGG-3′ and PH(Akt)-R: 5′- GCTGAGCTTATATGAGCCGGCTGGATAC-3′.
For expression of hLKB1, the open reading frame of hLKB1 was cloned into pENTR using the following nucleotides: hLKB1-F: 5′- CACC ATGGAGGTGGTGGACCC-3′ and hLKB1-R: 5′- TCACTGCTGCTTGCAGG-3′. For mutation of the farnesylation, lipid binding motif and construction of the kinase dead version, the following nucleotides were used in mutagenesis PCRs:
$hLKB1_{C430A}$-F: 5′- CGCCGGCTGTCGGCCGCTAAGCAGCAGTGAAAGGGT-3′,
$hLKB1_{R415AK416A}$-F: 5′- GCCCCCAACCCTGCCGCCGCGGCCTGCTCCGCCAGC-3′ and
$hLKB1_{D194A}$: 5′- ACCCTCAAAATCTCCGCCCTTGGCGTGGCCGAGGCA-3′.
Constructs were recloned into GFP-tagged destination vectors containing a One-Strep-Tag fused to the N terminus of GFP (USGW, modified TGW, Murphy lab, DGRC, expression in S2R cells) or into a modified EGFP-C1 vector (CGW, expression in mammalian cells) containing a gateway cassette using the gateway technology (Life technology).

Antibodies

Antisera directed against full length LKB1 were raised by injection of a fusion protein of LKB1 and MBP into two guinea pigs (Amsbio, Abingdon, UK).

Cell culture and cell viability assay

HeLa, IMR90, IGR37 and MDCK cells were obtained from ATCC. All cells were maintained in Dulbecco's modified Eagle's medium supplemented with 10% fetal calf serum, 2 mM Glutamine at 37 °C in a 5% CO_2 atmosphere and negatively tested for mycoplasma contamination by PCR. Cells were transfected using FUGENE (Promega) according to the manufacturer's instructions. For evaluation of cell viability upon energetic stress, 50×10^3 cells/well were transiently transfected in a 24well plate with GFP-hLKB1+STRADα constructs and treated for 12 h with 2.5 mM AICAR (Santa Cruz Inc.). GFP+STRADα were used as negative control. Cell viability was assessed in triplicates using MTT assay according to the manufacturer's instructions (SIGMA).

Western blotting and coimmunoprecipitation

Western blotting was done as previously described (Cidlinsky *et al.,* 2016). For mammalian cell culture experiments, HeLa or IGR37 cells were transiently transfected with the indicated constructs. 48 hours after transfection, cells were incubated with 2 mM AICAR for 1 h and harvested in lysis buffer (1% Triton X-100, 150 mM NaCl, 1 mM $CaCl_2$, 1 mM $MgCl_2$, 50 mM TRIS-HCl pH 7.5) supplemented with protease- and phosphatase inhibitors. For embryonic lysates, *lkb1*::GFP-LKB1 expressing embryos were collected from overnight plates. Coimmunoprecipitation using GFP-Trap (ChromoTek) of GFP-LKB1 with HA-tagged DmSTRADα (Stlk) and myc-tagged DmMo25 was done in embryonic lysates, which ubiquitously expressed the proteins using arm::GAL4. Primary antibodies used for western blotting were as follows: rabbit anti-Actin (1:1,000, sc-47778, Santa Cruz), mouse anti-S6K (1:500, sc-8418, Santa Cruz), rabbit phosphoT389-S6K (1:500, sc-11759, Santa Cruz), rabbit anti-phospho-T172-AMPK (1:200, sc-33524, Santa Cruz), rabbit anti-phospho-MARK1/2/3 (1:500, PA5-17495, Thermo Scientific), mouse anti-myc (1:100, 9E10, DSHB), rabbit anti-AMPK (1:400, sc-25792, Santa Cruz), guinea pig anti LKB1 (1:500, this study), mouse anti-GFP (1:500, sc-9996, Santa Cruz), mouse anti-HA (1:500, #11583816001, Roche), rabbit anti-GST (1:5,000, #G7781, SIGMA). For statistical analysis, three independent experiments were scored. Intensity of the bands was quantified by ImageJ.

Immunohistochemistry

Drosophila embryos were fixed in 4% formaldehyde, phosphate buffer pH 7.4 as described before (Sen *et al.*, 2012). Primary antibodies used for indirect immunofluorescence were as follows: guinea pig anti LKB1 (1:250, this study), rabbit anti Baz (1:2,000, kindly provided by A. Wodarz), mouse anti α-spectrin (3A9, 1:50, DSHB), mouse anti Dlg (4F10, 1:50, DSHB), rat anti DE-Cad (DCAD2, 1:25, DSHB), rabbit anti GFP (1:400, sc-8334, Santa Cruz Inc), guinea-pig anti Miranda (1:1,000, kindly provided by A. Wodarz). HeLa cells were fixed with 4% PFA in PBS and stained with the rabbit anti-phospho-Sad antibody (1:250) and a mouse anti-LKB1 antibody (1:200, sc-32245, Santa Cruz) in 10% goat serum.

Secondary antibodies conjugated with Alexa 488, Alexa 568 and Alexa 647 (Life Technology) were used at 1:400. Images were taken on a Zeiss LSM 710 Meta confocal microscope and processed using Adobe Photoshop.

For immunohistochemical staining of healthy skin, nevi and melanoma, a tissue micro array (TMA) of paraffin-embedded healthy skin, nevi and melanoma primary tumours was analysed. Paraffin sections were deparaffinized for 30 min at 72 °C, washed two times for

7 min in Xylol and subsequently re-watered in a descending sequence of ethanol/water mixture. Prior to staining sections were subjected for 5 min to heat-induced epitope-retrieval (HIER) using 1 mM Tris-EDTA-buffer (pH 8.5) at 120 °C. Sections were blocked in peroxidase-blocking solution (Dako, #S2023) for 5 min at room-temperature and washed 5 min with wash buffer (Dako, #S3006) prior to incubation with primary antibody diluted in antibody diluent (Dako, #S2022) for 30 min. Primary antibodies were as follows: rabbit anti-LKB1 (D60C5F10, 1:200, Cell Signaling), rabbit anti-phospho-Akt (1:20, Cell Signaling #4060), rabbit anti-PLD2 (1:1,000, Cell Signaling #13891) and rabbit anti-S6K-phospho-T389 S6K (1:50, Cell Signaling #9206). Subsequently, sections were washed with wash buffer and incubated for 30 min with HRP-coupled secondary antibody (Dako EnVision, # K5007). Stainings were developed after washing using DAB/chromogen solution (Dako, #K5007). To visualize cellular structures, stained sections were counterstained with hematoxylin (Merk, #10517505000) for 1 min and dehydrated in ethanol/xylol before embedding. The staining intensity was determined blinded for all tissue samples as followed: negative-0, weak-+, moderate-++ and strong-+++. LKB1 exhibited a strong expression in melanocytes *in situ*, so weak or negative intensity was scored as downregulation of the protein, whereas moderate staining was classified as slightly downregulated. Activated Akt was negative in healthy skin biopsies, so weak, moderate and strong staining was classified as upregulated. PLD2 expression was negative or weak in melanocytes *in situ*, thus moderate and strong staining was scored as upregulated. Phospho-S6K was strongly expressed in the nucleus but not in the cytoplasm of melanocytes but cytoplasmic staining occurred only in malignant tumours. Consequently, weak to strong cytoplasmic staining of phospho-S6K was classified as upregulated.

Lipid binding assays

Fusion proteins of the C terminus of LKB1 (aa 353–567) with MBP were expressed in E.coli and affinity purified. Lipid strips (Echelon) were incubated over night with purified MBP-LKB1 fusion proteins at 0.5 μg ml^{-1} in TBST containing 3% BSA, washed and probed with antibodies against MBP (1:1,000, Santa Cruz sc-73416) as described above.

For membrane floatation and *in vitro* kinase assays, lipids were obtained from Avanti Polar Lipids (Egg-PA, #840101, Egg-PC #840051, Brain PtdIns(4,5)P2 #840046) and Echelon (PtdIns(3,4,5)P3 #P-3916). Liposomes (10 mM total lipid concentration, either PC alone or PC:PA/PtdIns(3,4,5)P3/PtdIns(4,5)P2 in a 9:1 molar ratio) were prepared in LB buffer (30 mM Tris, 4 mM EGTA, pH 8.0) by extrusion through a 0.1 μm polycarbonate membrane

using a Mini-Extruder (Avanti Polar Lipids). The membrane floatation was performed as follows (Krahn *et al.*, 2010b): liposomes (100 µl of 10 mM total lipid concentration) were incubated on ice for 30 min with 1 µg recombinant protein. LB buffer (30 mM Tris, 4 mM EGTA, 2 M sucrose (pH 8.0)) was added to the incubation reaction to bring the final sucrose concentration to 1.6 M, and this mixture was overlaid with cushions containing 1.4 M, 0.4 M, and 0.25 M sucrose in the same buffer in a TLA-55 tube. After centrifugation at 186,000*g* (4 °C) for 45 min in a TLA-55 rotor (Beckman), the 0.25/0.4 M interphase (top fraction, T) and the loading fraction (bottom fraction, B) were collected and analysed by SDS-PAGE and western blot. For statistical analysis, three independent experiments were scored. Intensity of the bands was quantified by ImageJ.

In vitro kinase assay

OneStrep-GFP-LKB1 plus OneStrep-GFP-Stlk were precipitated from transfected S2R cells (2 mg total protein lysates) using Streptactin beads (IBA, Goettingen, Germany). The beads were washed five times in harsh washing buffer (50 mM TRIS pH 7.5, 500 mM NaCl) and one time in LKB1 kinase buffer (50 mM TRIS pH 7.5, 10 mM $MgCl_2$, 10 mM $MnCl_2$, 1 mM DTT, 100 µM ATP, phosphatase- and protease inhibitors). Immunoprecipitated proteins were then incubated with 2 µg of recombinant GST-DmAMPK$\alpha_{108\text{-}280}$ (=aa 108–280, containing the T-loop with the LKB1-phosphorylation site) and 0.3 µCi[$_{\gamma\text{-}32}$ATP] in kinase buffer for 1 h at 30 °C. The reaction was terminated by addition of SDS sample buffer and samples were subjected to SDS-PAGE. Phosphorylation was detected by exposure to X-ray films and quantified with Aida 2D Densitometry software.

For assays with human recombinant kinase complex (Supplemental Fig. 2.3b,c), 1 µg of a complex of recombinant hLKB1, STRADα and Mo25 (SIGMA) was used as described above replacing immunoprecipitated LKB1 protein. In this experiment, GFP-AMPKα1 from transfected HeLa cells (2 mg total protein lysate) was used as substrate as a recombinant fragment would have interfered with the autophosphorylation bands. After isolation of precipitated OneStrep-GFP-AMPK, recombinant hLKB1/STRADα/Mo25 was added and incubated as described above. Subsequently, OneStrep-GFP-AMPK was purified from the reaction mixture using Streptactin beads.

For kinase assays with addition of lipids, Liposomes were prepared as described above and added at 10 mM final concentration.

For statistical analysis, three independent experiments were scored. Intensity of the bands was quantified by ImageJ.

Transfection and analysis of neurons

Hippocampal neurons were isolated from the brains of E18 rat embryos and cultured as described previously (Yang *et al.*, 2014). Dissociated hippocampal neurons were plated at 70,000 cells per well in a 24 well plate and transfected 3 h after plating by calcium phosphate co-precipitation. Neurons were fixed at 3 DIV and permeabilized with 0.1% Triton X-100, 0.1% sodium citrate in PBS for 3 min on ice. Neurons were stained with the Tau-1 antibody as axonal marker (Chemicon, MAB3420; 1:300) and Alexa-Fluor-conjugated secondary antibodies (Molecular Probes; 1:300). The stage of neuronal differentiation and axon formation was determined according to published criteria (Schwamborn and Püschel, 2004). For each LKB1 variant, 3 different experiments with 100 analysed neurons in each were scored.

Statistics

All experiments were performed in triplicates. Error bars represent s.d. and statistical significance was determined using ANOVA: $P<0.0001$, ****$P<0.001$, ***$P<0.01$, **$P<0.05$, *$P>0.05$, not significant (NS).

Results

LKB1 localizes to the cortex of epithelial cells and neuroblasts

The activity of kinases can be modulated for instance by directly influencing their enzymatic activity (e.g., by a conformational change via phosphorylation) or by targeting the protein to different subcellular compartments. In cultured mammalian cells, LKB1 accumulates in the nucleus in many cell lines and only a minor fraction of the protein is found in the cytoplasm or at the cytocortex (Smith *et al.*, 1999a; Tiainen *et al.*, 1999; Song *et al.*, 2008). LKB1 has been demonstrated to shuttle from the cytoplasm into the nucleus and back, with its two co-factors, STRADα and Mo25 enhancing cytoplasmic localization and activating the kinase (Baas *et al.*, 2003; Boudeau *et al.*, 2003a; Dorfman and Macara, 2008). Whereas endogenous LKB1 accumulates predominately in the nucleus of non-transformed fibroblasts (Fig. 2.1A), epithelial cells (Madin Darby Canine Kidney, MDCK) exhibit a staining of endogenous LKB1 exclusively at the cell-cell contacts, partly overlapping with the AJ- and TJ markers E-Cadherin and ZO-1 (Fig. 2.1B) (Sebbagh *et al.*, 2009). Similar, endogenous LKB1 localizes to the (lateral) membrane in epithelial cells *in vivo* (colon or salivary glands) (Fig. 2.1C,D). Remarkably, polarized epithelial cells in culture (MDCK) and *in situ* (colon and salivary gland) do not exhibit nuclear staining of LKB1. In *Drosophila* cells endogenous LKB1 is also not found in the nucleus but localizes at the cortex of female germ line cells as well as at the lateral membrane in epithelial cells (Martin and St Johnston, 2003), whereas it shows a diffuse cytoplasmic pattern in neural stem cells of *Drosophila* larval neuroblasts (NBs) (Bonaccorsi *et al.*, 2007). Similar, the *Caenorhabditis elegans* orthologue, PAR-4, regulating asymmetric cell division of the zygote, localizes to the entire cell cortex (Watts *et al.*, 2000). To test which mechanisms target LKB1 to the cortex, we raised an antibody against LKB1 and confirmed that in epithelial cells of the embryonic epidermis, endogenous LKB1 is localized laterally, co-staining with α-spectrin (Fig. 2.1E), but also overlapping with the zonula adherens (ZA), marked by *Drosophila* E-Cadherin (DE-Cad) (Fig. 2.1E). Notably, in embryonic NBs, we detect a clear cortical LKB1 staining in interphase as well as during mitosis (Fig. 2.1F–H). However, in contrast to key regulators of asymmetric cell division like the apical localized Bazooka (Baz) protein and the basally segregated adaptor protein Miranda (Mir), LKB1 does not show a polarized distribution during mitosis (Fig. 2.1F–H). Thus, LKB1 localizes predominately to the (lateral) plasma membrane in polarized epithelial cells and NBs in *Drosophila* and mammals.

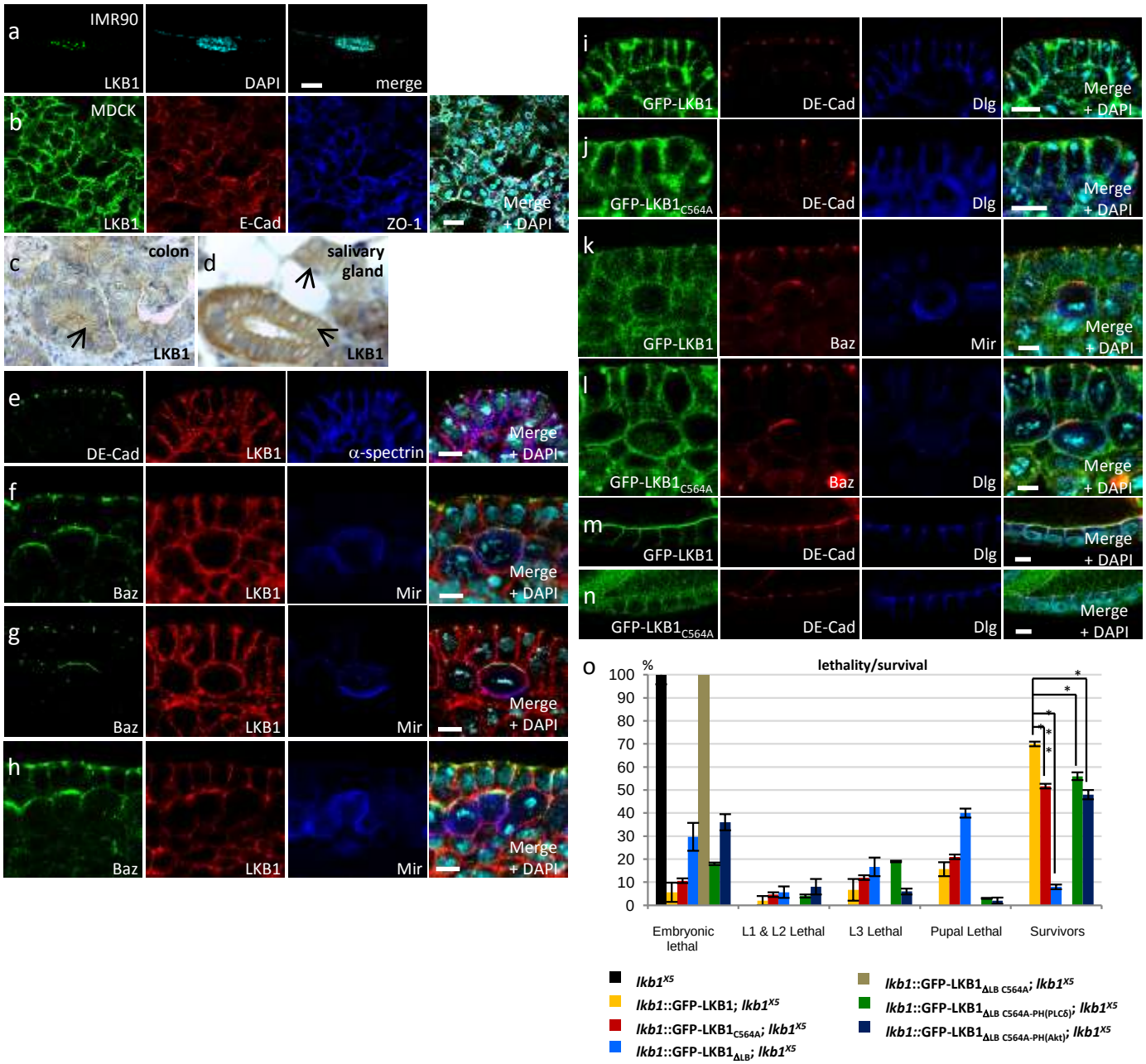

Fig. 2.1: LKB1 localizes to the plasma membrane in polarized epithelial cells and neuroblasts. (a) In non-transformed mammalian fibroblasts (IMR90 cells), endogenous LKB1 accumulates mostly in the nucleus. (b) In polarized epithelial cells (MDCK), LKB1 is targeted to the cell-cell contacts, partly colocalizing with E-Cadherin (E-Cad) and Zonula occludens protein 1 (ZO-1). (c,d) Sections of paraffin-embedded colon (c) and salivary gland tissues (d) show a localization of LKB1 at the lateral plasma membrane *in situ* (arrows). (e–h) LKB1 localizes to the lateral plasma membrane in epithelial cells of the *Drosophila* embryonic epidermis (e) and to the cortex of neuroblasts (f–h). (i–n) Wild-type GFP-LKB1 as well as farnesylation deficient LKB1 ($LKB1_{C564A}$) expressed from its endogenous promoter localize correctly to the (lateral) membrane of epithelial cells of the embryonic epidermis (i,j), of the follicular epithelium (m,n) and of neuroblasts (k,l). (o) Lethality tests of LKB1 variants as described in the methods section. Scale bars are 20 µm in a–d, 5 µm in e–n. Experiments were performed in triplicates. Error bars represent s.d. and statistical significance was determined using ANOVA: $P<0.0001$, ***$P<0.01$, *$P>0.05$, not significant (NS).

Farnesylation of LKB1 is not essential for its localization

The C-terminus of LKB1 can be farnesylated (Collins *et al.*, 2000; Houde *et al.*, 2014), establishing a putative membrane targeting domain—however, this modification does not seem to be important for its tumour suppressor function in mammals (Sapkota *et al.*, 2001) and for viability of mice (Houde *et al.*, 2014). In the *Drosophila* germ line, a block of farnesylation leads to a weaker cortical association and disturbed oocyte polarity (Martin and St Johnston, 2003). To test whether this is also true for epithelial cells and NBs, we used the endogenous LKB1 promoter to express a GFP-tagged LKB1 wild-type protein or an LKB1 version with a Cys564-Ala substitution in the fly (farnesylation-deficient LKB1, *lkb1*::GFP-LKB1$_{C564A}$). Wild-type GFP-LKB1 is expressed at similar protein level as endogenous LKB1 (Supplemental Fig. 2.1A) and localizes to the lateral cortex of epithelial cells and the cortical membrane in NBs indistinguishable from the endogenous protein (Fig. 2.1I,K). Surprisingly, in the embryonic epidermis and embryonic NBs, GFP-LKB1$_{C564A}$ shows the same subcellular localization as its wild-type counterpart (Fig. 2.1J,L). The farnesylation-deficient protein shows a more cytosolic distribution only in epithelial cells surrounding the oocyte (follicular epithelium) although a substantial fraction of the protein is still associated with the lateral membrane (Fig. 2.1N compared to wild-type GFP-LKB1 in Fig. 2.1M).
Notably, LKB1$_{C564A}$ expressed from its endogenous promoter is able to rescue an *lkb1*-null allele (*lkb1*^{X5}) to a large extent (52% surviving flies in comparison to 69% for wild-type LKB1, Fig. 2.1O), indicating that farnesylation of LKB1 is not essential for the function of the protein *in vivo*.

LKB1 directly binds to phospholipids

In order to further elucidate the targeting of LKB1 to the plasma membrane, we used Schneider R+ (SR+) cells as they do not exhibit an intrinsic polarity and do not express transmembrane proteins like DE-Cad, Crumbs or Echinoid, qualifying them as a model for the analysis of direct plasma membrane targeting. As expected, GFP-LKB1 localizes to the plasma membrane in transfected S2R+ cells (Fig. 2.2C). In contrast, the farnesylation motif alone (GFP fused to the last 15 amino acids of LKB1, GFP-LKB1$_{552\text{-}C}$) is not sufficient to target the protein to the cortex (Fig. 2.2D), which is in line with the hypothesis that stable

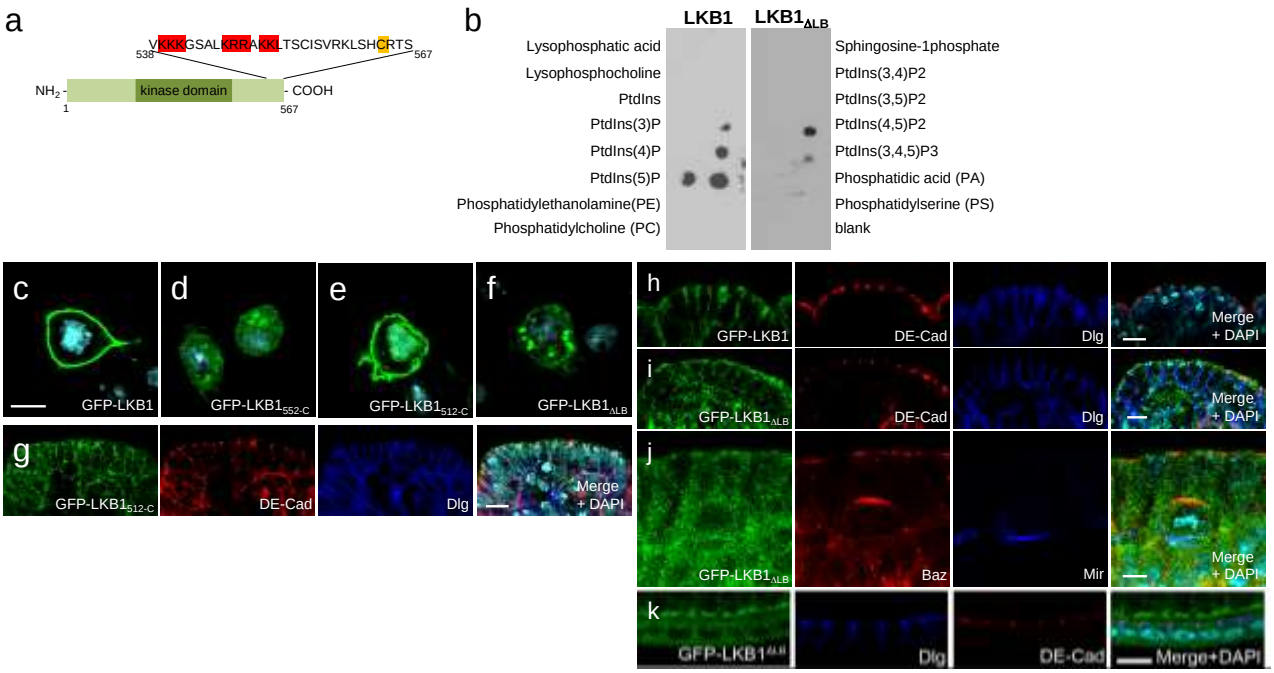

Fig. 2.2: LKB1 is recruited to the lateral plasma membrane by direct binding to phospholipids. (a) Schematic drawing showing *Drosophila* LKB1 with basic residues and the farnesylation motif within its C-terminal region highlighted. (b) Lipid overlay assay of recombinant LKB1 and LKB1$_{\Delta LB}$ (=LKB1$_{K546A\ R547A\ R548A\ K550A\ K551A\ K539A\ K540A\ K541A}$) using diverse lipids spotted on nitrocellulose membrane. (c–f) GFP-LKB1 and GFP-LKB1$_{512\text{-}C}$ localize to the cell cortex of transfected S2R cells (c,e), whereas a fusion protein of the last 16aa of LKB1 with GFP (GFP-LKB1$_{552\text{-}C}$) or GFP-LKB1$_{\Delta LB}$ does not (d,f). (g–j) GFP-LKB1$_{512\text{-}C}$ accumulates at the lateral membrane of epithelial cells in the embryonic epidermis (g), similar to full length GFP-LKB1 (h), whereas GFP-LKB1$_{\Delta LB}$ exhibits a cytosolic localization in epithelial cells of the embryonic epidermis (i) and of the follicular epithelium (k) as well as in neuroblasts (j). Scale bars are 5 µm.

membrane binding requires protein modifications (e.g., palmitoylation) or membrane binding domains (McTaggart, 2006) in addition to conjugation with farnesyl acid. In contrast, a longer C-terminal fragment of LKB1 (LKB1$_{512\text{-}C}$ and LKB1$_{536\text{-}C}$) exhibits a robust cortical localization apart from a nuclear staining (Fig. 2.2E; Supplemental Fig. 2.2A). Furthermore, in embryos, a substantial fraction of GFP-LKB1$_{512\text{-}C}$ localizes to the lateral membrane (Fig. 2.2G).

Membrane association can be achieved not only by the interaction with transmembrane or membrane associated proteins but also by the direct binding to the lipid bilayer. Several protein domains are known to facilitate protein–lipid interactions. Beside larger domains, polybasic motifs have been described for several proteins to bind to (phospho)-lipids, in particular to phosphatidic acid (Stace and Ktistakis, 2006). Indeed, a C-terminal polybasic motif (aa 539–551, termed lipid-binding motif=LB, Fig. 2.2A) facilitates a direct binding of

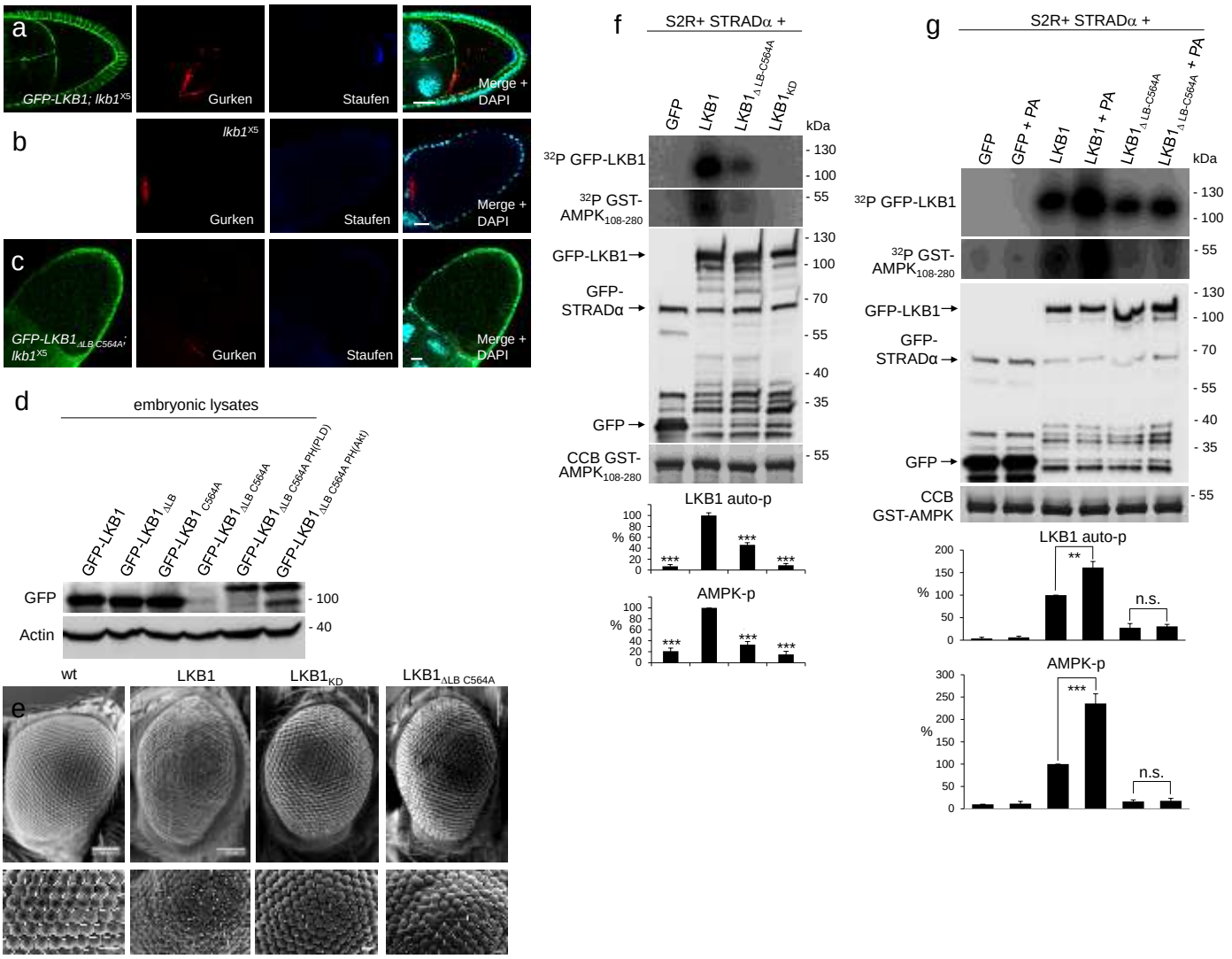

Fig. 2.3: Membrane-association of LKB1 is essential for its kinase activity and function *in vivo*. (a–c) Immunostainings of *lkb1*-mutant ovaries (b) exhibit a disturbed localization of Staufen, which is rescued by expression of GFP-LKB1 (a) but not of GFP-LKB1$_{\Delta LB\ C564A}$ (c). (d) Immunoblotting of LKB1 variants expressed in embryos demonstrating that the protein stability of GFP-LKB1$_{\Delta LB\ C564A}$ is strongly reduced. (e) Overexpression of LKB1, but not of a kinase-dead version of LKB1 (LKB1$_{D317A}$=LKB1$_{KD}$) or GFP-LKB1$_{\Delta LB\ C564A}$ results in an impaired eye morphology (‘rough eye’ phenotype). (f,g) *In vitro* kinase assays of GFP-LKB1/GFP-STRAD purified from transfected S2R cells demonstrate a strong decrease in the kinase activity of LKB1$_{\Delta LB\ C564A}$ measured by autophosphorylation (^{32}P GFP-LKB1) and phosphorylation of recombinant AMPK (^{32}P GST-AMPK$_{108-280}$) (f). The addition of PA-enriched liposomes (as described in materials and methods) increased the kinase activity of wild type but not of membrane-binding deficient LKB1 (g). Activity of GFP-LKB1 was set as 100%. Inputs were visualized by Western Blot against GFP (GFP, GFP-Stlk and GFP-LKB1) and by Coomassie Brilliant Blue staining (CCB, GST-AMPK$_{108-280}$) Scale bars are 5 µm in c–k and m, 100 µm in o and p, 10 µm in l and n. Experiments were performed in triplicates. Error bars represent s.d. and statistical significance was determined using ANOVA: P<0.001, ***P<0.01, **P<0.05, not significant (NS).

DmLKB1 to PA, PtdIns(5)P, PtdIns(3,4,5)P3 and PtdIns(4,5)P2 as determined by a lipid overlay assay (Fig. 2.2B). A strong binding to PA (and to some extent to PtdIns(3,4,5)P3 and PtdIns(4,5)P2) was confirmed in liposome flotation assays (Supplemental Fig. 2.2B). Mutation of this motif (mutation of Arg and Lys in LKB1-LB to Ala, $LKB1_{\Delta LB}$) abolished liposome association *in vitro* (Supplemental Fig. 2.2B) as well as membrane association in cultured cells (Fig. 2.2F) and in *Drosophila* epithelia and neural stem cells (Fig. 2.2H–K).

Membrane-bound LKB1 is crucial for *Drosophila* development

LKB1 has been implicated in various cellular functions, among them cell proliferation control, suppression of tumour growth and regulation of cell polarity in various cell types (Vaahtomeri and Mäkelä, 2011; Nakano and Takashima, 2012). To address the question whether membrane targeting of LKB1 is crucial for its physiological function, we performed rescue experiments with GFP-LKB1 expressed from its endogenous promoter. As indicated above, not only wild-type LKB1 but also $LKB1_{C564A}$ can rescue the embryonic lethality of maternal and zygotic mutant flies to a substantial extent, indicating that wild-type and farnesylation-deficient GFP-LKB1 can substitute endogenous LKB1 in all tissues (Fig. 2.1O). Notably, GFP-$DmLKB1_{\Delta LB}$ still exhibits a residual rescue capacity (8% of surviving flies in contrast to 69% for wild-type DmLKB1, (Fig. 2.1O), which might be due to a transient or weak membrane binding mediated by the farnesylation anchor. Indeed, removal of the farnesylation motif in GFP-$LKB1_{\Delta LB}$ (GFP-$LKB1_{\Delta LB\ C564A}$) totally abolishes the rescue capacity of the mutant protein and all mutant flies die during embryonic stages like the null allele $lkb1^{X5}$ (Fig. 2.1O). Moreover, *lkb1*-mutant flies expressing GFP-$LKB1_{\Delta LB\ C564A}$ exhibit the same polarity defects as the null allele alone (e.g., disruption of the anterior–posterior polarity of ovaries, Fig. 2.3C, compared with wild-type LKB1 rescue in A and *lkb1*-mutant phenotype in B).

Western blot analyses of lysates from embryos expressing LKB1 variants from the endogenous promoter reveal that GFP-$LKB1_{\Delta LB\ C564A}$ is unstable or rapidly degraded (Fig. 2.3D), indicating that the association of LKB1 with membranes is essential for protein stability. In contrast, transient membrane association of $LKB1_{\Delta LB}$, which is probably mediated by the farnesylation anchor, is sufficient for protein stabilization, as no differences in protein levels are detectable between wild-type LKB1 and lipid-binding-deficient LKB1 (Fig. 2.3D).

However, overexpression of GFP-DmLKB1$_{\Delta LB\ C564A}$ in *lkb1*-mutant flies using the UAS/GAL4 system instead of the endogenous *lkb1*-promoter does not result in detectable rescue capacity (Supplemental Fig. 2.3A). Similar, the overexpression phenotype (rough eye formation) of LKB1 is abolished in GFP-DmLKB1$_{\Delta LB\ C564A}$ similar to a kinase dead version (Fig. 2.3E). Thus, we assume that it is very unlikely that impaired functionality of GFP-DmLKB1$_{\Delta LB\ C564A}$ is only due to the instability of the protein.

To further substantiate this assumption, we fused two different heterologous membrane-binding domains to the C terminus of GFP-LKB1$_{\Delta LB\ C564A}$: The PH-domain of human phospholipase Cδ (Várnai and Balla, 1998) that preferentially binds to PtdIns(4,5)P2 (resulting in GFP-LKB1$_{\Delta LB\ C564A\text{-}PH(PLC\delta)}$), but is also capable of binding to PA with a high affinity (Pawelczyk and Matecki, 1999), and the PH-domain of human Akt1, (GFP-LKB1$_{\Delta LB\ C564A\text{-}PH(Akt1)}$) with a high affinity to PtdIns(3,4,5)P3 (Klippel *et al.*, 1997). Similar to PLCδ, Akt1 has recently been demonstrated to bind PA *in vitro* (Bruntz *et al.*, 2014). Strikingly, both chimeric proteins stabilize the protein expression of GFP-LKB1$_{\Delta LB\ C564A}$ (Fig. 2.3D), localize at least partly to the lateral plasma membrane (Supplemental Fig. 2.4A,B) and are capable of rescuing the *lkb1* null allele to a large extent (56 and 48% respectively, Fig. 2.1O). These results confirm our hypothesis that membrane association of LKB1 is crucial for its function *in vivo*.

To test whether membrane association is essential for the kinase function of LKB1, we performed *in vitro* kinase assays using the GFP-DmLKB1/STRADα complex purified from transfected S2R cells. Indeed GFP-DmLKB1$_{\Delta LB\ C564A}$ exhibits a strongly decreased kinase activity (46% in autophosphorylation and 30% in AMPK-phosphorylation relative to wild-type GFP-LKB1, Fig. 2.3F). Furthermore, addition of PA-enriched liposomes to GFP-DmLKB1/STRADα strongly increases the kinase activity of the LKB1 complex (autophosphorylation 1.6-fold and AMPK-phosphorylation 2.4-fold Fig. 2.3G).

Reduced kinase activity of LKB1$_{\Delta LB\ C654A}$ is neither due to impaired association with the canonical binding partners STRADα or Mo25, which enhance LKB1 activity, nor due to decreased substrate binding (Supplemental Fig. 2.3B). Therefore, these data suggest that the lipid binding capacity of DmLKB1 is essential for its kinase function.

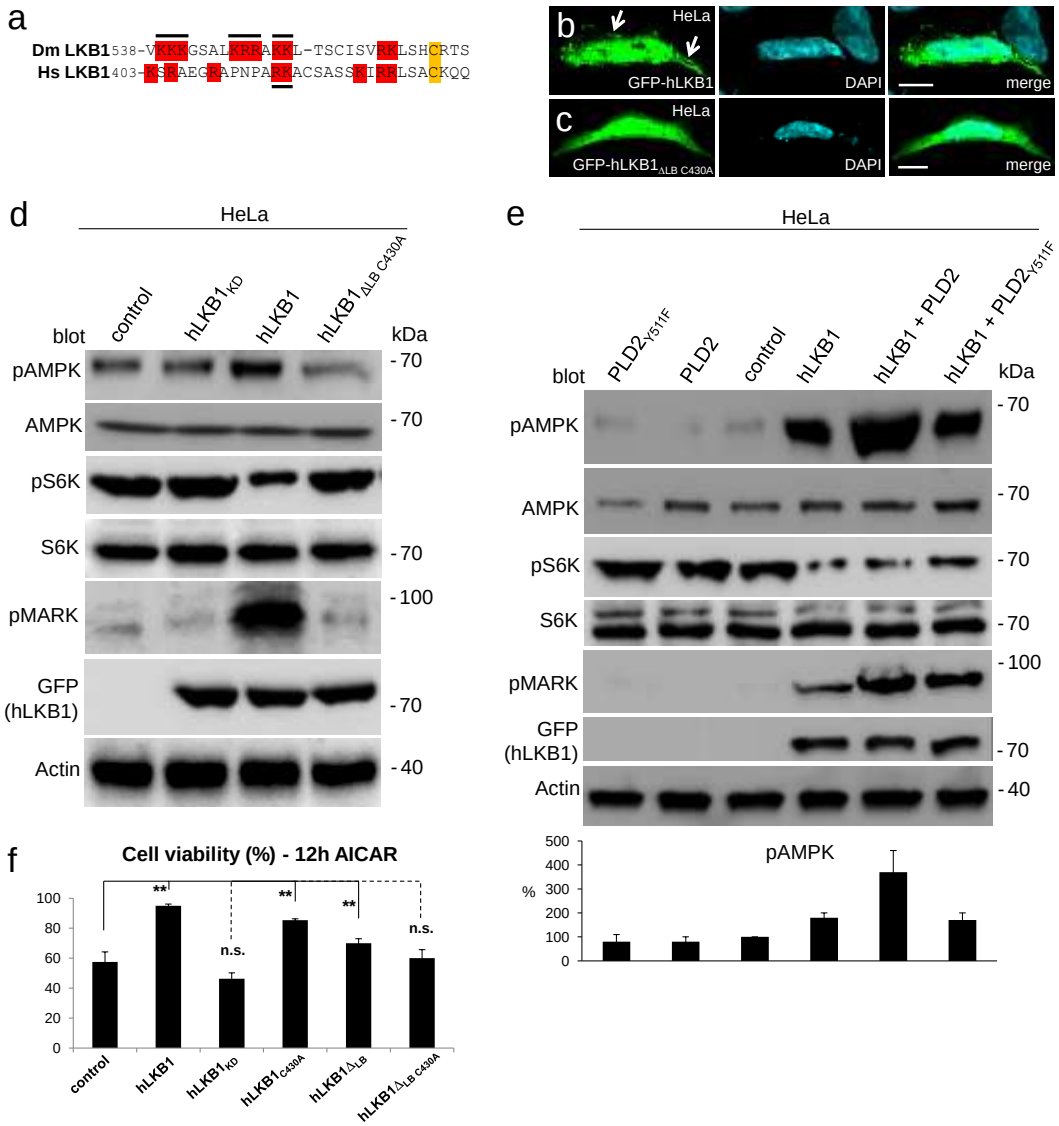

Fig. 2.4: Membrane binding of hLKB1 is essential for its function in mammalian cells. (a) Alignment of DmLKB1 and hLKB1 reveals several positively charged aa in the C terminus of hLKB1. Mutated residues are marked with bold lines. (b,c) GFP-hLKB1 localizes predominately to the nucleus and plasma membrane of HeLa cells cotransfected with STRADα (b), whereas GFP-hLKB1$_{\Delta LB\ C430A}$ is not recruited to the cortex (c). (d,e) Immunoblottings of lysates from transfected HeLa cells, which lack substantial LKB1 expression, demonstrate an increase of activated AMPK (phospho-T172 AMPK), activated MARK (phospho-MARK) and decreased mTOR activation (measured by phosphorylation of S6K) upon GFP-hLKB1+STRADα transfection, which is not observed in GFP-hLKB1$_{\Delta LB\ C430A}$+STRADα transfected cells (d). Co-transfection of PLD2 but not of a catalytically reduced variant (PLD$_{Y511F}$) together with hLKB1 results in a further increase of AMPK activation (e). The intensity of pAMPK bands was quantified (normalized against total AMPK) (e, lower panel, control was set as 100%). (f) Cell viability of HeLa cells under energetic stress (induced by incubation with AICAR for 12 h) was estimated using the MTT assay (as described in the methods section). Scale bars are 10 µm. Experiments were performed in triplicates. Error bars represent s.d. and statistical significance was determined using ANOVA: $P<0.01$, $^{**}P<0.05$, not significant (NS).

The function of human LKB1 depends on membrane binding

As association with the membrane is essential for LKB1 to accomplish its function during development of *Drosophila*, we further investigated whether this mechanism is conserved throughout evolution and controls the activity of human LKB1 (hLKB1). Similar to its fly homologue, mutation of the polybasic region at the C terminus of hLKB1 together with mutation of the farnesylation motif (Fig. 2.4A) resulted in an impaired membrane localization in HeLa cells (Fig. 2.4B,C).Activation of AMPK is one of the most important functions of LKB1 during tumour progression, which is further enhanced under energetic stress. As activated AMPK directly and indirectly inhibits mTOR (Arsham *et al.*, 2003; Kimura *et al.*, 2003; Inoki *et al.*, 2003b; Corradetti *et al.*, 2004; Shaw *et al.*, 2004a; Shaw *et al.*, 2005; Gwinn *et al.*, 2008; Shackelford *et al.*, 2009), the LKB1-AMPK pathway controls mTOR activity, e.g., upon aberrant activation of Akt, which occurs in various types of tumours with loss of function of PTEN or PI3-Kinase gain of function mutations (Menon and Manning, 2008). Loss of membrane binding capacity of hLKB1 strongly decreases its ability to activate AMPK in HeLa cells (Fig. 2.4D), which lack substantial endogenous LKB1 expression, and consequently leads to apoptosis in metabolically stressed cells (Fig. 2.4F). Apart from AMPK activation, $hLKB1_{\Delta LB\ C430A}$ fails to activate two other kinases of the AMPK-family, MARK (Fig. 2.4D) and SadA (Supplemental Fig. 2.5D). Furthermore, $hLKB1_{\Delta LB\ C430A}$ is no longer able to inhibit mTOR (as estimated by phosphorylation of p70-S6-Kinase 1, pS6K, Fig. 2.4D). Vice versa, addition of PA-enriched liposomes to a recombinant hLKB1/hSTRADα/hMo25 complex enhanced autophosphorylation of hLKB1 and AMPK phosphorylation *in vitro*, whereas Phosphatidylcholine (PC) alone or PtdIns(4,5)P2 and PtdIns(3,4,5)P3-enriched liposomes had only a small effect on the activity of hLKB1 (Supplemental Fig. 2.3C,D).

Overexpression of PLD2 enhances LKB1 activity

PA is generated (among other pathways) from PC by two isoforms of PLD, PLD1 and 2 (Gomez-Cambronero, 2014). Expression of PLD2 but not of a variant of PLD2 with a reduced catalytic activity (PLD2 Y511F (Henkels *et al.*, 2009)) together with hLKB1 results in a further increase of AMPK and MARK activation (Fig. 2.4E), suggesting that PLD2-induced production of PA enhances LKB1 activity *in vivo*. Conversely, inhibition of PLD reduces

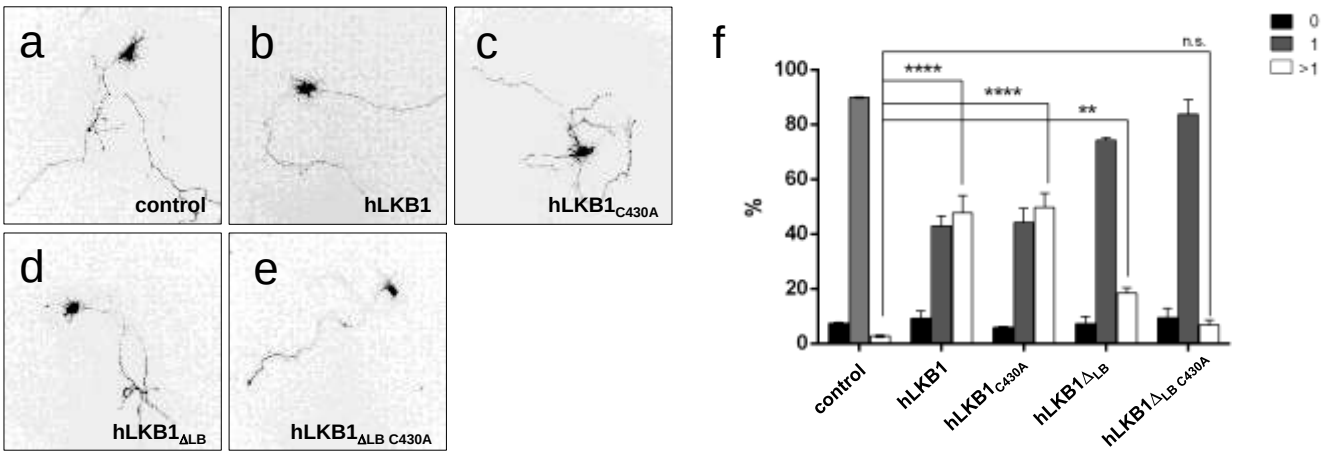

Fig. 2.5: Induction of multiple axons in primary rat hippocampal neurons depends on membrane binding of hLKB1. (a–f) Hippocampal neurons from E18 rat embryos were transfected at 0 d.i.v. with vectors for GFP (control), GFP-LKB1 or GFP fusion proteins for the indicated LKB1 mutants and STRAD and analysed at 3 d.i.v by staining with the Tau-1 antibody (axonal marker). Representative images of transfected neurons are shown. The scale bar is 20 μm. (f) The development of neuronal polarity was analysed by counting the number of neurons without an axon (0, black), with a single axon (1, gray) or with multiple axons (>1, white). Most primary rat hippocampal neurons transfected with GFP alone (control) develop only a single axon (a, quantified in f). In contrast, neurons overexpressing GFP-hLKB1+STRADα or GFP-hLKB1$_{C430A}$+STRADα (b,c,f) frequently establish two or more axons, whereas hLKB1 variants, which are deficient in membrane binding, fail to induce a multiple axon phenotype (d–f). Experiments were performed in triplicates. Error bars represent s.d. and statistical significance was determined using ANOVA: $P<0.0001$, ****$P<0.01$, **$P>0.05$, not significant (NS).

LKB1's capacity to activate AMPK (Supplemental Fig. 2.5B). However, basal levels of activated AMPK are maintained, indicating that other enzymes (e.g., Diacylglycerol kinase) can compensate loss of PLD activity. This is in line with the observation that *C. elegans*, *Drosophila* and mouse mutants lacking PLD enzymes do not exhibit as dramatic phenotypes as LKB1$_{\Delta LB\ C564A}$ (LaLonde *et al.*, 2005; Raghu *et al.*, 2009; Sato *et al.*, 2013).

Membrane-binding-deficient LKB1 fails to induce multiple axons

Overexpression of LKB1 induces the extension of multiple axons (Shelly *et al.*, 2007; Barnes *et al.*, 2007; Veleva-Rotse *et al.*, 2014). Consistently, overexpression of wild-type GFP-hLKB1

together with STRADα results in the formation of multiple axons by the majority of transfected rat hippocampal neurons in culture (Fig. 2.5B,F). Remarkably, expression of farnesylation-deficient hLKB1$_{C430A}$ induces this phenotype as efficiently as wild-type LKB1 (Fig. 2.5C,F). By contrast, mutation of the C-terminal basic region (hLKB1$_{\Delta LB}$) almost abolished the effect on axon formation (Fig. 2.5D,F). Inactivation of the farnesylation signal in lipid-binding-deficient hLKB1 (hLKB1$_{\Delta LB\ C430A}$) did result in further reduction of LKB1 activity in this assay (Fig. 2.5D,F). These results confirm the importance of the C-terminal membrane binding domain for the function of LKB1 in mammalian cells.

Expression of LKB1 is downregulated in malignant melanoma

As we have demonstrated that overexpression of PLD2 in cell culture results in increased activity of LKB1 (reflected by enhanced AMPK activation, Fig. 2.4E), we next assessed the pathophysiological relevance of our findings regarding tumour formation *in vivo*. Interestingly, expression of PLD2 is upregulated in several types of cancer, including melanoma, and high PLD2 expression correlates with poor survival rates of patients (Saito *et al.*, 2007; Henkels *et al.*, 2013). In cultured melanoma cells lacking detectable LKB1 expression (IGR37), membrane binding of LKB1 is essential for efficient AMPK (and MARK) activation, suppression of mTOR and cell survival under energetic stress (Supplemental Fig. 2.6).

Our data suggest that an aberrant increase in PLD expression in cancer cells will lead to increased PA levels and subsequent mTOR activation (Fang *et al.*, 2001; Foster *et al.*, 2014; Yoon *et al.*, 2015) only if in addition the expression of LKB1 is reduced, because PA-mediated LKB1/AMPK activation normally counteracts mTOR activity. To test this hypothesis, we investigated whether increased expression of PLD, aberrant activation of Akt and decreased LKB1 expression correlate with enhanced mTOR activity in melanoma. Indeed, biopsies of melanoma primary tumours show a strong correlation between these four parameters. In 81% of all analyzed tumours PLD2 expression as well as phospho-Akt and mTOR activity were elevated while the expression of LKB1 was decreased (Fig. 2.6A–E). Only 12% of the samples showed mTOR activation in the presence of stimulating phospho-Akt and PLD2-overexpression although LKB1 staining appeared normal, which might be explained by inactivating mutations of LKB1, which do not affect protein expression or stability. In contrast, melanocytes in biopsies of healthy skin exhibited a strong LKB1

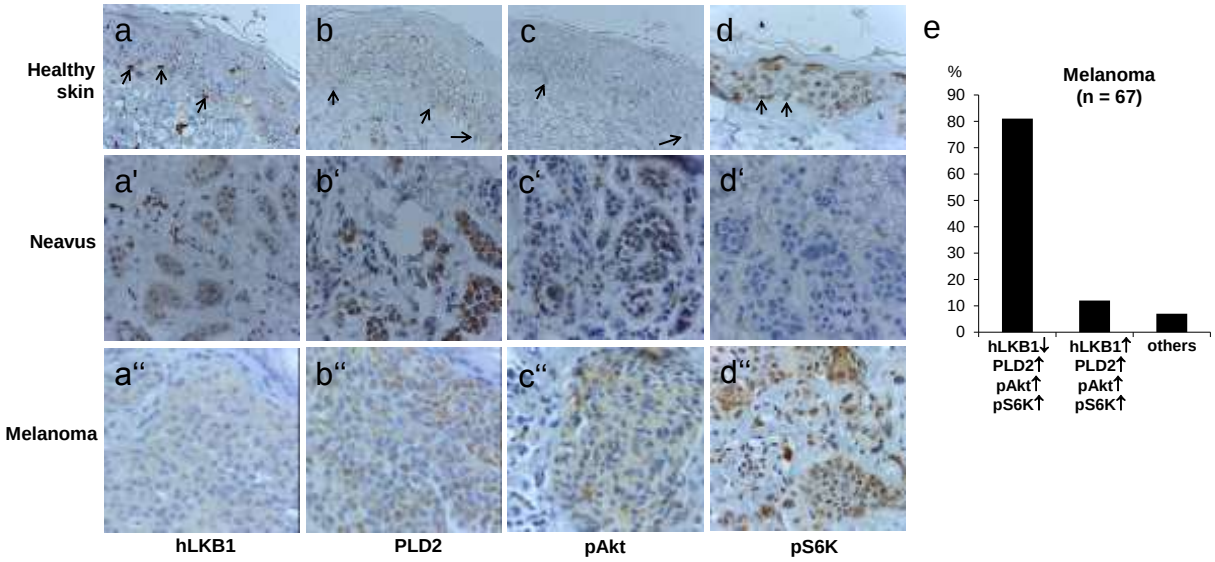

Fig. 2.6: Downregulation of hLKB1 correlates with increased mTOR signalling in malignant melanoma overexpressing PLD2. Immunostainings of paraffin-embedded tissue sections of normal skin (a–d), neavi (a′–d′) and primary malignant melanoma tumours (a″–d″). (a) hLKB1 is highly expressed in melanocytes in the *stratum basale* of the epidermis *in situ* (a, arrows), and still detectable at substantial levels (a′) whereas it is almost undetectable in the majority of malignant melanoma (a″). (b) PLD2 is not detectable in melanocytes of healthy skin sections (b, arrows) but becomes overexpressed in naevi (b′) and primary tumours (b″). (c) Akt is activated (indicated by staining of phospho Akt, pAkt) in naevi (c′) and malignant melanoma (c″), whereas it is not detectable in melanocytes of healthy skin samples (c). (d) Melanocytes in healthy skin biopsies (d) show only faint nuclear staining for phospho S6K (pS6K), which was used as to evaluate mTOR activation. Naevi (d′) exhibit only very few pS6K positive cells, whereas malignant melanoma show strong cytoplasmic and nuclear staining of pS6K (d″). (e) Quantification of melanoma biopsies scored for the indicated correlations. 'Others' are tumours, which do not exhibit increased phospho-Akt or PLD2 staining.

expression, as well as low level of PLD2, phospho-Akt and mTOR activation (Fig. 2.6A–D, arrows). Melanocytic nevi, a benign proliferation of melanocytes, which can give birth to malignant melanoma, show in many cases elevated PLD2 expression as well as activation of Akt, whereas LKB1 expression is still high in most cases, suppressing aberrant mTOR activation, which occurred only in 25% of the analyzed specimen (Fig. 2.6A'–D'). Thus in melanoma, loss of LKB1 in PLD2 overexpressing tumours may further contribute to mTOR activation, whereas in benign neoplasia higher LKB1 level counterbalance aberrant PLD2 activation.

Discussion

In this study, we have elucidated a conserved mechanism regulating LKB1 activity and function *in vivo* and during tumour suppression (Fig. 2.7). We have further established the first link between PLD-mediated production of PA and activation of LKB1. Our data suggest that membrane targeting of LKB1 by direct binding to PA is essential for the function of LKB1 during *Drosophila* development and for activation of AMPK and suppression of mTOR activity in cultured mammalian cells. Furthermore, downregulation of LKB1 in malignant melanoma specimen, which exhibit activated Akt and overexpression of PLD2, correlates with enhanced mTOR activity, indicating that the mechanism described in this study contributes to pathogenesis of malignant melanoma. In contrast to previous studies investigating the role of LKB1 farnesylation in the oocyte of *Drosophila* (Martin and St Johnston, 2003), we found farnesylation of LKB1 to be dispensable for the correct protein localization in the embryonic epidermis and NBs and for the function of LKB1 in *Drosophila* development. This observation is in line with previous findings from cultured mammalian cells and mice. In malignant melanoma cells, farnesylation-deficient LKB1 suppresses colony formation at similar degree as the wild-type kinase (Sapkota *et al.*, 2001). Furthermore, studies from knock-in mice show that mice homozygous for farnesylation deficient LKB1 are viable and do not exhibit any obvious phenotypes (Houde *et al.*, 2014). However, in these mice AMPK is less phosphorylated, whereas in cell culture experiments, no difference was found between wild-type and farnesylation deficient LKB1 (Denison *et al.*, 2009). Notably, several C-terminally truncated hLKB1 variants (due to nucleotide deletions or point mutations in STK11) with an intact kinase domain have been reported (Boudeau *et al.*, 2003d) and OMIM to be associated with Peutz-Jeghers syndrome, which might be due to the function of the C-terminal region in PA-mediated activation of LKB1. Apart from the association of LKB1 with STRADα/Mo25, membrane binding and PA-mediated activation of LKB1 is a newly described upstream mechanism, which controls LKB1 kinase activity and function *in vitro* and *in vivo*. The regulation of LKB1 function by membrane recruitment raises the question whether this depends primarily on membrane localization or whether lipid binding itself stimulates LKB1 activity. Several (phospho)-lipids have been demonstrated to activate or increase the activity of various serine/threonine kinases, including Phosphoinositide-dependent kinase 1 (PDK1, activated by PtdIns(3,4,5)P3) or PKCζ, Raf1, and mTOR (all activated by PA (Limatola *et al.*, 1994; Ghosh *et al.*, 1996; Fang *et al.*, 2001; Toschi *et al.*, 2009)). Fusion of GFP-LKB1$_{\Delta LB\ C564A}$ to lipid-binding domains (PH(PLCδ) and PH(Akt1))

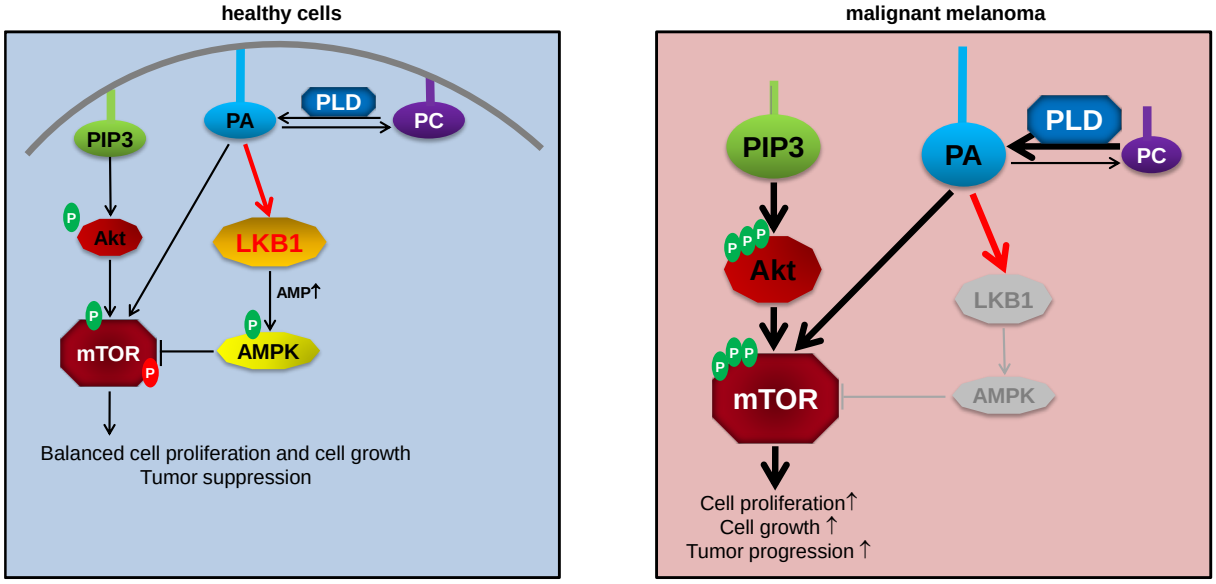

Fig. 2.7: Simplified model of LKB1 activation by PLD2-produced PA and its downstream effects on AMPK activation and mTOR inhibition. Under physiological conditions in non-tumourous cells, PA is produced by PLD (and other enzymes), resulting in an activation of mTOR and LKB1. Due to the inhibition of mTOR by LKB1-activated AMPK, the final result of increased PA level is a balanced cell proliferation and -growth. In contrast, in malignant melanoma, increased PI3K/Akt-signalling and enhanced production of PA by overexpression of PLD results in aberrant mTOR activation which is not counterbalanced by LKB1/AMPK and thus leads to increased cell proliferation and -growth and impaired tumour suppression.

resulted in a re-activation of GFP-LKB1$_{\Delta LB\ C564A}$ (Fig. 2.1O; Supplemental Fig. 2.4). Furthermore, the activity of LKB1$_{\Delta LB\ C564A}$ is strongly reduced in *in vitro* kinase assays (Fig. 2.3F,G). These findings could substantiate a hypothesis, in which the membrane functions as a scaffold for bringing together LKB1 and its cofactors (STRADα and Mo25) or its substrates. However, membrane binding deficient LKB1 robustly associates with its cofactors and one of its substrates (AMPK, Supplemental Fig. 2.3B). Moreover, addition of PA (but not of PtdIns(4,5)P2 or PtdIns(3,4,5)P3) is capable to substantially enhance the kinase activity of LKB1 *in vitro* (Fig. 2.3G; Supplemental Fig. 2.3C,D). Thus it is more likely, that in addition to membrane recruitment, PA functions to induce a conformational change of LKB1 thus enhancing its kinase activity. However we cannot exclude that in our *in vitro* kinase assays using immunoprecipitated proteins from transfected cells wild-type LKB1 might have co-immunoprecipitated with PA-enriched micelles, which enhanced its kinase activity in this experiment. Interestingly, PLD-produced PA activates both, LKB1 (this study) and mTOR (Fang *et al.*, 2001; Toschi *et al.*, 2009; Foster *et al.*, 2014; Yoon *et al.*, 2015). Up to now,

overexpression of PLD and increased levels of PA have been only assigned to pro-oncogenic pathways, in particular mTOR and Raf signalling (Ghosh *et al.*, 1996; Rizzo *et al.*, 1999; Zheng *et al.*, 2006; Shi *et al.*, 2007; Toschi *et al.*, 2009). Our data thus demonstrate the first anti-oncogenic mechanism of PLD function, which might counterbalance its pro-oncogenic effects as long as the LKB1-AMPK signalling axis is intact (Fig. 2.7). Notably, Mukhopadhyay *et al.* showed recently, that in a mesenchymal-like breast cancer cell line (MDA-MB-231), which expresses robust levels of endogenous LKB1 (in contrast to the majority of breast cancer metastases), activated PLD induces a reduction in phospho-AMPK (Mukhopadhyay *et al.*, 2015). Thus, PLD-mediated activation of LKB1 might be either cell type specific or depends on the basal activation of both signalling cascades, the LKB1-AMPK axis and the PI3K-AKT pathway.

The LKB1-AMPK signalling pathway is well described to play a crucial role for cell polarity, energy homeostasis and cell proliferation and is frequently disturbed in various types of cancer (Nakano and Takashima, 2012; Hardie and Alessi, 2013). As mentioned above, one particular function of AMPK is to counterbalance the pro-proliferative activity of mTOR (Arsham *et al.*, 2003; Kimura *et al.*, 2003; Inoki *et al.*, 2003b; Corradetti *et al.*, 2004; Shaw *et al.*, 2004a; Shaw *et al.*, 2005; Gwinn *et al.*, 2008; Shackelford *et al.*, 2009). Defects in the LKB1-AMPK signalling pathway (resulting in impaired inhibition of mTOR) have been already demonstrated to contribute to BRAF- and KRAS-induced melanoma formation in mouse models (Zheng *et al.*, 2009; Esteve-Puig *et al.*, 2009; Liu *et al.*, 2012b; Damsky *et al.*, 2015). Remarkably, somatic mutations in human STK11 (encoding LKB1) are rather rare in malignant melanoma (Rowan *et al.*, 1999; Guldberg *et al.*, 1999). However, our data demonstrate that downregulation of LKB1 protein expression can be observed in a majority of malignant melanoma samples and therefore most likely contributes to the pathogenesis of this type of skin cancer.

Our study provides strong evidences for an important and conserved regulatory mechanism, which facilitates membrane recruitment of LKB1 by PA and is essential for the kinase activity and function of LKB1 during development and tumour suppression. The dissection of upstream regulatory mechanisms of LKB1 contributes to a better understanding of the physiological regulation of LKB1 and their misregulation in tumours, which might be useful for the development of therapeutic approaches in the future.

Supplemental figures

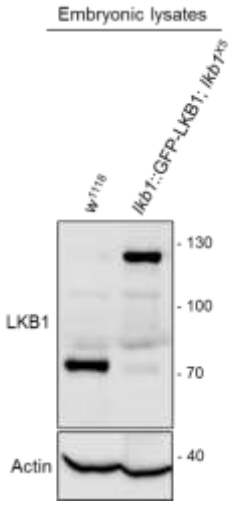

Supplemental Fig. 2.1: Expression of LKB1 by its endogenous promoter. Western blot analysis Immunoblotting of embryonic lysates from w1118 flies and homozygous mutants for lkb1X5, an lkb1 loss of function allele (Lee *et al.*, 2006), that express GFP-LKB1 from the endogenous lkb1 promoter shows comparable protein levels for endogenous and exogenous protein.

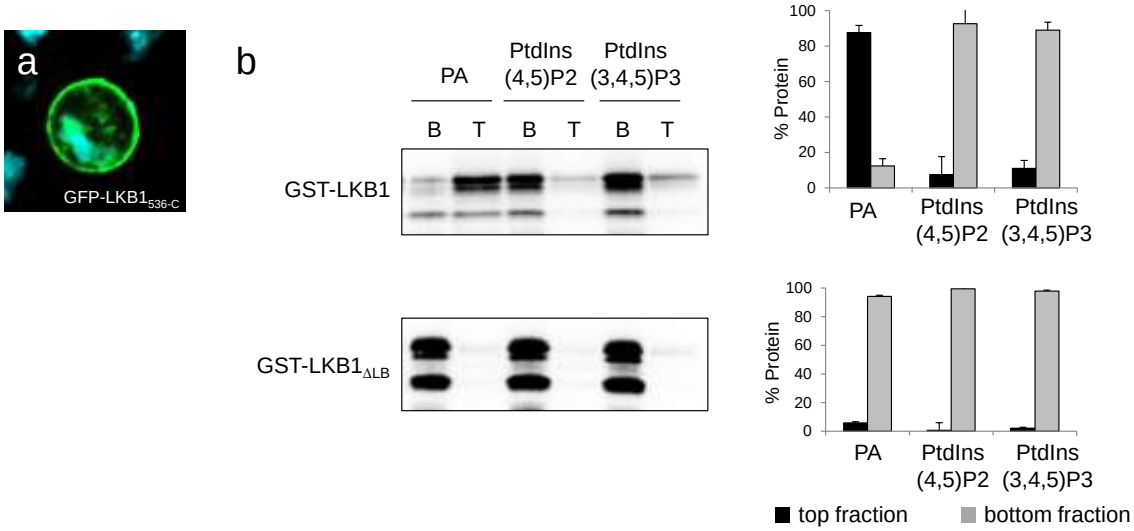

Supplemental Fig. 2.2: LKB1 binds to phosphatidic acid in liposome flotation assays. (a) GFP-LKB1 536-C localizes to the cell cortex of transfected S2R cells. (b) Recombinant GST-LKB1 or GST-LKB1 ΔLB was incubated with liposomes (see Methods section for further details), overlaid with a sucrose cushion and subjected to ultracentrifugation. Liposomes were harvested and loaded as top fraction (T), whereas unbound protein remained in the bottom fraction (B). n = 3, significance (wild type LKB1 versus LKB1 ΔLB): $p < 0.005$ for PA, n.s for PtdIns(4,5)P2 and $p < 0.05$ for PtdIns(3,4,5)P3.

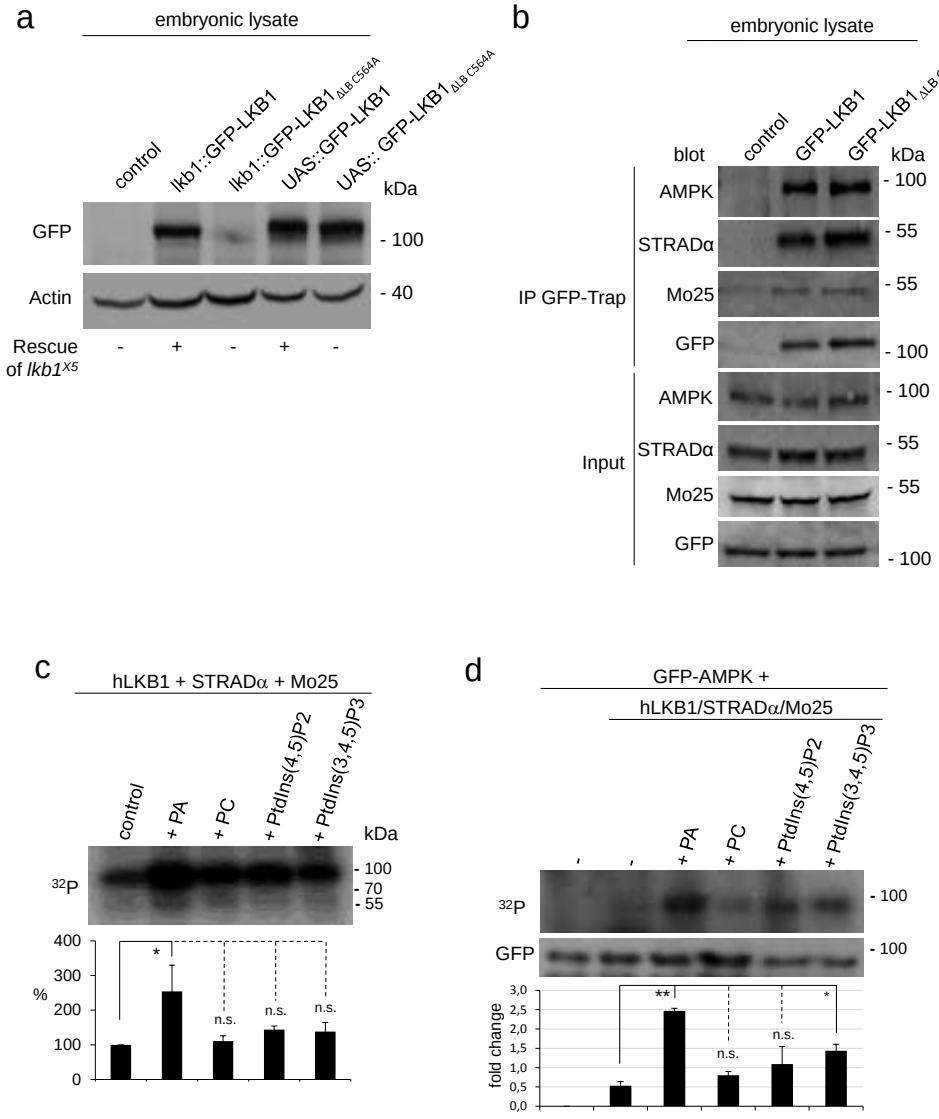

Supplemental Fig. 2.3: Lipid-binding of LKB1 is essential for its function. (a) Western Blotting of wild type or membrane binding deficient GFP-LKB1 expressed from its endogenous promoter (lkb1::GFP-LKB1) or ubiquitously expressed at endogenous levels using the UAS/GAL4 system (UAS::GFP-LKB1). Rescue capacity (viable flies: +) of these proteins in an lkb1x5-mutant background is indicated. (b) Coimmunoprecipitation of GFP-LKB1 or GFP-LKB1ΔLB C564A from embryonic lysates expressing GFP-LKB1 variants together with HA-tagged STRADα and myc-tagged Mo25. Embryos expressing only HA-STRADα and myc-Mo25 but no GFP-LKB1 served as a control. (c) Kinase activity of recombinant hLKB1/hSTRADα /hMo25 is strongly increased by addition of PC + PA, but only slightly by PC, PC + PtdIns(4,5)P2 or PC + PtdIns (3,4,5)P3. Lipids were prepared as liposomes as described in methods sections and applied in a 9:1 (PC:X) molar ratio. (d) *In vitro* kinase assays of GFP-AMPKα1 purified from transfected HeLa cells using recombinant LKB1/STRADα/Mo25 and indicated lipids. GFP-AMPK phosphorylation in the absence of LKB1 was not detectable. Phosphorylation of GFP-AMPK by LKB1in the absence of lipids

was set as 100%. Experiments were performed in triplicates. Error bars represent standard deviation and statistical significance was determined using ANOVA: $p < 0.0001$ ****, $p < 0.001$***, $p < 0.01$**, $p < 0.05$*, $p > 0.05$ not significant (n.s.).

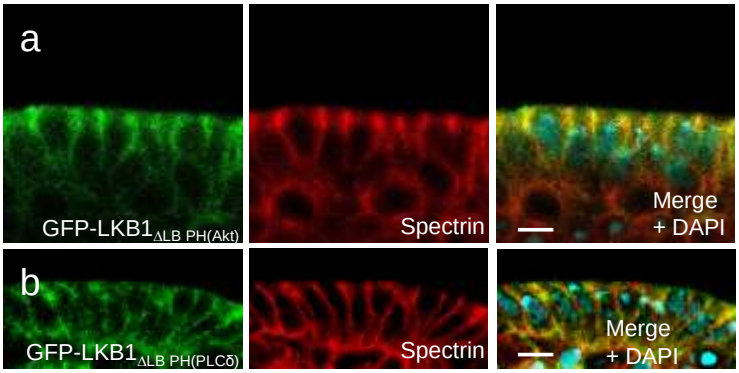

Supplemental Fig. 2.4: Localization of fusion proteins of GFP-LKB1ΔLB C564A with heterologous membrane-binding domains. (a and b) Immunostainings of embryos with GFP and α-spectrin reveal a substantial cortical localization of GFP-LKB1ΔLB C564A fused to the PH domain of Phospholipase C (PH(PLCδ), a) or to the PH domain of Akt1 (PH(Akt), b). Scale bars are 5µm.

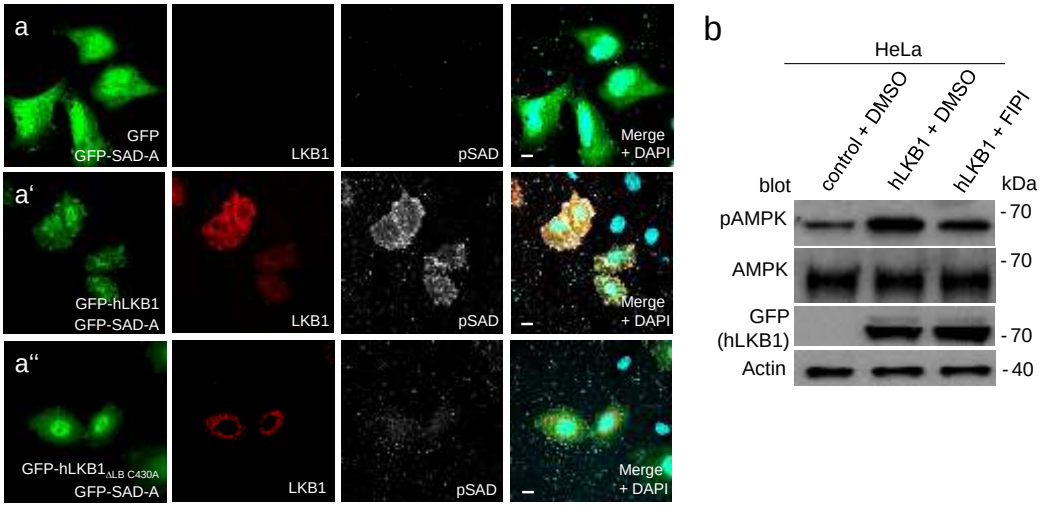

Supplemental Fig. 2.5: Activation of AMPK and AMPK-related kinases by LKB1. (a) HeLa cells were transfected with plasmids for GFP-SadA and GFP alone (a) or the indicated GFP-hLKB1 variants (a'-a'') and stained with antibodies specific for LKB1 (red) and activated Sad kinases (phosphorylated at S175 of SadA, pSAD, white). (b) Inhibition of PLD by 100nM 4-Fluoro-N-(2-(4-(5-fluoro-1H-indol-1-yl)piperidin-1-yl)ethyl)benzamide (FIPI) for 1h decreases the activation of AMPK by LKB1 in transfected HeLa cells. Scale bars are 5µm.

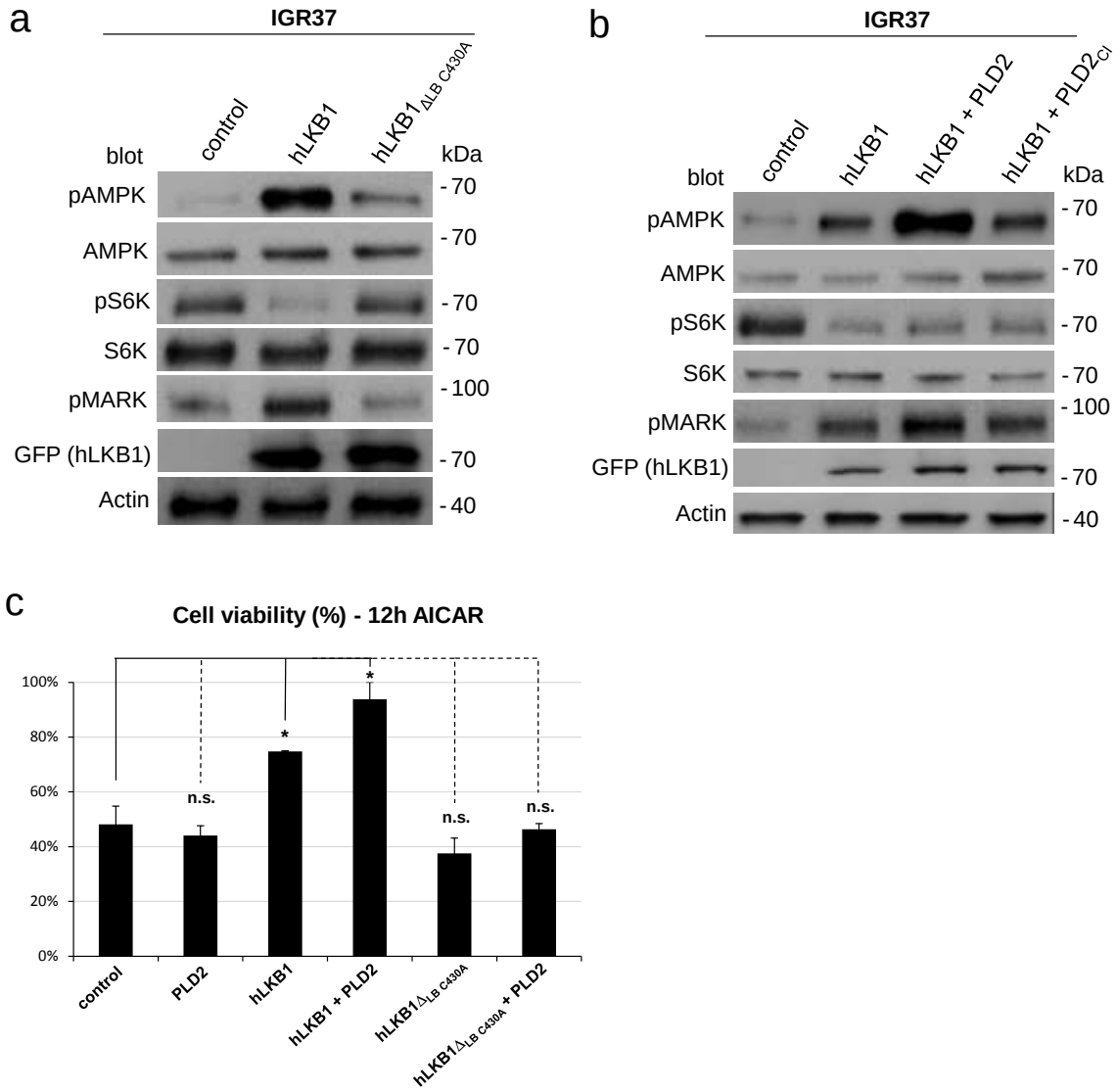

Supplemental Fig. 2.6: Activation of AMPK by LKB1 in malignant melanoma cells depends on membrane binding. (a and b) The activation of AMPK and MARK kinases by LKB1 in was analyzed by Western blot in IGR37 cells, which lack detectable LKB1 expression. Upon transfection of hLKB1, AMPK and MARK are activated, which is not seen in a membrane binding efficient LKB1 variant. This activation is further increased in the hLKB1+PLD2 double transfected cells (b). (c) Cell viability of IGR37 cells under energetic stress (induced by incubation with AICAR for 12h) was estimated using the MTT assay (as described in the methods section). Experiments were performed in triplicates. Error bars represent standard deviation and statistical significance was determined using ANOVA: $p < 0.0001$****, $p < 0.001$***, $p < 0.01$**, $p < 0.05$*, $p > 0.05$ not significant (n.s.).

Chapter 2: Upstream regulation of LKB1

Controlling the master – upstream regulation of the tumour suppressor LKB1

Authors: **Lars Kullmann** and Michael P. Krahn

Personal contributions: Wrote the manuscript and prepared the figures and table.

The tumour suppressor LKB1 is an essential serine/threonine kinase, which regulates various cellular processes such as cell metabolism, cell proliferation, cell polarity and cell migration. Germline mutations in the *lkb1* gene are the cause of the Peutz-Jeghers syndrome, which is characterized by benign polyps in the intestine and a higher risk for the patients to develop intestinal and extraintestinal tumours. Moreover, mutations and misregulation of LKB1 have been reported to occur in most types of tumours and are among the most common aberrations in lung cancer. LKB1 activates several downstream kinases of the AMPK family by direct phosphorylation in the T-loop. In particular the activation of AMPK upon energetic stress has been intensively analysed in various diseases, including cancer to induce a metabolic switch from anabolism towards catabolism to regulate energy homeostasis and cell survival.
In contrast, the regulation of LKB1 itself has long been only poorly understood. Only in the last years, several proteins and posttranslational modifications of LKB1 have been analysed to control its localization, activity and recognition of substrates. Here, we summarize the current knowledge about the upstream regulation of LKB1, which is important for the understanding of the pathogenesis of many types of tumours.

Introduction

The regulation of cell proliferation, energy metabolism, cell polarity and - migration are essential processes that have to be strictly controlled. The Liver Kinase B1 (LKB1, encoded by *STK11*) is a highly conserved serine/threonine kinase that functions as a tumour suppressor. Germline mutations in *STK11* cause the Peutz-Jeghers syndrome (PJS), an autosomal dominant disorder, which is characterized by cutaneous mispigmentations, benign gastrointestinal polyps and a high risk for the patients to develop tumours (Hemminki *et al.*, 1998; Mehenni *et al.*, 1998; Jansen *et al.*, 2009). The risk of PJS patients to develop cancer is highest in the gastrointestinal tract, however female patients bear also an increased risk to develop breast cancer (Hearle *et al.*, 2006). Somatic mutations or loss of LKB1 are also found in several other types of cancer, such as non-small cell lung cancer (NSCLC), cervical cancer, ovarian cancer, breast cancer, pancreatic cancer and malignant melanoma (Rowan *et al.*, 1999; Guldberg *et al.*, 1999; Sanchez-Cespedes *et al.*, 2002; Carretero *et al.*, 2004; Matsumoto *et al.*, 2007; Wingo *et al.*, 2009; Morton *et al.*, 2010; Gill *et al.*, 2011; Tanwar *et al.*, 2014; George *et al.*, 2016; Dogliotti *et al.*, 2017). Only in the pathogenesis of salivary gland tumours, LKB1 seems to play no role (Cidlinsky *et al.*, 2016). In NSCLC, genetic alterations of the *STK11* gene are among the most common mutations in these tumours. Moreover, loss of LKB1 is associated with a poor survival rate of breast cancer patients (Shen *et al.*, 2002; Sengupta *et al.*, 2017).

LKB1 forms a ternary complex with the pseudokinase STRADα and the scaffolding protein MO25, which promote nuclear export of the complex and enhance the kinase activity of LKB1. Together with the AMP-activated protein kinase (AMPK) LKB1 acts as a cellular energy sensor. Under energy deprivation LKB1 phosphorylates AMPK to inhibit mTORC1, Acety-CoA carboxylase and HMG-CoA-Reductase, thus inhibiting anabolic processes (Woods *et al.*, 2003). Additionally, LKB1 phosphorylates 12 AMPK related kinases in their activation loop: SAD-A/B (BRSK2 and BRSK1), NUAK1/2 (ARK5 and SNARK), SIK1/2/3, MARK1/2/3/4 and SNRK (Lizcano *et al.*, 2004; Jaleel *et al.*, 2005). Given that LKB1 regulates such a broad number of other kinases it could be considered as a “master kinase”. Beyond the role of LKB1 in metabolism and cell proliferation it is involved in the establishment of cell polarity by activating MARKs, which in turn regulate the formation of the Par complex (Benton and St Johnston, 2003a; Lizcano *et al.*, 2004; Granot *et al.*, 2009; Amin *et al.*, 2009). In *Drosophila*, LKB1 has been described to regulate cell polarity by activation of AMPK, which in turn indirectly enhances the phosphorylation non-muscle

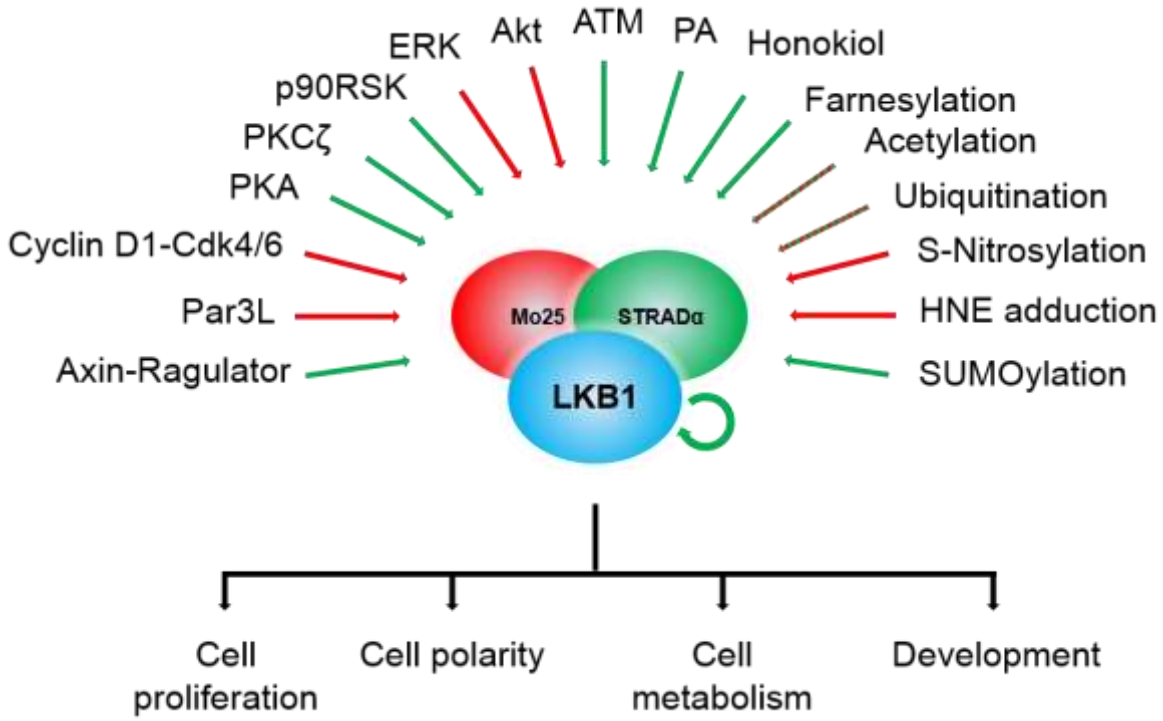

Figure 3.1: Schematic summary of upstream regulatory factors affecting LKB1 function in its four core functions. Red arrows represent inhibitory functions whereas green arrows indicate an activation of LKB1.

myosin regulatory light chain (Lee *et al.*, 2007; Bultot *et al.*, 2009). Furthermore, by activating SAD-A/B and NUAK1 in neurons LKB1 regulates axon determination (Barnes *et al.*, 2007; Courchet *et al.*, 2013).

Although at lot is known about the downstream functions of LKB1, the upstream mechanisms, which regulate the localization and function of this master kinase have long been less well characterized. Only over the recent years, several interaction partners and posttranslational modifications have been reported to regulate localization and function of LKB1, which will be summarised in this review.

Non-covalent regulation by interaction partners

The LKB1-STRADα-Mo25 complex

LKB1 can either localize in the nucleus or in the cytoplasm. The N-terminal nuclear localization sequence (NLS) of LKB1 is recognized by Importin-α, which mediates the nuclear translocation (Smith *et al.*, 1999a; Dorfman and Macara, 2008). Binding to the

pseudokinase STRADα (STe20 Related ADaptor) and the scaffolding protein MO25 (mouse protein 25) enhances nuclear export (Boudeau *et al.*, 2003a; Baas *et al.*, 2003; Dorfman and Macara, 2008). STRADα translocates LKB1 into the cytoplasm by binding to the export factors CRM1 or Exportin7 and maintains LKB1 in the cytoplasm by outcompeting Importin-α for binding to the NLS of LKB1 (Dorfman and Macara, 2008). Moreover, STRADα and MO25 drastically enhance the kinase activity of LKB1 (~9 fold) (Boudeau *et al.*, 2003a). In line with these results, the LKB1 mutant SL26 in PJS, which was lacks the amino acids 303 – 306 cannot bind to STRADα and accumulates in the nucleus, which probably mediates its pathogenicity as the SL26 mutant is still catalytically active (Nezu *et al.*, 1999; Baas *et al.*, 2003; Boudeau *et al.*, 2004). The crystal structure of the LKB1/-STRADα-MO25 complex provides further insights into the formation of the active complex (Zeqiraj *et al.*, 2009): STRADα binds LKB1 as a pseudosubstrate and mediates its conversion in an active conformation, whereas Mo25 is required to stabilize the active conformation of the LKB1 activation loop (Zeqiraj *et al.*, 2009). However, no structural data are available for the N- and C-terminus of LKB1, as in this study, only the kinase domain of LKB1 (aa 43 – 347) and the pseudokinase domain of STRADα (aa 59 – 431) have been analysed. This might be of particular interest, as the C-terminus contains several important phosphorylation sites as well as a farnesylation motif and a lipid-binding domain (Collins *et al.*, 2000; Sapkota *et al.*, 2001; Sapkota *et al.*, 2002a; Sapkota *et al.*, 2002b; Baas *et al.*, 2003; Xie *et al.*, 2006; Bai *et al.*, 2012; Dogliotti *et al.*, 2017).

The scaffolding protein AXIN

One of the major targets of LKB1 in order to regulate metabolism and proliferation under energetic stress is AMPK. AMPK is sensitized for an increase in the AMP/ATP ratio: A single AMP molecule binds to the γ-subunit of the heterotrimeric AMPK, which enhances the affinity to a second AMP molecule. Upon AMP binding the catalytic domain in the α-subunit becomes exposed, which is then phosphorylated and activated at a conserved residue (T172) within the activation loop (T-loop) by LKB1. The activated kinase in turn phosphorylates Tuberin (TSC2) and Raptor to antagonize mTORC1 and thereby blocks the energy consuming protein synthesis.

Recent studies demonstrated a more complex mechanisms of the LKB1 dependent regulation of AMPK (Zhang *et al.*, 2013b; Zhang *et al.*, 2014). In hepatocytes, AXIN functions as a scaffold by binding directly to LKB1 and AMPK and promotes the phosphorylation of AMPK in an AMP dependent manner. Consequently, knock down of *AXIN* in mice causes an

enhanced fatty liver as a result of insufficient AMPK activation (Zhang *et al.*, 2013b). Furthermore, in mouse embryonic fibroblasts the AXIN-LKB1-AMPK complex is recruited to the late endosome and forms a complex with the v-ATPase-Ragulator complex (Zhang *et al.*, 2014). This complex formation is essential for the activation of AMPK by LKB1, because the tissue specific knock out of *LAMTOR1* (a component of the Ragulator complex) eliminates AMPK activation (Zhang *et al.*, 2014).

Interestingly, in addition to the well-known energy sensor AMPK, which is activated by AMP, a novel AMP-independent mechanism has been described: Upon energetic stress the concentration of fructose-1,6-bisphosphate (FBP) decreases and unoccupied Aldolase, which splits FBP into dihydroxyacetone phosphate (DHAP) and glyceraldehyde 3-phosphate (G3P), promotes the formation of the v-ATPase-Ragulator-AXIN-LKB1-AMPK complex to activate AMPK (Zhang *et al.*, 2017a).

It still remains to be investigated whether AXIN is a general activator of LKB1's function or whether it regulates specifically the substrate recognition and phosphorylation of AMPK. Interestingly, AXIN is well known as a core component of the β-catenin destruction complex, functioning as being an important regulator of the Wnt pathway, which is frequently targeted in tumour cells (Tortelote *et al.*, 2017). Thus, AXIN might be a converging point, integrating LKB1/AMPK- and Wnt signalling.

Membrane localization of LKB1

In *Drosophila* and mammalian epithelial cells and fly neural stem cells, LKB1 is localized to the (lateral) plasma membrane, which is mediated by an C-terminal lipid binding domain and a farnesylation motif (C430) (Collins *et al.*, 2000; Sapkota *et al.*, 2001; Sebbagh *et al.*, 2009; Dogliotti *et al.*, 2017). Via its lipid binding motif, which is composed of several positively charged amino acids (lysines and arginines), human and *Drosophila* LKB1 bind to phosphatidic acid, which enhances its kinase activity and activation of downstream kinases (at least AMPK, MARKs and SAD kinases) (Dogliotti *et al.*, 2017). The membrane association of LKB1 is essential *in vivo* to ensure protein stability and to promote polarization of the *Drosophila* oocyte as well as survival and development of the fly. Furthermore, activation of AMPK in human cervical carcinoma (HeLa) and melanoma (IGR37) cells depends on membrane-binding of LKB1 (Dogliotti *et al.*, 2017). The role of LKB1 farnesylation will be discussed later in this review. In polarized MDCK cells, E-Cadherin (E-Cad) contributes to the membrane localization of LKB1 and promotes the phosphorylation of AMPK (Sebbagh *et*

al., 2009). However, this regulation seems to be rather indirect and does more likely depend on the overall integrity of the apical-basal cell polarity (Sebbagh *et al.*, 2009).

Par3L

The asymmetric cell division is a key feature of stem cells, where one daughter cell maintains its stem cell identity and the other one differentiates. In mouse mammary stem cells, the protein Par3-like (Par3L), but not Par3 itself, binds to LKB1 and inhibits its ability to activate AMPK (Huo and Macara, 2014). Loss of Par3L causes a decrease of mouse mammary stem cells, suggesting a role for LKB1 in stem cell maintenance, which has been also reported for human embryonic stem cells and haematopoietic stem cells (Nakada *et al.*, 2010; Gurumurthy *et al.*, 2010; Gan *et al.*, 2010; Lai *et al.*, 2012). In differentiated cells (Caco-2 human colon carcinoma cells), knockout of Par3L enhances the activation of AMPK, reduces cell proliferation and enhances cell death (Li *et al.*, 2017).

Honokiol

Beside the cell intrinsic mechanisms to activate LKB1 several recently published studies report that the polyphenol Honokiol (HNK) from *Magnolia grandiflora* efficiently activates the LKB1-AMPK axis (Nagalingam *et al.*, 2012; Seo *et al.*, 2015; Avtanski *et al.*, 2015; Sengupta *et al.*, 2017). Upon HNK treatment of breast cancer cells, the expression of LKB1 is enhanced by an unknown mechanism (Nagalingam *et al.*, 2012; Avtanski *et al.*, 2015). Moreover, the expression of the deacetylases SIRT1 and SIRT3 increases, which deacetylate LKB1 to promote its cytoplasmic localization and activation (acetylation of LKB1 will be discussed later) (Avtanski *et al.*, 2015). Enhanced expression and activity of LKB1 results in increased expression of the micro RNA miR-34a, which in turn inhibits the expression of epithelial-mesenchymal transition (EMT) markers, such as Zeb1 and Slug. Thus, the HNK dependent upregulation of LKB1 in breast cancer cells inhibits EMT and reduces their migratory capacity (Avtanski *et al.*, 2015). In addition to the inhibition of EMT, HNK treated breast cancer cell display a reduced expression of the stemness transcription factors Nanog, Oct4 and Sox2 (Avtanski *et al.*, 2015; Sengupta *et al.*, 2017), which is most likely mediated by a decreased phosphorylation of Stat3 upon HNK treatment. Finally, in a xenograft mouse model HNK treatment inhibits breast tumour growth depending on LKB1 (Nagalingam *et al.*, 2012; Sengupta *et al.*, 2017). Taken together, the HNK mediated activation of LKB1 might become a promising treatment for breast cancer patients in the future. However, on the

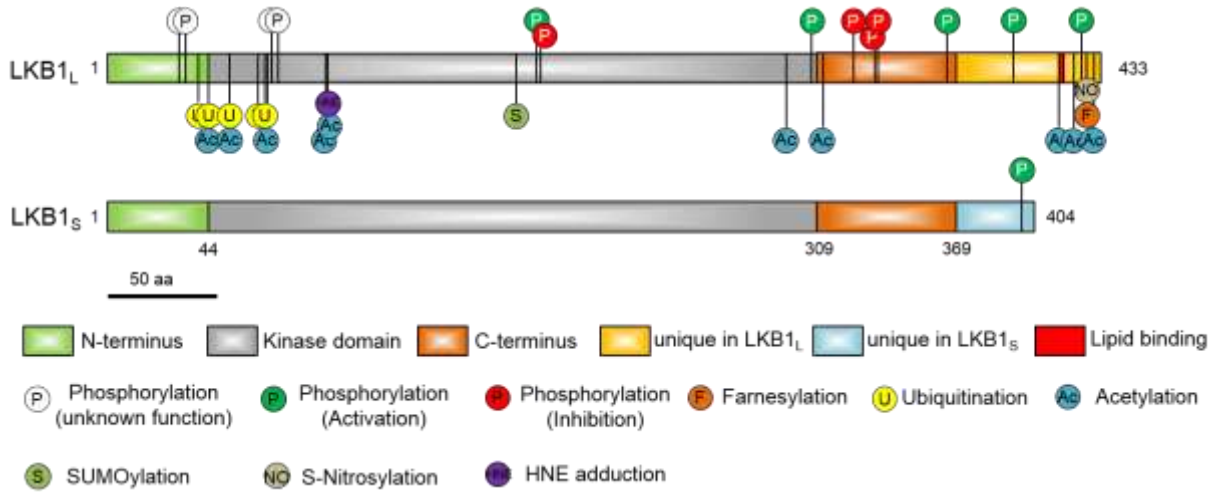

Figure 3.1: Schematic summary of posttranslational modifications of human LKB1

Posttranslational protein modifications

molecular basis, several important questions regarding the underlying mechanism are still unclear.

Posttranslational protein modifications

Phosphorylation

Phosphorylation is the most common posttranslational modification and can either affect the conformation of the phosphorylated protein or create a novel interaction surface for other proteins. At least ten residues of LKB1 have been reported to be phosphorylated (Table 1), whereof some are autophosphorylation sites (S31, T185, T189, T336 and T402) and others residues are phosphorylated by other kinases (S307, S325, S334, T366, S399 and S428) (Alessi *et al.*, 2006; Xie *et al.*, 2009; Liu *et al.*, 2012a; Zhu *et al.*, 2013). However, not all phosphorylation events affect the (kinase) function of LKB1: None of the phospho-deficient or phospho-mimetic mutants of S31, S325, T336 and T366 displayed a significant change in their catalytic activity *in vitro* (Sapkota *et al.*, 2002a). By contrast, the phospho-mimetic LKB1 T336E mutant prevented LKB1 from suppressing growth of a human malignant melanoma cell line, suggesting an autoinhibitory function of this autophosphorylation site (Sapkota *et al.*, 2002a). Phosphorylated T336 is bound by 14-3-3ζ, which interferes with the LKB1-AMPKα interaction (Bai *et al.*, 2012). With respect to the autophosphorylation of T189 contradictory functions have been reported. Either this residue is not phosphorylated at all or autophosphorylation of T189 negatively regulates LKB1 activity in a human fibrosarcoma *cell* line (Karuman *et al.*, 2001b; Sapkota *et al.*, 2002a).

In addition to its autophosphorylation, LKB1 is phosphorylated by PKCζ (Xie *et al.*, 2006; Xie *et al.*, 2008; Xie *et al.*, 2009). Activation of PKCζ by either peroxynitrite or metformin in endothelial cells induces the phosphorylation of LKB1 at S428, which enhances the nuclear export of LKB1 to mediate its association with AMPK in order to activate it (Xie *et al.*, 2006; Xie *et al.*, 2008). In addition to the activation of AMPK in response to S428 phosphorylation, LKB1 phosphorylates and activates the lipid phosphatase PTEN to inhibit Akt signaling (Song *et al.*, 2008). Moreover, PKCζ phosphorylates LKB1 at S307 (Xie *et al.*, 2009). This phosphorylation is also important to enhance the nucleo-cytoplasmic shuttling of LKB1 in peroxynitrite stimulated cells to activate AMPK. Loss of the phosphorylation sites S307 and S428 attenuates the association of LKB1 with STRADα and the export factor CRM1 and thus decreases the cytoplasmic accumulation of LKB1 in an adenocarcinoma cell line (Xie *et al.*, 2009). Consequentially, the phosphorylation-deficient LKB1 S307A mutant has a reduced capacity to suppress angiogenesis and cannot efficiently protect cells from apoptosis (Xie *et al.*, 2009).

Apart from PKCζ, S428 is also a phosphorylation site for p90 ribosomal S6 kinase (p90-RSK) and cAMP-dependent protein kinase (PKA) (Collins *et al.*, 2000; Sapkota *et al.*, 2001; Martin and St Johnston, 2003). The p90-RSK mediated phosphorylation of S428 depends on ERK stimulation, whereas PKA phosphorylates S428 in response to adenylyl cyclase activation (Sapkota *et al.*, 2001). In melanoma cells, phosphorylation of S428 is essential to suppress cell growth and does not affect the farnesylation at C433 (Sapkota *et al.*, 2001). The PKCζ/PKA/p90-RSK mediated phosphorylation of LKB1 at S428 is crucial for axon differentiation: Only wild type LKB1, but not the S428A mutant, is capable of phosphorylating SAD-A/B in order to promote axon differentiation (Barnes *et al.*, 2007; Shelly *et al.*, 2007). Furthermore, phosphorylation of LKB1 S428 by PKA is essential for LKB1 localization and the myelination of Schwann cells (Shen *et al.*, 2014). Notably, other studies reports that S428 phosphorylation of LKB1 is not essential to suppress cell growth of melanoma cells and to activate AMPK and SAD-A/B *in vitro* and *in vivo* (Bright *et al.*, 2008; Fogarty and Hardie, 2009; Houde *et al.*, 2014).

The pleiotropy of studies with partly contradicting results indicates that LKB1 S428 phosphorylation might be cell-type specific (maybe even compartment specific) and probably depends on the cellular context regarding cell proliferation, cell cycle, migration and metabolism.

In mammals, two splice variants of LKB1 are expressed: $LKB1_L$ (long) and $LKB1_S$ (short), which are both widely expressed (Towler *et al.*, 2008; Denison *et al.*, 2009). The two protein

variants differ only in their last 63 amino acids, hence, $LKB1_S$ lacks the critical residues S428 and C430. $LKB1_S$ is essential for spermatogenesis, since male *lkb1*$_S$ null mice are sterile (Towler *et al.*, 2008). However, despite the lack of S428 in $LKB1_S$ it is still phosphorylated by PKCζ at its C-terminus at S399, which is unique in $LKB1_S$ (Zhu *et al.*, 2013). Phosphorylation of S399 in $LKB1_S$ promotes its nuclear export followed by the activation of AMPK and is therefore thought to be the functional equivalent to S428 in $LKB1_L$ (Zhu *et al.*, 2013).

Another phosphorylation site in LKB1 is S325 (Sapkota *et al.*, 2002a). Subsequent studies managed to identify ERK and Cyclin D1-Cdk4/6 as the responsible kinases for the phosphorylation of LKB1 at this residue (Zheng *et al.*, 2009; Casimiro *et al.*, 2017). In melanoma cells, which express the oncogenic B-Raf^{V600E} variant, constitutively active ERK phosphorylates LKB1 at this residue. This phosphorylation decreases the affinity of LKB1 to AMPK and consequently leads to a reduction of AMPK activation. The authors confirmed their cell culture data in tissue samples of human melanoma, where the phosphorylation and activation of ERK associates with inactive AMPK (Zheng *et al.*, 2009). In addition to ERK, LKB1 is also phosphorylated at S325 by Cyclin D1-Cdk4/6 (Casimiro *et al.*, 2017). Like phosphorylation by ERK, Cyclin D1-Cdk4/6 mediated LKB1 S325 phosphorylation also suppresses AMPK activation and the stress-induced activation of AMPK is enhanced in *cyclin D1*$^{-/-}$ cells. Likewise, in mammary gland tissue of conditional *cyclin D1*$^{-/-}$ mice, the phosphorylation of AMPK and the level of autophagy are enhanced. (Casimiro *et al.*, 2017)
A previous study reported that mutations of S325 to alanine or glutamic acid did not affect the catalytic activity of LKB1 (Sapkota *et al.*, 2002a). However, this inhibitory modification of LKB1 affects its substrate recognition rather than its kinase activity (Zheng *et al.*, 2009). In the context of tumour progression the misregulation of B-Raf and Cyclin D1 is a common variation (Bartkova *et al.*, 1994; Davies *et al.*, 2002). Hence, affected tumours antagonize the tumour suppressor function of the LKB1-AMPK axis, which enhances their malignancy.

The kinases Akt and LKB1 display antagonistic functions to control cell proliferation: Akt activates mTOR signalling, whereas LKB1 inhibits it via AMPK activation (Inoki *et al.*, 2003b; Shaw *et al.*, 2004a). However, Akt act as an upstream regulator of LKB1, as it directly phosphorylates S334 of LKB1. Upon phosphorylation, 14-3-3 binds to LKB1 and antagonizes the interaction with STARDα. Consequentially, LKB1 is sequestered in the nucleus as fails to inhibit cell proliferation (Liu *et al.*, 2012a).

Table 3.1: Summary of described posttranslational modifications.

PTM	Residue	Enzyme	Function	Reference
Phosphorylation	S31	unknown	unknown	*Sakopta et al., 2002*
	T32	unknown	unknown	*Liu et al., 2012*
	S69	unknown	unknown	*Liu et al., 2012*
	T71	unknown	unknown	*Liu et al., 2012*
	T185	LKB1	Activation	*Baas et al., 2003*
	T192 (Xenopus) T189 (mammals)	LKB1	Inhibition	*Su et al., 1996 Karuman et al., 2001*
	S307	PKCζ	Association with STRADα and cytoplasmic translocation	*Xie et al., 2009*
	S325	ERK, Cyclin D1-Cdk4/6	Suppression of LKB1-AMPK interaction	*Sakopta et al., 2002 Zheng et al., 2009 Casimiro et al., 2017*
	S334	Akt	14-3-3 binding, nuclear retention and inhibition	*Liu et al., 2012*
	T336	LKB1	14-3-3 ζ binding, inhibition of AMPK phosphorylation	*Sakopta et al., 2002 Bai et al., 2012*
	T366	ATM	Activation in response to ionizing radiation	*Sakopta et al., 2002*
	S399	PKCζ	Nuclear export and activation, only in LKB1s	*Zhu et al., 2013*
	T402	LKB1	Activation	*Baas et al., 2003*
	S428 (human) S431 (mouse) S562 *(Drosophila*)	p90 RSK, PKA and PKCζ	Activation	*Sakopta et al., 2001 Martin and St Johnston, 2003 Xie et al., 2006*
Ubiquitination	K41, K44, K48, K62, K63	Skp2-SCF	Activation, promotes the interaction with Mo25	*Lee et al., 2015*
	unknown	CHIP	Degradation	*Gaude et al., 2012*
	unknown	HERC2	Degradation upon recruitment by SIRT1	*Bai et al. 2016*

PTM	Residue	Enzyme	Function	Reference
SUMOylation	K178	unknown	Promotes the interaction with AMPK under energetic stress	*Ritho et al., 2015*
Neddylation	unknown	unknown	Stabilization of LKB1	*Barbier-Torres et al., 2015*
Farnesylation	C430	unknown	Membrane localization	*Collins et al., 2000* *Sapkota et al., 2001*
Acetylation	K44	unknown	unknown	*Lan et al., 2008*
	K48	unknown	SIRT1 deacetylates LKB1 to promote its cytoplasmic localization and binding to STRADα	*Lan et al., 2008*
	K64	unknown	SIRT1 recruits HERC2 to acetylated K64 to promote the proteasomal degradation of LKB1 in endothelial cells	*Bai et al., 2016*
	K96	unknown	unknown	*Lan et al., 2008*
	K97	unknown	unknown	*Lan et al., 2008*
	K296	unknown	unknown	*Lan et al., 2008*
	K311	unknown	unknown	*Lan et al., 2008*
	K416	unknown	unknown	*Lan et al., 2008*
	K423	unknown	unknown	*Lan et al., 2008*
	K431	unknown	unknown	*Lan et al., 2008*
***S*-Nitrosylation**	C430	none	Promotes LKB1 degradation	*Liu et al., 2015*
HNE adduktion	K97	none	Inhibition	*Dolinsky et al., 2009* *Calamaras et al., 2012*

Beside the role of LKB1 at the membrane, LKB1 might have an additional function in the nucleus: In response to ionizing radiation LKB1 becomes phosphorylated at T366 by the protein kinase ataxia-telangiectasia mutated (ATM), which is known for its function in DNA damage response (Sapkota *et al.*, 2002b). Another study investigating the ATM mediated phosphorylation of LKB1 T366 finds that ATM activates LKB1 in the cytoplasm upon treatment with reactive oxygen species (Alexander *et al.*, 2010). Subsequently, mTORC1 is inhibited by the ATM-LKB1-AMPK axis, inducing autophagy (Alexander *et al.*, 2010).

Ubiquitination

The ubiquitination of proteins is a posttranslational modification that is involved in many different cellular processes in addition to its well-known function during protein degradation. LKB1 associates with the chaperon heat-shock protein 90 (Hsp90) and the co-chaperon Cdc37, which is essential to stabilize LKB1 by protecting it from ubiquitin dependent degradation (Nony *et al.*, 2003; Boudeau *et al.*, 2003b). Hsp90 binds to the kinase domain of LKB1 and pharmacological inhibition of Hsp90 causes an enhanced LKB1 degradation (Boudeau *et al.*, 2003b; Nony *et al.*, 2003). Moreover, the G163D mutation of LKB1, which has been found in a testicular tumour, has an impaired capacity to interact with Hsp90/Cdc37. Since LKB1 G163D still has some catalytic activity, the loss of the Hsp90/Cdc37 mediated stabilization might the reason of its pathogeny (Ylikorkala *et al.*, 1999; Nony *et al.*, 2003). The LKB1-Hsp90-Cdc37 complex does not include STRADα and in contrast to the LKB1-STRADα-Mo25 complex lacks a catalytic activity (Gaude *et al.*, 2012). The degradation of LKB1 upon Hsp90 inhibition depends on the binding of Hsp/Hsc70 to the C-terminus of LKB1. Hsp/Hsc70 then recruits the carboxyl terminus of Hsc70-interacting protein (CHIP), which is an E3-ubiquitin ligase that drives the degradation of LKB1. Thus, the two chaperone complexes Hsp90-Cdc37 and Hsp/Hsc70-CHIP regulate the stability of LKB1 (Gaude *et al.*, 2012).

Beyond protein degradation, ubiquitination can have the opposite effect on proteins. LKB1 is also polyubiquitinated by the Skp2-SCF ubiquitin ligase, which activates the LKB1-AMPK axis (Lee *et al.*, 2015a). The polyubiquitination of LKB1 takes place on five lysine residues (K41, K44, K48, K62 and K63) at the N-terminus of LKB1. Moreover, LKB1 is modified by a Lys-63-linked polyubiquitination, which has previously been described to activate other kinases (Yang *et al.*, 2010; Lee *et al.*, 2015a). Mechanistically, the polyubiquitination of LKB1 is crucial for the interaction with Mo25 and thus, for the integrity of the LKB1-STRADα-Mo25 complex. Surprisingly, oncogenic H-Ras promotes the polyubiquitination and activation of LKB1. In specimen of hepatocellular carcinoma both, LKB1 and Skp2 are upregulated and associate with a poor survival rate (Lee *et al.*, 2015a). Although LKB1 is classified as a tumour suppressor, its activation by Skp2 in response to oncogenic H-Ras suggest that it also exhibits pro-oncogenic potential. Furthermore, these data highlight again cell type specific functions of LKB1 and an ambivalent role in tumorigenesis, which should be explored in more detail in the future.

SUMOylation

The SUMOylation of proteins is a posttranslational modification that involves the covalent attachment of a SUMO (Small Ubiquitin-like Modifier) protein to a substrate. Similar to ubiquitination SUMOylation requires an activating enzyme (E1), a conjugating enzyme (E2) and a ligating enzyme (E3) (Geiss-Friedlander and Melchior, 2007).

Energetic stress promotes the SUMO1 modification of LKB1 on lysine 178 (Ritho *et al.*, 2015). Moreover, LKB1 seems to be SUMOylated at other lysine residues under normal conditions as well. The SUMO1 modification on K178 during energy deprivation promotes the interaction with AMPK and its activation, whereas LKB1 K178R fails to activate AMPK. AMPKα bears a SUMO-interacting motif (SIM), which promotes the association with LKB1 and mutating the SIM decreases this interaction and the activation of AMPK. Cells that express the LKB1 K178R mutant do not display an increased level of mitophagy under energetic stress, which would be essential for their fitness (Ritho *et al.*, 2015). Notably, only a marginal proportion of LKB1 protein seems to be SUMOylated, suggesting that only a small pool of the kinase might be capable of AMPK activation. Future studies must address the questions about the role of LKB1 SUMOylation *in vivo* and whether the phosphorylation of other substrates, in particular members of the AMPK-family kinases depends on LKB1 SUMOylation, too.

Farnesylation

Farnesylation is a posttranslational modification of proteins that can mediate a transient membrane association. LKB1 is farnesylated at the C-terminus on the conserved cysteine 430. Nevertheless, the LKB1 localization is not restricted to the plasma membrane, but rather occurs in the nucleus and the cytoplasm as well, depending on the cell type and -status (Collins *et al.*, 2000; Sapkota *et al.*, 2001; Dogliotti *et al.*, 2017). A farnesylation-deficient LKB1 has been reported to disable its membrane localization (Collins *et al.*, 2000), however recent studies show that although the membrane localization is affected, a substantial amount of LKB1 still localizes at the plasma membrane (Houde *et al.*, 2014; Dogliotti *et al.*, 2017). The farnesylation of LKB1 has been reported to regulate the mesenchymal polarization and localizes LKB1 to the leading edge of motile cells (Konen *et al.*, 2016; Wilkinson *et al.*, 2017). Nonetheless, transgenic flies and mice that cannot be farnesylated at C433 (or C564 in *Drosophila*) are viable without obvious defects (Houde *et al.*, 2014; Dogliotti *et al.*, 2017). Similar, LKB1 C433A retained its ability to suppress cell growth (Sapkota *et al.*, 2001). In *Drosophila*, the farnesylation-deficient LKB1 C564A has a slightly decreased capacity to

rescue an *lkb1* null allele and in mice loss of the LKB1 farnesylation results in a decreased activation of AMPK (Houde *et al.*, 2014; Dogliotti *et al.*, 2017). Given that the loss of LKB1 farnesylation does not affect its catalytic activity (Sapkota *et al.*, 2001), LKB1 farnesylation is likely to be a fine tuning mechanism to target the kinase to the plasma membrane during specific cellular processes, such as cell migration or under non-physiological energetic stress.

Acetylation

LKB1 is strongly acetylated and at least ten lysine residues have been identified as potential modification sites (K44, 48, 64, 96, 97, 296, 311, 416, 423 and 431) (Lan *et al.*, 2008; Bai *et al.*, 2016). The protein deacetylase SIRT1 specifically deacetylates LKB1 on K48, which enhances the interaction with STRADα, LKB1's cytoplasmic localization and consequently the activation of AMPK (Lan *et al.*, 2008). In line with these results, the hepatic overexpression of SIRT1 leads to an elevated activation of AMPK (Hou *et al.*, 2008). Similar, SIRT1 is activated by the polyphenol Resveratrol, which in turn activates AMPK in mouse skeletal muscles through LKB1 deacetylation (Price *et al.*, 2012). In contrast to the LKB1 promoting function of SIRT1 in the liver, in endothelial cells, SIRT1 targets LKB1 for proteasomal degradation. The endothelial degradation of LKB1 promotes proliferation and inhibits endothelial senescence (Zu *et al.*, 2010). The SIRT1 mediated degradation does not depend on its deacetylase activity, but rather requires a scaffolding function. SIRT1 binds to acetylated K64 and subsequently recruits the E3-ubiquitin ligase HERC2. HERC2 then ubiquitinates LKB1 in the nucleus to downregulate the amount of acetylated LKB1 (Bai *et al.*, 2016).

Neddylation

Neddylation is a posttranslational modification that relies on the attachment of NEDD8 to target proteins. Analogous to ubiquitination and SUMOylation, neddylation requires E1, E2 and E3 enzymes. The level of neddylation is enhanced in hepatocellular carcinoma (HCC) and LKB1 is a neddylation target. The stability of LKB1 seems to depend on its neddylation, because upon the pharmacologic inhibition of NEDD8-activating enzymes the amount of LKB1 decreases in HCC. Furthermore, the decrease of LKB1 promotes the metabolic switch from oxidative phosphorylation towards glycolysis. Inhibition of neddylation enhanced apoptosis in HCC, which is reversible by LKB1 overexpression (Barbier-Torres *et al.*, 2015). Taken together, the neddylation mediated stabilization of LKB1 seems to be disadvantageous in HCC.

S-Nitrosylation

S-Nitrosylation is a posttranslational protein modification, where nitric oxide (NO) is attached to a cysteine residue. In response to stimulation of macrophages with lipopolysaccharides (LPS) the inducible NO-synthase (iNOS) generates NO as an innate immune response (MacMicking *et al.*, 1995). However, a side effect of the increased NO synthesis might be the S-Nitrosylation of proteins. In LPS-challenged macrophages, LKB1 is S-Nitosylated on C430, which causes an enhanced degradation by the ubiquitin-proteasome system. Inhibition of iNOS after LSP challenge reduces the mortality of mice and enhances the LKB1 protein level (Liu *et al.*, 2015). Thus, the S-Nitrosylation of LKB1 in challenged macrophages seems to further challenge the cells.

HNE adduktion

Under oxidative stress the electrophilic aldehyde 4-Hydroxynonenal (HNE) is produced as a result of an enhanced lipid peroxidation. HNE can bind to proteins and diminish the catalytic activity of enzymes and an increase of HNE is found in patients with cardiomyopathy (Schaur, 2003; Mali and Palaniyandi, 2014). In cardiomyocytes, LKB1 is affected by a HNE modification (Dolinsky *et al.*, 2009; Calamaras *et al.*, 2012, 2015). The HNE adduction takes place on K97 and HNE-modified LKB1 is inactive and fails to activate AMPK, resulting in an elevated mTORC1 activity and consequently an enhanced protein synthesis (Dolinsky *et al.*, 2009; Calamaras *et al.*, 2012, 2015). Activation of the LKB1-AMPK axis with Resveratrol reduces the HNE modification of LKB1 and reverses the mTORC1 activation. Furthermore, in a mouse model for hypertension and left ventricular hypertrophy Resveratrol treated animals have a reduced cardiac hypertrophy (Dolinsky *et al.*, 2009). Thus, an elevated production of HNE in cardiomyocytes promotes the progression of cardiomyopathies by inhibiting LKB1, which results in an enhanced mTORC1 dependent anabolism.

Concluding remarks

An increasing number of publications demonstrate that the master kinase LKB1 is regulated by various inputs – binding partners and targeting to subcellular compartments as well as posttranslational modifications. However, not for all of them an *in vivo* relevance is not yet clear. Besides its known deletion/mutation and downregulation of transcription, regulation of the protein stability by posttranslational modifications and/or interaction partners has emerged as an important mechanism to reduce active LKB1 levels, which certainly contributes to the

pathogenesis of tumours and might be a promising approach for the development of cancer therapies.

Although LKB1 is capable of phosphorylating and thereby activating several kinases (mostly of the AMPK-family), most studies focus on AMPK as this is supposed to be a key enzyme in metabolism and tumour suppression. However, whether other LKB1 substrates are affected by the upstream regulatory mechanisms or whether it establishes a substrate specificity of LKB1 often remains to be investigated in the future. Furthermore, a possible interplay between the distinct posttranslational modifications and between these and described interaction partners is still poorly understood and might contribute to the complexity of LKB1's regulation.

Chapter 3: Oligomerization and lipid-binding stabilize Bazooka

Oligomerization and lipid-binding of Bazooka function redundantly to promote protein stability and ensure epithelial polarization in *Drosophila*

Authors: **Lars Kullmann** and Michael P. Krahn

Personal contributions: Performed all experiments, data analysis, discussion of results and writing most of the manuscript.

Apical-basal polarity is an important characteristic of epithelia and *Drosophila* neural stem cells. The conserved Par-complex, which consists of the atypical protein kinase C and the scaffold proteins Baz and Par6, is a key player in the establishment of apical-basal cell polarity. Membrane recruitment of Baz has been described to be accomplished by several mechanisms, which might function in redundancy, to ensure the correct localization of the complex. Here, we dissected the role of the oligomerization domain and the lipid-binding motif of Baz *in vivo* in the *Drosophila* embryo. We found that these domains function in redundancy to promote the apical junctional localization of Baz. However, inactivation of only one domain is not sufficient to disrupt the function of Baz during apical-basal polarization of epithelial cells and neural stem cells. Moreover, oligomerization stabilizes Baz by protecting it from degradation. Notably, we found that the mutation of both domains results in a strongly impaired protein stability and a phenotype characterized by embryonic lethality and an impaired apical-basal polarity in the embryonic epithelium and neural stem cells, resembling a *baz*-loss of function allele. Strikingly, the binding of Baz to the transmembrane proteins E-Cadherin, Echinoid and Starry Night was not affected in this mutant protein. Our findings reveal a redundant function of the oligomerization and the lipid-binding domain, which is required for protein stability, correct subcellular localization and apical-basal cell polarization.

Introduction

Apical-basal polarity is a hallmark of epithelial tissues and is essential during development and tissue homeostasis. In monolayered epithelial cells, the apical plasma membrane domain faces towards the outer environment or a lumen and the basal domain contacts the basement membrane. This polarity is achieved by the distinct position of conserved protein complexes along the apical-basal axis: The Crumbs complex (consisting of the transmembrane protein Crumbs and the adaptor proteins PATJ and Stardust) and the Par-complex determine the apical domain identity, whereas the Scribble-Lethal-Giant-Larvae and Discs large complexes counterbalance their activity at the basolateral domain (Goldstein and Macara, 2007; Pocha and Knust, 2013). Both apical junctional complexes, the Crumbs and the Par-complex overlap in the so called subapical region and at the adherens junctions (AJs) (Harris and Peifer, 2005; Krahn *et al.*, 2010a; Sen *et al.*, 2015; Koch *et al.*, 2016).

Bazooka (Baz), the *Drosophila* homolog of *C. elegans* and vertebrate Par3, is a scaffold protein and forms together with Par6 and aPKC the ternary Par complex (Wodarz *et al.*, 2000a; Petronczki and Knoblich, 2001; Suzuki and Ohno, 2006). Par3/Baz acts as an apical cue to establish the AJ by positioning *Drosophila* E-Cadherin (DE-Cad) and mediates the formation of the tight junctions in cultured mammalian cells (Hirose *et al.*, 2002; Harris and Peifer, 2004; Chen and Macara, 2005; Horikoshi *et al.*, 2009). Furthermore, Par3 acts as an exocyst receptor to regulate the delivery of membrane proteins (Lalli, 2009; Ahmed and Macara, 2017).

In addition, Baz is required to establish apical-basal polarity and correct spindle orientation of *Drosophila* neural stem cells (neuroblasts, NBs), which is essential for their asymmetric cell division (Kuchinke *et al.*, 1998a; Wodarz *et al.*, 1999; Schober *et al.*, 1999). NBs originate from the embryonic neuroectoderm and initially inherit their apical-basal polarization. During their asymmetric cell divisions, the Par-complex localizes to the apical cortex of the NB, which maintains its stem cell identity after asymmetric division, whereas proteins of the basal domain are segregated into the second daughter cell, the ganglion mother cell, which further differentiates into two neurons or glia cells (Wodarz, 2005; Zhong and Chia, 2008; Knoblich, 2008).

In epithelial cells, the kinase Par1 inhibits the formation of the Par complex in the baso-lateral region by phosphorylating Baz at two conserved residues (Ser151 and Ser1085). Binding of 14-3-3 proteins to these phosphorylated residues prevents the oligomerization and association with aPKC (Hurd *et al.*, 2003a; Benton and St Johnston, 2003a). In NBs, the protein

phosphatase PP2A counteracts the Par1 phosphorylation and thereby promotes the maturation of the Par complex (Krahn *et al.*, 2009). Vice versa, at least in mammalian cells, Par1 is excluded at the apical domain by aPKC-mediated phosphorylation (Hurov *et al.*, 2004). Furthermore, aPKC phosphorylates and inhibits Lgl at the apical cortex of NBs, which leads to a release of Par6 and aPKC from Lgl to promote the formation of the mature Par complex and the asymmetric localization of Numb and Miranda to the basal region (Betschinger *et al.*, 2003; Wirtz-Peitz *et al.*, 2008). The mutual antagonism of basal and apical protein complexes maintains a border between both regions in epithelia and neural stem cells.

Within the ternary Par complex, Par6 activates aPKC by replacing its pseudosubstrate domain (Graybill *et al.*, 2012), whereas the aPKC binding region of Baz inhibits aPKC kinase activity (Soriano *et al.*, 2016). The phosphorylation of Ser980 of Baz by aPKC leads to the dissociation of Baz/PAR-3 and aPKC whereupon Crumbs outcompetes phosphorylated Baz for binding to aPKC (Nagai-Tamai *et al.*, 2002; Harris and Peifer, 2005; Morais-de-Sá *et al.*, 2010). Furthermore, Baz recruits the Crumbs adaptor Stardust during early embryogenesis, which is released upon aPKC-mediated phosphorylation of Baz (Krahn *et al.*, 2010a; Sen *et al.*, 2015). Thus, Baz/Par3 functions as an important polarity cue, recruiting the Par-complex to the apical junctions.

Notably, how exactly Baz/Par3 itself localizes to the plasma membrane is still not fully clarified: Baz/PAR-3 contains an oligomerization domain (OD) at its N-terminus (Mizuno *et al.*, 2003; Benton and St. Johnston, 2003b; Feng *et al.*, 2007; Li *et al.*, 2010a; Zhang *et al.*, 2013a) and three PDZ (PSD-95, Disc Large, ZO-1) domains, which interact with the cell adhesion molecule Echinoid (Ed) and Armadillo (Arm), the Drosophila homologue of ß-catenin, which in turn stabilizes DE-Cad and thereby localizes Baz to the AJs (Wei *et al.*, 2005). In mammalian Par3, PDZ2 was suggested to directly bind to phospholipids of the plasma membrane (Wu *et al.*, 2007) and we have demonstrated previously, that a C-terminal phosphoinositide lipid binding (LB) domain of Baz directly binds to $PtdIns_{(4,5)}P_2$ (PIP2) and $PtdIns_{(3,4,5)}P_3$ (PIP3) to tether Baz to the cell cortex (Krahn *et al.*, 2010b), which was confirmed for mammalian Par3, too (Horikoshi *et al.*, 2011). However, deletion of any of these domains in Baz on its own disrupts the localization of the protein (Krahn *et al.*, 2010b; Krahn *et al.*, 2010a; McKinley *et al.*, 2012).

In this study we report that impaired oligomerization of Baz enhances degradation of the protein, but affects only mildly the rescue capacity of the mutant protein. We confirmed that the OD and LB motifs mediate the correct localization of the protein in redundancy.

Consequently, loss of both domains results in Baz degradation, which leads to the disruption of apical-basal cell polarity in epithelial cells of the embryonic epidermis and embryonic NBs and consequently embryonic lethality.

Material and Methods

DNA and constructs

Cloning of Baz pENTR was described before (Krahn *et al.*, 2009). For expression plasmids, we recloned Baz pENTR variants into UGW, UWS and PWG vectors (modified from UGW, UWG and PWG, which were obtained from the Drosophila Genomic Resource Center as described before (Sen *et al.*, 2012) using the gateway technology (Life Technologies). The following primer were used to introduce the mutants in Baz pENTR:

Baz1-968: 5'-ACAAACTCGGGCTGAGGATCCGGAGGTCACGCCTCCAAGGTG–3'

BazV14D-F: 5' - GGCGACGTTCGCATTCTG GAT CCCTGTGGTTCCGGC - 3'

BazD68K-F: 5' - GTCCGCGACGTGGCC AAA GATCGGGAGCAGATATTG - 3'

BazK1173K1174A-F: 5' - AAGTCGTCGCGGGCCGCGGCGCCAAGCATACTGCGC - 3'

Fly stocks and genetics

In all experiments, we used the *baz*$^{815-8}$ allele, which is a null allele. *baz* germline clones were generated with *baz*$^{815-8}$ FRT19A using the dominant female sterile technique (Chou and Perrimon, 1996). Homozygous mutant embryos were identified by loss of mCherry signal (from *FM7-sqh::mCherry*) in Western Blots. For immunofluorescence of germline clones, male embryos were selected by the absence of Sxl staining.

Ubi::GFP-Baz, Ubi::Baz-OneStrep and UASp::Baz-GFP transgenes were generated using phiC31-mediated germline transformation and attP40 was used as landing site (Groth *et al.*, 2004). For overexpression of Baz during early embryogenesis, we used mat-tub::GAL4 (#6356) (obtained from the Bloomington Drosophila Stock Center).

Lethality test

To test the lethality of embryos, 100 embryos of each genotype were tested in three biological replicates. Embryos derived from germline clones were selected against mCherry. The embryos were kept at 25°C on apple juice agarose plates and the amount of dead embryos, larval stage 1/2 (L1/2), larval stage 3 (L3), pupae and survivors was counted.

Cuticle preparation

Cuticle preparations were done as described previously (Wieschaus and Nusslein-Volhard, 1986). The cuticle phenotypes were classified into the four categories wild type, shrunken with holes, holes and cuticle rest.

Real time PCR Analysis

Embryos from overnight apple juice agar plates were used to isolate total RNA with TRIzol (Life Technologies) according to the manufactures instructions. To convert the RNA into cDNA, 1µg total RNA was used for reverse transcription with the qScript cDNA Synthesis Kit (Quantabio). Real time PCR was performed using the SensiFAST™ SYBR No-ROX Kit (Bioline) and the LightCycler 480 II (Roche). Relative expression levels of genes of interest were calculated as *Δ*Ct values normalized to the rp49 control. The following primers were used: Baz qPCR F 5‘-GTCCGTTTGTGACGCAGGTG-3’, Baz qPCR R 5‘-GGTCGGCGCGCCCACCCTTC-3’, rp49 F 5’-GCGGGTGCGCTTGTTCGATCC-3‘ rp49 R 5’-CCAAGGACTTCATCCGCCACC-3‘.

Cell culture

Drosophila S2R cells were kept at 25 °C in Drosophila Schneider medium supplemented with 10% FCS and 1% penicillin and streptomycin and passaged every three to four days.
Cells were transfected with FuGene HD (Promega) according to the manufactures instructions and allowed to grow for additional three to four days after transfection.

Antibody production

To produce sera against the N-terminus of Baz, a rabbit and a guinea pig were immunized with the recombinant GST-Baz1-318 (Eurogentec Inc.).

Immunofluorescence

Embryos were fixed in 4% formaldehyde, phosphate buffer pH 7.4 as previously described (Krahn *et al.*, 2009). The following primary antibodies were used for immunofluorescence: chicken anti GFP (1:2.000, Aves Labs Inc., #GFP-1020), mouse anti Dlg (1:25, DSHB, #4F3), rat anti DE-Cad (1:5, DSHB, #DCAD2), rabbit anti Baz (1:1.000, this study), Gp anti Baz (1:500, this study), rat anti Mir (1:1.000, gift from A. Wodarz), rabbit anti aPKC (1:500, Santa Cruz, #sc-216), mouse anti Sxl (1:25, DSHB, #M114). Secondary antibodies conjugated with Alexa 488, Alexa 568 and Alexa 647 (Life Technologies) were used at 1:400. Images were taken with a Zeiss LSM710 and processed with ImageJ.

Embryonic lysates, immunoprecipitation and Western Blotting

For embryonic lysates, embryos from overnight apple juice agar plates were collected and dechorionated in 50% bleach. The embryos were lysed in lysis buffer (1% Triton X-100, 150

mM NaCl, 1 mM $CaCl_2$, 1 mM $MgCl_2$, and 50 mM Tris-HCl, pH 7.5) supplemented with protease inhibitors. After incubation for 20 min at 4°C the lysates were centrifuged and SDS sample buffer was added before boiling at 95°C for 5 min.

For immunoprecipitation, transfected S2R+ cells were lysed in lysis buffer supplemented with protease inhibitors. After centrifugation, cell lysates were added to StrepTactin beads for precipitation of OneStrep tagged Baz proteins for 45 min at 4°C. The beads were washed three times in lysis buffer and 2 x SDS sample buffer was added before boiling at 95°C for 5 min. followed by Western blotting. Western blotting was performed according to standard protocols. The following primary antibodies were used in this study: mouse anti GFP (1:500, Santa Cruz #sc-9996), rabbit anti GST (1:5.000, Sigma #G7781), mouse anti c-Myc (1:100, DSHB, #9E10), mouse anti Actin (1:1.000, Santa Cruz #sc-47778), rabbit anti Baz (1:1.000, a gift from A. Wodarz).

In vitro crosslinking

The first 81 amino acids of wt or BazV14D D68K were fused to GST and purified from E.coli (strain BL21*) using glutathione beads (Macherey-Nagel). For in vitro crosslinking experiments, 5 µM recombinant protein was incubated in PBS for 1h on ice. Subsequently formaldehyde was added to a final concentration of 2% and incubated for 10 min at room temperature. The reaction was quenched by adding Tris to a final concentration of 250 mM. Then 5 x SDS sample buffer was added before boiling at 65°C for 5 min. The crosslinked proteins were analyzed by Western Blotting.

Statistical analysis

Data were analyzed using one-way ANOVA followed by Turkey's post hoc test with Graphpad Prism 6. All plots are expressed as the mean ± standard deviation (s.d.).

Results

Oligomerization and lipid binding promote Baz localization redundantly

Baz functions on the top of a hierarchy regulating apical-basal polarization in the epidermis of the developing *Drosophila* embryo. However, it is still not fully understood, how Baz itself is recruited to the membrane. To analyze the contribution of structural domains of Baz to its localization in the *Drosophila* embryonic epithelium we generated transgenic flies that express GFP-tagged *baz* transgenes (Fig. 4.1A). The *baz* constructs were expressed with the *ubiquitin* promoter, which resulted in a weak overexpression of the full length protein (Fig. 4.1B).

GFP-Baz co-localizes with the AJ marker DE-Cad at the AJs (Fig. 4.2B), similar to endogenous Baz (Fig. 4.2A) and can fully rescue the embryonic lethality of the baz^{815-8} null allele (91,4 ± 2,8% hatched L1 larvae) (Fig. 4.1A).

To analyse the function of the N-terminal oligomerization domain, we generated a oligomerization-deficient version of Baz, Baz V14D D68K (hereafter BazΔOD), which has been reported to abolish the self-association of two N-terminal monomers in rat Par3 (Feng *et al.*, 2007). Indeed, BazΔOD had a strongly attenuated capacity to self-associate *in vivo* and *in vitro* (Fig. 4.1C-D). Surprisingly, in lethality tests with baz^{815-8} germ line clones (GLCs), which are deprived of maternal Baz mRNA and protein, GFP-BazΔOD rescued the embryonic lethality of the baz^{815-8} null allele almost as efficient as wild type Baz (61,0 ± 0,6%) (Fig. 4.1A). Furthermore, GFP-BazΔOD localizes to the AJs in epithelial cells of the embryonic epithelium indistinguishable from its wild type counterpart (Fig. 4.2C compared to Fig. 4.2A and B).

Baz is capable of binding to the phospholipids PIP2 and PIP3 (Krahn *et al.*, 2010b). However, mutation of the lipid binding domain of Baz (GFP-BazK1173-1174A = BazΔLB, Fig. 4.6B) did not attenuate the apical junctional localization of GFP-BazΔLB or its rescue capacity (95,3 ± 5,3%) (Fig. 4.1A and Fig. 4.2D). In contrast, a variant of Baz which cannot oligomerize or bind to phospholipids (GFP-BazΔODΔLB) displayed a cytoplasmic localization and failed to rescue the baz^{815-8} mutant (Fig. 4.1A and Fig. 4.2E). Thus, Baz oligomerization and binding to phospholipids function in redundancy to target the protein to the apical junctions and ensure its function. This is confirmed by the finding, that a Baz

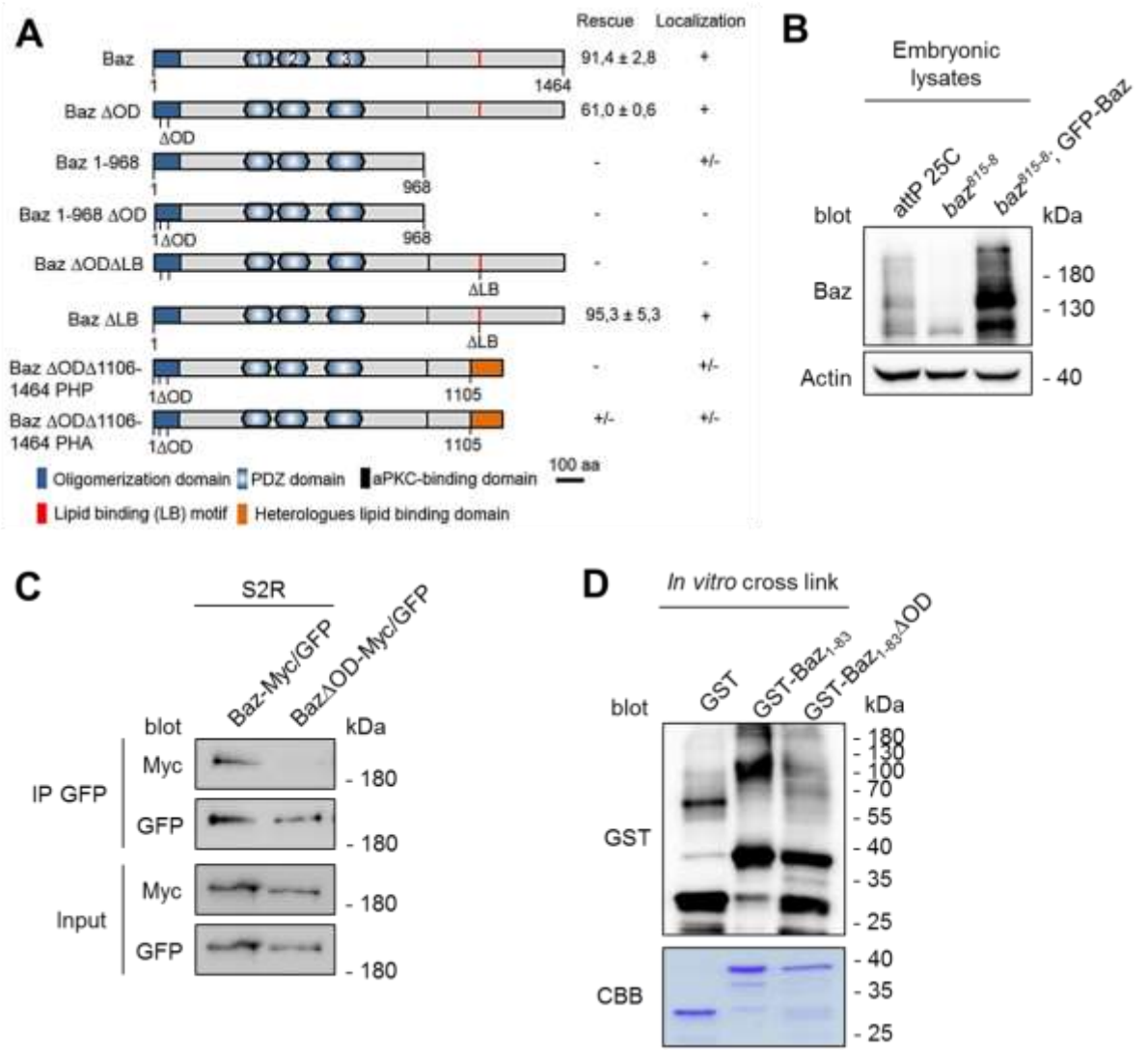

Fig. 4.1: Oligomerization of Baz is dispensable for viability (A) Schematic representation of different Baz deletion constructs. All constructs were expressed from the same genomic locus (attP40) with an N-terminal GFP-tag under the control of the *ubiquitin* promotor. The ΔOD mutation (V14DD68K) prevents oligomerization and the ΔLB mutation (K1173-74A) abolishes membrane binding. The ability to rescue the embryonic lethality of baz^{815-8} germ lines clones was quantified and the localization determined, where "+" indicates the wild type situation, "+/-"indicates a lateral cortical localization and "-"indicates a cytoplasmic localization. (B) Expression of GFP-Baz in the baz^{815-8} mutant background results in a weak overexpression compared towards endogenous Baz. (C) Co-immunoprecipitation of GFP and Myc tagged Baz or BazΔOD in S2R cells. Mutations of the OD domain strongly attenuate the capacity of Baz to self-associate. (D*) In vitro* crosslinking of the Baz OD domain (aa 1-83). Mutations of the OD domain (V14DD68K) strongly impair the formation of oligomers *in vitro*.

variant encoding the first 968 amino acids (GFP-Baz1-968), which includes the oligomerization domain, is localized to the apical junctions with a slight baso-lateral mislocalization (Suppl. Fig. 4.1). Mutation of the oligomerization domain in GFP-Baz1-968

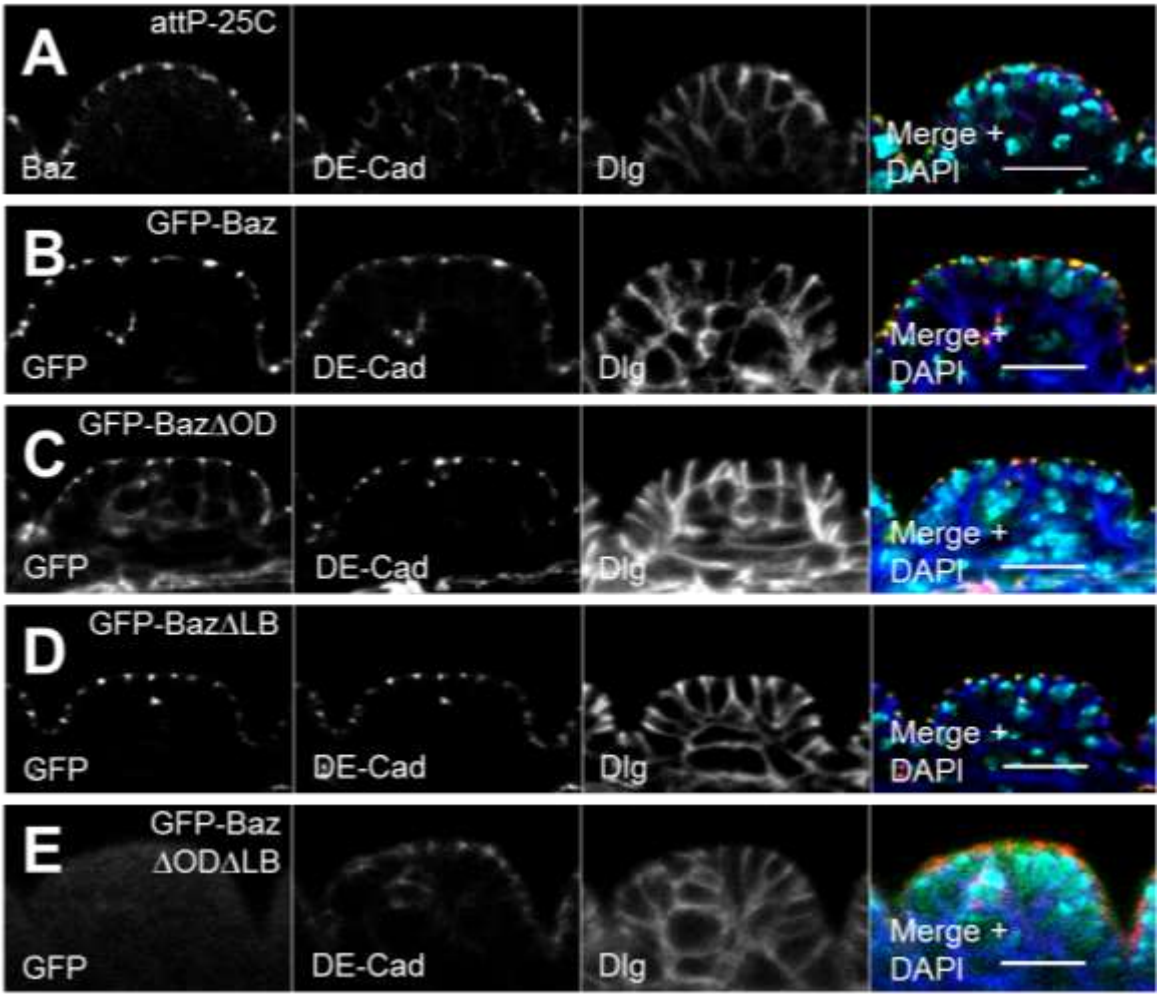

Fig. 4.2: Oligomerization and lipid-binding promote Baz localization redundantly. (A) In immunostainings of the *Drosophila* embryonic epithelium, endogenous Baz (green) co-localizes with DE-Cadherin (DE-Cad, red) at the apical junctions. Disc large (Dlg, blue) was stained as a lateral marker. (B) The localization of GFP-Baz is indistinguishable from the endogenous protein. (C) The oligomerization-deficient GFP-BazΔOD displays an accumulation at the AJ, overlapping with DE-Cad. (D) The localization of a lipid-binding deficient GFP-BazΔLB protein is similar to wild type Baz. (E) The GFP-BazΔODΔLB double mutant is absent from the cell cortex and displays a diffuse cytoplasmic localization. All transgenes were expressed in a wild type background. Scale bars are 10 µm

(GFP-Baz1-968ΔOD) abolishes its cortical localization (Suppl. Fig. 4.1). Notably, GFP-Baz1-968 did not rescue the embryonic lethality of baz^{815-8}, most likely due to a lack of the C-terminal part of the protein, which includes the aPKC-binding region.

Taken together, the N-terminal oligomerization domain and the C-terminal LB motif of Baz contribute redundantly to the localization of the protein. Based on the rescue capacity of the Baz variants we found that neither the oligomerization nor the binding to phospholipids are essential for viability.

Binding to phospholipids is not sufficient for the function of Baz

To further investigate the role of the LB motif regarding the localization and function of Baz we substituted the C-terminus including the intrinsic LB motif of GFP-BazΔOD by the Pleckstrin homology (PH) domains of either PLCδ (BazΔODΔ1106-1464-PHP) or Akt1 (BazΔODΔ1106-1464-PHA) (Fig. 4.1A). The PH domain of PLCδ specifically binds to $PtdIns_{(4,5)}P_2$ (PIP2) (Várnai and Balla, 1998), whereas the PH domain of Akt1 binds to $PtdIns_{(3,4,5)}P_3$ (PIP3) (James *et al.*, 1996). Baz itself binds both, PIP2 and PIP3 *in vitro* (Krahn *et al.*, 2010b).

In the epithelium of transgenic embryos, both GFP-BazΔODΔ1106-1464-PHP and GFP-BazΔODΔ1106-1464-PHA had a cortical localization and punctual enrichments at the AJ where they co-localized with DE-Cad (Suppl. Fig. 4.1). However, only GFP-BazΔODΔ1106-1464-PHA rescued occasionally the zygotic baz^{815-8} allele (<1%), but not embryos, which have been depleted for the maternal and zygotic protein expression (GLCs). Moreover, expression of both variants together, GFP-BazΔODΔ1106-1464-PHP and GFP-BazΔODΔ1106-1464-PHA in a *baz*-mutant background did not produce surviving animals, indicating that either simultaneous binding of one Baz molecule to PIP2 and PIP3 is essential or that the C-terminus (aa 1106-1464) is essential for Baz' function in our experimental set up, which differs from previous studies, which used proteins overexpressed by the UAS/GAL4 system (Krahn *et al.*, 2010b; McKinley *et al.*, 2012).

BazΔODΔLB fails to polarize the epithelium of the embryonic epidermis

To better understand why BazΔODΔLB failed to rescue baz^{815-8} mutant embryos, we analysed the epithelium of GLCs. To exclude the possibility that the N-terminal GFP-tag interferes with the function of Baz, we created transgenic flies, which express Baz transgenes fused with a small OneStrep-tag (OneS) at the C-terminus under the control of the *ubiquitin* promotor. As the GFP-variants, Baz-OneS displayed a strong rescue capacity of the embryonic lethality in baz^{815-8} GLCs, whereas BazΔODΔLB-OneS displayed a complete embryonic lethality (Fig. 4.3). To test if the overexpression of BazΔODΔLB might help to overcome the embryonic lethality of baz^{815-8} GLCs, we expressed UASp::Baz-GFP and UASp::BazΔODΔLB-GFP with mat-Tub::Gal4 in baz^{815-8} GLCs (Fig. 4.5A). Baz-GFP rescues the embryonic lethality of

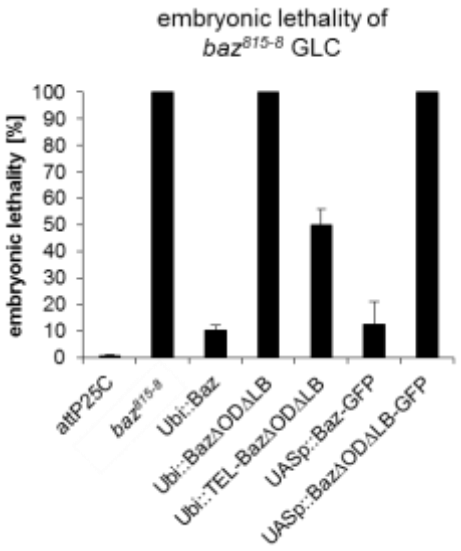

Fig. 4.3: Loss of oligomerization and lipid-binding causes embryonic lethality. Baz variants that carry an C-terminal One-Strep (OneS) tag were expressed under the *ubiquitin* promoter and tested for their capacity to rescue baz^{818-8} germ line clones. Baz-OneS efficiently rescues the lethality of the baz^{818-8} allele (10,5 ± 1,8% embryonic lethality). BazΔODΔLB-OneS failed to rescue the embryonic lethality. Fusion of the oligomerization domain of the human TEL protein (aa 45 – 115) to the N-terminus of Baz restores its function and rescues embryonic lethality of baz^{815-8} to a large extent (50,0 ± 6,1% embryonic lethality). Similar, wild type Baz-GFP overexpressed with mat-Tub::Gal4 using the Gal4/UAS-system had comparable efficiencies as the constitutively expressed variant (12,7 ± 8,5%), whereas overexpression of BazΔODΔLB-GFP failed to rescue (100% embryonic lethality). Bars represent the mean ± s.d.

GLCs to the same extend as Baz-OneS (87,3 ± 8,5% and 89,5 ± 1,8%, respectively), whereas BazΔODΔLB-GFP expressing GLCs failed to escape embryonic lethality (Fig. 4.3).

Next, we evaluated the phenotypes of embryonic cuticles of *baz* GLCs expressing the different rescue constructs. The Cuticle is secreted from the epidermis and allows drawing a conclusion of its integrity, in particular the formation of a function apical domain. We divided the observed phenotypes in five groups (hatched (=normal cuticle), wild type (= dead but cuticle without obvious defects), cuticle rest, holes and shrunken with holes). As expected the baz^{815-8} mutant displayed large cuticle hole or some cuticle rest (Suppl. Fig. 4.2). In contrast to the null allele, most animals of Baz-OneS hatch and the dead embryos had either a wild type or shrunken cuticle phenotype (4,8% or 5,7%, respectively, Suppl. Fig. 4.2). BazΔODΔLB-OneS partially rescued the baz^{815-8} phenotype, because some embryos developed further and had either a wt or shrunken with holes phenotype (2,3% or 23,3%, respectively, Suppl. Fig. 4.2).

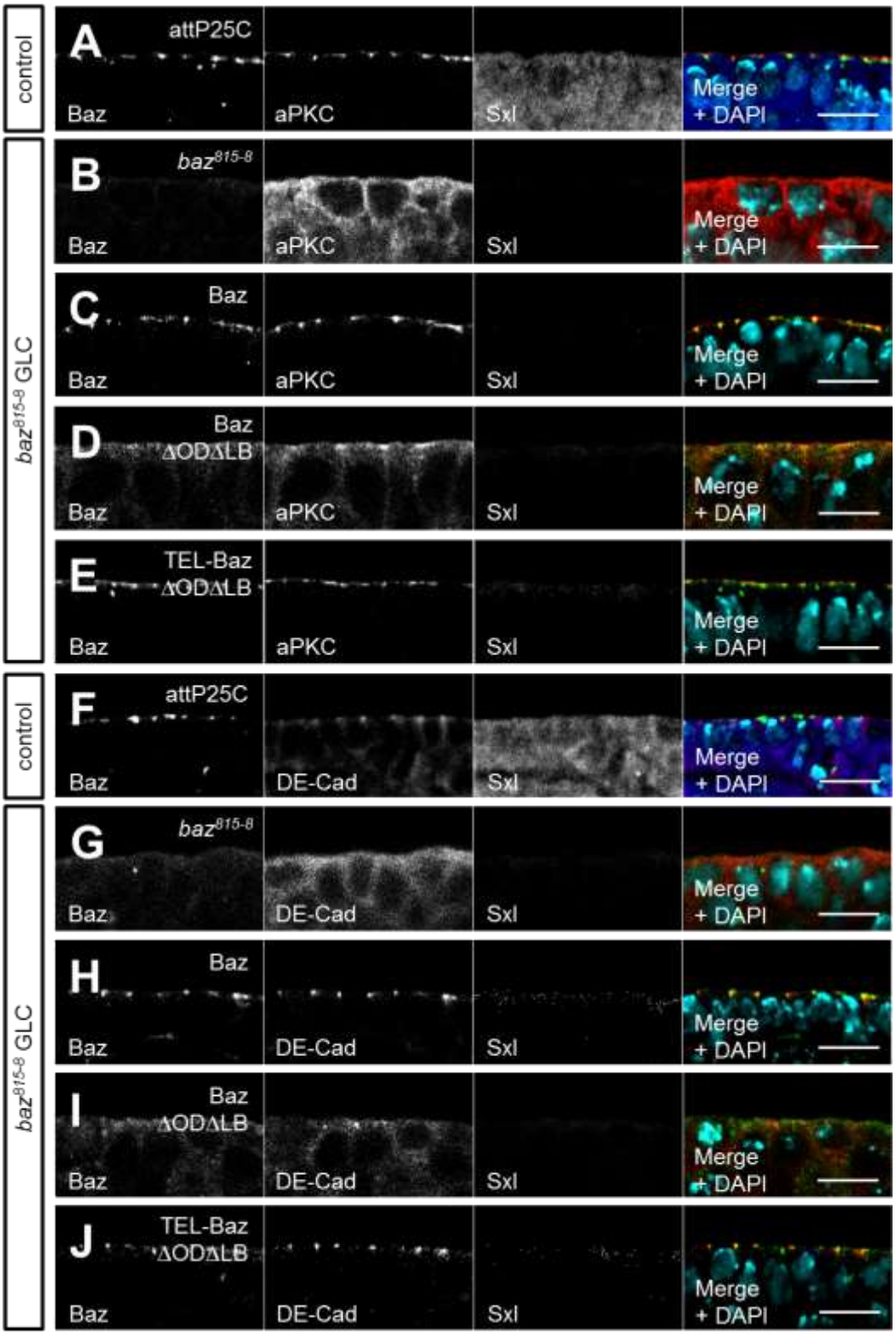

Fig. 4.4: Epithelial polarization requires the functional redundancy of the OD and LB domains. (A) Immunostaining of endogenous Baz (green), aPKC (red) and Sxl (blue) in the embryonic epidermis. (B-E) Immunostaining of Baz variants and endogenous aPKC in the embryonic epidermis of *baz*$^{818-8}$ germ line clones. Hemizygous mutant embryos were identified by the absence of Sxl staining. (B) Loss of Baz in the embryonic epidermis of disrupts epithelial polarization and aPKC accumulates in the cytoplasm. (C) Baz-OneS

efficiently recruits aPKC to the apical junctions, such as endogenous Baz, whereas BazΔODΔLB-OneS displays a cytoplasmic mislocalization (D). BazΔODΔLB-OneS rescues some aPKC to the apical junctions, but the majority of the protein still accumulates in the cytoplasm. (E) TEL-BazΔODΔLB-OneS localizes at the apical junctions and is capable of recruiting aPKC to rescue the defects of BazΔODΔLB-OneS. (F-J) Immunostaining of Baz (green), DE-Cad (red) and Sxl (blue) in the embryonic epidermis demonstrate a loss of AJ in *baz*$^{815-8}$ germ line clones, which can be rescued by wild type Baz and (H) and TEL-BazΔODΔLB-OneS (J) but not by BazΔODΔLB-OneS (I). Scale bars are 10 µm

Interestingly, fusion of the heterologous oligomerization domain of the human TEL protein (residues 45-115 (Kim *et al.*, 2001)) to the N-terminus of BazΔODΔLB-OneS (TEL-BazΔODΔLB-OneS) partly restores the rescue capacity of the mutant Baz protein.

Furthermore, TEL-BazΔODΔLB-OneS embryos had a milder phenotype, as most dead embryos had a wild type or shrunken cuticle phenotype (21,9% and 17,9%, respectively, Suppl. Fig. 4.2).

Next, we scored for the localization of polarity markers in the embryonic epithelium by immunostainings. Hemizygous mutant embryos derived from GLC were identified by the lack of Sex lethal (Sxl) staining. As expected, in the epithelium of *baz*$^{815-8}$ GLCs we did not detect a signal for Baz, whereas aPKC exhibited a cytoplasmic localization (Fig. 4.4B). *Baz*-OneS and TEL-BazΔODΔLB-OneS both had a robust apical localization and recruited aPKC to the apical junctions, similar to endogenous Baz (Fig. 4.4A, C and E). In contrast, BazΔODΔLB-OneS showed a cytoplasmic mislocalization (Fig. 4.4D). Nevertheless, BazΔODΔLB-OneS managed to recruit some aPKC to the apical junctions, but the majority of the aPKC protein still accumulates in the cytoplasm (Fig. 4.4D). In general, the overall structure of the epithelium was disrupted in BazΔODΔLB-OneS embryos.

Then, we examined the assembly of intact AJ by scoring for the localization of DE-Cad in *baz*$^{815-8}$ GLCs (Fig. 4.4F-J). Baz-OneS and TEL-BazΔODΔLB-OneS both showed an apical junctional targeting of DE-Cad comparable to the wild type control (Fig. 4.4F, H, J). Unlike as for aPKC we did not see a localization of DE-Cad in the apical region or at the plasma membrane in BazΔODΔLB-OneS expressing *baz*$^{815-8}$ GLCs (Fig. 4.4I).

In summary, BazΔODΔLB-OneS has only a weak capability to polarize the embryonic epithelium and displayed strong cuticle defects, as well as an impaired function, since aPKC was inefficiently and DE-Cad not at all recruited to the apical junctions. Restoring the oligomerization capacity of Baz by fusing the oligomerization domain of TEL to BazΔODΔLB-OneS restores its functionality to a large extent.

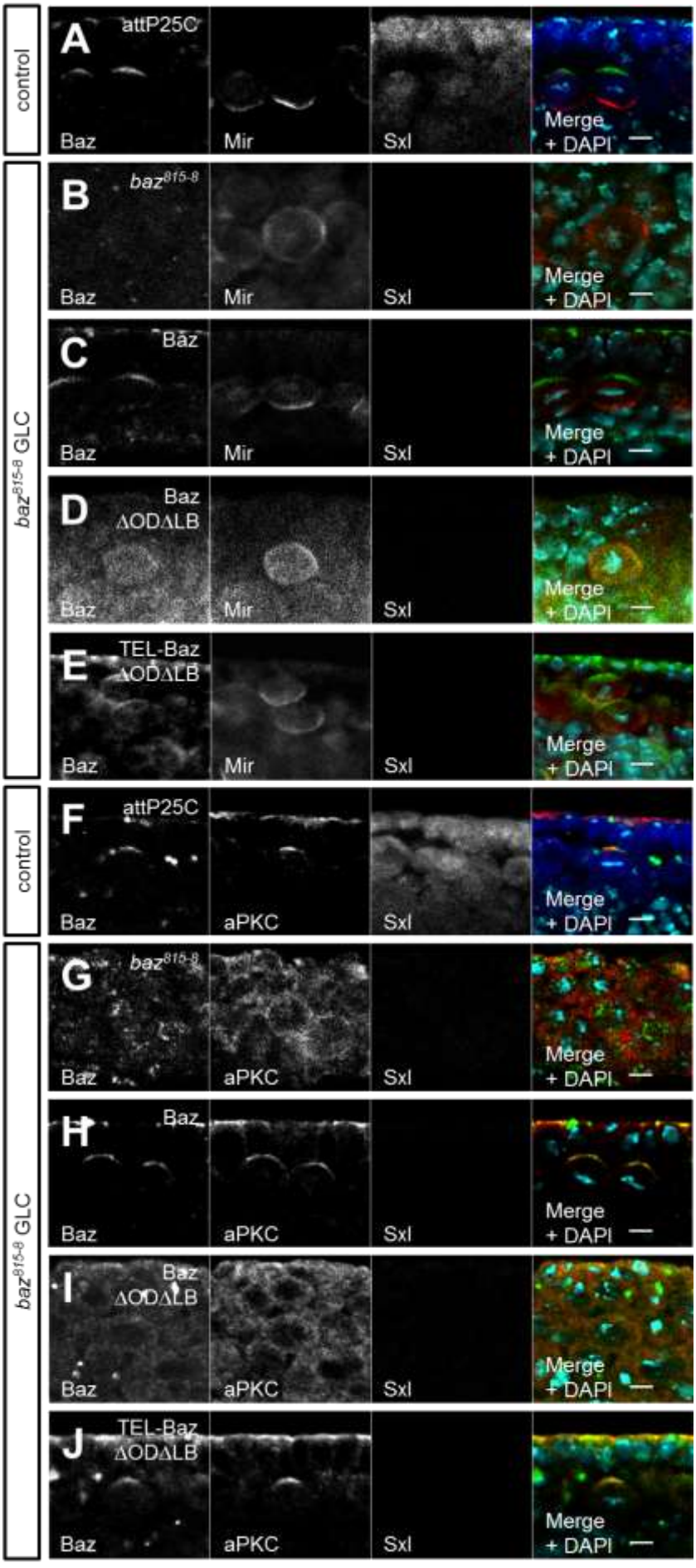
control
A
attP25C
Baz
Mir
Sxl
Merge
+ DAPI
baz815-8 GLC
B
baz815-8
C
Baz
D
Baz
ΔODΔLB
E
TEL-Baz
ΔODΔLB
control
F
attP25C
aPKC
G
baz815-8
H
Baz
I
Baz
ΔODΔLB
J
TEL-Baz
ΔODΔLB

Fig. 4.5: Neuroblast polarity requires Baz's capacity to either self-associate or to bind lipids. (A) Immunostaining of endogenous Baz (green), Mir (red) and Sxl (blue) in embryonic metaphase NBs. Baz localizes at the apical cortex, whereas Mir accumulates basally. (B-E) Immunostaining of Baz variants (green) and endogenous Mir (red) in embryonic NBs of *baz*$^{818\text{-}8}$ germ line clones during metaphase. Hemizygous mutant embryos were identified by the absence of Sxl staining. (B) Loss of Baz in *baz*$^{818\text{-}8}$ germ line clones disrupts NB polarity and Mir localization. (C) Baz-OneS rescues NB polarity, whereas BazΔODΔLB-OneS does not localize at the cortex and fails to polarize NBs (D). (E) TEL-BazΔODΔLB-OneS restores apical-basal polarity in metaphase NBs, such as wild type Baz. (F) Immunostaining of endogenous Baz (green), aPKC (red) and Sxl (blue) in embryonic metaphase NBs. Baz recruits aPKC to the apical pole of metaphase NBs. (G) aPKC accumulates in the cytoplasm in metaphase NBs of *baz*$^{818\text{-}8}$ germ line clones. (H, J) Baz-OneS and TEL-BazΔODΔLB-OneS both show a comparable localization and recruit aPKC to the apical pole. (I) In contrast, BazΔODΔLB-OneS localizes in the cytoplasm, such as endogenous aPKC. Scale bars are 5 µm

Apical-basal polarity of embryonic NBs is disrupted in BazΔODΔLB embryos

Similar to polarization of the epithelium of the embryonic epidermis, Baz is also required for the establishment of apical-basal polarity of dividing NBs. Hence we investigated if BazΔODΔLB-OneS had similar phenotypes in embryonic NBs as in the epithelium. Baz accumulates at the apical cortex, recruiting aPKC and Par6, whereas the scaffold protein Miranda (Mir) is restricted to the basal region of metaphase NBs (Fig. 4.5A). Basal segregation of Mir depends on the apical formation of the Par complex (Rolls *et al.*, 2003; Atwood and Prehoda, 2009). Therefore, we analysed the localization of Baz variants and Mir in NBs of *baz*$^{815\text{-}8}$ GLCs. We found that BazΔODΔLB-OneS phenocopied the *baz* null allele, as Mir is not restricted to the basal region of NBs in both genotypes but can be found more or less all around the cortex (Fig. 4.5B, D). BazΔODΔLB-OneS also failed to localize to the apical membrane of NBs, but rather displayed a weak cytoplasmic localization (Fig. 4.5D). Like in the epithelium Baz-OneS and TEL-BazΔODΔLB-OneS rescued the asymmetric distribution of Mir and localized to the apical membrane in metaphase NBs, such as the control (Fig. 4.5A, C, E).

In contrast to the epithelium where aPKC displayed at least a minimal polarization in BazΔODΔLB-OneS GLC, its localization in NBs is cytoplasmic, similar to the *baz* null allele (Fig. 4.5G, I). As expected, Baz-OneS and TEL-BazΔODΔLB-OneS recruit aPKC to the

apical cortex comparable to endogenous protein (Fig. 4.5F, H, J).
Thus, the functional redundancy of the OD and the LB motif are essential to polarize embryonic NBs, since neither Mir nor aPKC exhibited a correct localization in BazΔODΔLB-OneS GLC.

BazΔODΔLB is still recruited to the cortex by transmembrane proteins

In order to elucidate the mechanism why BazΔODΔLB-OneS fails to accumulate at the apical junctions and why it is non-functional, we tested whether the membrane recruitment by its described interacting transmembrane proteins is disturbed. Therefore, we used *Drosophila* S2R cells as a model system, because they do not exhibit a polarity or detectable amounts of polarity proteins (Krahn *et al.*, 2010b). In S2R cells, Baz-GFP clearly localizes to the cell cortex (Fig. 4.6A), whereas BazΔLB-GFP appears in cytoplasmic aggregates (Fig. 4.6B), indicating that in S2R cells cortical localization of Baz depends exclusively on the binding to phospholipids. Co-transfection of BazΔLB-GFP with DE-Cad-RFP or Ed-RFP led to the formation of cell-cell contacts of transfected cells. Both proteins recruited BazΔLB-GFP to the artificial cell-cell contacts (Fig. 4.6C-D). Additionally, the intracellular domain of the atypical cadherin Starry night (Stan) fused to the extracellular domain of DE-Cad also recruited BazΔLB-GFP to ectopic cell-cell contacts (Fig. 4.6E). By contrast, the Stan isoform Flamingo, which lacks the C-terminal PDZ binding motif did not recruit lipid binding deficient Baz (data not shown). Expression of BazΔODΔLB-GFP alone or together with DE-Cad, Ed or Stan showed that BazΔODΔLB-GFP was recruited to the cell-cell contacts, such as its oligomerizing counterpart (Fig. 4.6F-I). Thus, BazΔODΔLB is still able to interact with its reported recruiting transmembrane proteins. This is in line with the observation, that deletion of the PDZ domains, which facilitate binding to Stan, Ed and Arm/DE-Cad, does not disturb the localization of GFP-BazΔLB (Fig. 6J).

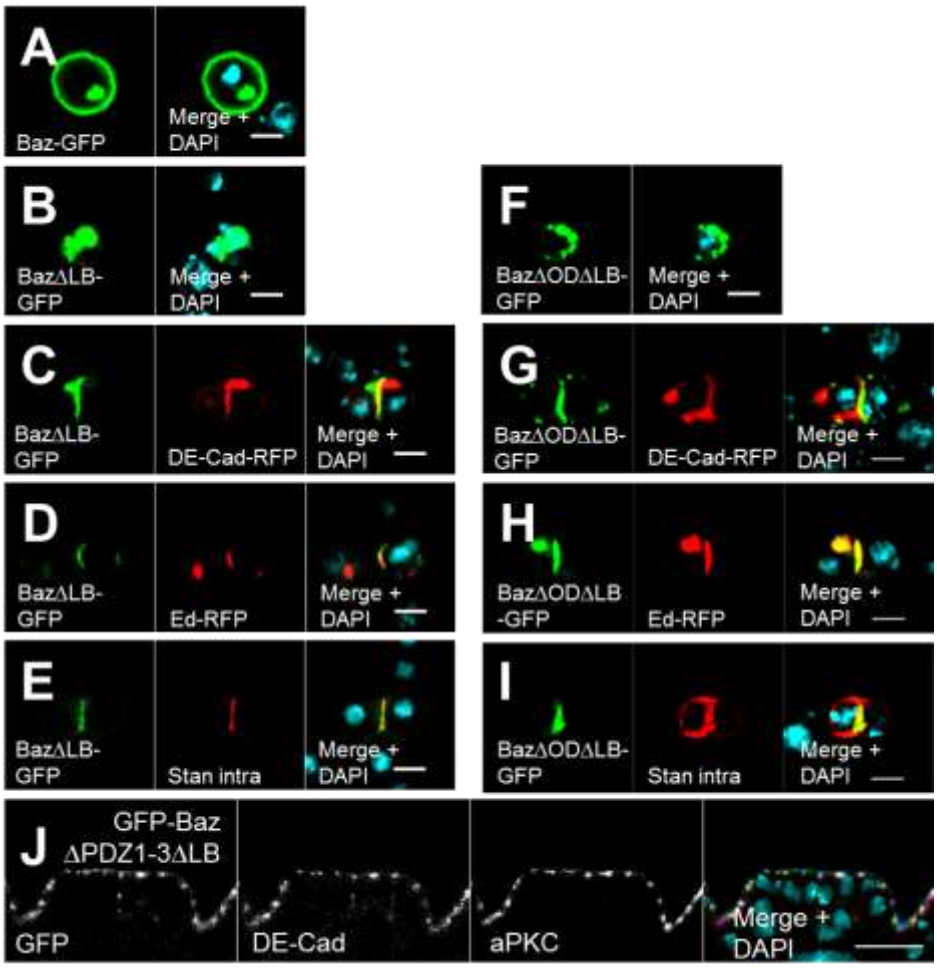

Fig. 4.6: Recruitment of Baz by DE-Cad, Ed and Stan does not depend on self-association or lipid-binding of Baz. (A) Wild type Baz-GFP was expressed with the *ubiquitin* promoter in S2R cells and localizes at the plasma membrane. (B) BazΔLB-GFP accumulates in cytoplasmic aggregates. (C, D) DE-Cad-RFP and Ed-RFP recruit BazΔLB-GFP to artificial cell-cell contacts. (E) Similar, the intracellular domain of Stan, fused to the extracellular and transmembrane domain of DE-Cad (DE-CadΔintra-StanΔextra) targets BazΔLB-GFP to cell-cell contacts. DE-CadΔintra-StanΔextra was detected with an anti DE-Cad antibody, which recognizes the extracellular domain of DE-Cad. (F-I) In the same experimental setup with BazΔODΔLB-GFP, the double mutant was efficiently recruited by DE-Cad, Ed and Stan without apparent differences. (J) Deletion of all three PDZ domains in BazΔLB does not affect the localization of the mutant protein at the apical junctions (green = GFP- BazΔPDZ1-3 ΔLB, red = DE-Cad, blue = aPKC). Scale bars are 5 μm in A-I and 10 μm in J.

Oligomerization protects Baz from degradation

Despite its capacity to interact with transmembrane proteins, BazΔODΔLB-OneS is non-functional and does not localize to the apical junctions. Therefore, we tested, whether simultaneous loss of oligomerization and lipid binding affects the protein stability, we blotted *baz*$^{815-8}$ GLC rescued with GFP-Baz and Baz-OneS variants to detect the exogenous Baz protein. Indeed, we observed that loss of the dimerization domain caused a reduced amount of Baz protein in the embryo, which is further enhanced upon the loss of the LB motif (Fig. 4.7A, C). In contrast, mutation of the LB motif alone did not affect the amount of protein (Fig. 4.7C). Similar, the amount of BazΔODΔLB-OneS protein is strongly reduced in lysates of GLC (Fig. 4.7A), whereas Baz-OneS and TEL-*Baz*ΔODΔLB-OneS were not affected by enhanced protein degradation (Fig. 4.7A). The reduced amount of *Baz*ΔODΔLB-OneS was not due to impaired gene expression, because all transgenes were expressed from the same promoter and genomic location and exhibited comparable mRNA levels with no significant differences (Fig. 4.7B).

Finally, we tested, whether the phenotypes observed in *Baz*ΔODΔLB rescued embryos are only due to protein degradation of the mutant protein. Strikingly, overexpression of wild type Baz-GFP, but not *Baz*ΔODΔLB-GFP rescued the embryonic lethality of *baz*$^{815-8}$ (Fig. 4.3) although both proteins are expressed at comparable levels (Suppl. Fig. 4.3A). Moreover, *Baz*ΔODΔLB-GFP is still cytoplasmic, whereas its wild type counterpart localizes to the apical junctions (Suppl. Fig. 4.3C in comparison to B). These data suggest, that *Baz*ΔODΔLB fails to localize to the apical junctions, accumulates in the cytoplasm and is rapidly degraded.

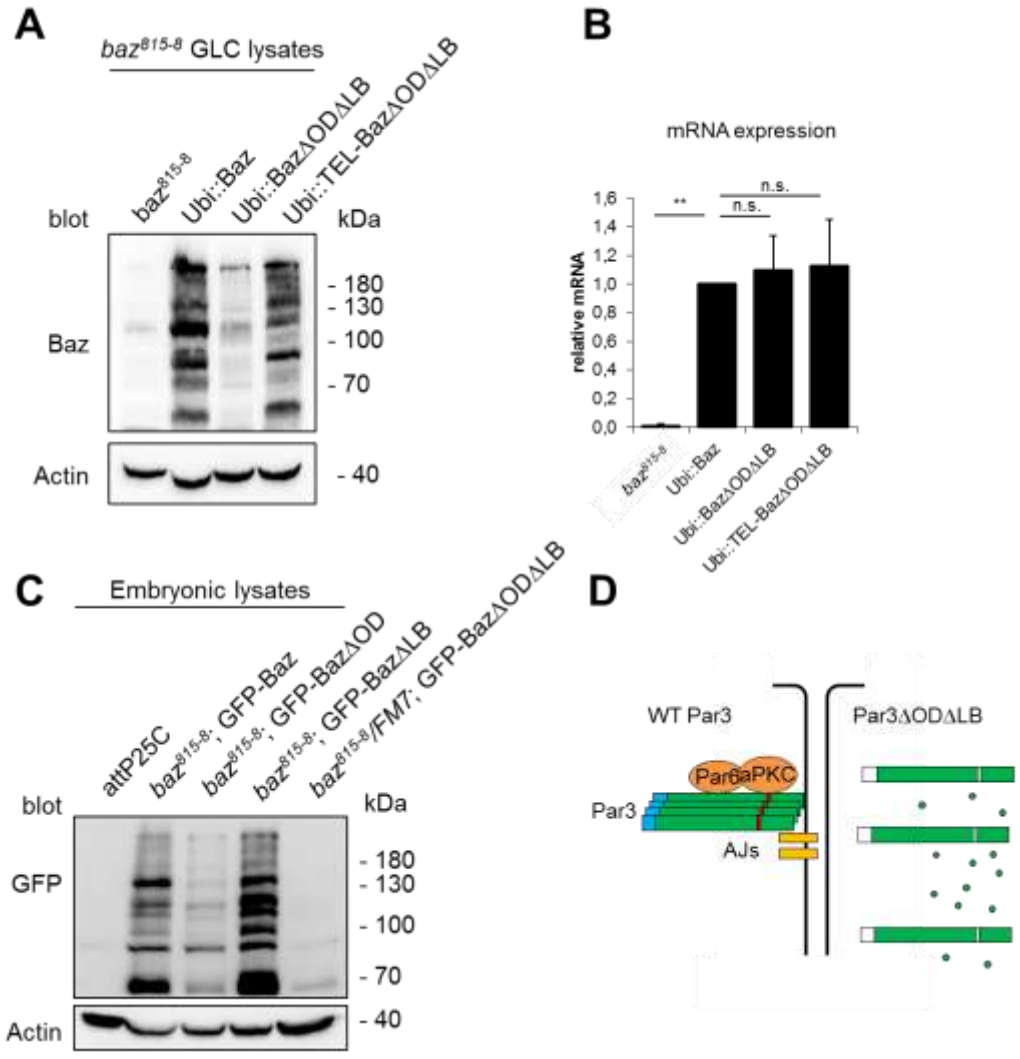

Fig. 4.7: Oligomerization and lipid binding are crucial for Baz' stabilization. (A) Lysates of *baz*$^{818-8}$ germ line clones that express different Baz variants were blotted against Baz. Actin was used as loading control. Loss of Baz oligomerization and lipid binding (BazΔODΔLB) strongly decreases the amount of Baz protein. TEL-BazΔODΔLB-OneS rescues the degradation of BazΔODΔLB-OneS. (B) qPCR of total RNA from the *baz*$^{818-8}$ germ line clones shows that all transgenes were expressed without significant differences (One-way ANOVA followed by Turkey's post-hoc test, n.s. $p>0.05$, * $p< 0.05$, ** $p< 0.01$). Bars represent the mean ± s.d.. (C) Embryonic lysates of different GFP-Baz variants in a *baz*$^{818-8}$ genetic background were blotted against GFP. Actin was used as loading control. Loss of oligomerization reduces the stability of GFP-BazΔOD, which is drastically enhanced upon the mutation of the lipid binding motif in GFP-BazΔODΔLB. However, mutation of the lipid-binding motif alone (GFP-BazΔLB) does not affect the protein stability. (D) Scheme of the functional redundancy between the OD and LB domains.

Discussion

Taken together, the oligomerization domain of Baz is not essential for viability of the Drosophila embryo, but contributes to the stability of the protein and the functional redundancy of the oligomerization domain and the LB motif are indispensable for the function of Baz during Drosophila embryogenesis (Fig. 4.7D).

This is in contrast to previous findings, reporting an important role for the oligomerization domain for Baz/Par3 localization in *Drosophila* and mammalian cells (Mizuno *et al.*, 2003; Benton and St. Johnston, 2003b). This discrepancy might be explained by the different setups: In contrast to previous studies (Benton and St. Johnston, 2003b; Krahn *et al.*, 2010b; McKinley *et al.*, 2012) using overexpressed proteins with the UAS/GAL4 system in rescue experiments, we used a constitutive expression, which resulted in a rather mild overexpression. Nonetheless, the slightly reduced rescue capacity (61% of BazΔOD in contrast to 91% for wild type Baz) and the redundant function of the OD underline the importance of Baz self-association. The fact, that the heterologous oligomerization domain of TEL can rescue the defects of *Baz*ΔODΔLB suggests, that the OD promotes indeed self-association instead of interaction with other binding partners.

In line with previous results (Krahn *et al.*, 2010b; McKinley *et al.*, 2012), we found that the lipid-binding domain of Baz/Par3 is dispensable for the localization and function of the protein – however, it can to a far extent compensate the loss of the OD. We further demonstrate here that protein stability of Baz depends on membrane localization, as BazΔODΔLB is rapidly degraded, whereas fusion of heterologous lipid-binding domains or an oligomerization domain rescues the protein stability (Suppl. Fig. 4.1E and Fig. 4.7A).

Finally, one important question remains: How does the OD contribute to the localization of Baz? One likely possibility is that Baz forms oligomers, which are then recruited to the plasma membrane by a transmembrane- or membrane-associated protein. Previous studies have identified three transmembrane proteins (DE-Cad, Ed, Stan) as interaction partners of Baz, which might be capable of recruiting the protein to the membrane (Wei *et al.*, 2005; Wasserscheid *et al.*, 2007). Work from Harris and Peifer nicely demonstrated that Baz functions upstream of at least DE-cadherin in the polarization of the embryonic epidermis (Harris and Peifer, 2004). However, it is still unclear, how Baz is initially localized to the plasma membrane of epithelial cells during early embryonic development. Therefore, we tried to abolish the expression of DE-Cadherin, Ed and Stan in early embryos using triple GLCs, which unfortunately did not produce any eggs (data not shown), indicating that these three

genes are involved in oogenesis, too. Nonetheless, we observed that *Baz*ΔODΔLB is still able to interact with DE-Cad, Ed and Stan (Fig. 4.6). This is surprising as *in vivo*, none of these interaction partners seem to be capable of targeting the mutant protein to the apical junctions, although they are all expressed in the embryonic epidermis. Thus, we can exclude DE-Cadherin, Ed and Stan to be involved in the recruitment of Baz oligomeric complexes. Moreover, the fact, that deletion of all three PDZ domains in BazΔLB does not disturb the correct apical junctional localization of the mutant protein (Fig. 6J), suggests that another domain is essential for the recruitment of Baz oligomers. Finally, the identification of an up to now undescribed protein (complex) binding oligomerized Baz / Par-complex remains a task for future studies.

Supplemental figures

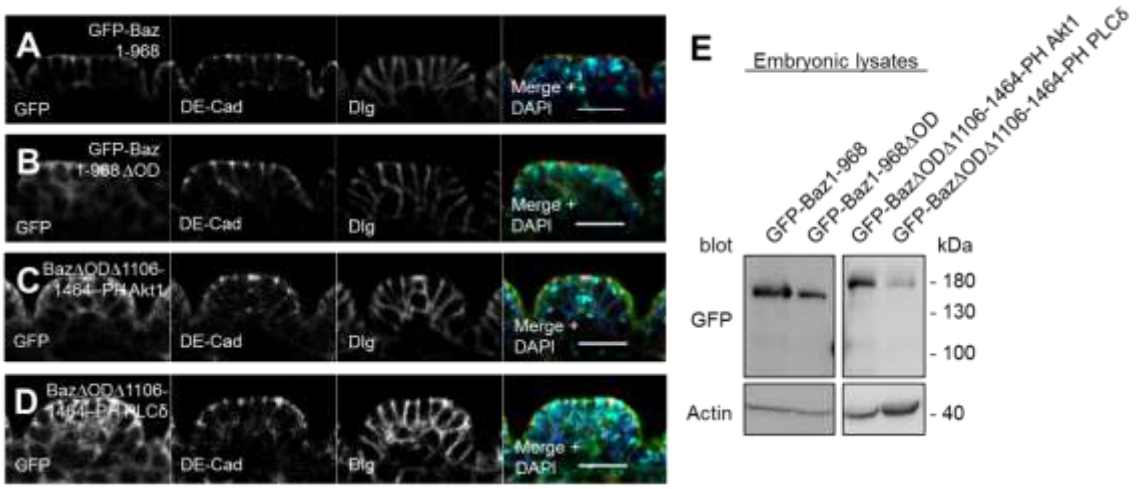

Supplemental Fig. 4.1: Localization of Baz variants in the embryonic epidermis. (A-D) Immunostainings of different GFP-Baz variants in the embryonic epidermis. All transgenes were expressed with the *ubiquitin* promotor in a wild type background. GFP (green), DE-Cad (red) and Dlg (blue) were stained. (A) GFP-Baz1-968 localizes mainly at the apical junctions with some baso-lateral mislocalization. (B) Mutation of the OD domain in this truncated protein causes a cytoplasmic accumulation of GFP-Baz1-968ΔOD. (C, D) Chimeric proteins that carry the pleckstrin homology (PH) domains of either human PLCδ or Akt1 fused to the C-terminus GFP-BazΔOD1-1105 promote a cortical localization in the embryonic epidermis. (E) Western blot of embryonic lysates of the Baz variants (A-D). The Baz variants were detected with a GFP antibody and Actin was used as a loading control. Scale bars are 10 µm

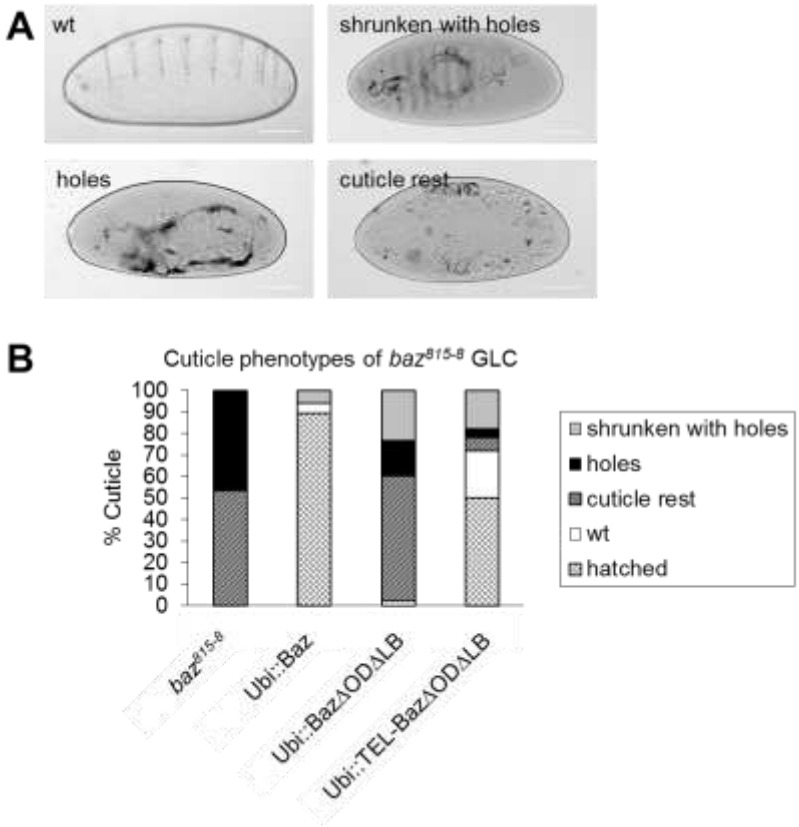

Supplemental Fig. 4.2: Cuticle phenotypes of Baz variants. (A) Cuticle phenotypes were classified into the four categories wt, shrunken with holes, holes and cuticle rests. (B) The cuticle phenotypes of *baz*$^{818-8}$ germ line clones that express different Baz variants with the *ubiquitin* promoter were quantified (n=300 per genotype). Embryos that normally developed and hatched are also included as "hatched". *baz*$^{818-8}$ germ line clones display holes or cuticle rests. Embryos that express Baz-OneS hatch to a large extend (89,5%) or display either wt or shrunken with hole phenotypes. No embryos hatch upon the expression of BazΔODΔLB-OneS. Most embryos have either cuticle rests or holes phenotypes (58,1 and 16,3%, respectively). Nevertheless, some embryos develop further and have a wt or shrunken with holes phenotype (2,3 and 23,3%, respectively). The chimeric TEL-BazΔODΔLB-OneS protein rescues the BazΔODΔLB phenotypes to a large extent as half of the embryos hatch (50,2 %) or have either wt or shrunken with holes phenotypes (21,9 and 17,9%, respectively). Scale bars are 200µm

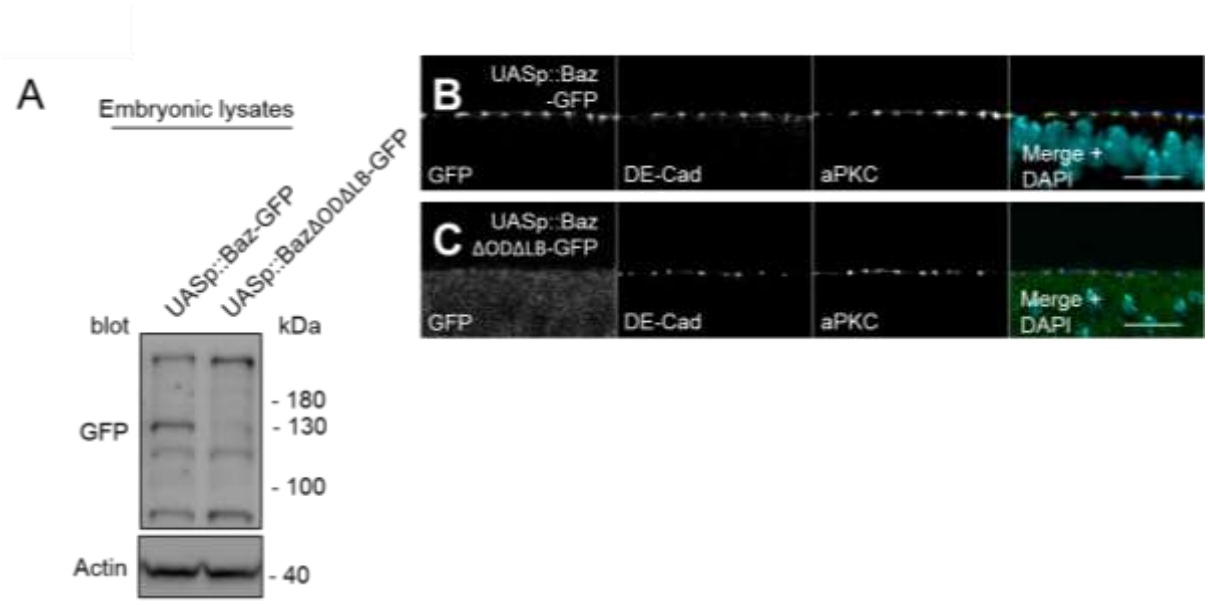

Supplemental Fig. 4.3: Expression of Baz variants with the UAS/Gal4-system. (A) Western blot of embryonic lysates from embryos that express Baz-GFP and BazΔODΔLB-GFP with the *UASp* promotor, driven by *mat-Tub::Gal4*. The Baz variants were detected with a GFP antibody and Actin was used as a loading control. (B, C) Immunostaining of Baz variants (green), DE-Cad (red) and aPKC (blue) in the embryonic epidermis. (B) Baz-GFP localizes at the apical junction, (C) whereas BazΔODΔLB-GFP displays a diffuse cytoplasmic localization. Scale bars are 10µm

Chapter 4: Structural analysis of the Par3 - Par6 interaction

Structural basis for the interaction between the cell polarity proteins Par3 and Par6

Authors: Fabian A. Renschler, Susanne R. Bruekner, Paulin L. Salomon, Amrita Mukherjee, **Lars Kullmann**, Mira C. Schütz-Stoffregen, Christine Henzler, Tony Pawson, Michael P. Krahn and Silke Wiesner.

Personal contributions: Preparation of *Drosophila* embryos for immunofluorescence, S2R cell culture experiments, data analysis and discussion of results

Polarity is a fundamental property of most cell types. The Par protein complex is a major driving force in creating asymmetrically localized protein networks and consists of atypical protein kinase C (aPKC), Par3, and Par6. Dysfunction of this complex causes developmental abnormalities and diseases such as cancer. However, how Par3 interacts with Par6 has remained enigmatic. Here, we identified a PDZ domain-binding motif (PBM) in Par6 that was essential for Par3 interaction *in vitro* and Par3-mediated membrane localization of Par6 in cultured cells. In fly embryos, we observed that the PBM functions in redundancy with the PDZ domain to target Par6 to the cortex of epithelial cells. Our structural analyses by x-ray crystallography and NMR spectroscopy showed that both the Par3 PDZ1 and PDZ3 domains but not the PDZ2 engage in canonical PDZ:PBM interactions with the Par6 motif that we identified. Par3 thus has the potential to recruit two Par6 proteins simultaneously. This may facilitate the assembly of polarity protein networks through multivalent PDZ domain interactions.

Introduction

Most cell types in multicellular organisms require an unequal distribution of proteins, lipids and mRNA for their function (Nelson, 2003). This phenomenon is referred to as cell polarity. During development, the differential segregation of cell fate determinants (anterior-posterior polarity) forms the basis for asymmetric cell division and ultimately the generation of body axes and cell diversity. In differentiated cells, partitioning of the cell membrane into functionally discrete domains enables cells to execute their specialized functions within an organism. Epithelia are a classic example of polarized cells and display an apico-basal polarity. While the apical side faces the exterior or lumen, the basal domain is directed towards the interior extracellular matrix and interstitial space in tissues and organs. The lateral cell surface allows neighboring epithelial cells to adhere and to communicate through cell-cell junctions. However, epithelial cells can also lose their polarity and acquire a migratory, mesenchymal character. While this process is vital for embryonic development and tissue repair, it is also adversely a key event in cancer metastasis. Elucidating the basic mechanisms underlying cell polarity thus has broad implications for our understanding of developmental and oncogenic processes.

Although polarized cells vary substantially in their morphology and function, polarity depends in all cell types on the Par (*par*titioning-defective) protein complex that is conserved across the animal phyla (Ohno, 2001). The Par complex constitutes the major molecular machinery for creating the mutually exclusive signaling networks that cover large areas of the cell cortex in all polarized cells. In epithelia, the Par complex is a key polarity regulator at the apical surface and engages in intricate signaling networks with the Crumbs complex and cell adhesion proteins such as E-cadherin and nectins (Shotgun (Shg) and Echinoid (Ed), respectively, in *Drosophila*) to form and maintain cell junctions (Nelson, 2003; Tepass, 2012).

The Par complex comprises atypical protein kinase C (aPKC) and two scaffolding proteins, Par3 (Bazooka (Baz) in *Drosophila*) and Par6 (Fig. 5.1A). While a single set of genes encodes the Par complex in invertebrates, this gene family has expanded to two Par3 (Par3 and Par3L), two aPKC (PKCλ/ι and PKCζ) and three Par6 (Par6α, Par6β and Par6γ) genes in vertebrates (Noda *et al.*, 2001; Gao *et al.*, 2002; Suzuki *et al.*, 2003). Par6 and aPKC hetero-dimerize with high affinity *via* their N-terminal PB1 (Phox and Bem1) domains (Fig. 5.1A) (Suzuki *et al.*, 2001; Hirano *et al.*, 2005). In addition, Par6 contains a Crib (Cdc42/Rac interactive binding) motif directly preceding a PDZ protein-protein interaction domain. Par3

contains an N-terminal PB1-like homo-oligomerization domain (NTD) (Zhang *et al.*, 2013a), three central PDZ domains and a C-terminal region with an aPKC phosphorylation site (Nagai-Tamai *et al.*, 2002; Krahn *et al.*, 2010b; Morais-de-Sá *et al.*, 2010; Soriano *et al.*, 2016). Whether Par3 interacts directly with Par6 has remained controversial. The Par3 PDZ1 domain has been described to hetero-dimerize with the Par6 Crib-PDZ domain (Lin *et al.*, 2000; Joberty *et al.*, 2000; Li *et al.*, 2010b) (Fig. 5.1A). However, these reports disagree on whether the Par6 Crib motif is essential for the Par3:Par6 interaction. Moreover, the *in vivo* relevance of this interaction has been debated (Li *et al.*, 2010b), and lastly the Par3:Par6 interaction has been reported to be indirect, requiring aPKC as a linker molecule (Suzuki *et al.*, 2001; Nagai-Tamai *et al.*, 2002). Given these controversial observations, we sought to investigate the mechanism of Par3:Par6 association on a structural and functional level.

PDZ domain interactions are a recurring theme in polarity and cell-cell adhesion protein networks. PDZ domains fold into a six-stranded antiparallel β-sheet capped by two α-helices (Morais Cabral *et al.*, 1996) and predominantly bind with low affinity (typically in the μM range (Wiedemann *et al.*, 2004; Stiffler *et al.*, 2007)) to short (4-15 amino acids (aa)), disordered sequences at the C-termini of target proteins, so-called PDZ-binding motifs (PBMs). This interaction results in an augmentation of the PDZ β-sheet by an antiparallel β-strand formed by the PBM. The four C-terminal residues constitute the specificity-determining core PBM (Appleton *et al.*, 2006) that can be categorized into three classes depending on the aa at the -2 position relative to the C-terminus: X-[S/T]-X-φ-COO^- (class I), X-φ-X-φ-COO^- (class II) and X-[D/E]-X-φ-COO^- (class III), with X being any aa and φ being a hydrophobic residue (Songyang *et al.*, 1997). In addition, PDZ domains can recognize internal peptide sequences (Penkert *et al.*, 2004) or homo- or hetero-dimerize in some cases (Lin *et al.*, 2000; Joberty *et al.*, 2000; Li *et al.*, 2010b).

Here, we uncover the molecular basis of the Par3:Par6 interaction. We have identified a previously unrecognized, highly conserved PBM in Par6 that is important for Par6 localization *in vivo* and essential for Par3:Par6 interaction *in vitro*. We find that both the Par3 PDZ1 and PDZ3 but not the PDZ2 domain can associate through canonical PDZ:PBM interactions with the Par6 PBM and show that one Par3 protein has the potential to recruit two Par6 molecules simultaneously. *In vivo*, we find that the Par6 PBM is critical for Par3-mediated membrane recruitment of Par6 in cultured Drosophila Schneider cells (S2R) and plays a role in Par6 localization to the cell cortex in fly embryonic epidermal cells. In sum, our results provide important structural and functional details on the role of Par3 and Par6 in organizing polarity complexes.

Methods

Reagents and Constructs

Par3 and Par6 constructs were cloned from *C. elegans* cDNA, S2R cell cDNA or a synthetic gene fragment (LifeTechnologies) containing the Par3 PDZ domains (*Drosophila melanogaster*), and pK-myc-Par3b (*Hs*. Par3) and pK-myc-Par6C (*Hs*. Par6α) vectors purchased from Addgene (plasmid #19388 and #15474). For NMR studies, gene fragments amplified by PCR were cloned into the following vectors: pETZ2.1a (His_6-Z domain-TEV) for *Ce*. Par3 and Par6 constructs; pET-M30 (His_6-GST-TEV) for *Dm*. Par3 PDZ constructs; pET-M41 (His_6-MBP-TEV) for the *Dm*. Par3 PDZ1:Par6 PBM fusion, *Dm*. Par6 PDZ and Crib-PDZ and *Hs*. Par3 PDZ domains and the *Hs*. Par3:Par6α PBM fusion constructs; pRTDuet-GB1 (His_6-GB1-TEV) for all Par6 and Shg PBM peptides. For GST pull down experiments, a gene fragment containing the three *Dm*. Par3 PDZ domains was cloned into a pETM30-HA (His_6-GST-TEV-HA) vector, while full-length and truncated *Dm*. Par6 constructs were cloned into a pET-M11-Sumo (His_6-Sumo-TEV) vector.

For S2R cell transfection, *Dm*. Par3 and *Dm*. Par6 were cloned into pENTR vectors. Site-directed mutagenesis was carried out with the Par6 pENTR vector as DNA template using the following primers:

Par6 ΔPDZ: 5’-GTGCCGGAAACGCATGGTGGAGGTGGAGGTCCGGCCAATCAGCGC-3’

Par6 ΔPBM: 5’-ACGATAATGGCCAGCGATTAAATCGATGGAGTGCTGCATTTG-3’.

Par3 and wild-type and mutant Par6 variants were subsequently subcloned into pUGW and pURW vectors of the *Drosophila* Gateway Collection (DGRC) (Sen *et al.*, 2012), respectively. For co-immunoprecipitation studies, the Myc-tag in the pK-myc-Par3b vector was replaced by a Flag-tag using QuikChange mutagenesis. All deletions in the *Hs*. Par6α gene were generated by QuikChange mutagenesis using the pK-myc-Par6C vector as DNA template. For a complete list of constructs, see Supplemental Table 5.3.

Expression and purification of recombinant proteins

All recombinant proteins were expressed in *E. coli* BL21-CodonPlus (DE3) RIL cells (Stratagene) and purified by Ni-affinity and size-exclusion chromatography. To facilitate peptide production, the Par6 and Shg PBMs were fused at their N-termini to the immunoglobulin binding domain B1 of streptococcal protein G (GB1) domain followed by a

TEV protease cleavage site. For all NMR binding experiments, non-specific binding of GB1 alone was tested. For NMR studies, unlabeled His_6-GB1-Par6 and His_6-GB1-Shg peptides or *dm*Par3 PDZ domains were expressed in LB medium, while ^{15}N- or ^{13}C,^{15}N-labeled His_6-GB1-Shg, Par3 PDZ or Par6 (Crib-)PDZ domains were expressed in M9 minimal medium with $^{15}NH_4Cl$ or $^{15}NH_4Cl$ and ^{13}C-glucose as sole sources of nitrogen and carbon. All NMR constructs were buffer exchanged into NMR buffer (20 mM Na phosphate pH 6.5 or 7.5, 150 mM NaCl, 1 mM DTT, and 0.03% NaN_3) for triple resonance and CSP experiments.
Proteins for pull down experiments were expressed as His_6-GST-HA-tagged *Dm.* Par3 and His_6-Sumo-tagged *Dm.* Par6 proteins in *E. coli* BL21-CodonPlus (DE3) RIL cells (Stratagene) in LB medium and purified by Ni-affinity chromatography. Subsequently, buffer was exchanged by dialysis to 50 mM Na phosphate pH 7.5, 150 mM NaCl, 1 mM DTT, 10 % glycerol for Par6 proteins or to 20 mM Na phosphate pH 6.5, 150 mM NaCl, 1 mM DTT, and 10 % glycerol for Par3 proteins.

Pull down assays

Dm. Par3 proteins containing an N-terminal His_6-GST-HA-tag were incubated with glutathione beads (Macherey-Nagel) at 1 µM concentration together with 65 µM *Dm.* Par6 proteins that contained an N-terminal His_6-Sumo-tag for 1 h at 4 °C in PD buffer (50 mM Na phosphate pH 7.5, 150 mM NaCl, 10% glycerol, 2 mM DTT). The beads were washed four times with PD buffer and specifically bound proteins eluted with PD buffer supplemented with 25 mM reduced GSH. Eluted proteins were precipitated with 10% (w/v) TCA (Sigma) on ice followed by centrifugation. Protein pellets were resuspended in SDS loading buffer, resolved by SDS-PAGE and detected by Coomassie staining.

S2R cell culture

Immunostainings of transfected Schneider 2R cells was carried out as previously described (Krahn *et al.*, 2010b). In brief, S2R cells were transfected using FUGENE (Promega) with Ubi::GFP-Par6 variants alone or together with Ubi::RFP-Baz. Cells were fixed with paraformaldehyde and imaged with a Zeiss LSM 710 Meta confocal microscope. For RNAi-mediated downregulation of aPKC was performed as described (Krahn *et al.*, 2009). In brief, a ~ 300bp dsRNA fragment was taken up by the cells and processed to several siRNAs. One dsRNA thus results in several siRNAs and thereby reduces the probability of off-targets. The efficiency of dsRNA-mediated gene knock down of aPKC was confirmed by a Western blot of S2R cell lysates using aPKC (1:1000, Santa Cruz sc-216, 1:1000) and mouse actin (1:1000,

Santa Cruz sc-47778) antibodies. The following oligonucleotides were used to amplify a fragment of aPKC mRNA for *in vitro* transcription into dsRNA:
aPKC-dsRNA-F: 5'-ACTTCGCGTTCTCCGC-3',
aPKC-dsRNA-R: 5'-TTGCTAGCTGGGTAAAATATTTTGA-3'.

HEK293T cell culture and co-immunoprecipitation

HEK293T cells were transfected with N-terminally Flag-tagged *Hs.* Par3 in a pKFlag and N-terminally Myc-tagged *Hs.* Par6α in a pKMyc expression vector using Lipofectamin (Invitrogen), grown in DMEM supplemented with 10% Fetal Bovine Serum (Invitrogen), 2 mM L-glutamine (Invitrogen), penicillin (Invitrogen) and streptomycin (Invitrogen) and harvested three days after transfection. Cells were lysed in NET buffer (50 mM Tris-HCl pH 8.0, 150 mM NaCl, 0.1% (w/v) Triton X-100, 1 mM EDTA) supplemented with Proteinase Inhibitor Cocktail (Roche). The supernatants were incubated with Flag M2 antibody (2 ug/mg cell lysate) and subsequently with GammaBind Plus Sepharose (GE Healthcare) for 1 h each at 4 °C. The beads were washed three times with NET buffer and once with Triton-free NET buffer. Immunoprecipitated proteins were eluted with SDS loading buffer, separated by SDS-PAGE and immunoblotted using mouse Flag M2 (1:1000) (Sigma) as primary and HRP-coupled mouse IgG (1:10.000) as secondary antibody (ThermoScientific) or mouse Myc-HRP (1:5000) (LifeTechnologies) antibody. Western blots were imaged by chemiluminescence.

Fly stocks and genetics

Fly stocks were cultured on standard cornmeal agar food and maintained at 25 °C. Transgenic flies of Ubi::GFP-Par6 variants were established using the Phi-C31-Integrase system with attP40 in a wild-type background (Groth *et al.*, 2004). Fly embryo lysates were applied to SDS-PAGE and immuno-blotted using rabbit GFP (1:500, sc8334, Santa Cruz) and mouse actin (1:1000, Santa Cruz sc-47778) antibodies to ensure uniform expression of the Par6 mutants. Western blots were imaged by chemiluminescence. To evaluate the function of GFP-Par6 and GFP-Par6 ΔPDZ, ΔPBM and ΔPDZΔPBM mutants in a *Par6*-null background, the transgenes were backcrossed into a homozygous *par6* $^{\Delta 226}$ mutant background (Petronczki and Knoblich, 2001). However, only the wild-type and ΔPBM transgenes can rescue the embryonic lethality of *par6*$^{\Delta 226}$ mutant flies and be kept as stable stocks.

Immunohistochemistry

Drosophila stage 6-7 or stage 11 embryos were fixed in 4% formaldehyde, phosphate buffer

pH 7.4 as previously described (Sen *et al.*, 2012). The primary antibodies used for indirect immunofluorescence were as follows: mouse aPKC (PKCζ, 1:500, sc17781, Santa Cruz), rabbit GFP (1:500, sc8334, Santa Cruz) and guinea pig Baz (1:500). Secondary antibodies conjugated with Alexa 488, Alexa 568 and Alexa 647 (Life Technologies) were used at 1:400. Images of the epidermis were taken from stage 11 embryos on a Zeiss LSM 710 Meta confocal microscope or at stage 6-7 on a Leica SP8 confocal microscope. For correlation analysis, the images displayed in Fig. 5.3 and Supplemental Fig. 5.6 were partitioned in three regions covering almost the entire image. Pearson's correlation coefficients were estimated after automatic thresholding using the Costes' approach as implemented in the JACoP v2.0 plugin of ImageJ (Fiji) (Costes *et al.*, 2004; Bolte and Cordelières, 2006; Schindelin *et al.*, 2012).

NMR spectroscopy

CSP studies were performed with 75-100 μM samples of ^{15}N-labeled protein in NMR buffer (20 mM Na phosphate pH 6.5 (individual PDZ domains or Shg PBM) or 7.5, 150 mM NaCl, 1 mM DTT, and 0.03% NaN_3) by recording ^{1}H,^{15}N-HSQC experiments on a 600 MHz Bruker Avance-III spectrometer at 20 °C for the *Dm*. and *Ce*. Par3 and Par6 PDZ domains and at 30 °C for the human proteins. For CSP studies with the *dm*Par3 PDZ1-3 Δβ2-3loop module, we recorded ^{1}H,^{15}N-TROSY experiments at 600 MHz and 30 °C in 20 mM Na phosphate pH 7.5, 150 mM NaCl and 1 mM DTT. Backbone resonance assignment for the *Dm*. Par3 PDZ domains was performed at 20 °C and at 25 °C for the *Hs*. Par3 PDZ2 and PDZ3 domains by recording 3D HNCACB, HNCOCACB, CCONH and HNH-NOESY spectra at 600 or 800 MHz. NMR data were processed using the nmrPipe/nmrDraw software suite (Delaglio *et al.*, 1995) and analyzed using XEasy (Bartels *et al.*, 1995) and Sparky (Lee *et al.*, 2015b). Figures displaying NMR spectra were produced with nmrView (onemoonscientific.com). Average CSPs used for binding site mapping were calculated in ppm as $((\Delta\delta_{1H})^2 + (0.25*\Delta\delta_{15N})^2)^{0.5}$, where Δδ is the difference in chemical shift at a nine-fold stoichiometric excess of Par6 PBM *vs*. the respective reference in the absence of ligand. For binding site mapping, a homology model of the *dm*Par3 PDZ3 domain was generated using HHPred (Alva *et al.*, 2016), while PDB entries 2KOM and 2KOH were used for binding site mapping for the *hs*Par3 PDZ2 (Jensen *et al.*, 2010) and PDZ3 (Tyler *et al.*, 2010) domains, respectively. Of note, a highly similar structure exists for the PDZ2 domain of rat Par3 (Wu *et al.*, 2007).

Two-dimensional line shape fitting analysis

$^{1}H,^{15}N$-CSP studies for the *Dm*. Par3 PDZ domains were quantified using TITAN (Waudby *et al.*, 2016) according to instructions and online documentation (http://www.nmr-titan.com and https://bitbucket.org/cwaudby/titan/wiki/Home). Spectra were acquired with 1024 and 128 points in the ^{1}H and ^{15}N dimensions, respectively, and processed with exponential window functions with a line broadening of 4 Hz and 8 Hz. Spectra were zero-filled to 4096 and 1024 points in the ^{1}H and ^{15}N dimensions, respectively. In order to obtain comparable results for different ligands, the same cross peaks were used for the analysis of each PDZ domain (Supplemental Table 5.4). Errors were estimated with bootstrapping statistics on 100 replica. Figures for line shape analyses were prepared with TITAN.

X-ray crystallography

The *Dm*. Par3 PDZ1:Par6 fusion construct was crystallized in 0.1 M BisTris pH 6.5, 2 M $(NH_4)_2SO_4$. Diffraction data were collected at 100 K using a wavelength of 1 Å and a PILATUS 6M-F detector at the beamline PXII of the Swiss Light Source (PSI, Villigen, Switzerland). Data were processed using XDS (Kabsch, 2010) and molecular replacement was performed using Phaser (McCoy *et al.*, 2007). The structure was finalized by iterative manual modeling with Coot (Emsley *et al.*, 2010) and refinement with Phenix (Adams *et al.*, 2010). Each asymmetric unit contains two protein chains with virtually identical conformations (backbone r.m.s.d. of 0.031 Å for the PDZ1 domain and the core PBM). All figures displaying protein structures were generated using PyMOL (http://www.pymol.org/).

Sequence alignment

Multiple sequence alignments were performed with MUSCLE (Edgar, 2004) and displayed with ClustalX (Larkin *et al.*, 2007). The position weighted matrix for the Par6 PBM was created with WebLogo 3.4 (Crooks *et al.*, 2004) using all Par6 PBMs displayed in Supplemental Fig. 4.3. The overall height of the stack indicates the sequence conservation at that position, while the height of a symbol within the stack indicates the relative frequency of each aa at that position.

Results

Par6 contains a PBM that associates with the Par3 PDZ1 domain

In order to elucidate the molecular details of the Par3:Par6 interaction, we performed nuclear magnetic resonance (NMR) binding studies. This method is a powerful tool to study biomolecular interactions (Williamson, 2013; Wiesner and Sprangers, 2015), since the measured chemical shifts of atomic nuclei, that is the peak positions in NMR spectra, are highly sensitive to changes in the local chemical environment. In a standard experiment, an unlabeled binding partner is titrated to an isotope-labeled, NMR-visible protein. This results in concentration-dependent changes of the chemical shifts for the residues contacting the ligand (chemical shift perturbation; CSP) that can be used to obtain dissociation constants (Supplemental Fig. 5.1). Together with chemical shift assignments, this enables the mapping of the ligand binding surface on a protein structure with close to atomic resolution.

Previous studies indicated a hetero-dimerization of the Par3 PDZ1 and the Par6 PDZ domains (Lin *et al.*, 2000; Joberty *et al.*, 2000; Li *et al.*, 2010b). To investigate the mechanism of Par3:Par6 interaction, we first recorded $^{1}H,^{15}N$-correlation NMR spectra of the ^{15}N-labeled PDZ1 domain of human Par3. Surprisingly, we observed that this PDZ domain was largely unfolded in isolation (Supplemental Fig. 5.2A). The domain architectures of the Par complex proteins are highly conserved in metazoans suggesting that Par3 and Par6 interact in a similar manner (Ohno, 2001). We therefore investigated next whether the *Drosophila melanogaster* (*Dm.*) or *Caenorhabditis elegans* (*Ce*.) Par3 PDZ1 domains interact with the respective Par6 PDZ or Crib-PDZ domains. Although both the *Dm*. and *Ce*. Par3 PDZ1 domains were folded in isolation, we observed only very few changes in the NMR spectra of the ^{15}N-labeled Par3 PDZ1 domains upon addition of the respective unlabeled Par6 PDZ (Supplemental Fig. 5.2B,C) or upon addition of the unlabeled Par3 PDZ1 domains to the respective ^{15}N-labeled Par6 Crib-PDZ domains (Supplemental Fig. 5.2D,E). Similarly, neither the *Dm*. Par3 (*dm*Par3) PDZ2 nor the PDZ3 domain induced substantial CSPs in the ^{15}N-labeled *Dm*. Par6 (*dm*Par6) Crib-PDZ domain in our NMR experiments (Supplemental Fig. 5.2F,G). We thus conclude that the Par3 PDZ domains do not associate directly with the Par6 (Crib-)PDZ domain.

In search of an alternative binding mechanism we revisited the Par6 protein sequence and identified a previously unrecognized class II (φ-X-φ-COO^{-}) PBM at its C-terminus (Fig. 5.1B). This motif is highly conserved in metazoans (Fig. 5.1B) with the notable exception of

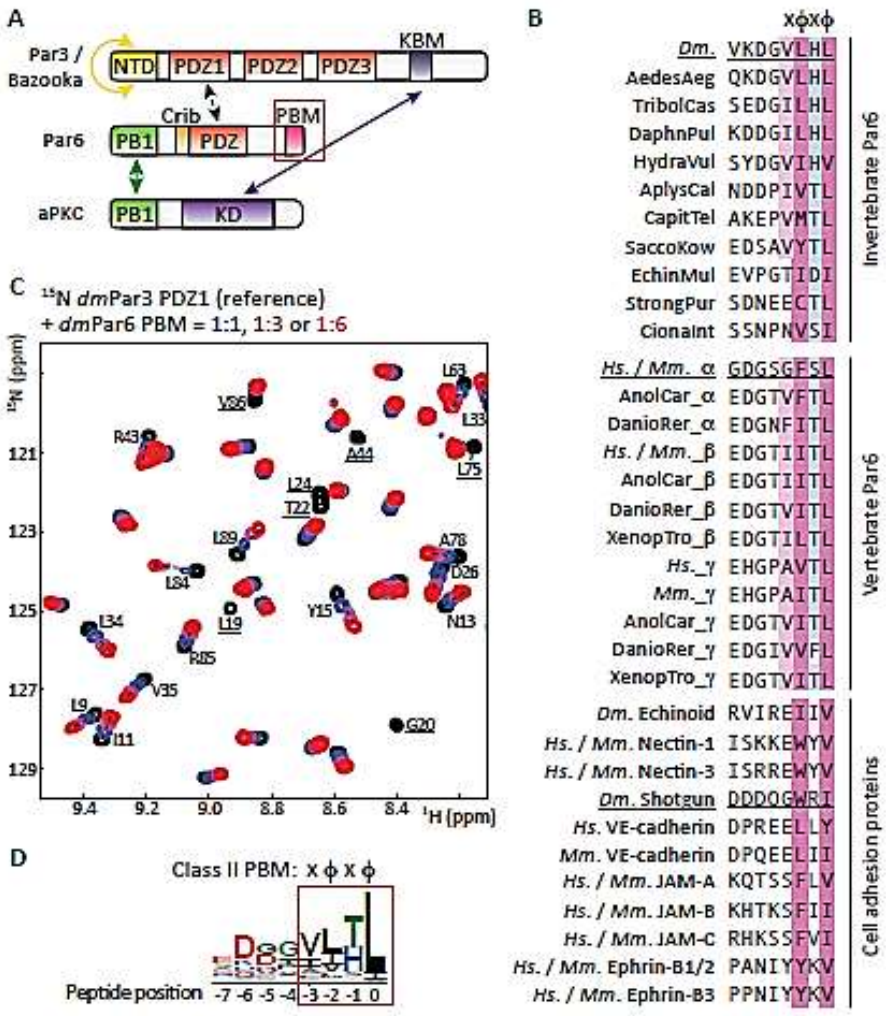

Fig. 5.1: The Par6 C-terminus contains a class II PBM that interacts with the Par3 PDZ1 domain. (A) Reported interactions (shown as arrows) within the Par complex. The controversial PDZ-PDZ interaction is indicated with a dashed arrow. The Par6 PBM identified in this study is boxed in red. (B) Amino acid sequences of the eight C-terminal residues of vertebrate and invertebrate Par6 and known cell adhesion interaction partners (Lin *et al.*, 1999; Itoh *et al.*, 2001; Ebnet *et al.*, 2001; Ebnet *et al.*, 2003; Takekuni *et al.*, 2003; Latorre *et al.*, 2005; Iden *et al.*, 2006; Nakayama *et al.*, 2013). Conserved hydrophobic (φ) residues are in dark pink for the 0 and -2 positions, and in light pink for the -3 position, while polar residues at the -1 position are in blue. Organism abbreviations are expanded in Supplemental Fig. 4.3. PBMs used in this study are underlined. (C) Overlay of a representative region of the ^{1}H,^{15}N-HSQC spectra of the *Dm*. Par3 (*dm*Par3) PDZ1 domain in the absence (black) and presence of increasing stoichiometric amounts of *dm*Par6 PBM as indicated. Dashed lines indicate the directions of chemical shift changes. Chemical shift assignments are shown for the most affected peaks. Peaks broadened beyond detection upon ligand binding are underlined. In CSP figures, residue numbers correspond to the respective NMR or X-ray construct (see Supplemental Table 5.3) for clarity. (D) Sequence conservation of the Par6 PBM shown as position weight matrix (Crooks *et al.*, 2004) (PWM; bottom panel) based on the sequences shown in Supplemental Fig. 5.3.

nematodes (Supplemental Fig. 5.3), and we therefore focused our further efforts on the *Dm*. Par3 and Par6 proteins. To assess whether the identified Par6 PBM can interact with the Par3 PDZ domains we performed NMR CSP experiments. We observed large peak shifts (more than one peak width) and line broadening for numerous residues in the ^{15}N-labeled *dm*Par3 PDZ1 domain upon addition of an unlabeled peptide containing the eight C-terminal residues of *dm*Par6 (Fig. 5.1C) as expected for two proteins that specifically interact with each other. This shows that in the *Drosophila* proteins the Par3 PDZ1 domain can directly interact with the Par6 PBM *in vitro*. In support of this, epithelial cell polarity also critically depends on interactions of the Par3 PDZ domains with cell adhesion proteins through PBMs that are highly similar to the Par6 PBM (Fig. 5.1B,D) (Lin *et al.*, 1999; Itoh *et al.*, 2001; Takekuni *et al.*, 2003; Ebnet *et al.*, 2003; Iden *et al.*, 2006).

The Par6 PBM is important for Par3 interaction *in vitro* and in cell culture

To investigate the importance of the Par6 PBM for Par3 binding, we performed *in vitro* GST pull down experiments using recombinant GST-tagged *dm*Par3 fragment containing all three PDZ domains and Sumo-tagged *dm*Par6 variants (Fig. 5.2A). The Par3 PDZ1-3 domains efficiently pulled down wild-type Par6 (Fig. 5.2B; lane 10). By contrast, deletion of the PBM (ΔPBM) (Fig. 5.2B; lane 12), the region C-terminal of the PDZ domain (PB1-CribPDZ) (Fig. 5.2B; lanes 14) or the region C-terminal of the Crib motif (PB1-Crib) (Fig. 5.2B; lanes 16) essentially abolished Par6 binding to the Par3 PDZ1-3 domains. Of note, GST alone did not pull down any of the Par6 constructs in a control experiment (Fig. 5.2B; lanes 9, 11, 13, and 15). These pull down experiments thus confirm our NMR experiments and show a direct and essential interaction of the Par6 PBM with the Par3 PDZ domains *in vitro*.

To explore whether the Par6 PBM is important for Par3 interaction in cells, we transiently transfected *Drosophila* S2R cells with wild-type GFP-tagged Par6 or deletion constructs (Fig. 5.2A) in the absence (Fig. 5.2C-F) or presence of RFP-tagged Par3 (Fig. 5.2G-J). All Par6 variants were cytosolic in the absence of Par3 (Fig. 5.2C-F). In the presence of Par3 however, wild-type Par6 showed a strong co-localization with Par3 at the cell cortex (Fig. 5.2G). A Par6 mutant lacking the PDZ domain (ΔPDZ) was still recruited to the plasma membrane in the presence of Par3 (Fig. 5.2H) with only a small fraction of Par6 remaining cytosolic. In contrast, membrane targeting of Par6 was strongly reduced when we co-transfected Par3 and

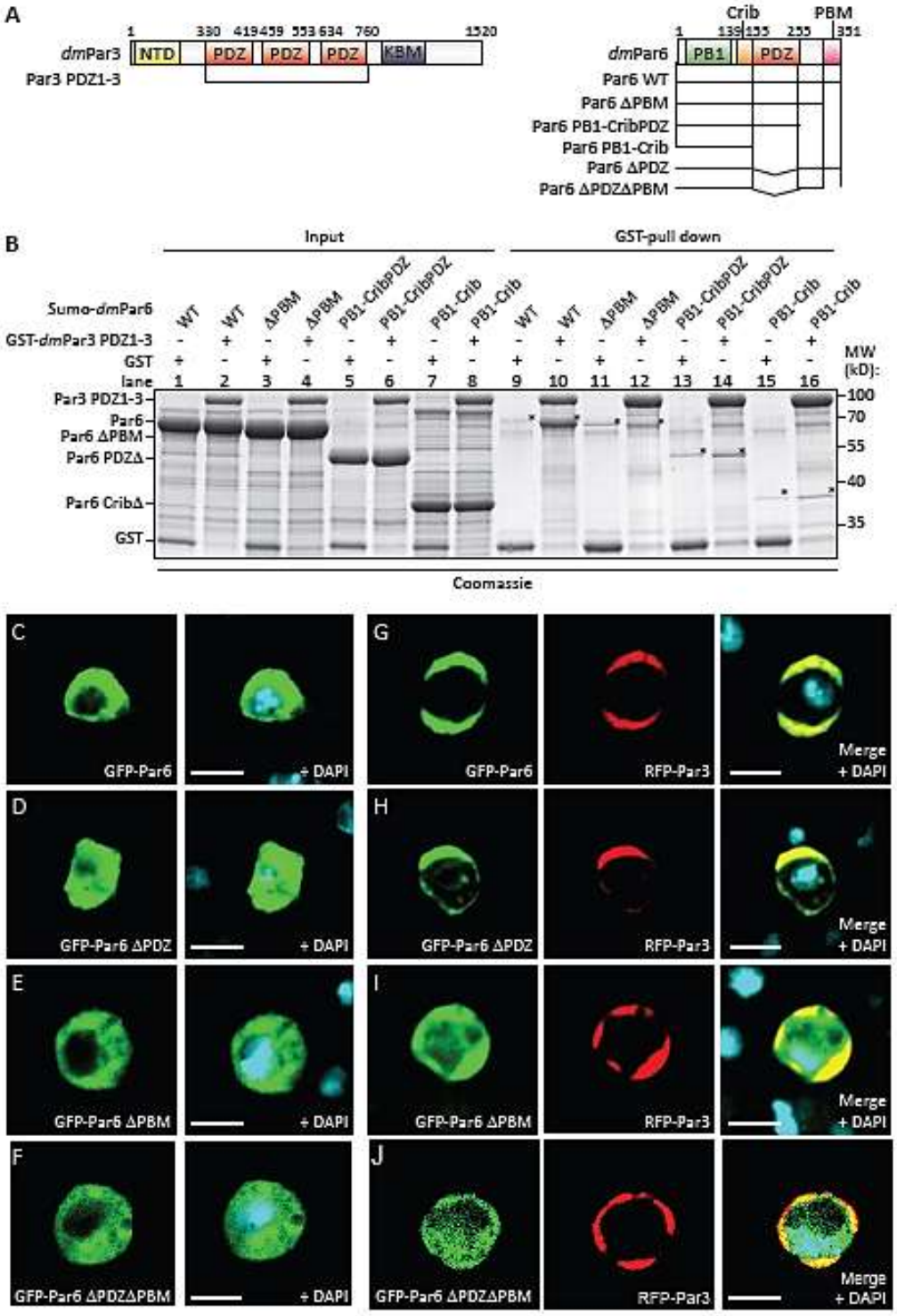

Fig. 5.2: The Par6 PBM is essential for Par3 interaction and Par3-mediated cortical targeting. (A) Schematic representation of the *dm*Par3 and *dm*Par6 constructs used for GST pull down experiments and Par6 recruitment assays. (B) GST pull down experiments using GST or GST-tagged *dm*Par3 PDZ1-3 module incubated with WT or truncated Sumo-tagged *dm*Par6 as indicated. Input and associated Par6 were detected along with GST and GST-*dm*Par3 PDZ1-3 by Coomassie staining. Par6 proteins in the pull downs are highlighted with asterisks. (C-J) Representative fluorescence images of S2R cells transiently transfected with GFP-Par6 variants in the absence (C-F) or presence of RFP-Par3 (G-J). The scale bar corresponds to 5 μm.

a Par6 mutant that lacked the PBM (ΔPBM) (Fig. 5.2I) or a mutant lacking both the PDZ domain and the PBM (ΔPDZΔPBM) (Fig. 5.2J). To assess whether Par3-mediated membrane targeting of Par6 may depend on endogenous aPKC, we performed Par6 recruitment assays in S2R cells where we knocked down aPKC by RNAi (Supplemental Fig. 5.4A). We observed that wild-type Par6 was still efficiently recruited to the cell cortex in the presence of Par3 (Supplemental Fig. 5.4B). In contrast, membrane targeting was compromised for all Par6 mutants (Supplemental Fig. 5.4C-E). aPKC knockdown thus only affects the localization of the Par6 ΔPDZ mutant (Supplemental Fig. 5.4D versus Fig. 5.2H), but not the ΔPBM and ΔPDZΔPBM mutants. This suggests that the PDZ domain may have an additional function in Par6 localization in the presence of aPKC. In line with our NMR binding studies and *in vitro* assays, these *in vivo* results show that the PBM of Par6 plays an important role in the interaction with Par3 and in Par3-mediated localization of Par6 to the cell cortex.

The PBM functions in redundancy with the PDZ domain in Par6 localization *in vivo*

To explore the *in vivo* relevance of our findings, we generated transgenic flies expressing GFP-tagged Par6 under a constitutive promoter (Sen *et al.*, 2012) and analyzed the embryos at stage 11 (Fig. 5.3). As expected, we observed that wild-type GFP-Par6 accumulated predominately at the cell-cell contacts of epidermal cells and co-localized with Par3 and aPKC (Fig. 5.3A). Deletion of the Par6 PBM or the PDZ domain alone mildly but consistently reduced cortical localization of Par6 (Fig. 5.3B,C). In contrast, deletion of both the PDZ domain and the PBM caused an almost complete mislocalization of this Par6 mutant to the cytosol (Fig. 5.3D). Of note, all GFP-Par6 variants were expressed similarly in fly embryos (Supplemental Fig. 5.5A). Thus, both the PDZ domain and the PBM contribute to correct Par6 localization *in vivo* with deletion of both domains resulting in almost complete mislocalization of Par6. Yet, This may reflect an indirect association between Par3 and Par6 *via* aPKC as suggested previously (Suzuki *et al.*, 2001; Nagai-Tamai *et al.*, 2002) and / or Par6 recruitment by other epithelial cell polarity regulators such as Crumbs or Stardust that bind to the Par6 PDZ domain (Hurd *et al.*, 2003b; Penkert *et al.*, 2004; Lemmers *et al.*, 2004; Wang *et al.*, 2004; Kempkens *et al.*, 2006; Whitney *et al.*, 2016).

Of these other polarity regulators Stardust is already expressed early on in fly embryos, whereas Crumbs is only expressed at later stages (Krahn *et al.*, 2010a; Sen *et al.*, 2015). To

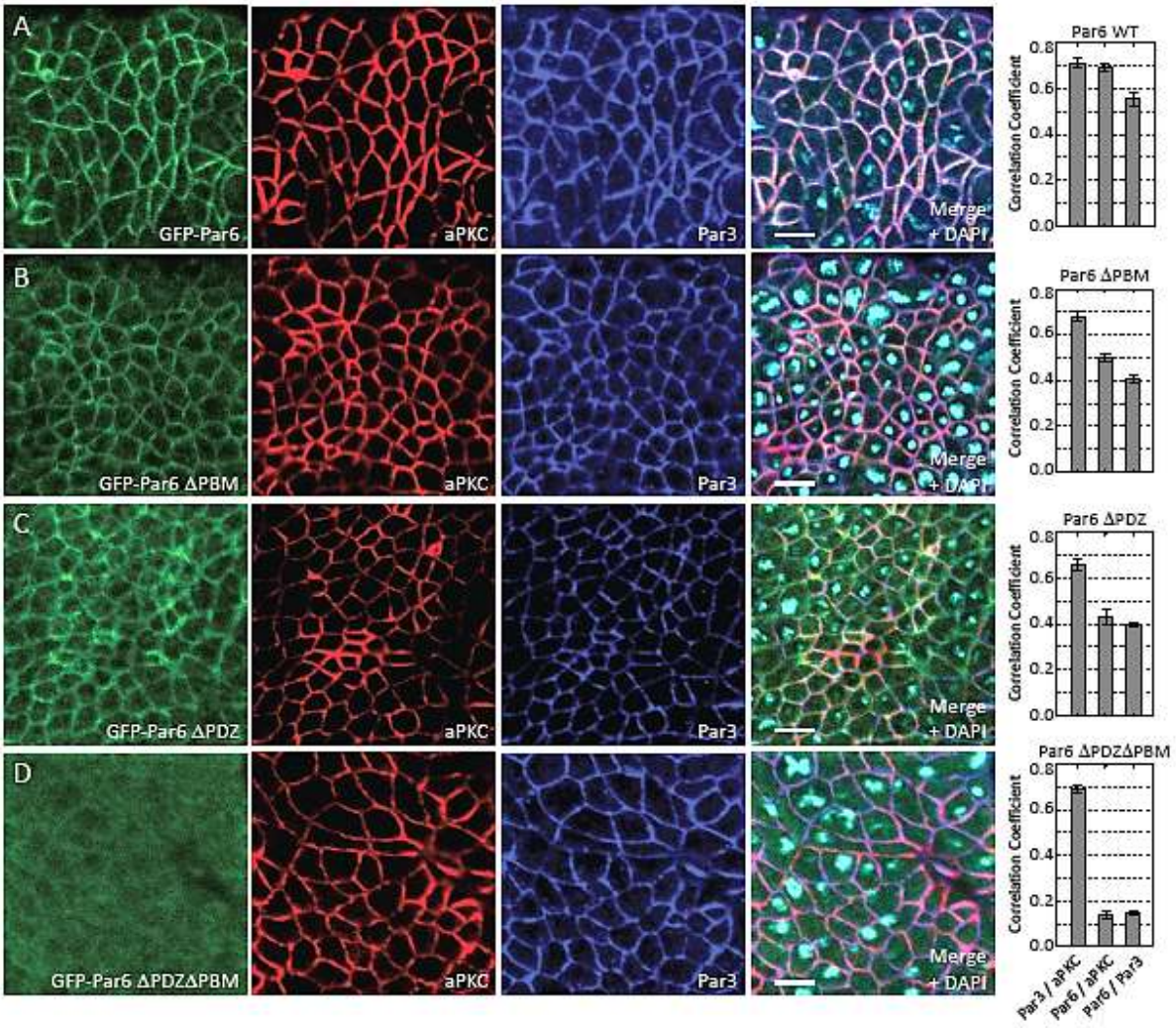

Fig. 5.3: Recruitment of Par6 to the cell cortex in fly epithelia depends on both the PBM and the PDZ domain. (A-D) Localization of aPKC, Par3 and GFP-Par6 variants in the epithelia of fly embryos (stage 11). The scale bar corresponds to 5 µm. Pearson's correlation coefficients (PCC) of Par6, aPKC, and Par3 fluorescence intensities were determined using the Costes' approach (Costes *et al.*, 2004). The average PCCs estimated independently for three different regions of each image are plotted along with their standard deviations (right hand panels).

examine whether the observed localization of the Par6 variants may differ between developmental stages, we analyzed Par6 localization in fly embryos during gastrulation (stage 6-7) and found that Par6 localization at stage 6-7 was highly similar to stage 11 (Supplemental Fig. 5.5B-E). Most notably, the ΔPDZΔPBM mutant resulted in strong Par6 mislocalization both at stage 6-7 and stage 11. This demonstrates that *in vivo* Par6 recruitment to the cell cortex critically depends on both the PDZ domain and the PBM and points to a functional redundancy of these domains in Par6 localization *in vivo*.

In a *par6*-null background (*par6* $^{\Delta 226}$) (Petronczki and Knoblich, 2001), we found that wild-

type GFP-Par6 and GFP-Par6 ΔPBM restored viability as well as aPKC and Par3 localization (Supplemental Fig. 5.6), while the GFP-Par6 ΔPDZ and GFP-Par6 ΔPDZΔPBM could not rescue the lethality of the *par6*-null allele. Similarly to our observations in the wild-type background, lack of the PBM caused in stage 11 embryos a mild localization defect for Par6, but not for Par3 and aPKC (Supplemental Fig. 5.6B). This confirms that the PBM contributes to the correct localization of Par6 *in vivo* under physiological conditions and suggests that it functions in redundancy with the PDZ domain to fully establish epithelial polarity.

Structural analysis of the Drosophila Par3 PDZ1:Par6 PBM complex

Having established the importance of the Par6 PBM for Par3 interaction and Par3-mediated localization *in vitro* and *in vivo*, we sought to gain structural insight into the Par3:Par6 complex. To this end, we crystallized a *Dm*. Par3:Par6 fusion construct comprising the Par3 PDZ1 domain and the C-terminal PBM octapeptide of Par6 (VKDGVLHL; core PBM is underlined) and solved the X-ray structure of the PDZ1:PBM complex (Supplemental Table 5.1). Both the Par3 PDZ1 domain and the Par6 core PBM are well defined with the PDZ1 domain adopting the typical PDZ fold and the core PBM forming the canonical antiparallel β-strand with the PDZ1 β2-strand (Fig. 5.4A, Supplemental Fig. 5.7A). The C-terminal carboxylate group is involved in an extensive hydrogen bond network with the backbone of the PDZ1 β1-2 loop (Fig. 5.4A). The hydrophobic residues at the 0 and -2 positions of the PBM are deeply buried in a hydrophobic pocket formed by the carboxylate binding loop (Leu^{19}), the β2 (Leu^{21}, Ala^{23}, Leu^{24}, Pro^{25}), β3 (Leu^{33}) and β6 (Leu^{84}, Val^{86}) strands and the α2 helix (Val^{71}, Leu^{75}, Leu^{79}) of the PDZ1 domain (Fig. 5.4A, Supplemental Fig. 5.7B). Overall, our structure is highly similar to other PDZ:PBM complexes such as the INADL PDZ3 in complex with a phage display-derived class II PBM peptide (Fig. 5.4B) (Ernst *et al.*, 2014) and Par3 PDZ3:PBM complexes (Supplemental Fig. 5.7C,D) (Feng *et al.*, 2008; Tyler *et al.*, 2010). Outside the core PBM, we observed less well-defined electron density for the Par6 peptide and three residues of the GS-linker (Supplemental Fig. 5.8A,B) indicating an additional antiparallel β-strand formed by the last aa of the GS-linker and the -7 and -6 PBM

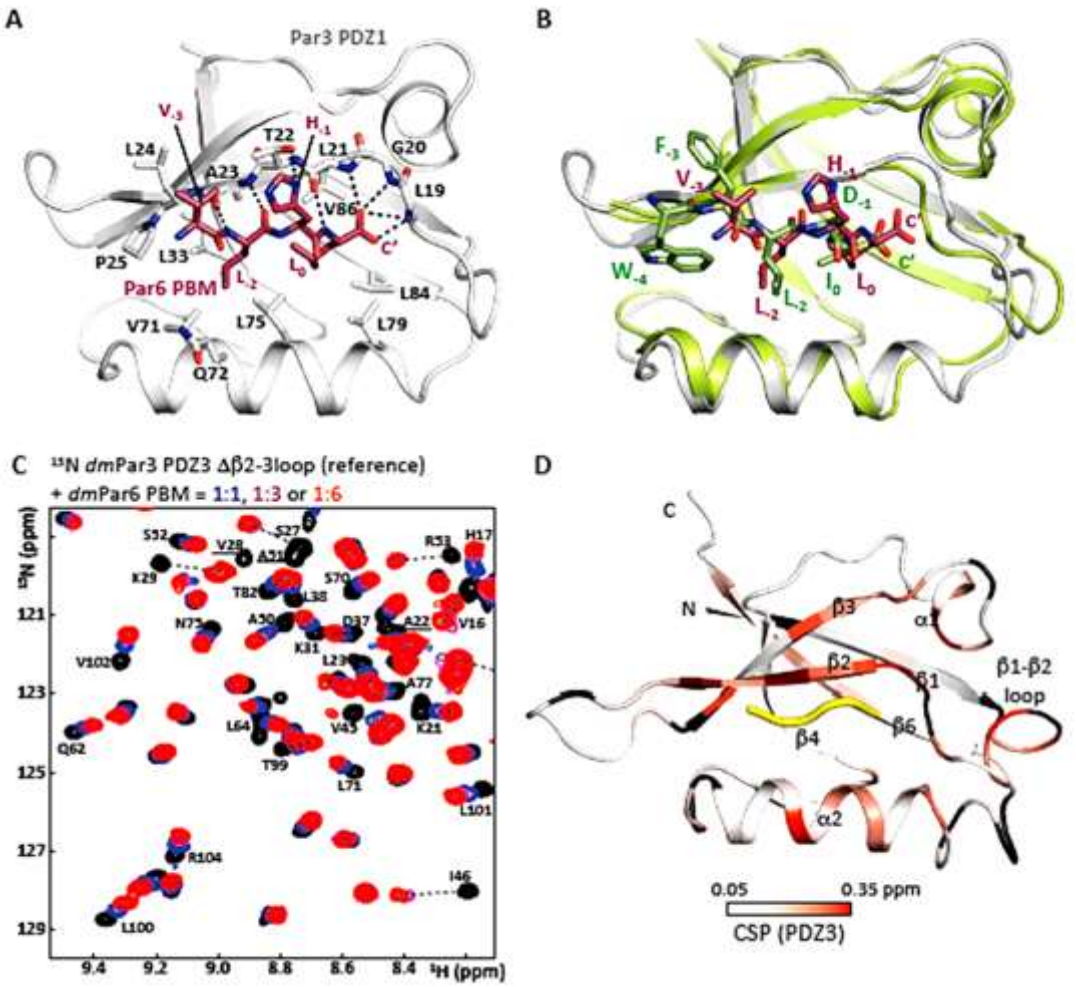

Fig. 5.4: The *Dm.* Par3 PDZ1 and PDZ3 domains interact with Par6 through canonical PDZ:PBM interactions. (A) Interaction network of the Par6 core PBM (dark pink) with the Par3 PDZ1 domain (grey). Residues involved in hydrogen bonds (dashed lines) and side-chain interactions are shown in stick representation with carbon, nitrogen and oxygen atoms colored in grey (PDZ1) / dark-pink (PBM), blue and red, respectively. (B) The Par3 PDZ1 : Par6 PBM complex is highly similar to the INADL PDZ3 in complex with a phage-derived class II PBM peptide (PDB code: 4Q2N, (*39*)) shown in green (backbone r.m.s.d. = 1.64 Å). (C) As Fig. 4.1C, but for the Par3 PDZ3 Δβ2-3loop domain. (D) Binding surface of the *dm*Par6 PBM mapped onto a PDZ3 homology model and colored with a linear gradient from white (CSP ≤ 0.05 ppm; cut-off) to red (CSP = 0.35 ppm). Unassigned residues are colored in dark grey, while residues broadened beyond detection in the PDZ3 are in dark red. The Par6 core PBM is shown in yellow and was modeled by superposition of the *dm*Par3 PDZ1:PBM and PDZ3 structures.

residues. However, the consistently high B-factors (Supplemental Table 5.1, Supplemental Fig. 5.8C,D) strongly suggest that the residues outside the core PBM are not stably structured. To validate key interactions of the Par6 PBM with the Par3 PDZ1 domain in our crystal structure, we substituted each of the three C-terminal positions in the *dm*Par6 peptide with

Ala (Par6 L349A (L_{-2}A), H350A (H_{-1}A) and L351A (L_0A)) and tested the Par3 binding capabilities of the PBM mutants in NMR experiments (Supplemental Fig. 5.8E). Consistent with our crystal structure, both the L_{-2}A and the L_0A mutations led to an almost complete loss of Par6 binding, while the H_{-1}A mutation lessened CSPs in the Par3 PDZ1 domain as compared to the wild-type PBM (Supplemental Fig. 5.8E versus Fig. 5.1C). In sum, our results demonstrate that Par6 associates with Par3 through a canonical PDZ:PBM interaction that crucially depends on the -2 and 0 positions of the Par6 PBM.

The Par3 PDZ1 and PDZ3 domains both recognize the Par6 PBM

We noticed that the residues in the PDZ1 domain contacting the 0 and -2 PBM positions are well-conserved in all three Par3 PDZ domains (Supplemental Fig. 5.9). We therefore also tested the binding specificities of the Par3 PDZ2 and PDZ3 domains towards the Par6 PBM. To this end, we performed NMR binding studies with the individual *dm*Par3 PDZ2 and PDZ3 domains and the *dm*Par6 PBM peptide. In contrast to the PDZ1 domain, we observed virtually no CSPs for the Par3 PDZ2 domain upon addition of the Par6 PBM (Supplemental Fig. 5.10A). The Par3 PDZ2 domain thus possesses binding specificities that are distinct from the Par3 PDZ1 domain.

The PDZ3 domain contains a long, disordered insertion in the β2-3 loop that is unique to *dm*Par3 (Supplemental Fig. 5.9). Since this extension severely compromised spectral quality, we used a PDZ3 domain with a truncated β2-3 loop (PDZ3 Δβ2-3loop) for our NMR studies (Supplemental Fig. 5.9). As for the PDZ1 domain, addition of the Par6 PBM induced numerous, large CSPs in the ^{15}N-labeled PDZ3 Δβ2-3loop (Fig. 5.4C). This demonstrates that the truncated PDZ3 domain is functional and interacts readily with the *dm*Par6 PBM. To map the observed CSPs onto the surface of the PDZ3 domain, we obtained chemical shift assignments for the PDZ3 domain and generated a homology model of the Par3 PDZ3 domain. As the PDZ1 domain, in this model the PDZ3 domain binds the Par6 PBM in a canonical manner mainly involving the carboxylate binding loop, the β2 strand and the α2 helix (Fig. 5.4D).

To obtain quantitative insights into the Par3 PDZ interactions with the Par6 PBM, we determined dissociation constants (K_d values) by NMR line shape fitting for the chemical shift titrations of the *Dm*. Par3 PDZ1 and PDZ3 domains with the Par6 PBMs. Of note, since the PDZ2 domain did exhibited no CSPs upon addition of the Par6 PBM, we did not fit these

data. We found that the Par6 PBM bound to the PDZ1 domain with a moderate affinity of 216 ± 4 μM and to the PDZ3 domain with a tighter affinity of 54 ± 1 μM for the PDZ3 domain (Supplemental Table 5.2, Supplemental Fig. 5.11, 5.12). Next, we quantitatively addressed the importance of the three C-terminal positions in the Par6 PBM for PDZ1 binding (Supplemental Fig. 5.8E and 5.13). We found that mutation of the C-terminal position (L_0A) weakened the affinity of the PDZ1 domain for the Par6 PBM to 2.5 ± 0.4 mM, for the -1 position ($H_{-1}A$) to 964 ± 60 μM and for the -2 position ($L_{-2}A$) to 4.0 ± 1.1 mM, respectively (Supplemental Table 5.2, Supplemental Fig. 5.13). This confirms that these mutations in the core PBM indeed strongly compromise binding to the Par3 PDZ1 domain and that these residues are thus important determinants for the interaction with the Par3 PDZ1 domain.

Overall, dissociation constants of up to a few hundreds of μM have been observed for physiologically relevant PDZ interactions (Stiffler *et al.*, 2007). Consistent with our analyses of cultured S2R cells (Fig. 5.2 and Supplemental Fig. 5.4) and fly embryos (Fig. 5.3 and Supplemental Fig. 5.5-6), this shows that the interaction of the newly identified Par6 PBM plays a role in Par3 PDZ binding *in vitro* and is physiologically relevant *in vivo*.

Par3 can interact with two Par6 proteins simultaneously *in vitro*

In polarized cells, Par complexes form micrometer-sized clusters that cover the apical plasma membrane. Yet, how Par complexes assemble into these sizeable protein networks is largely unknown. A prerequisite for forming higher order networks is that the proteins involved are multivalent, that is they contain multiple independent binding sites, and engage in a multitude of weak (μM-affinity) interactions. To test whether the first and third PDZ domain of Par3 fulfill this requirement, we recorded $^{1}H,^{15}N$-correlation spectra of the ^{15}N-labeled Par3 PDZ1-3 module that contains all three PDZ domains (PDZ1-3 Δβ2-3loop) and examined its Par6 binding capability. In this construct the Δβ2-3 loop in the PDZ3 domain was removed to improve spectral quality (see above). The NMR spectra of the Par3 PDZ1-3 module and the individual PDZ domains superimpose well (Fig. 5.5A-C), and resonance assignments of the individual domains could be transferred to the PDZ1-3 module. This demonstrates that the individual PDZ domains in Par3 are structurally largely independent. Addition of unlabeled Par6 PBM to the PDZ1-3 construct resulted in CSPs comparable to the isolated PDZ domains (Fig. 5.5D-F versus 5.1C, 5.4C, Supplemental Fig. 5.10A). This shows that the Par3 PDZ

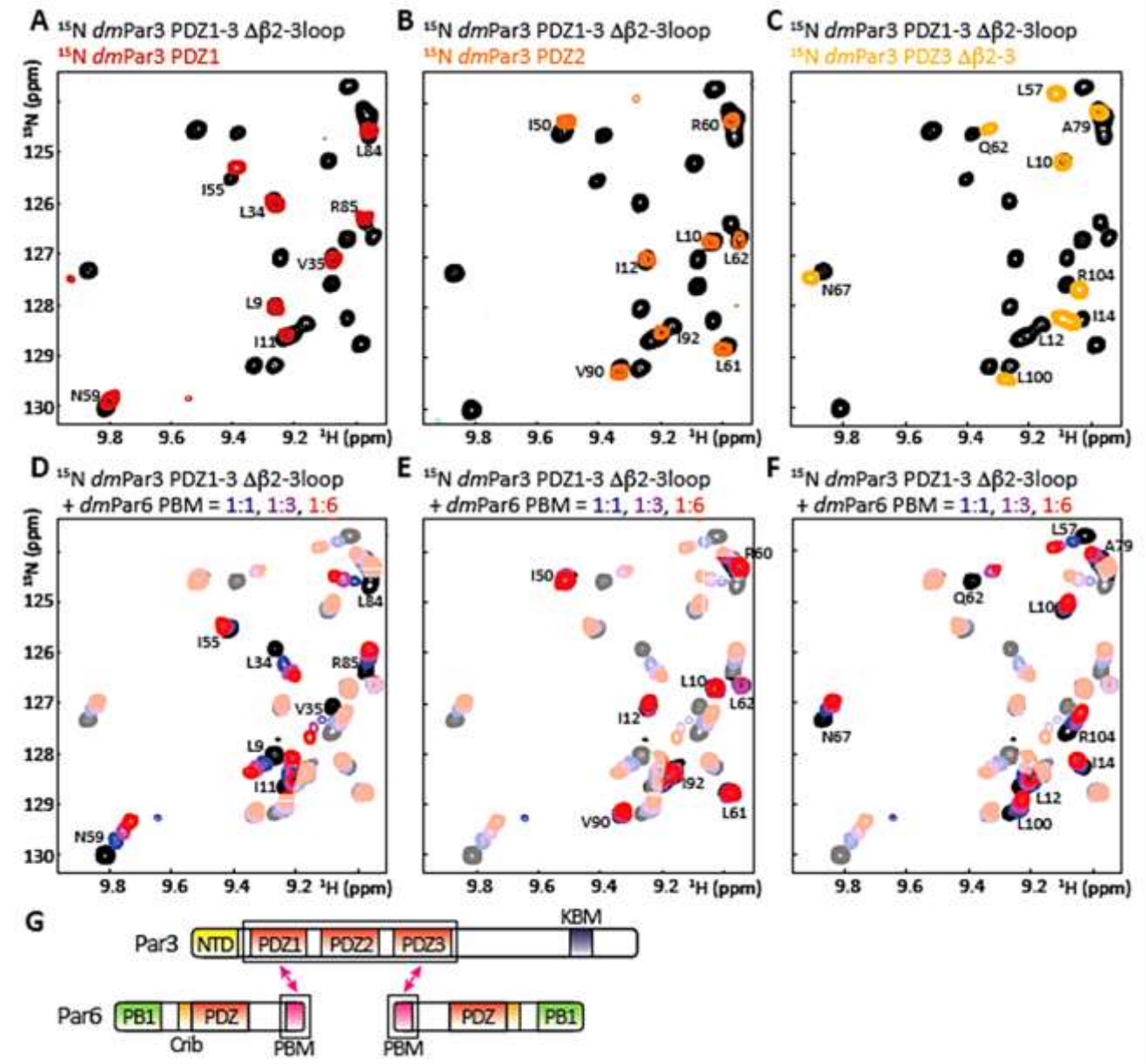

Fig. 5.5: Par3 can interact with two Par6 proteins simultaneously. Overlay of $^{1}H,^{15}N$-TROSY spectra of the Par3 PDZ1-3 Δβ2-3loop module with the isolated PDZ1 (A), PDZ2 (B) and PDZ3 Δβ2-3loop domains (C). (D-F) Overlay of $^{1}H,^{15}N$-TROSY spectra of the Par3 PDZ1-3 Δβ2-3loop module in the absence (black) and presence of *dm*Par6 C-terminal peptide as indicated. Peaks not corresponding to the PDZ1 (D), PDZ2 (E) or PDZ3 Δβ2-3loop (F) domain within the PDZ1-3 module are shown in opaque to highlight the changes of the individual domains within the entire module. Indicated resonance assignments correspond to the respective PDZ domain as shown in the panels on top and correspond to the respective NMR or X-ray construct (Supplemental Table 5.2). (G) Schematic representation of the Par3:Par6 interactions as mapped by NMR spectroscopy highlighting the 1:2 stoichiometry of the complex *in vitro*.

domains act as functionally independent entities within the PDZ1-3 module and that *in vitro* one Par3 protein can simultaneously interact with two Par6 proteins through its PDZ1 and PDZ3 domains (Fig. 5.5G). Par3 thus has the potential to engage in weak, multivalent interactions with Par6 and may thereby promote the assembly of large-scale clusters of Par complexes at the cell membrane *in vivo*.

The Par6 PBM can compete with the PBM of E-cadherin for Par3 binding

Cell adhesion proteins such as cadherins and nectins are well-known interaction partners of Par3 and contain conserved class II PBMs that are highly similar to the Par6 PBM (Fig. 5.1B and Supplemental Fig. 5.7C). In fact, the VE-cadherin PBM interacts with the PDZ3 domain of murine Par3 with a K_d of ~ 6 μM (Tyler *et al.*, 2010) and thus ~ 9-fold (PDZ3) and ~ 36-fold (PDZ1) tighter than its *Dm*. counterparts with the Par6 PBM (Supplemental Table 5.2). To address whether the Par6 PBM could compete with such ligands for Par3 binding, we performed NMR CSP studies with the ^{15}N-labeled *Dm*. Par3 PDZ domains and added increasing amounts of unlabeled Shg PBM to the individual domains. Similarly to the Par6 PBM, both the Par3 PDZ1 (Fig. 5.6A) and PDZ3 (Fig. 5.6B) domains show large CSPs for numerous peaks in the ^{1}H,^{15}N-correlation spectra upon addition of the Shg PBM. In contrast, the PDZ2 domain displayed only few changes (Supplemental Fig. 5.10B). Line shape fitting analyses for the Shg PBM chemical shift titrations of all three *Dm*. Par3 PDZ domains yielded K_d values of 128 ± 4 μM for the PDZ1, 954 ± 45 μM for the PDZ2 and 0.6 ± 0.1 μM for the PDZ3 domain (Supplemental Table 5.2, Supplemental Fig. 5.11C,D, Supplemental Fig. 5.14 and Supplemental Fig. 5.12C,D). The *Dm*. Par3 PDZ domains thus bind tighter to the PBM of Shg than to the Par6 PBM albeit only by a factor of ~ 2 for the PDZ1 domain.

To evaluate whether the PBM of Par6 and Shg compete for binding to the Par3 PDZ1 or PDZ3 domains, we performed a set of NMR experiments on the ^{15}N-labeled Shg PBM. First, we recorded ^{1}H,^{15}N-correlation spectra of the peptide in the presence or absence of unlabeled *Dm*. Par3 PDZ1 or PDZ3 domain. In both cases, this resulted in PDZ:Shg complex formation as indicated by the observed CSPs (Fig. 5.6C,D). Subsequently, we added Par6 PBM to the PDZ:Shg complex in a step-wise manner and observed for both the PDZ domains a release of

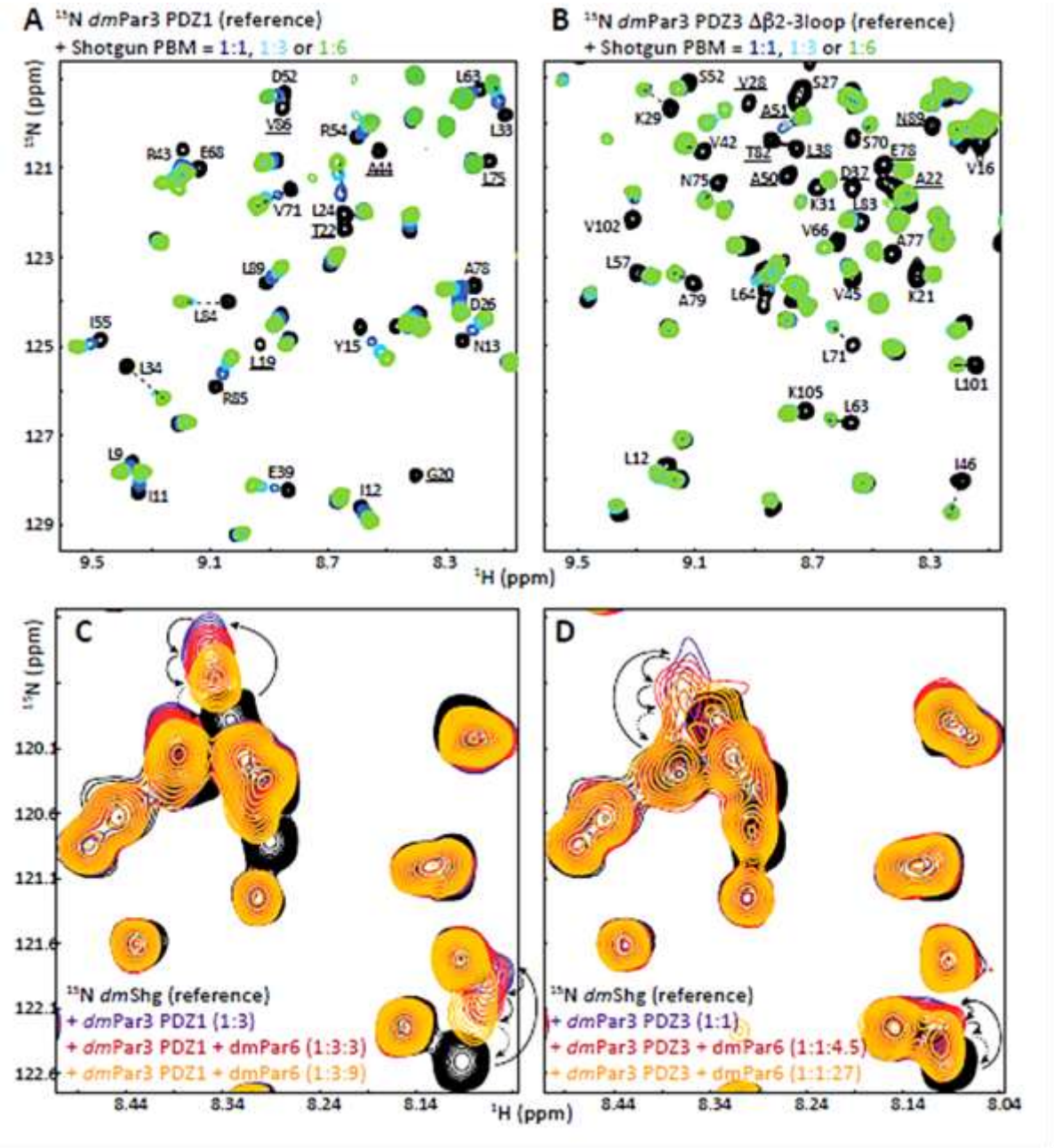

Fig. 5.6: The Par6 PBM can compete with Shg for Par3 binding. (A) Overlay of ^{1}H,^{15}N-HSQC spectra of the *Dm*. Par3 PDZ1 domain in the absence and presence of the Shg PBM peptide as indicated. (B) as (A), but for the *Dm*. Par3 PDZ3 Δβ2-3loop domain. (C) Overlay of ^{1}H,^{15}N-HSQC spectra of the Shg PBM fused to GB1 in the absence (black) or presence of *dm*Par3 PDZ1 domain (purple) and upon step-wise addition of the Par6 PBM (red and orange). Arrows indicate the successive reversal of the chemical shifts from the Shg:PDZ complex towards the unbound Shg PBM. (D) as (C), but for the PDZ3 PDZ3 Δβ2-3loop domain.

the Shg peptide as indicated by chemical shift changes that reverted towards the unbound Shg peptide (Fig. 5.6C,D). This demonstrates that the Par6 PBM can indeed compete with Shg for Par3 PDZ binding. The relatively high stoichiometric amounts of Par6 PBM required to

outcompete the Shg peptide from the PDZ3 domain reflect the large difference in binding affinities (Supplemental Table 5.2). Ultimately, the question of direct competition between the Par6 PBM and other PBM-containing ligands for Par3 binding *in vivo* would require determining the specific subcellular concentrations of Par3, Par6 and other binding partners, the binding affinities within the fully assembled Par complex and the exact chronological order of binding events in cells. These are certainly highly interesting, though challenging topics for future studies.

The PDZ:PBM interaction is conserved in the human Par3 and Par6 proteins

To explore whether the PDZ:PBM interactions that mediate Par3:Par6 association in *Drosophila* are conserved in the human proteins, we co-transfected human embryonic kidney (HEK) 293T cells with Flag-tagged human Par3 (*hs*Par3) and Myc-tagged wild-type or truncated *hs*Par6α. Co-immunoprecipitation (co-IP) experiments with the cell lysates showed that full-length Par6α readily co-precipitated with Par3, while deletion of the Par6α PBM (ΔPBM) abrogated Par3 binding (Fig. 5.7A). In contrast, the amounts of Par6α ΔPDZ that co-immunoprecipitated with Par3 were comparable with wild-type Par6α, while deletion of both the Par6α PDZ domain and the PBM (ΔPDZΔPBM) again abrogated Par3 binding. Consistent with our *in vitro* and *in vivo* data for the *Drosophila* Par3:Par6 interaction, this demonstrates that the Par6 PBM is important also for the interaction of the human proteins.

To examine whether the mode of interaction and the specificities of the individual PDZ domains towards the Par6 PBM are conserved among human and *Drosophila* Par3, we performed NMR binding studies. Since the human Par3 PDZ1 domain is unfolded in isolation (Supplemental Fig. 5.2A), we fused the eight C-terminal residues of *hs*Par6α to the C-terminus of the *hs*Par3 PDZ1 domain separated by a 15-aa GS-linker. This led to a well-dispersed $^{1}H,^{15}N$-correlation spectrum of the ^{15}N-labeled PDZ1:PBM fusion demonstrating that the Par6α PBM induces the folding of the PDZ1 domain and hence interacts with the Par3 PDZ1 domain (Fig. 5.7B). Addition of unlabeled Par6α PBM peptide to the ^{15}N-labeled *hs*Par3 PDZ2 domain resulted in a few, though partially substantial CSPs (Fig. 5.7C, Supplemental Fig. 5.10C) indicating that the human Par3 PDZ2 domain binds to the Par6α PBM. In contrast, the PDZ3 domain displayed numerous, large CSPs in the presence of Par6α

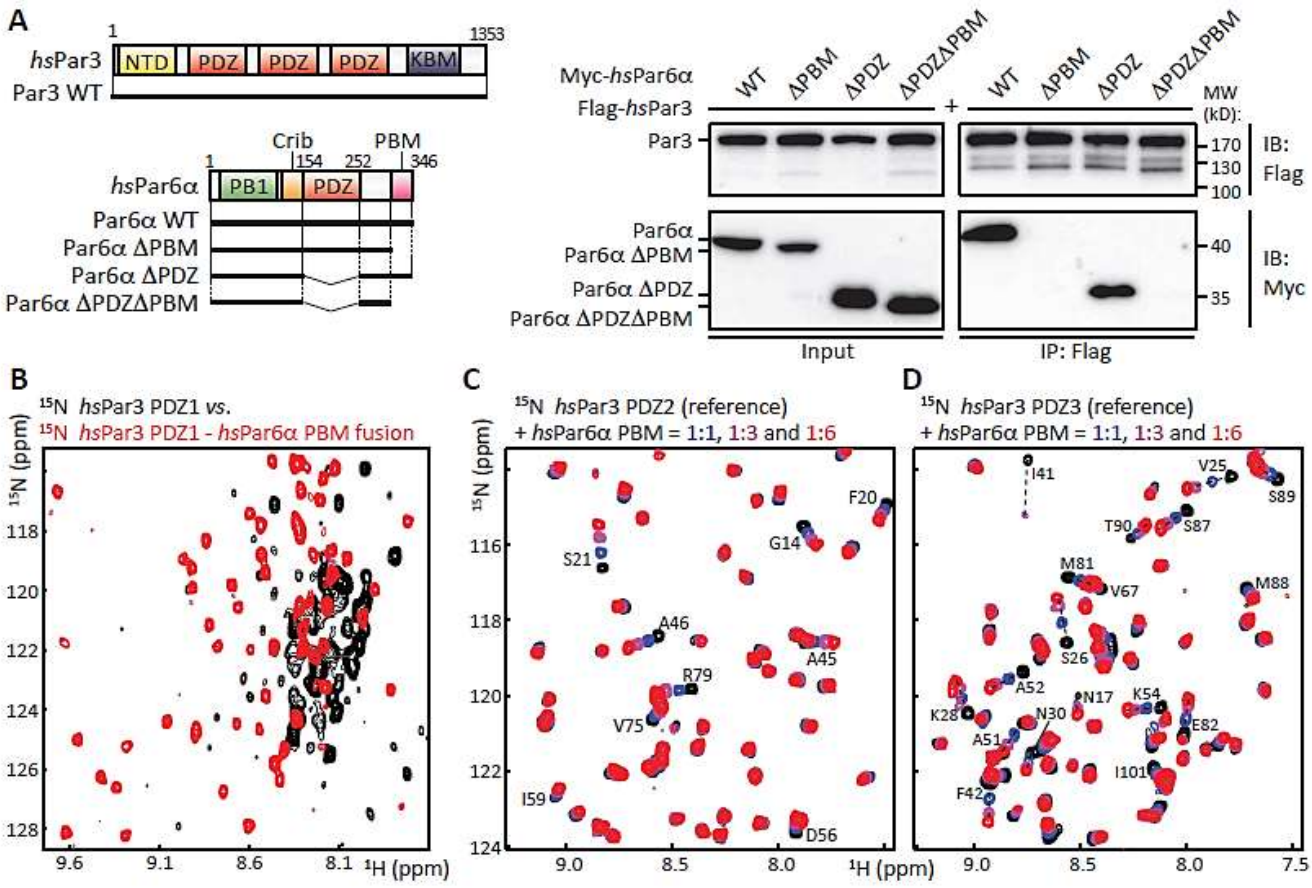

Fig. 5.7: The PDZ:PBM interaction is conserved in the human Par3:Par6 complex. (A) Schematic representation of the *hs*Par3 and *hs*Par6α constructs used for co-immunoprecipitation (IP) experiments (left). Right panel: Cell lysates of HEK293T cells co-transfected with human Flag-tagged Par3 and Myc-tagged Par6α variants were subjected to Flag-antibody IP followed by immunoblotting (IB) with Flag and Myc antibodies. Equal amounts of protein were confirmed by IB as shown (Input). (B) Overlay of ^{1}H,^{15}N-correlation spectra of the *hs*Par3 PDZ1 domain in isolation and fused to the *hs*Par6α PBM. (C,D) Overlay of ^{1}H,^{15}N-correlation spectra of the PDZ2 (C) and the PDZ3 (D) domains in the absence and presence of *hs*Par6α PBM peptide as indicated.

(Fig. 5.7D). Mapping of the observed CSPs on the structures of the human Par3 PDZ2 and PDZ3 domains shows that both domains can engage the Par6α PBM through canonical PDZ:PBM interactions (Supplemental Fig. 5.10C,D). Altogether, these results demonstrate that the Par3 PDZ:Par6 PBM interactions as well as the functions of the Par3 PDZ domains are largely conserved in the human and *Drosophila* proteins.

Discussion

In this study, we have identified a previously unrecognized PDZ-binding motif in Par6 that mediates canonical PDZ:PBM interactions with the PDZ1 and PDZ3 domains of Par3. This interaction mode is conserved amongst the human and *Drosophila* Par3 and Par6 proteins. We demonstrate that the PBM, but not the PDZ domain, of Par6 is essential for interaction with Par3 *in vitro*. Yet, the PBM seems to function in redundancy with the PDZ domain in Par6 localization in fly epithelia, as the individual deletions only mildly reduce cortical localization *in vivo*, and deletion of both the PBM and the PDZ domain are required for almost complete mislocalization of Par6.

Overall, we found no indication of a heterodimerization of the human, *Dm.* or *Ce.* Par3 PDZ domains with the respective Par6 (Crib-)PDZ domain by NMR (Supplemental Fig. 5.2), in GST-pull down (Fig. 5.2B) or co-IP experiments (Fig. 5.7A) nor in recruitment assays in S2R cells (Fig. 5.2D). Our results thus provide important, novel insights into Par complex assembly and contrast previous findings that Par3 and Par6 associate through PDZ:PDZ interaction (Lin *et al.*, 1999; Joberty *et al.*, 2000; Li *et al.*, 2010b). In support of our findings, Par3 associates in epithelial cells with various cell adhesion proteins possessing class II PBMs that are highly similar to the Par6 PBM (Fig. 5.1B) and we show here that the *Dm*. Par3 PDZ1 and PDZ3 domains also interact with the major cell adhesion protein E-cadherin (Shg) (Fig. 5.6A,B). These interactions have been shown to be crucial for the establishment and maintenance of cell junctions and epithelial cell polarity (Lin *et al.*, 1999; Itoh *et al.*, 2001; Takekuni *et al.*, 2003; Ebnet *et al.*, 2003; Iden *et al.*, 2006; Tepass, 2012). Of note, as in the case of Par6, these adhesion protein interactions are conserved among human and *Drosophila* Par3. In sum, this supports the notion that class II PBMs constitute a general binding motif for the Par3 PDZ1 and PDZ3 domains to recruit polarity and cell adhesion proteins for the establishment and maintenance of cell polarity. Nematodes may constitute a notable exception, as not only their Par6 but also their cadherin (HRM-1) proteins lack a detectable, C-terminal PBM (Supplemental Fig. 5.3). Future studies will thus be required to elucidate the exact mechanism of Par3 PDZ interactions and their role in cell polarity in nematodes.

The individual PDZ binding preferences allow for multivalent Par3 interactions

Tandem arrangement of PDZ domains is a well-known mechanism for scaffolding proteins to assemble different components of a signaling cascade through multivalent interactions (Tsunoda *et al.*, 1997). This is based on the fact that interaction domains embedded in proteins can in general fold and function independently (Pawson and Nash, 2003). We find that the isolated Par3 PDZ1 and PDZ3 domains can both independently interact with the Par6 PBM (Fig. 5.5D,F and 5.7B,D) and thus may function in redundancy. Indeed, these functional redundancies allow each Par3 molecule to simultaneously recruit two Par6 proteins *in vitro* (Fig. 5.5G). Together with Par6:aPKC hetero-dimerization and Par3 homo-oligomerization, this provides a basis for the role of Par3 in enforcing the spatial segregation and the assembly of large-scale, self-organizing Par complex networks at the cell cortex *in vivo*.

Concluding remarks

The mode of Par3:Par6 interaction has remained controversial. In a sense, this reflects the challenges of delineating the specific functions of proteins and even more importantly their individual domains and motifs in cell polarity. Functional coupling, redundant interactions, differences in organism strains, cell types and protein constructs and finally the existence of paralogs severely hamper *in vivo* analyses of polarity proteins (Nagai-Tamai *et al.*, 2002; Fievet *et al.*, 2013). Moreover, the composition of polarity complexes is dynamic and may depend on the cell type or developmental context (Henrique and Schweisguth, 2003). Lastly, different populations of polarity proteins may even co-exist within a single cell (Goehring *et al.*, 2011). Altogether, this poses enormous obstacles for functional analyses as phenotypes may be obscured in mutation studies. Detailed structural analyses are thus essential to unambiguously determine the molecular basis of polarity complex formation. Moreover, the fact that PBMs require a free C-terminus for their function posits that C-terminal tagging for fluorescence microscopy or immunoblotting likely abrogates not only Par3:Par6 association, but possibly also other, yet unidentified Par6 PBM interactions. Altogether, this may explain some of the controversy about the Par3:Par6 interaction.

The fact that almost all polarity and cell adhesion proteins contain either at least one PDZ domain or a PBM emphasizes the importance of PDZ:PBM interactions in the assembly of

cell polarity and adhesion signaling networks. Our work illustrates the difficulties in predicting PDZ specificities, as the marked differences in Par6 and Shg recognition of the Par3 PDZ2 (Fig. 5.5D-F, 5.6A,B and Supplemental Fig. 5.10B, Supplemental Table 5.2) were unexpected on the sequence level (Supplemental Fig. 5.9). A detailed characterization of the functional specificities and redundancies of PDZ domains, as presented here, is therefore indispensable to decipher their contribution to polarity protein localization and function. Ultimately, this will help to predict PDZ domain function and provide a better understanding of the interaction networks underlying the establishment, maintenance and loss of cell polarity and hence critical developmental and carcinogenic processes.

Supplemental figures

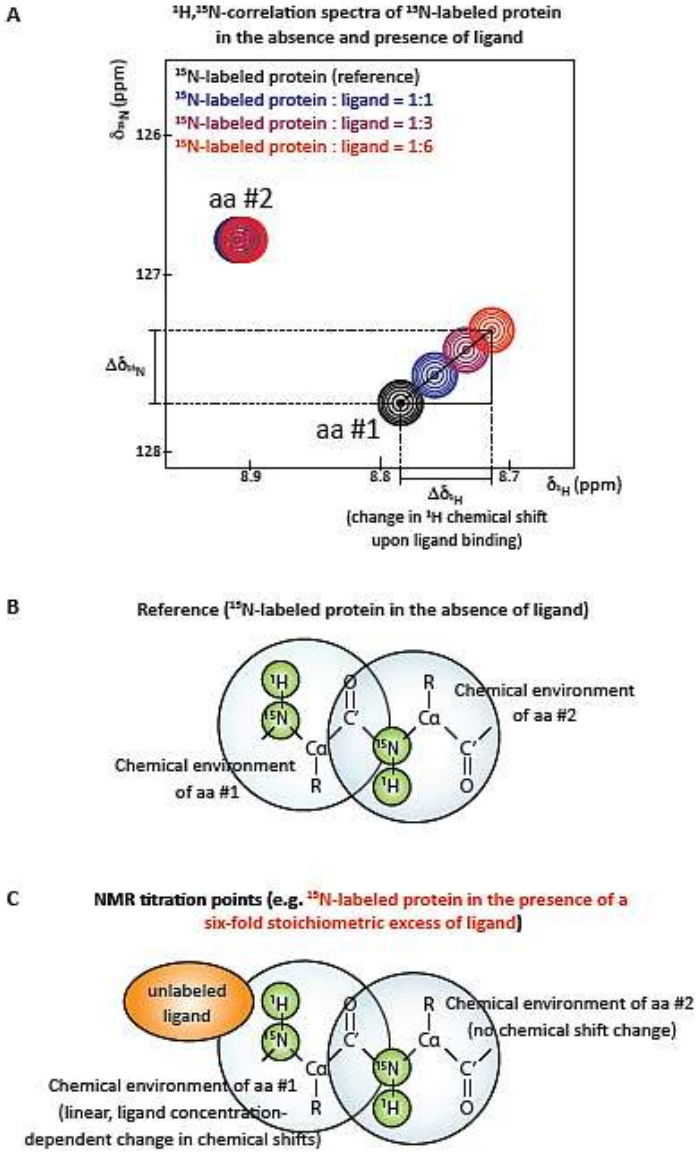

Supplemental Fig. 5.1: Chemical shift perturbation experiments. (A) Exemplary overlay of ^{1}H,^{15}N-correlation spectra of a ^{15}N-labeled protein in the absence and presence of an unlabeled binding partner at varying stoichiometric ratios. A region of the spectrum containing the NMR signals of two consecutive amino acids in the protein sequence is shown. (B) Chemical structure of the protein backbone highlighting the ^{1}H and ^{15}N atoms (green spheres) observed in the H,N-correlation spectra. The position of a peak in the spectrum strongly depends on the local chemical environment of the respective amino acid (indicated by light-blue spheres). Therefore, in contrast to an unfolded protein, peaks are distributed over a wide range of ^{1}H and ^{15}N chemical shifts in a folded protein. (C) Ligand binding (shown in orange) induces a change in the chemical environment, and hence in the chemical shifts, of those amino acids that participate in ligand binding (aa #1), but not of those that are located outside the binding pocket (aa #2).

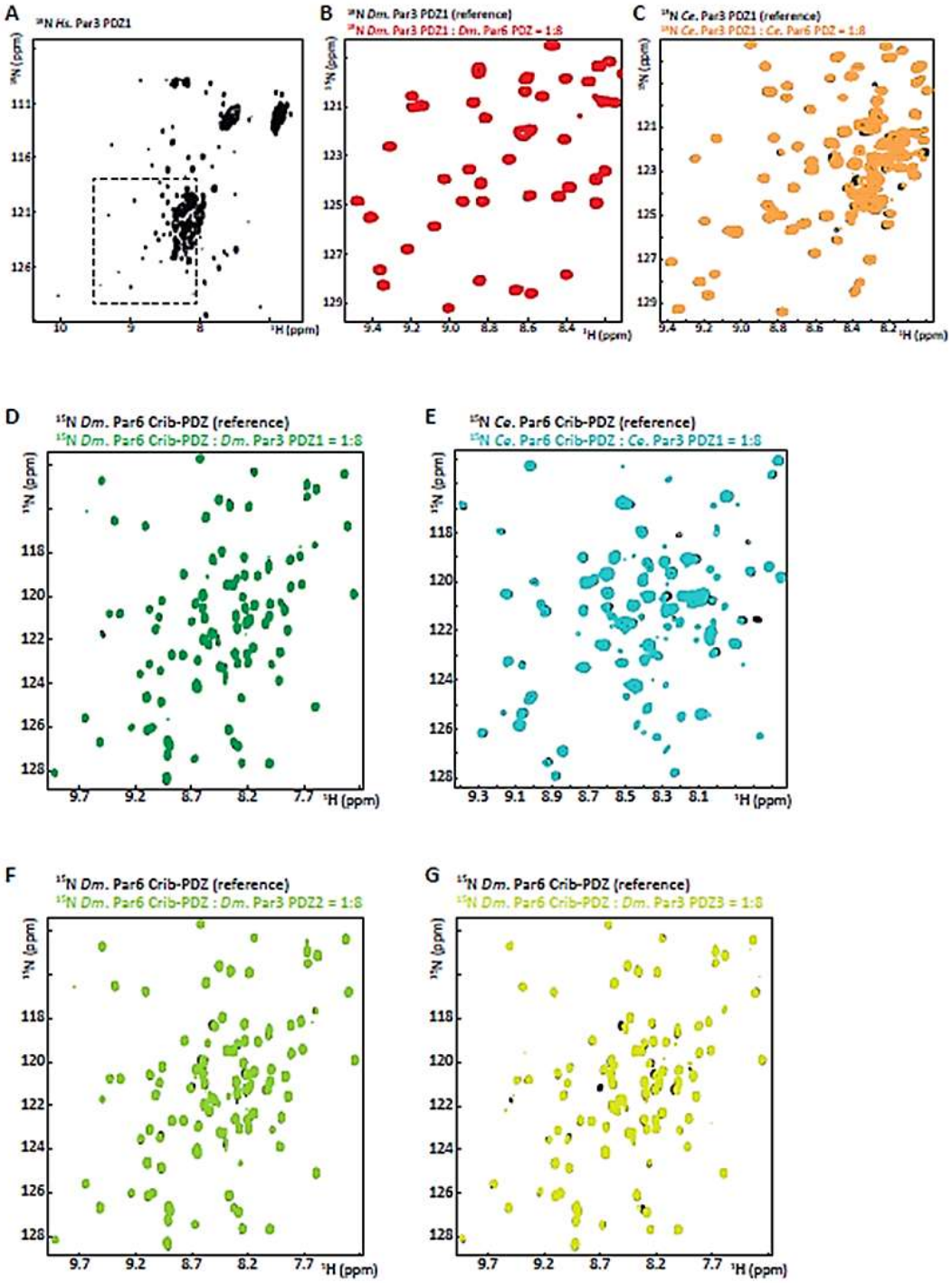

Supplemental Fig. 5.2: The Par3 PDZ1 domain does not interact directly with the Par6 (Crib-)PDZ domain. (A) $^{1}H,^{15}N$-correlation spectrum of the ^{15}N-labeled *Hs*. Par3 PDZ1 domain showing that the domain is largely unstructured in isolation. The boxed region is magnified in Fig. 4.7B. (B,C) Overlay of $^{1}H,^{15}N$-correlation spectra of the *D. melanogaster* (B) and *C. elegans* (C) Par3 PDZ1 domains in the absence and presence of a stoichiometric excess of the respective Par6 PDZ domain as indicated. (D,E) As (B,C) but for the *D. melanogaster* (D) and *C. elegans* (E) Par6 semiCRIB-PDZ constructs in the absence and presence of a stoichiometric excess of the Par3 PDZ1 domains as indicated. (F,G) As (B,C) but for the *D. melanogaster* Par6 Crib-PDZ construct in the absence and presence of a stoichiometric excess of the Par3 PDZ2 (F) and PDZ3 (G) domains as indicated.

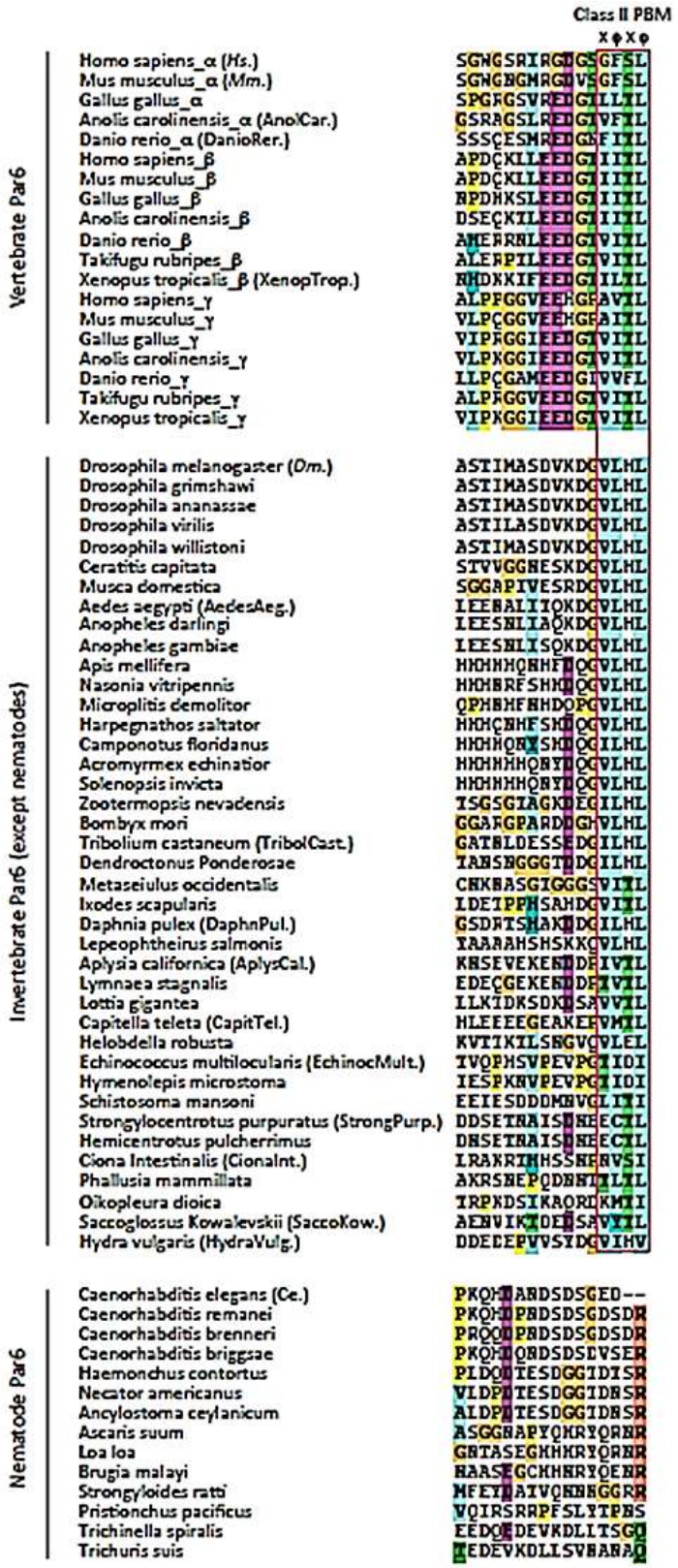

Supplemental Fig. 5.3: The Par6 C-terminus contains a conserved class II PDZ binding motif. Sequences of the C-terminal 16 aa of various vertebrate (top), invertebrate (center) and nematode (bottom) Par6 proteins. The class II PBM is highlighted with a red box and conserved in all metazoans with the exception of nematodes. Conserved residues were color-coded with ClustalX (Crooks *et al.*, 2004).

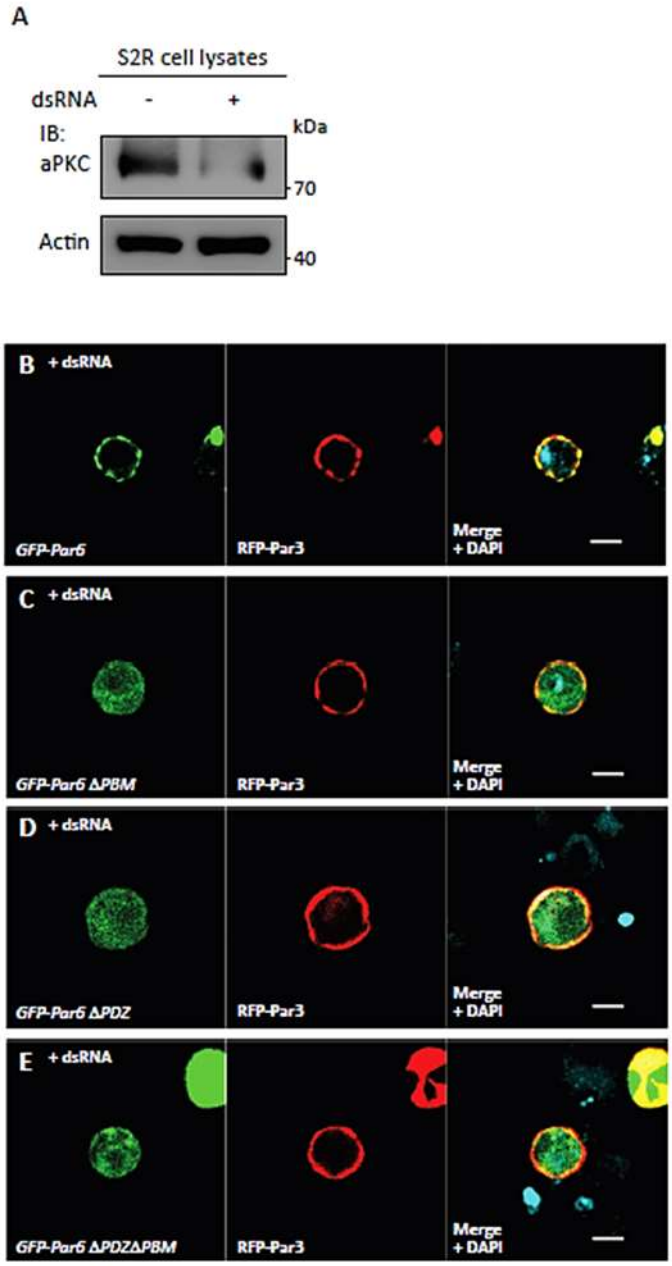

Supplemental Fig. 5.4: Par6 localization in S2R cells upon aPKC knockdown. (A) Western blot analysis of aPKC expression in S2R cell lysates in the absence or presence of dsRNA for aPKC knockdown. (B-E) As Fig. 5.2G-J, but for S2R cells where aPKC is knocked down by RNAi.

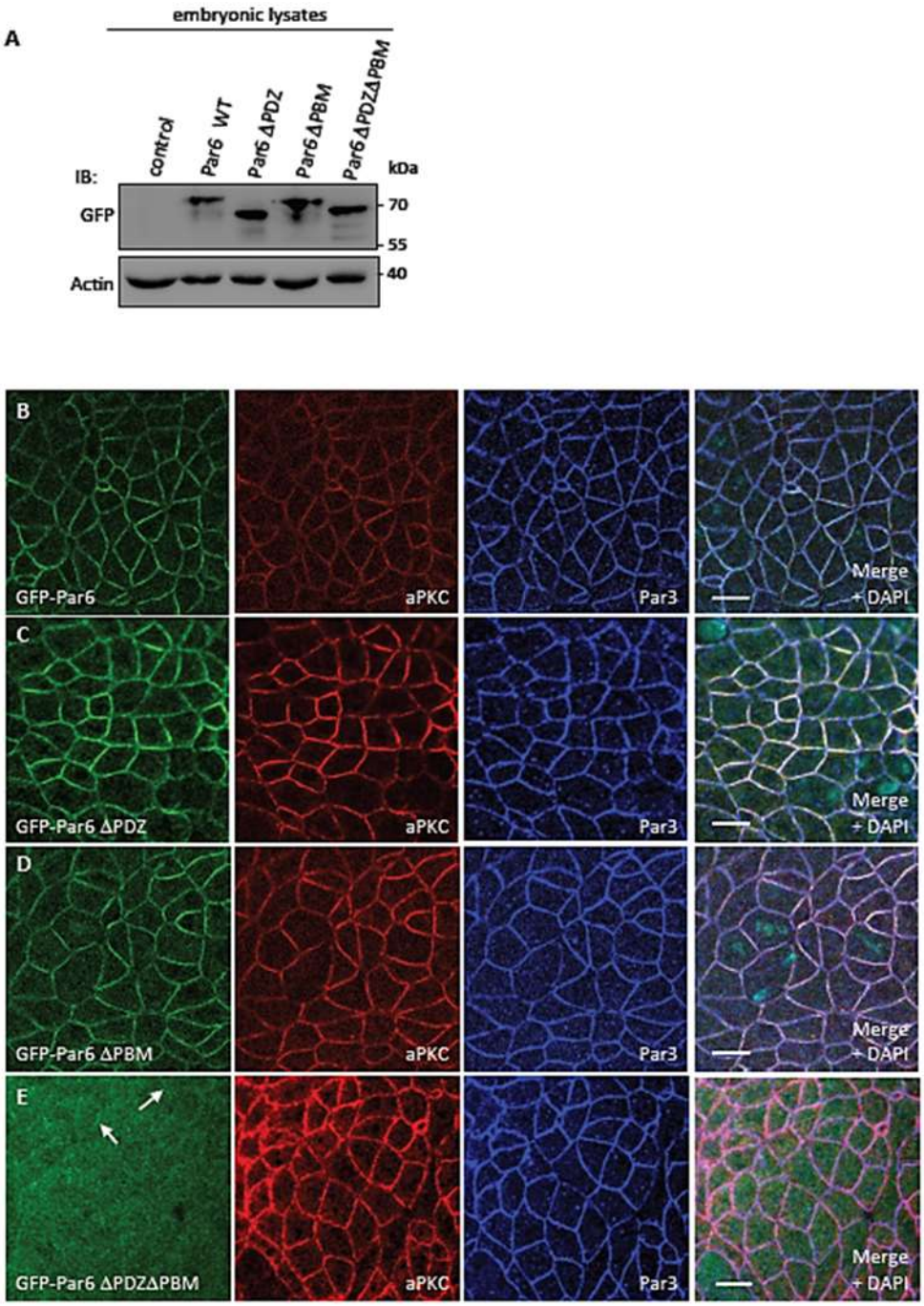

Supplemental Fig. 5.5: Expression of Par6 variants in fly embryos and localization of Par6 variants in transgenic flies during gastrulation. (A) Western blot analysis of GFP-Par6 expression in fly embryo lysates showing that all Par6 variants are stable and expressed similarly in a WT background. (B-E) Localization of aPKC, Par3 and GFP-Par6 variants in the epithelia of fly embryos during gastrulation (stage 6-7). The scale bar corresponds to 5 μm. Arrows in (E) highlight small fractions of Par6 that still localize to the cell cortex.

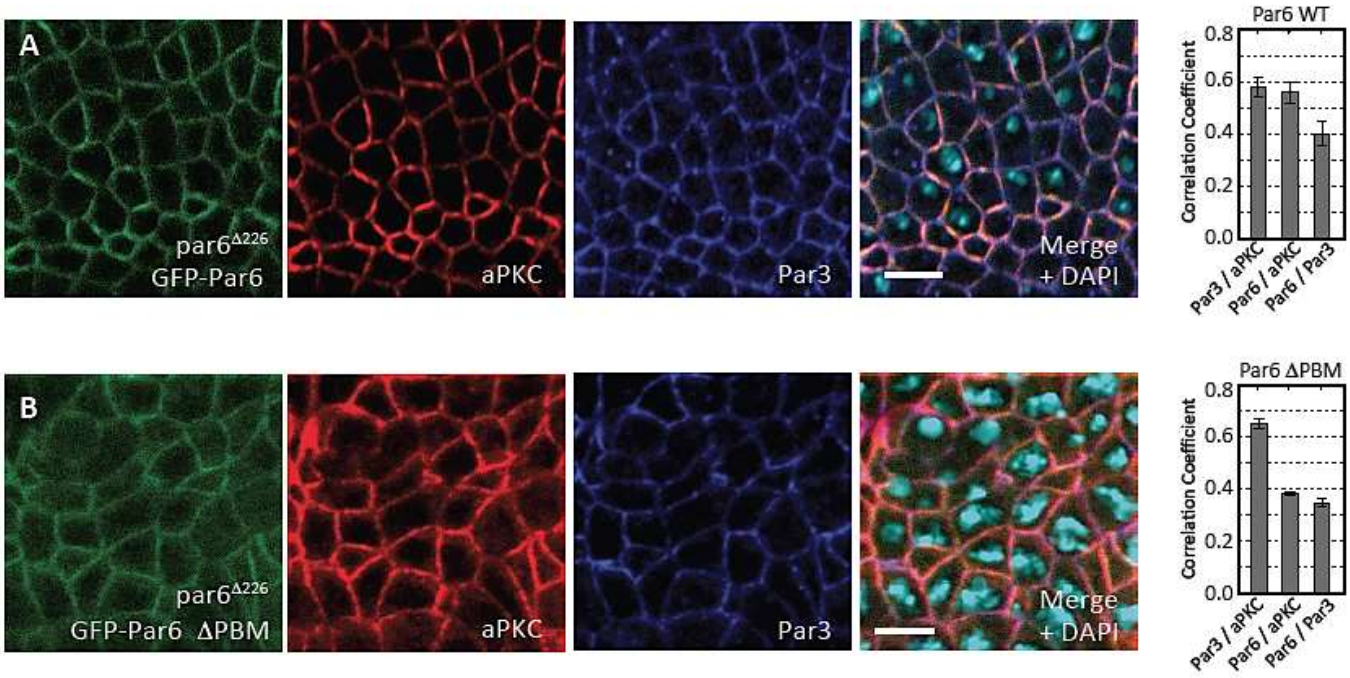

Supplemental Fig. 5.6: Par6 localization in *Par6*-null fly embryos. (A,B) As Fig. 5.3, but for GFP-Par6 WT (A) and GFP-Par6 ΔPBM (B) in a *par6* $^{\Delta 226}$ (*par6-null*) background.

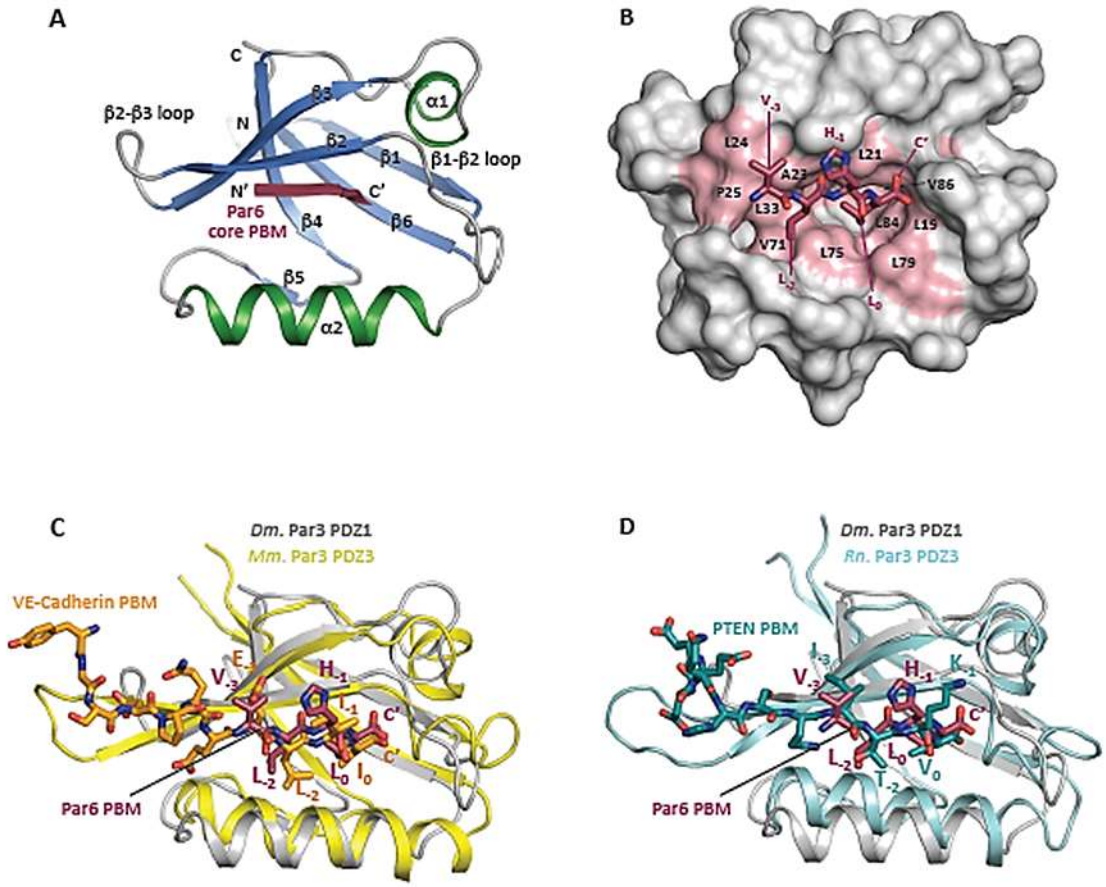

Supplemental Fig. 5.7: Crystal structure of the Par3 PDZ1 : Par6 PBM complex. (A)

Ribbon representation of the crystal structure of the Par3 PDZ1 : Par6 PBM complex with α helices and β strands in the PDZ1 domain colored in green and blue, respectively, and the β-strand formed by the Par6 core PBM (VLHL) shown in dark-pink. Secondary structure elements are labeled. (B) Surface representation of the Par3 PDZ1 domain highlighting the hydrophobic pocket (light-pink) surrounding the Par6 core PBM. (C,D) Structure superposition of the *Dm*. Par3 PDZ1:Par6 PBM complex (grey for the PDZ1 domain and raspberry for the PBM) with the *Mm*. Par3 PDZ3 domain (yellow) in complex with the PBM of VE-Cadherin (orange) (PDB-ID: 2KOH (Ernst *et al.*, 2014)) (C) and with the *Rn*. Par3 PDZ3 domain (cyan) in complex with the PBM of the PTEN phosphatase (dark cyan) (PDB-ID: 2K20 (Petronczki and Knoblich, 2001) (D). Otherwise as in Fig. 5.4B.

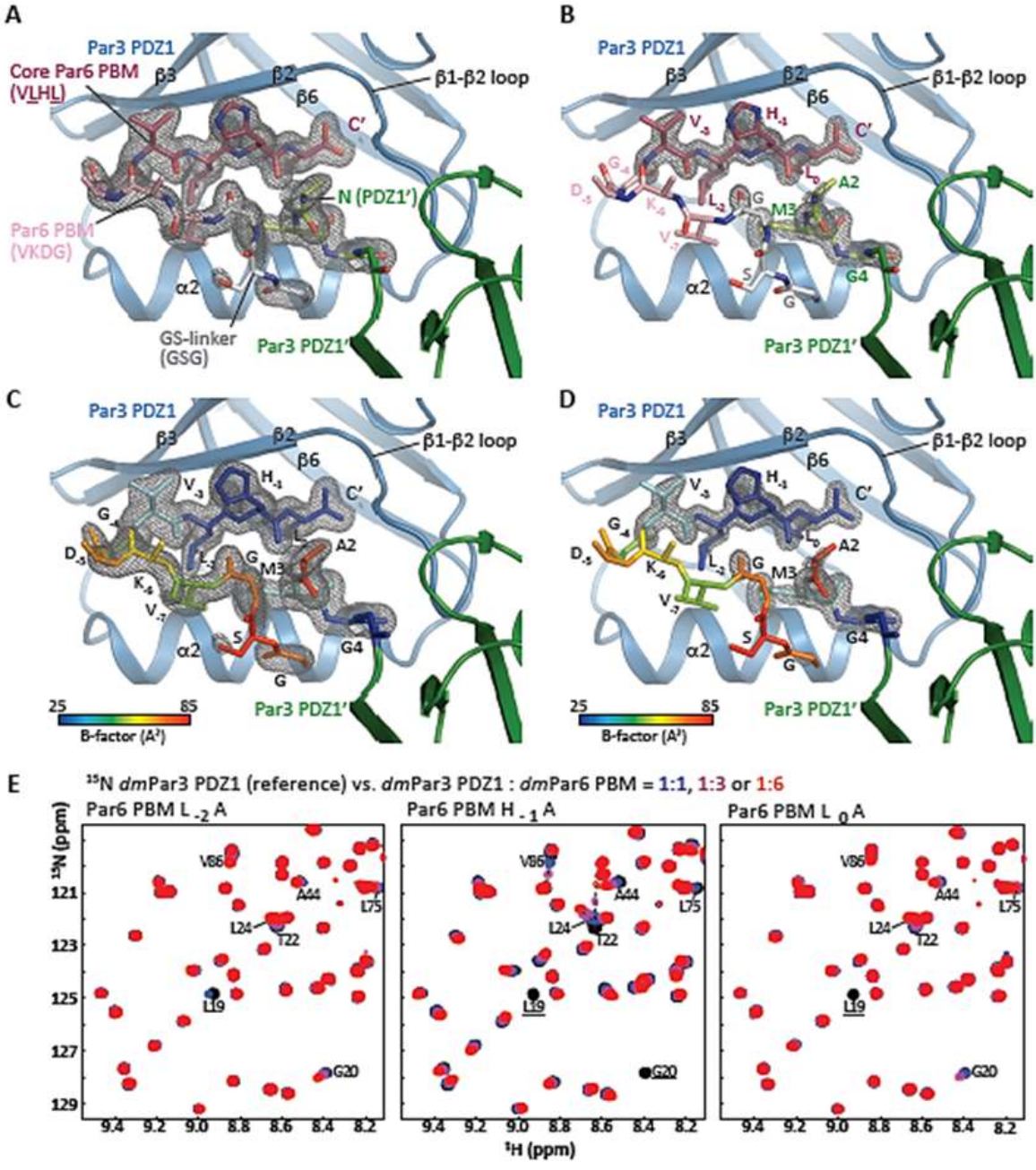

Supplemental Fig. 5.8: Ligand electron density and importance of the 0 and -2 position of the Par6 PBM for PDZ interaction. (A-D) Ribbon representation of the two Par3 PDZ1

domains in the asymmetric unit of the crystal (blue and green). The electron difference density of the Par6 PBM, the three C-terminal residues of the GS-linker and the three N-terminal residues of the neighboring PDZ1 domain is shown as $2F_O$-F_C map contoured at a σ level of 1.0 (A,C) and 2.0 (B,D). (C,D) As (A,B), but displaying the B-factor distribution of the PBM highlighting the increased flexibility of the residues outside the core PBM. The color scale for B-factors ranges from blue ($\leq$ 25 Å^2) to red ($\geq$ 85 Å^2). (E) NMR titration experiments with ^{15}N-labeled Par3 *dm*Par3 PDZ1 domain and Par6 core PBM mutants as indicated. Otherwise as Fig. 5.1C.

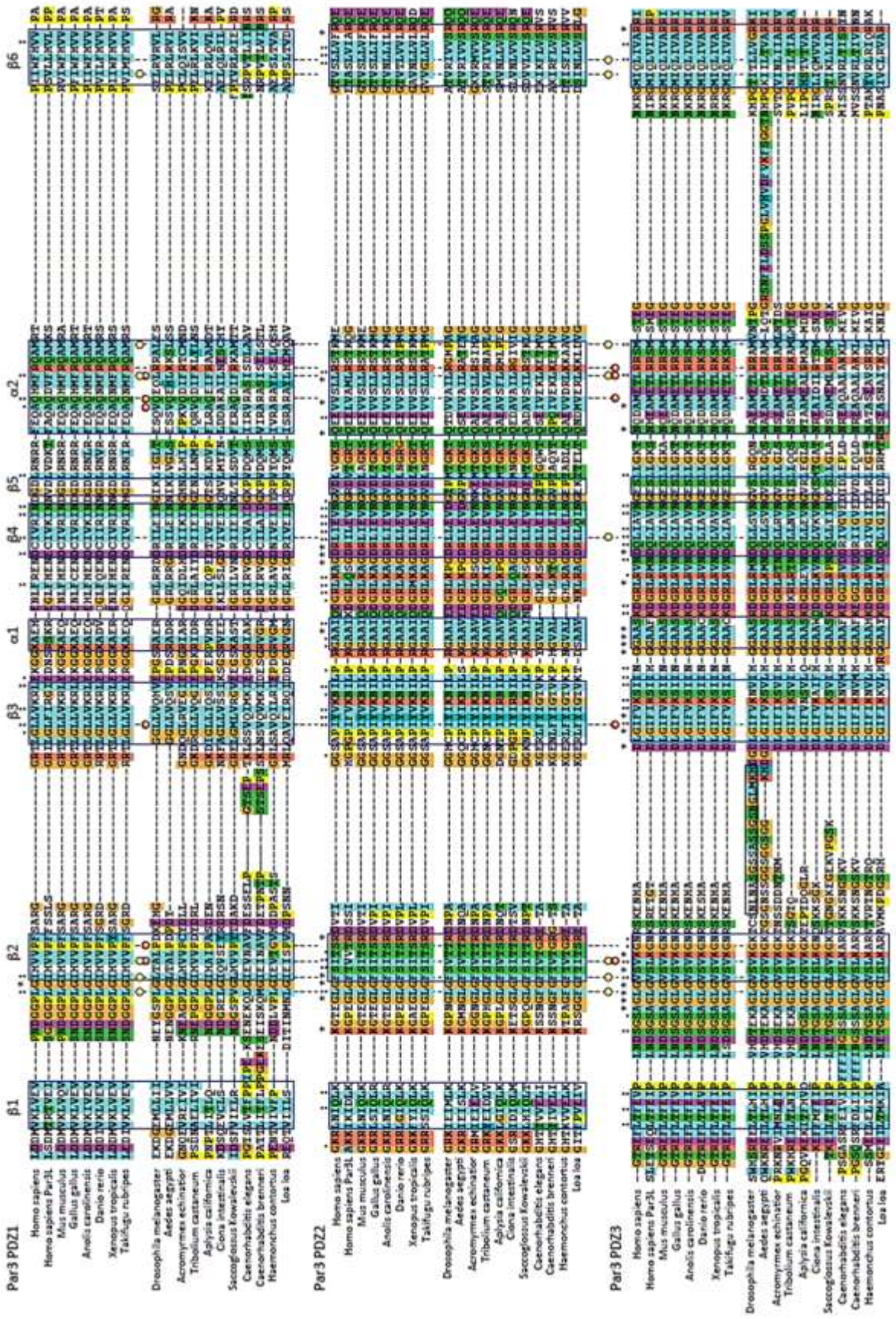

Supplemental Fig. 5.9: Structure-based sequence alignment of Par3 PDZ domains. Protein sequences of the individual Par3 PDZ domains were aligned with MUSCLE (Larkin *et al.*, 2007), manually edited where necessary to match known Par3 PDZ structures (PDB-

ID: 2KOM (Waudby *et al.*, 2016) for PDZ2 and 2KOH (Ernst *et al.*, 2014) for PDZ3) and color-coded with ClustalX (Crooks *et al.*, 2004). Secondary structure elements based on the *dm*Par3 PDZ1 : *dm*Par6 PBM complex are shown with blue boxes and denoted on the top. Residues within 5 Å proton-proton distance of the PBM are highlighted with circles and dashed lines (red: -2 position; yellow: 0 position) for the Par3 PDZ1:Par6 and the highly similar Par3 PDZ3:VE-cadherin complex (Ernst *et al.*, 2014). This shows that all residues contacting the specificity-determining 0 and -2 positions of the PBM are highly conserved and thus do not allow a specificity prediction based on sequence alignments. The region deleted in the *dm*Par3 PDZ3 Δβ2-3loop construct is indicated with a black box.

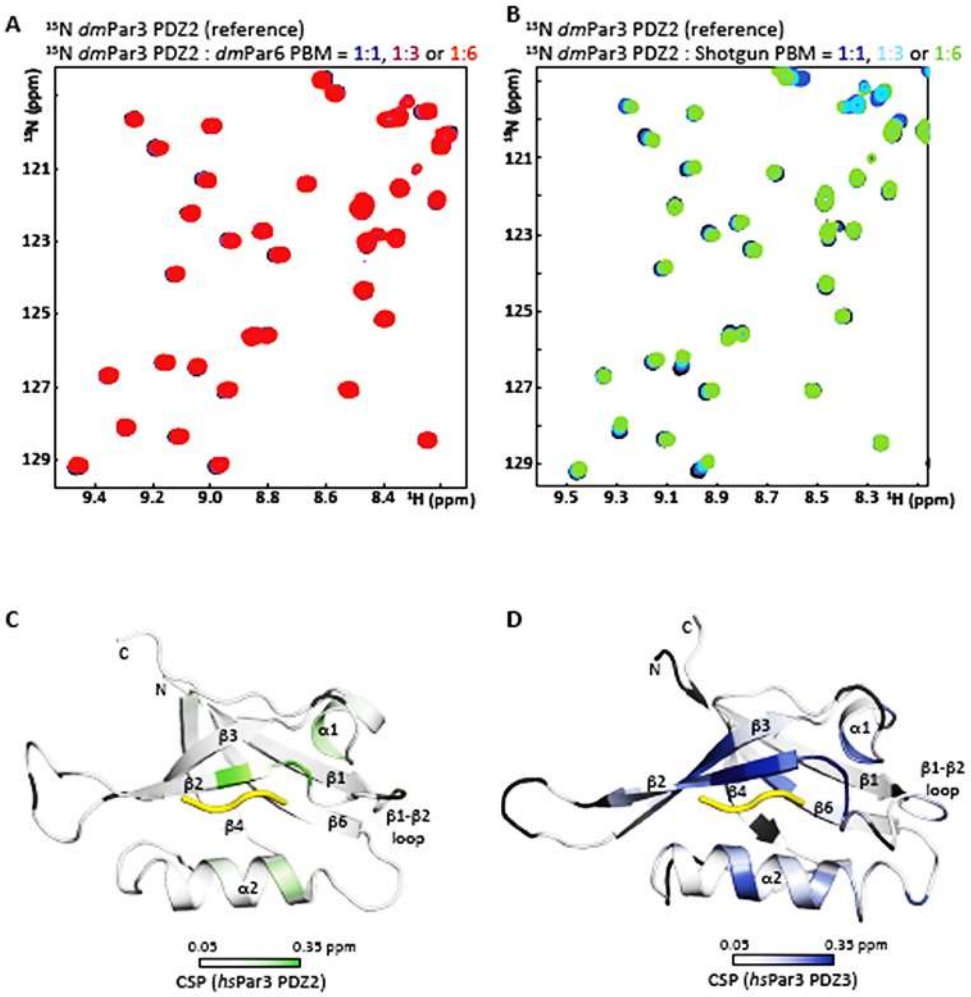

Supplemental Fig. 5.10: Interaction of the *dm*Par6 and Shg PBMs with the *dm*Par3 PDZ2 domain and Par6:Par3 interactions in the human proteins. (A,B) NMR titration of the ^{15}N-labeled *dm*Par3 PDZ2 domain with Par6 (A) or Shg (B) PBM as indicated. (C,D) CSPs induced by the *hs*Par6α PBM mapped onto the structures of the human Par3 PDZ2 (PDB-ID: 2KOM (Waudby *et al.*, 2016); left panel) and rat Par3 PDZ3 domain (PDB-ID: 2K20 (Petronczki and Knoblich, 2001); right panel) and colored with a linear gradient from white (CSP ≤ 0.05 ppm) to green (C) or blue (D) (CSP = 0.35 ppm). Residues broadened beyond detection in the PDZ3 are shown in dark-blue. Secondary structure elements are labeled (for PDZ2 β1: aa 5-12, β2: aa 20-24, β3: aa 35-40, α1: aa 45-49, β4: aa 56-61, β5: aa

64-65, α2: aa 71-80, β6: aa 86-93; for PDZ3 β1: aa 6-14, β2: aa 25-31, β3: aa 38-46, α1: aa 51-54, β4: aa 62-67, β5: aa 70-71, α2: aa 77-89, β6: aa 97-105). Otherwise as Fig. 5.4D.

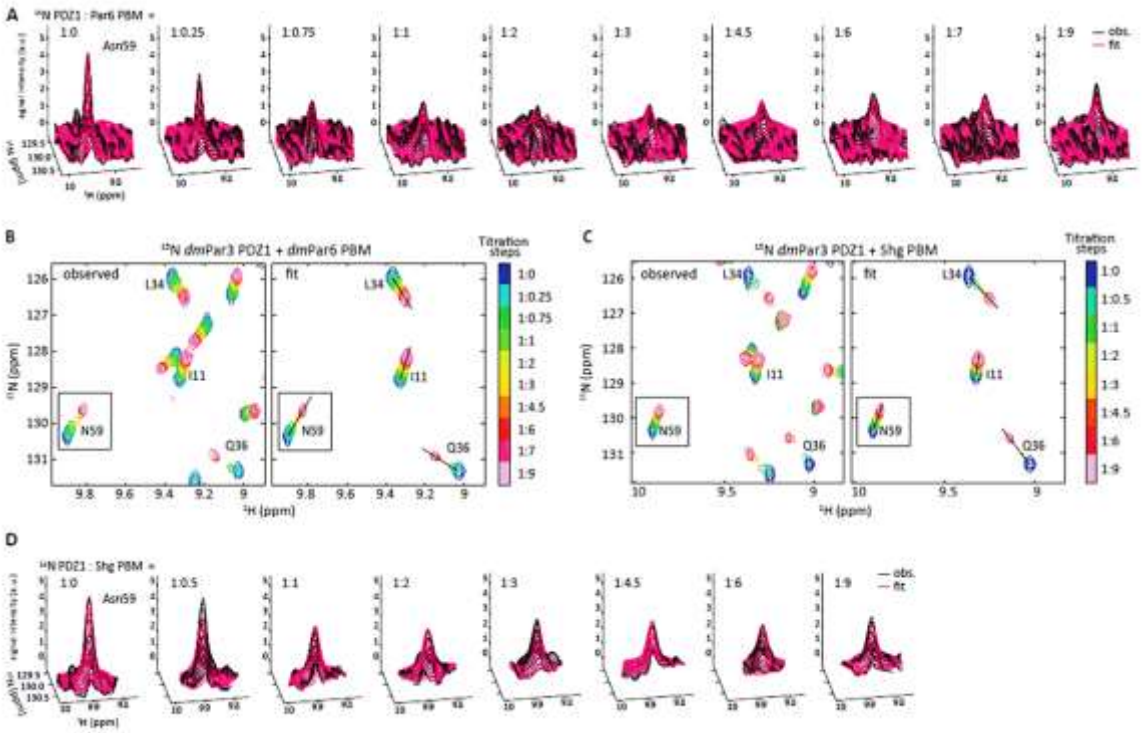

Supplemental Fig. 5.11: Line shape fitting analyses of the *dm*Par3 PDZ1 interactions with the PBMs of *dm*Par6 or Shg. (A) 2D line shape fit of the Asn^{59} cross peak in the individual ^{1}H,^{15}N-HSQC spectra of the *dm*Par3 PDZ1 domain in the absence or presence of Par6 PBM. Observed data are presented as black lines, while fits are shown in magenta. Each panel represents the fit of one titration point at the indicated stoichiometric ratio of PDZ:PBM. (B,C) Representative region of the NMR titration of ^{15}N-labeled *dm*Par3 PDZ1 with Par6 (B) or Shg (C). Contour plots of observed CSPs are shown in the left panel, while the fit of the cross peaks is presented in the right panel with black lines indicating the course of the fit CSPs between the reference point and the estimated saturation point. Titration steps are color coded as indicated. The Asn^{59} cross peak shown in (A) and (D) is boxed. (D) as (A) but for the Shg PBM.

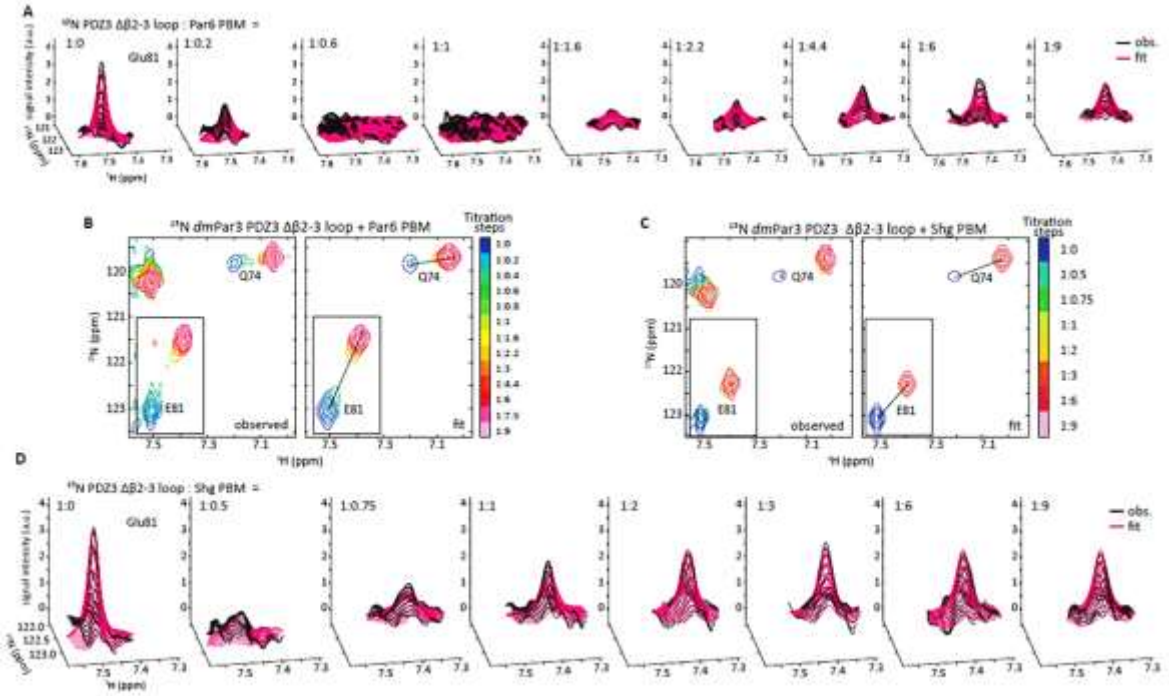

Supplemental Fig. 5.12: Line shape fitting analyses of the *dm*Par3 PDZ3 Δβ2-3loop interactions with the PBMs of *dm*Par6 and Shg. (A-D) as in Supplemental Fig. 5.11, but for the dmPar3 PDZ3 Δβ2-3loop and the Glu^{81} cross peak (A,D).

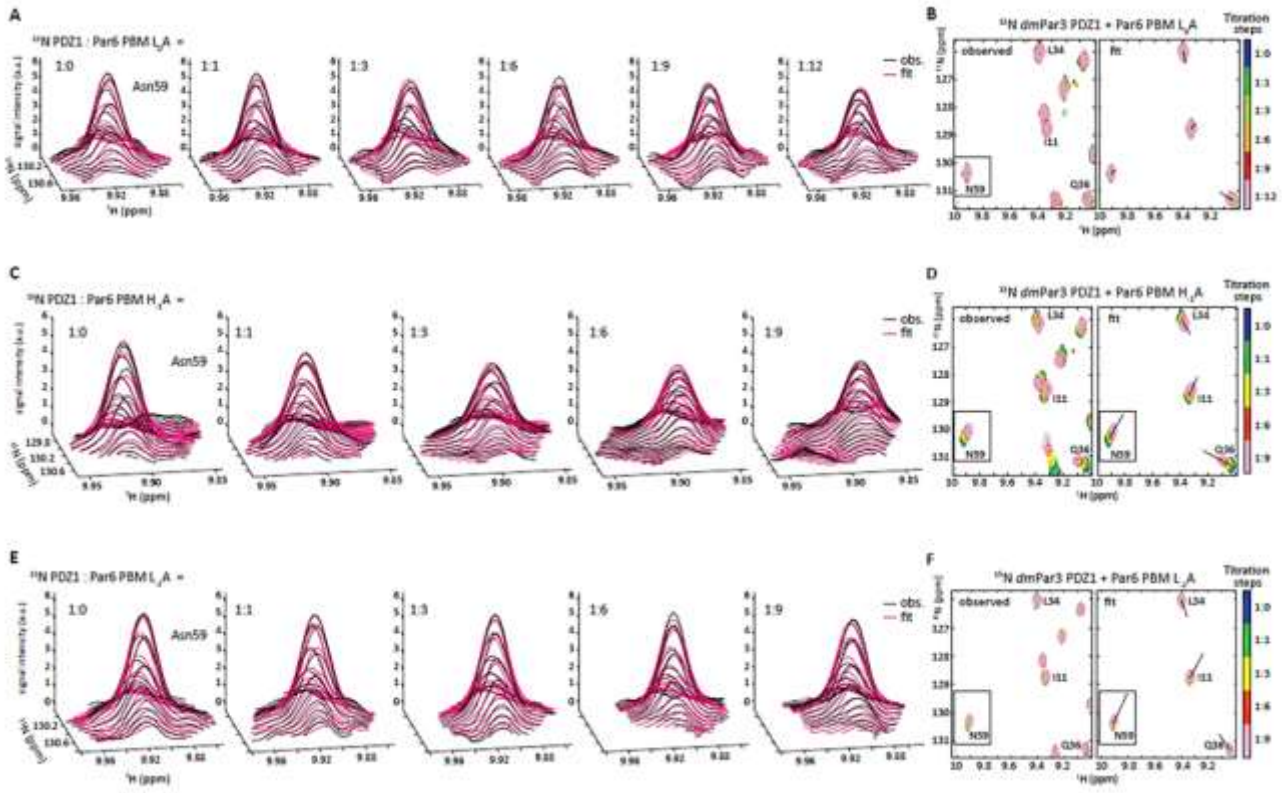

Supplemental Fig. 5.13: Line shape fitting analyses of the *dm*Par3 PDZ1 interactions with mutant *dm*Par6 PBMs. (A,B) As in Supplemental Fig. 5.11A, but for the Par6 L_0A

mutant. (C-F) as in (A,B), but for the Par6 $H_{-1}A$ (C,D) and $L_{-2}A$ (E,F) mutants.

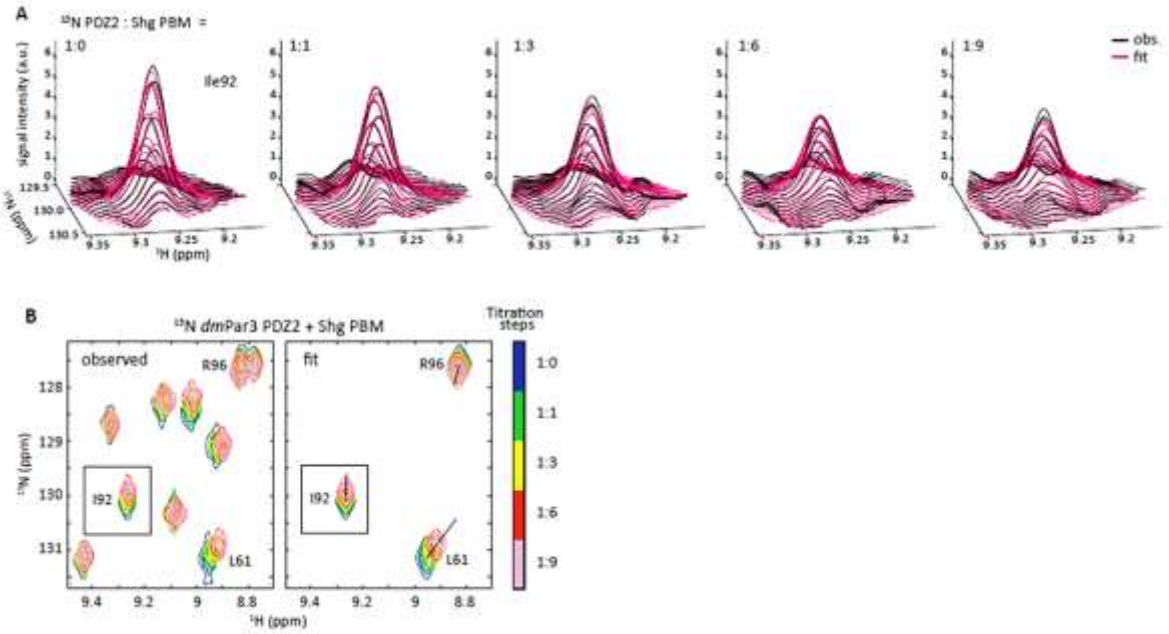

Supplemental Fig. 5.14: Line shape fitting analyses of the *dm*Par3 PDZ2 interactions with the Shg PBM. (A, B) as in Supplemental Fig. 5.11, but for the dmPar3 PDZ2 and the Ile^{92} cross peak.

Supplemental Table 5.1. Statistics of X-ray data collection and model refinement for the *dm*Par3 PDZ1:dmPar6 PBM complex[1]

Data collection	
Resolution (Å)	40.96 – 1.50 (1.59 – 1.50) [2]
Completeness (%)	99.8 (98.7)
No. of unique reflections	86,611 (13,880)
Redundancy	5.13 (4.88)
CC1/2* (%)	99.9 (70.2)
I / σI	18.78 (2.12)
Wilson B-Factor (Å^2)	31.13
FreeR (% of reflections)	5

Crystal properties	
Space group	$P3_1$
Unit cell dimensions	
a, *b*, *c* (Å)	60.88, 60.88, 65.05
α, β, γ (°)	90.00, 90.00, 120.00
Solvent content (%)	57.4
Refinement	
Resolution (Å)	40.96 – 1.50 (1.53 – 1.50)
R_{work} (%) / R_{free} (%)	14.03 / 16.91
R.m.s.d. bond lengths (Å)	0.02
R.m.s.d. bond angles (°)	1.64
B-Factor (Å^2) (Overall)	32.18
PDZ domain	29.04
Peptide (core PBM / outside core PBM)	35.83 / 68.32
Solvent	45.19
No. of atoms (Total)	1796
PDZ domain / peptide / solvent	1508 / 138 / 150
Ramachandran (%) (Favored / allowed / outliers)	98 / 2 / 0

[1]Number of crystals equals one.

[2]Values in parentheses are for highest-resolution shell.

Supplemental Table 5.2. Dissociation constants (K_d values) in μM for the *Dm*. Par3 PDZ domains and their interactions with the PBMs of Par6 and Shg.[1]

Ligand	**PDZ1**	**PDZ2**	**PDZ3**
Par6	216 ± 4	n.d.	54 ± 1
Par6 $L_{-2}A$	2486 ± 357	n.d.	n.d.
Par6 $H_{-1}A$	964 ± 60	n.d.	n.d.
Par6 L_0A	4049 ± 1113	n.d.	n.d.
Shg	128 ± 4	954 ± 45	0.6 ± 0.1

[1] K_d values are given in μM and were determined by line shape fitting of NMR CSP experiments. Errors were estimated with bootstrapping statistics on 100 replica.

Discussion

Establishing a cellular polarity is a fundamental process and is a prerequisite for development and the control of cellular processes. This study aimed to provide a better understanding of the function and the regulation of key proteins that are essential for epithelial development and the regulation of cellular homeostasis.

The scaffold protein Baz/Par3 and the serine/threonine kinase LKB1 cooperate to establish the initial polarization of epithelial cells. In addition, LKB1 controls the metabolism and proliferation of differentiated cells. Baz and LKB1 were the subjects of this study and further characterized.

Within this study a so far uncharacterized lipid binding (LB) domain of LKB1 has been identified. *In vitro* experiments managed to show that LKB1 prefers binding to PA, but also to some extend to PtdIns(5)P, PtdIns(4,5)P2 and PtdIns(3,4,5)P3. Notably, binding to PA activated LKB1, which was essential for *Drosophila* development, mouse axon formation and to counteract mTOR activity in human cancer cell lines. Understanding the mechanism by which potent tumour suppressors, such as LKB1 are activated is important in biomedical science to develop and improve new strategies to treat human diseases. Here, using *Drosophila* as a model organism an unknown mechanism to activate LKB1 has been described which is also conserved in humans. Thus, although it can be challenging to study human diseases like cancer in *Drosophila* the principle mechanisms of cell proliferation control are conserved.

Moreover, it could have been shown that oligomerization and lipid binding of Baz function redundantly to promote the apical localization of Baz in the embryonic epithelium and NBs. Strikingly, neither oligomerization nor lipid binding were essential for viability, whereas loss of both led to embryonic lethality. Moreover, a novel function of the oligomerization domain has been identified, as an oligomerization-deficient protein is destabilized. Additionally, the organization of the Par complex has been further analyzed. Although the general functions of the Par complex (Baz/Par6/aPKC) in the establishment of a cell polarity became more obvious in recent years, the formation of the complex itself remained controversial. However, using a combined approach of structural biology and *in vivo* analysis a detailed study about the Par3-Par6 interaction revealed novel insights in the complex assembly. A C-terminal PDZ binding motif (PBM) of Par6 binds to the PDZ1 and PDZ3 domains of Par3, whereas the previously reported PDZ-PDZ domain interaction of Par3 and Par6 was dispensable. Considering the Par complex as a ternary complex is misleading, because of Par3's capacity

to bind two Par6 proteins simultaneously *in vitro* and form homo-oligomers. Thus, it is more likely that the Par complex forms large clusters, which surround the apical domain. In addition, a C-terminal PBM of DE-Cad is capable of binding the PDZ1 and PDZ3 domains of Par3 independent of Armadillo. Therefore, an alternative mechanism to target Par3 to the plasmamembrane has been described.

The membrane association of LKB1

This study identified a novel lipid binding (LB) domain of LKB1 and highlighted that the membrane association of LKB1 provides an important cue to activate its catalytic activity. Membrane-binding of LKB1 could be shown to be important for the development of *Drosophila* and its function as a tumour suppressor in mammalian cells. LKB1 has previously been reported to localize at the plasmamembrane of *Drosophila* and mammalian cells (Collins *et al.*, 2000; Sapkota *et al.*, 2001; Martin and St Johnston, 2003; Sebbagh *et al.*, 2009). It has been assumed that this cortical localization is mediated by the addition of a farnesyl moiety, which serves as a membrane anchor (Collins *et al.*, 2000; Martin and St Johnston, 2003). However, *in vivo* the farnesylation of LKB1 seems to be dispensable. Farnesylation-deficient melanoma cells were still capable to suppress cell growth (Sapkota *et al.*, 2001) and a transgenic farnesylation-deficient knock-in mouse had only a decreased capacity to activate AMPK, but had otherwise no obvious defects (Houde *et al.*, 2014). Likewise, the farnesylation-deficient flies in this study had a slightly decreased capacity to rescue an *lkb1* null allele, but were viable. By contrast, loss of the identified LB domain strongly reduced LKB1's ability to rescue the mutant. Moreover, the double mutant (LKB1ΔLB C564A) completely failed to give rise to viable offspring. Thus, although the farnesylation of LKB1 seems to have an effect on its activity, the major mechanism that recruits LKB1 to the plasmamembrane and fully activates it was its LB domain rather than farnesylation.

LKB1 preferentially bound to PA, but binding to other lipids (PtdIns(5)P, PtdIns(4,5)P2 and PtdIns(3,4,5)P3) has also been observed. In response to PA binding the kinase activity of LKB1 was strongly enhanced *in vitro*. PA is mainly produced by PLD and activates also other kinases, such as mTOR (Fang *et al.*, 2001). Since LKB1 and its major target to counteract cell proliferation are activated by the same mechanism, a novel autoregulation of the activation and repression of mTOR signaling has been identified. The association of elevated PLD2 expression and mTOR activity (as measured by the phosphorylation of S6K) with

simultaneous loss of LKB1 in histological samples of human melanoma supports the hypothesis of an auto-regulatory effect.

Binding of LKB1 to PtdIns(5)P was not further investigated in this study, because PtdIns(5)P is a low-abundant phospholipid and enriched in endomembranes (Sarkes and Rameh, 2010; Ramel *et al.*, 2011), whereas this study focused on epithelial cells in which LKB1 localizes at the plasmamembrane. However, with respect to data from non-epithelial cells (mouse hepatocytes and embryonic fibroblasts) LKB1 localizes on late endosomes in a complex containing AMPK, v-ATPase, Ragulator and AXIN, which is essential to activate LKB1 (Zhang *et al.*, 2013b; Zhang *et al.*, 2014). Although PtdIns(5)P is more prominent in the membrane of the early endosome, it is also incorporated into the late endosome (Ramel *et al.*, 2011). The mechanism by which LKB1 is activated on late endosomes is not understood, yet. Thus, PtdIns(5)P might contribute to the activation of LKB1 on endosomes. In a human fibroblast cell line (IMR90) no cortical localization could be observed, which raises the question if LKB1 simply localizes in the cytoplasm or in association with endosomes. By using a fluorescent reporter that is fused to a PtdIns(5)P binding domain a possible coincidence of the lipid and LKB1 on endosomes could be analyzed.

The elevated degradation of membrane-binding deficient LKB1 (LKB1ΔLB C564A) in *Drosophila* supports the idea of an endomembrane localization of LKB1. LKB1ΔLB C564A was absent from the plasmamembrane and accumulated in the cytoplasm, such as hLKB1 in a fibroblast cell line (IMR90), but without the capacity to associate with lipids. In *Drosophila*, LKB1ΔLB C564A was in contrast to LKB1 affected by enhanced degradation. Therefore, binding to either the plasmamembrane or to endomembranes might be a mechanism to protect LKB1 from degradation. Accordingly, in flies that express membrane-binding deficient LKB1 fused to the PH domains of either PLCδ or Akt1 (to mediate membrane binding), the transgenes were not affected by enhanced protein degradation. Nevertheless, a cell type specific membrane association of LKB1 could be another explanation. Moreover, the C-terminus of LKB1, which harbors the LB domain is affected by several posttranslational modification, including phosphorylation and acetylation (Sapkota *et al.*, 2001; Lan *et al.*, 2008). Strikingly, in non-polarized HEK293 cells, LKB1 has been reported to be acetylated on lysine 416 (Lan *et al.*, 2008), which is essential for binding lipids. This acetylation might interfere with the membrane association of LKB1, but a role of this modification *in vivo* has not been analyzed, yet.

Regarding the degradation of LKB1 two E3 ubiquitin ligases (CHIP and HERC2) have already been described to promote the proteasomal degradation of LKB1 (Gaude *et al.*, 2012;

Bai *et al.*, 2016). Given that a decreased amount of LKB1 is frequently found in various tumours, identifying other E3 ubiquitin ligases that target LKB1 for degradation would help to develop new strategies to treat cancer or to discover new biomarker. Some molecules that inhibit specific E3 ubiquitin ligases are currently undergoing clinical trials (Bielskienė *et al.*, 2015).

The PA mediated activation of LKB1

Given that LKB1 was activated upon binding to PA it remains to be investigated how this activation occurs on the molecular level. The structure of the LKB1/STRADα/Mo25 complex has previously been resolved (Zeqiraj *et al.*, 2009). Based on the reported crystal structure of the complex, binding of STRADα to LKB1 causes an allosteric activation of LKB1, which is stabilized by Mo25. However, in this study only truncated variants of STRADα (residues 59 – 431) and LKB1 (residues 43 – 347) have been analyzed (Zeqiraj *et al.*, 2009). Therefore, a putative role in the activation of LKB1 of the either the N- or C-terminus remains enigmatic. Loss of the membrane binding capacity of LKB1 did not affect its association with STRADα (Stlk in *Drosophila*), Mo25 and AMPK in the *Drosophila* embryo. Nevertheless, this complex had a significantly decreased catalytic activity and failed to rescue an *lkb1* null allele. The chimeric proteins that were fused to the PH domains of either PLCδ or Akt1 were able to restore the membrane localization of LKB1 and to rescue the null allele to a large extend. *In vitro*, the addition of PA to the recombinant human LKB1/STRADα/Mo25 complex strongly enhances its kinase activity, whereas adding either PtdIns(4,5)P2 or PtdIns(3,4,5)P3 led only to a moderate activation. This indicates the specific association of LKB1 with PA is required to fully activate its catalytic activity.

In order to better understand the PA-dependent activation of LKB1 at the molecular level the structure of LKB1 in complex with liposomes containing PA could be determined by NMR. The conformational change of LKB1 upon binding to PA should induce a chemical shift perturbation (CSP), if the conformation of LKB1 changes upon binding PA. Therefore PA-containing liposomes could be titrated to LKB1, which also allows determining the dissociation constant (K_D-value) that will provide information about the strength of the interaction. Knowing the structure of the PA-activated LKB1 will help to gain insight to the (mis)regulation of this important tumour suppressor. To this end, sequence optimized variants of the human LKB1 and the membrane-binding deficient form have been generated, because

of an inefficient translation of the human codon sequences in *E. coli* (data not shown). Moreover, an attempt to gain insight into the PA-dependent regulation of LKB1 using atomic force microscopy (AFM, in cooperation with AG Gießibl, University of Regensburg) has been made. AFM bears the potential to provide structural information of molecules at atomic resolution. Nevertheless, although we were able to visualize lipid head groups of a lipid bilayer, which was adsorbed on mica, we could not acquire structural information about membrane-bound recombinant LKB1 (data not shown).

The functional redundancy of the OD and LB motif

The N-terminal oligomerization domain (OD) of Baz/Par3 is highly conserved among animals and has been described to be essential in *Drosophila* and mammalian cells (MDCK) to target Baz/Par3 to the plasmamembrane (Benton and St. Johnston, 2003b; Mizuno *et al.*, 2003). In addition, loss of the OD results in a severely compromised capacity to rescue a *baz* null allele (Benton and St. Johnston, 2003b). However, this study found that the OD is neither essential to tether Baz to the plasmamembrane nor for viability of *Drosophila* embryos. BazΔOD localizes entirely at the apical junctions, overlapping with DE-Cad. Likewise, mutating the lipid binding (LB) domain did not affect the localization or rescue ability as well, which is in line with previous data (Krahn *et al.*, 2010b). Surprisingly, loss of both domains (BazΔODΔLB) completely abolished the cortical localization, ability to rescue a null allele and protein stability of Baz. This indicates a functional redundancy between the OD and LB motif, which cannot be compensated by any other domain (e.g. the PDZ domains) of Baz. Given that a chimeric protein, which carries the oligomerization domain of the human TEL protein efficiently restores the function of BazΔODΔLB, oligomerization *per se* rather than a specific feature of the OD is enough for the function of Baz in the absence of the lipid binding motif.

Although Baz has been reported to localize to the plasmamembrane by binding to Ed, Arm and Stan via its PDZ domains (Wei *et al.*, 2005; Wasserscheid *et al.*, 2007), none of these proteins seems to be capable to initially recruit Baz to the plasmamembrane. Strikingly, the interaction of BazΔODΔLB with any of these proteins was impaired, as all of them managed to recruit BazΔODΔLB to artificial cell-cell contacts in S2R cells. This suggests a role for oligomerization and lipid binding as important initial cues to tether Baz to the plasmamembrane. The observation that the simultaneous loss of the PDZ (interacts with Ed,

Arm and Stan) domains and the LB motif did not affect the apical localization of Baz further highlights the role of the OD and LB motif for the localization of Baz, rather than the PDZ domains. Nevertheless, loss of all PDZ domains causes embryonic lethality (Krahn *et al.*, 2010b), whereas mutating either the OD or LB motif can be compensated and produces viable offspring. The PDZ domains of Baz/Par3 have been reported to bind directly to phospholipids *in vitro* (Wu *et al.*, 2007; Yu and Harris, 2012), however in cell culture experiments the PDZ domains were not able to mediate a cortical localization of BazΔLB. This suggests, that the association of the PDZ domains with phospholipids is either not relevant *in vivo* (at least not in S2R cells) or is restricted to a certain function of Baz. Although the PDZ domains seem to be dispensable for the initial recruitment of Baz to the plasmamembrane they become indispensable during further development. The initial recruitment of Baz to the plasmamembrane neither requires the OD nor the LB motif, but rather a specific function, which is mediated in redundancy by them.

Oligomerization promotes the stability of Baz

In addition to the role of the OD in localizing Baz, this study described a novel function of the OD to maintain the stability of Baz. Mutations that affect the critical residues, which are required to mediate the self-association of Baz, markedly reduce the amount of Baz protein. The enhanced degradation of oligomerization-deficient Baz was rescued by fusing the heterologous OD of the human TEL protein to the Baz N-terminus. Therefore, although oligomerization is not essential for viability it contributes to the stability of Baz. However, it remains to be investigated by which mechanism the amount of BazΔOD protein decreases. Oligomerization-deficient Baz could either be prone to aberrant targeting of proteases or E3-ubiquitin ligases that promote its proteasomal degradation. Baz has previously been reported to have multiple truncated variants (based on observations from western blots), which arise either from proteolytic cleavage or proteasomal degradation (Krahn *et al.*, 2009). Thus, the self-assembly of Baz might shield the protein from degradation.

In future studies it could become an objective to identify potential Baz proteases or E3-ubiquitin ligases that degrade Baz. The immunoprecipitation of wildtype and oligomerization-deficient Baz followed by mass spectrometry could be a promising approach to analyze potential differences in the interactome of both proteins. Another approach for the analysis of dimer-specific interaction partner would be bimolecular complementation affinity purification

(BiCAP) (Croucher *et al.*, 2016), which is also followed by mass spectrometry. The loss of Baz's oligomerization could favor the interaction with its degrading enzymes, which might facilitate their identification.

Novel insights into the structural organization of the Par complex

This study provided a novel understanding of the molecular organization of the Par complex. The current model of the Par complex supposes that Par6 binds to the first PDZ domain of Baz/Par3 via its own PDZ domain, which might also require its CRIB motif (Lin *et al.*, 2000; Joberty *et al.*, 2000). However, the data shown here reject this model. PDZ domains are frequently bound by proteins that harbor a PDZ binding motif (PBM). Here, a so far undescribed PBM at the C-terminus of Par6 has been identified. Loss of the Par6 PBM abolishes the interaction with the PDZ domains of Baz *in vitro* and a recombinant Par6 CRIB-PDZ protein fails to bind the Baz PDZ domains. In addition, Par6ΔPDZ is efficiently recruited to the cell cortex by Baz in S2R cells. Finally, the NMR spectra of neither Par6 PDZ nor Par3 PDZ changed upon incubation with each other, which indicates that the two domains do not interact with each other. Furthermore, in contrast to previous studies we found that Par6 binds in addition to the first PDZ domain of Baz also to the third PDZ domains, which enables Baz to bind two Par6 proteins simultaneously. The interaction between the Par6 PBM and the Baz PDZ3 domain were even four times stronger than between Par6 PBM and Baz PDZ1. Taken together, the interaction between Par6 and Baz does not depend on a PDZ-PDZ interaction, but rather on the PBM of Par6. Nevertheless, in the epidermis of *Drosophila* embryos the PDZ domain and the PBM of Par6 function redundantly to recruit Par6 to the apical junctions. Moreover, embryos that express Par6ΔPBM overcome the embryonic lethality of a *par6* null allele, whereas Par6ΔPDZ expressing embryos die. The importance of the Par6 PDZ domain for embryonic viability is most likely due to its function of binding to the ECR1 domain of Sdt to join the Crb complex or to directly bind the PBM of Crb upon the apical exclusion of Baz (Lemmers *et al.*, 2004; Wang *et al.*, 2004; Morais-de-Sá *et al.*, 2010; Whitney *et al.*, 2016; Koch *et al.*, 2016). Given that Baz also forms a complex with Sdt prior to the expression of Crb (Krahn *et al.*, 2010a), Par6ΔPBM could associate with the Baz-Sdt complex by binding Sdt during gastrulation and afterwards join to the Crb complex. Binding either directly to Baz (via PBM) or indirectly in complex with Sdt (via PDZ domain) could

explain the functional redundancy and would be in line with the cytoplasmic localization of the double mutant (Par6ΔPDZΔPBM).

In addition to the novel PBM-PDZ interaction of Par6 and Baz, this study further showed a direct interaction of DE-Cad and Baz for the first time. In *Drosophila*, the interaction of Baz and DE-Cad has been described to be indirect and requires Arm (Wei *et al.*, 2005). By contrast, mammalian VE-Cad binds directly with its C-terminal PBM to the first and third PDZ domains of Par3, which is essential for the polarization of endothelial cells (Iden *et al.*, 2006). Similar to the mammalian system, DE-Cad contains a class II PBM that mediates the interaction with the first and third PDZ domain of Baz as well. Notably, the interaction of the DE-Cad PBM with the third PDZ domain of Baz is more than 50 times stronger compared towards the PBM of Par6. However, both PBM's compete with each other for binding to the third PDZ domain of Baz *in vitro*. The cellular context of this competition has not been determined, yet, but the stronger affinity of the DE-Cad PBM towards Baz might contribute to the observation of an apical exclusion of Baz (Nam and Choi, 2003; Vogelmann and Nelson, 2004; Harris and Peifer, 2005; Martin-Belmonte *et al.*, 2007; Morais-de-Sá *et al.*, 2010; Doerflinger *et al.*, 2010). To date two mechanisms have been described, which promote the segregation of Baz from the SAR towards the AJ. First, the phosphorylation of Baz by aPKC induces the dissociation of the Par complex and the translocation of Baz to the AJ (Morais-de-Sá *et al.*, 2010). Second, the phosphorylation of Arm by Pak4 is essential for the retention of Baz at the AJ in *Drosophila* photoreceptor cells (Walther *et al.*, 2016). The direct association of DE-Cad with Baz might contribute to the accumulation of Baz at the AJ by sequestering it. The role of Baz's accumulation at the AJ *in vivo* still remains to be investigated, but it might be necessary for Baz as an exocyst receptor to regulate the delivery of cell adhesion proteins to the AJ.

References

Adams, P. D., P. V. Afonine, G. Bunkóczi, V. B. Chen, I. W. Davis, N. Echols, J. J. Headd, and L.-W. Hung, *et al.* 2010. PHENIX: A comprehensive Python-based system for macromolecular structure solution. *Acta Crystallogr D Biol Crystallogr* 66(Pt 2):213–221.

Ahmed, S. M., and I. G. Macara. 2017. The Par3 polarity protein is an exocyst receptor essential for mammary cell survival. *Nat Commun* 8:14867.

Alessi, D. R., K. Sakamoto, and J. R. Bayascas. 2006. LKB1-dependent signaling pathways. *Annu Rev Biochem* 75:137–163.

Alexander, A., S.-L. Cai, J. Kim, A. Nanez, M. Sahin, K. H. MacLean, K. Inoki, and K.-L. Guan, *et al.* 2010. ATM signals to TSC2 in the cytoplasm to regulate mTORC1 in response to ROS. *Proc Natl Acad Sci U S A* 107(9):4153–4158.

Alva, V., S.-Z. Nam, J. Söding, and A. N. Lupas. 2016. The MPI bioinformatics Toolkit as an integrative platform for advanced protein sequence and structure analysis. *Nucleic Acids Res* 44(W1):W410-5.

Amin, N., A. Khan, D. St Johnston, I. Tomlinson, S. Martin, J. Brenman, and H. McNeill. 2009. LKB1 regulates polarity remodeling and adherens junction formation in the Drosophila eye. *Proc Natl Acad Sci U S A* 106(22):8941–8946.

Anderson, J. M., and C. M. van Itallie. 2009. Physiology and function of the tight junction. *Cold Spring Harb Perspect Biol* 1(2):a002584.

Appleton, B. A., Y. Zhang, P. Wu, J. P. Yin, W. Hunziker, N. J. Skelton, S. S. Sidhu, and C. Wiesmann. 2006. Comparative structural analysis of the Erbin PDZ domain and the first PDZ domain of ZO-1. Insights into determinants of PDZ domain specificity. *J Biol Chem* 281(31):22312–22320.

Arsham, A. M., J. J. Howell, and M. C. Simon. 2003. A novel hypoxia-inducible factor-independent hypoxic response regulating mammalian target of rapamycin and its targets. *J Biol Chem* 278(32):29655–29660.

Atwood, S. X., C. Chabu, R. R. Penkert, C. Q. Doe, and K. E. Prehoda. 2007. Cdc42 acts downstream of Bazooka to regulate neuroblast polarity through Par-6 aPKC. *J Cell Sci* 120(Pt 18):3200–3206.

Atwood, S. X., and K. E. Prehoda. 2009. aPKC phosphorylates Miranda to polarize fate determinants during neuroblast asymmetric cell division. *Curr Biol* 19(9):723–729.

Avtanski, D. B., A. Nagalingam, M. Y. Bonner, J. L. Arbiser, N. K. Saxena, and D. Sharma. 2015. Honokiol activates LKB1-miR-34a axis and antagonizes the oncogenic actions of leptin in breast cancer. *Oncotarget* 6(30):29947–29962.

Baas, A. F., J. Boudeau, G. P. Sapkota, L. Smit, R. Medema, N. A. Morrice, D. R. Alessi, and H. C. Clevers. 2003. Activation of the tumour suppressor kinase LKB1 by the STE20-like pseudokinase STRAD. *EMBO J* 22(12):3062–3072.

Bai, B., A. W. C. Man, K. Yang, Y. Guo, C. Xu, H.-F. Tse, W. Han, and M. Bloksgaard, *et al.* 2016. Endothelial SIRT1 prevents adverse arterial remodeling by facilitating HERC2-mediated degradation of acetylated LKB1. *Oncotarget* 7(26):39065–39081.

Bai, Y., T. Zhou, H. Fu, H. Sun, and B. Huang. 2012. 14-3-3 interacts with LKB1 via recognizing phosphorylated threonine 336 residue and suppresses LKB1 kinase function. *FEBS Lett* 586(8):1111–1119.

Barbier-Torres, L., T. C. Delgado, J. L. García-Rodríguez, I. Zubiete-Franco, D. Fernández-Ramos, X. Buqué, A. Cano, and V. Gutiérrez-de Juan, *et al.* 2015. Stabilization of LKB1 and Akt by neddylation regulates energy metabolism in liver cancer. *Oncotarget* 6(4):2509–2523.

Bardeesy, N., M. Sinha, A. F. Hezel, S. Signoretti, N. A. Hathaway, N. E. Sharpless, M. Loda, and D. R. Carrasco, *et al.* 2002. Loss of the Lkb1 tumour suppressor provokes intestinal polyposis but resistance to transformation. *Nature* 419(6903):162–167.

Barnes, A. P., B. N. Lilley, Y. A. Pan, L. J. Plummer, A. W. Powell, A. N. Raines, J. R. Sanes, and F. Polleux. 2007. LKB1 and SAD kinases define a pathway required for the polarization of cortical neurons. *Cell* 129(3):549–563.

Bartels, C., T. H. Xia, M. Billeter, P. Güntert, and K. Wüthrich. 1995. The program XEASY for computer-supported NMR spectral analysis of biological macromolecules. *J Biomol NMR* 6(1):1–10.

Bartkova, J., J. Lukas, H. Müller, D. Lützhøft, M. Strauss, and J. Bartek. 1994. Cyclin D1 protein expression and function in human breast cancer. *Int J Cancer* 57(3):353–361.

Baumgartner, S., J. T. Littleton, K. Broadie, M. A. Bhat, R. Harbecke, J. A. Lengyel, R. Chiquet-Ehrismann, and A. Prokop, *et al.* 1996. A Drosophila neurexin is required for septate junction and blood-nerve barrier formation and function. *Cell* 87(6):1059–1068.

Benton, R., and D. St Johnston. 2003a. Drosophila PAR-1 and 14-3-3 inhibit Bazooka/PAR-3 to establish complementary cortical domains in polarized cells. *Cell* 115(6):691–704.

Benton, R., and D. St. Johnston. 2003b. A Conserved Oligomerization Domain in Drosophila Bazooka/PAR-3 Is Important for Apical Localization and Epithelial Polarity. *Current Biology* 13(15):1330–1334.

Betschinger, J., F. Eisenhaber, and J. A. Knoblich. 2005. Phosphorylation-induced autoinhibition regulates the cytoskeletal protein Lethal (2) giant larvae. *Curr Biol* 15(3):276–282.

Betschinger, J., K. Mechtler, and J. A. Knoblich. 2003. The Par complex directs asymmetric cell division by phosphorylating the cytoskeletal protein Lgl. *Nature* 422(6929):326–330.

Bielskienė, K., L. Bagdonienė, J. Mozūraitienė, B. Kazbarienė, and E. Janulionis. 2015. E3 ubiquitin ligases as drug targets and prognostic biomarkers in melanoma. *Medicina (Kaunas)* 51(1):1–9.

Bilder, D., M. Li, and N. Perrimon. 2000. Cooperative regulation of cell polarity and growth by Drosophila tumor suppressors. *Science* 289(5476):113–116.

Bilder, D., M. Schober, and N. Perrimon. 2003. Integrated activity of PDZ protein complexes regulates epithelial polarity. *Nat Cell Biol* 5(1):53–58.

Bolte, S., and F. P. Cordelières. 2006. A guided tour into subcellular colocalization analysis in light microscopy. *J Microsc* 224(Pt 3):213–232.

Bonaccorsi, S., V. Mottier, M. G. Giansanti, B. J. Bolkan, B. Williams, M. L. Goldberg, and M. Gatti. 2007. The Drosophila Lkb1 kinase is required for spindle formation and asymmetric neuroblast division. *Development* 134(11):2183–2193.

Boudeau, J., A. F. Baas, M. Deak, N. A. Morrice, A. Kieloch, M. Schutkowski, A. R. Prescott, and H. C. Clevers, *et al.* 2003a. MO25alpha/beta interact with STRADalpha/beta enhancing their ability to bind, activate and localize LKB1 in the cytoplasm. *EMBO J* 22(19):5102–5114.

Boudeau, J., M. Deak, M. A. Lawlor, N. A. Morrice, and D. R. Alessi. 2003b. Heat-shock protein 90 and Cdc37 interact with LKB1 and regulate its stability. *Biochem. J.* 370(Pt 3):849–857.

Boudeau, J., G. Sapkota, and D. R. Alessi. 2003c. LKB1, a protein kinase regulating cell proliferation and polarity. *FEBS Lett* 546(1):159–165.

Boudeau, J., G. Sapkota, and D. R. Alessi. 2003d. LKB1, a protein kinase regulating cell proliferation and polarity. *FEBS Lett* 546(1):159–165.

Boudeau, J., J. W. Scott, N. Resta, M. Deak, A. Kieloch, D. Komander, D. G. Hardie, and A. R. Prescott, *et al.* 2004. Analysis of the LKB1-STRAD-MO25 complex. *J Cell Sci* 117(Pt 26):6365–6375.

Bright, N. J., D. Carling, and C. Thornton. 2008. Investigating the regulation of brain-specific kinases 1 and 2 by phosphorylation. *J Biol Chem* 283(22):14946–14954.

Bruntz, R. C., H. E. Taylor, C. W. Lindsley, and H. A. Brown. 2014. Phospholipase D2 mediates survival signaling through direct regulation of Akt in glioblastoma cells. *J Biol Chem* 289(2):600–616.

Bultot, L., S. Horman, D. Neumann, M. P. Walsh, L. Hue, and M. H. Rider. 2009. Myosin light chains are not a physiological substrate of AMPK in the control of cell structure changes. *FEBS Lett* 583(1):25–28.

Calamaras, T. D., C. Lee, F. Lan, Y. Ido, D. A. Siwik, and W. S. Colucci. 2012. Post-translational modification of serine/threonine kinase LKB1 via Adduction of the Reactive Lipid Species 4-Hydroxy-trans-2-nonenal (HNE) at lysine residue 97 directly inhibits kinase activity. *J Biol Chem* 287(50):42400–42406.

Calamaras, T. D., C. Lee, F. Lan, Y. Ido, D. A. Siwik, and W. S. Colucci. 2015. The lipid peroxidation product 4-hydroxy-trans-2-nonenal causes protein synthesis in cardiac myocytes via activated mTORC1-p70S6K-RPS6 signaling. *Free Radic Biol Med* 82:137–146.

Calles, A., L. M. Sholl, S. J. Rodig, A. K. Pelton, J. L. Hornick, M. Butaney, C. Lydon, and S. E. Dahlberg, *et al.* 2015. Immunohistochemical Loss of LKB1 Is a Biomarker for More Aggressive Biology in KRAS-Mutant Lung Adenocarcinoma. *Clin Cancer Res* 21(12):2851–2860.

Carling, D., V. A. Zammit, and D. G. Hardie. 1987. A common bicyclic protein kinase cascade inactivates the regulatory enzymes of fatty acid and cholesterol biosynthesis. *FEBS Lett* 223(2):217–222.

Carrera, A. C. 2004. TOR signaling in mammals. *J Cell Sci* 117(Pt 20):4615–4616.

Carretero, J., P. P. Medina, R. Pio, L. M. Montuenga, and M. Sanchez-Cespedes. 2004. Novel and natural knockout lung cancer cell lines for the LKB1/STK11 tumor suppressor gene. *Oncogene* 23(22):4037–4040.

Casimiro, M. C., G. Di Sante, A. Di Rocco, E. Loro, C. Pupo, T. G. Pestell, S. Bisetto, and M. A. Velasco-Velázquez, *et al.* 2017. Cyclin D1 Restrains Oncogene-Induced Autophagy by Regulating the AMPK-LKB1 Signaling Axis. *Cancer Res* 77(13):3391–3405.

Chen, X., and I. G. Macara. 2005. Par-3 controls tight junction assembly through the Rac exchange factor Tiam1. *Nat Cell Biol* 7(3):262–269.

Chou, T. B., and N. Perrimon. 1996. The autosomal FLP-DFS technique for generating germline mosaics in Drosophila melanogaster. *Genetics* 144(4):1673–1679.

Cidlinsky, N., G. Dogliotti, T. Pukrop, R. Jung, F. Weber, and M. P. Krahn. 2016. Inactivation of the LKB1-AMPK signaling pathway does not contribute to salivary gland tumor development - a short report. *Cell Oncol (Dordr)* 39(4):389–396.

Collins, S. P., J. L. Reoma, D. M. Gamm, and M. D. Uhler. 2000. LKB1, a novel serine/threonine protein kinase and potential tumour suppressor, is phosphorylated by cAMP-dependent protein kinase (PKA) and prenylated in vivo. *Biochem J* 345 Pt 3:673–680.

Corradetti, M. N., K. Inoki, N. Bardeesy, R. A. DePinho, and K.-L. Guan. 2004. Regulation of the TSC pathway by LKB1: Evidence of a molecular link between tuberous sclerosis complex and Peutz-Jeghers syndrome. *Genes Dev* 18(13):1533–1538.

Costes, S. V., D. Daelemans, E. H. Cho, Z. Dobbin, G. Pavlakis, and S. Lockett. 2004. Automatic and quantitative measurement of protein-protein colocalization in live cells. *Biophys J* 86(6):3993–4003.

Courchet, J., T. L. Lewis, S. Lee, V. Courchet, D.-Y. Liou, S. Aizawa, and F. Polleux. 2013. Terminal axon branching is regulated by the LKB1-NUAK1 kinase pathway via presynaptic mitochondrial capture. *Cell* 153(7):1510–1525.

Crooks, G. E., G. Hon, J.-M. Chandonia, and S. E. Brenner. 2004. WebLogo: A sequence logo generator. *Genome Res* 14(6):1188–1190.

Croucher, D. R., M. Iconomou, J. F. Hastings, S. P. Kennedy, J. Z. R. Han, R. F. Shearer, J. McKenna, and A. Wan, *et al.* 2016. Bimolecular complementation affinity purification (BiCAP) reveals dimer-specific protein interactions for ERBB2 dimers. *Sci Signal* 9(436):ra69.

Dahmani, R., P.-A. Just, A. Delay, F. Canal, L. Finzi, C. Prip-Buus, M. Lambert, and P. Sujobert, *et al.* 2015. A novel LKB1 isoform enhances AMPK metabolic activity and displays oncogenic properties. *Oncogene* 34(18):2337–2346.

Damsky, W., G. Micevic, K. Meeth, V. Muthusamy, D. P. Curley, M. Santhanakrishnan, I. Erdelyi, and J. T. Platt, *et al.* 2015. mTORC1 activation blocks BrafV600E-induced growth arrest but is insufficient for melanoma formation. *Cancer Cell* 27(1):41–56.

Davies, H., G. R. Bignell, C. Cox, P. Stephens, S. Edkins, S. Clegg, J. Teague, and H. Woffendin, *et al.* 2002. Mutations of the BRAF gene in human cancer. *Nature* 417(6892):949–954.

Delaglio, F., S. Grzesiek, G. W. Vuister, G. Zhu, J. Pfeifer, and A. Bax. 1995. NMRPipe: A multidimensional spectral processing system based on UNIX pipes. *J Biomol NMR* 6(3):277–293.

Denison, F. C., N. J. Hiscock, D. Carling, and A. Woods. 2009. Characterization of an alternative splice variant of LKB1. *J Biol Chem* 284(1):67–76.

Ding, L., G. Getz, D. A. Wheeler, E. R. Mardis, M. D. McLellan, K. Cibulskis, C. Sougnez, and H. Greulich, *et al.* 2008. Somatic mutations affect key pathways in lung adenocarcinoma. *Nature* 455(7216):1069–1075.

Doerflinger, H., N. Vogt, I. L. Torres, V. Mirouse, I. Koch, C. Nüsslein-Volhard, and D. St Johnston. 2010. Bazooka is required for polarisation of the Drosophila anterior-posterior axis. *Development* 137(10):1765–1773.

Dogliotti, G., L. Kullmann, P. Dhumale, C. Thiele, O. Panichkina, G. Mendl, R. Houben, and S. Haferkamp, *et al.* 2017. Membrane-binding and activation of LKB1 by phosphatidic acid is essential for development and tumour suppression. *Nat Commun* 8:15747.

Dolinsky, V. W., A. Y. M. Chan, I. Robillard Frayne, P. E. Light, C. Des Rosiers, and J. R. B. Dyck. 2009. Resveratrol prevents the prohypertrophic effects of oxidative stress on LKB1. *Circulation* 119(12):1643–1652.

Dorfman, J., and I. G. Macara. 2008. STRADalpha regulates LKB1 localization by blocking access to importin-alpha, and by association with Crm1 and exportin-7. *Molecular Biology of the Cell* 19(4):1614–1626.

Ebnet, K., M. Aurrand-Lions, A. Kuhn, F. Kiefer, S. Butz, K. Zander, M.-K. Meyer zu Brickwedde, and A. Suzuki, *et al.* 2003. The junctional adhesion molecule (JAM) family members JAM-2 and JAM-3 associate with the cell polarity protein PAR-3: A possible role for JAMs in endothelial cell polarity. *J Cell Sci* 116(Pt 19):3879–3891.

Ebnet, K., A. Suzuki, Y. Horikoshi, T. Hirose, M. K. Meyer Zu Brickwedde, S. Ohno, and D. Vestweber. 2001. The cell polarity protein ASIP/PAR-3 directly associates with junctional adhesion molecule (JAM). *EMBO J* 20(14):3738–3748.

Edgar, R. C. 2004. MUSCLE: Multiple sequence alignment with high accuracy and high throughput. *Nucleic Acids Res* 32(5):1792–1797.

Emsley, P., B. Lohkamp, W. G. Scott, and K. Cowtan. 2010. Features and development of Coot. *Acta Crystallogr D Biol Crystallogr* 66(Pt 4):486–501.

Eneling, K., L. Brion, V. Pinto, M. J. Pinho, J. I. Sznajder, N. Mochizuki, K. Emoto, and P. Soares-da-Silva, *et al.* 2012. Salt-inducible kinase 1 regulates E-cadherin expression and intercellular junction stability. *FASEB J* 26(8):3230–3239.

Ernst, A., B. A. Appleton, Y. Ivarsson, Y. Zhang, D. Gfeller, C. Wiesmann, and S. S. Sidhu. 2014. A structural portrait of the PDZ domain family. *J Mol Biol* 426(21):3509–3519.

Esteve-Puig, R., F. Canals, N. Colomé, G. Merlino, and J. A. Recio. 2009. Uncoupling of the LKB1-AMPKalpha energy sensor pathway by growth factors and oncogenic BRAF. *PLoS ONE* 4(3):e4771.

Fang, Y., M. Vilella-Bach, R. Bachmann, A. Flanigan, and J. Chen. 2001. Phosphatidic acid-mediated mitogenic activation of mTOR signaling. *Science* 294(5548):1942–1945.

Fehon, R. G., I. A. Dawson, and S. Artavanis-Tsakonas. 1994. A Drosophila homologue of membrane-skeleton protein 4.1 is associated with septate junctions and is encoded by the coracle gene. *Development* 120(3):545–557.

Feng, W., H. Wu, L.-N. Chan, and M. Zhang. 2007. The Par-3 NTD adopts a PB1-like structure required for Par-3 oligomerization and membrane localization. *EMBO J* 26(11):2786–2796.

Feng, W., H. Wu, L.-N. Chan, and M. Zhang. 2008. Par-3-mediated junctional localization of the lipid phosphatase PTEN is required for cell polarity establishment. *J Biol Chem* 283(34):23440–23449.

Ferlay, J., I. Soerjomataram, R. Dikshit, S. Eser, C. Mathers, M. Rebelo, D. M. Parkin, and D. Forman, *et al.* 2015. Cancer incidence and mortality worldwide: Sources, methods and major patterns in GLOBOCAN 2012. *Int J Cancer* 136(5):E359-86.

Fievet, B. T., J. Rodriguez, S. Naganathan, C. Lee, E. Zeiser, T. Ishidate, M. Shirayama, and S. Grill, *et al.* 2013. Systematic genetic interaction screens uncover cell polarity regulators and functional redundancy. *Nat Cell Biol* 15(1):103–112.

Fletcher, G. C., E. P. Lucas, R. Brain, A. Tournier, and B. J. Thompson. 2012. Positive feedback and mutual antagonism combine to polarize Crumbs in the Drosophila follicle cell epithelium. *Curr Biol* 22(12):1116–1122.

Fogarty, S., and D. G. Hardie. 2009. C-terminal phosphorylation of LKB1 is not required for regulation of AMP-activated protein kinase, BRSK1, BRSK2, or cell cycle arrest. *J Biol Chem* 284(1):77–84.

Foster, D. A., D. Salloum, D. Menon, and M. A. Frias. 2014. Phospholipase D and the maintenance of phosphatidic acid levels for regulation of mammalian target of rapamycin (mTOR). *J Biol Chem* 289(33):22583–22588.

Gan, B., J. Hu, S. Jiang, Y. Liu, E. Sahin, L. Zhuang, E. Fletcher-Sananikone, and S. Colla, *et al.* 2010. Lkb1 regulates quiescence and metabolic homeostasis of haematopoietic stem cells. *Nature* 468(7324):701–704.

Gao, L., I. G. Macara, and G. Joberty. 2002. Multiple splice variants of Par3 and of a novel related gene, Par3L, produce proteins with different binding properties. *Gene* 294(1-2):99–107.

Gaude, H., N. Aznar, A. Delay, A. Bres, K. Buchet-Poyau, C. Caillat, A. Vigouroux, and C. Rogon, *et al.* 2012. Molecular chaperone complexes with antagonizing activities regulate stability and activity of the tumor suppressor LKB1. *Oncogene* 31(12):1582–1591.

Geiss-Friedlander, R., and F. Melchior. 2007. Concepts in sumoylation: A decade on. *Nat Rev Mol Cell Biol* 8(12):947–956.

Genova, J. L., and R. G. Fehon. 2003. Neuroglian, Gliotactin, and the Na+/K+ ATPase are essential for septate junction function in Drosophila. *J Cell Biol* 161(5):979–989.

George, S. H. L., A. Milea, R. Sowamber, R. Chehade, A. Tone, and P. A. Shaw. 2016. Loss of LKB1 and p53 synergizes to alter fallopian tube epithelial phenotype and high-grade serous tumorigenesis. *Oncogene* 35(1):59–68.

Getsios, S., A. C. Huen, and K. J. Green. 2004. Working out the strength and flexibility of desmosomes. *Nat Rev Mol Cell Biol* 5(4):271–281.

Ghosh, S., J. C. Strum, V. A. Sciorra, L. Daniel, and R. M. Bell. 1996. Raf-1 kinase possesses distinct binding domains for phosphatidylserine and phosphatidic acid. Phosphatidic acid regulates the translocation of Raf-1 in 12-O-tetradecanoylphorbol-13-acetate-stimulated Madin-Darby canine kidney cells. *J Biol Chem* 271(14):8472–8480.

Gill, R. K., S.-H. Yang, D. Meerzaman, L. E. Mechanic, E. D. Bowman, H.-S. Jeon, S. Roy Chowdhuri, and A. Shakoori, *et al.* 2011. Frequent homozygous deletion of the LKB1/STK11 gene in non-small cell lung cancer. *Oncogene* 30(35):3784–3791.

Goehring, N. W., C. Hoege, S. W. Grill, and A. A. Hyman. 2011. PAR proteins diffuse freely across the anterior-posterior boundary in polarized C. elegans embryos. *J Cell Biol* 193(3):583–594.

Goldstein, B., and I. G. Macara. 2007. The PAR proteins: Fundamental players in animal cell polarization. *Dev Cell* 13(5):609–622.

Gomez-Cambronero, J. 2014. Phospholipase D in cell signaling: From a myriad of cell functions to cancer growth and metastasis. *J Biol Chem* 289(33):22557–22566.

Goodwin, J. M., R. U. Svensson, H. J. Lou, M. M. Winslow, B. E. Turk, and R. J. Shaw. 2014. An AMPK-independent signaling pathway downstream of the LKB1 tumor suppressor controls Snail1 and metastatic potential. *Mol Cell* 55(3):436–450.

Granot, Z., A. Swisa, J. Magenheim, M. Stolovich-Rain, W. Fujimoto, E. Manduchi, T. Miki, and J. K. Lennerz, *et al.* 2009. LKB1 regulates pancreatic beta cell size, polarity, and function. *Cell Metab* 10(4):296–308.

Graybill, C., B. Wee, S. X. Atwood, and K. E. Prehoda. 2012. Partitioning-defective protein 6 (Par-6) activates atypical protein kinase C (aPKC) by pseudosubstrate displacement. *J Biol Chem* 287(25):21003–21011.

Groth, A. C., M. Fish, R. Nusse, and M. P. Calos. 2004. Construction of transgenic Drosophila by using the site-specific integrase from phage phiC31. *Genetics* 166(4):1775–1782.

Guldberg, P., P. thor Straten, V. Ahrenkiel, T. Seremet, A. F. Kirkin, and J. Zeuthen. 1999. Somatic mutation of the Peutz-Jeghers syndrome gene, LKB1/STK11, in malignant melanoma. *Oncogene* 18(9):1777–1780.

Gurumurthy, S., S. Z. Xie, B. Alagesan, J. Kim, R. Z. Yusuf, B. Saez, A. Tzatsos, and F. Ozsolak, *et al.* 2010. The Lkb1 metabolic sensor maintains haematopoietic stem cell survival. *Nature* 468(7324):659–663.

Guyer, R. A., and I. G. Macara. 2015. Loss of the polarity protein PAR3 activates STAT3 signaling via an atypical protein kinase C (aPKC)/NF-κB/interleukin-6 (IL-6) axis in mouse mammary cells. *J Biol Chem* 290(13):8457–8468.

Gwinn, D. M., D. B. Shackelford, D. F. Egan, M. M. Mihaylova, A. Mery, D. S. Vasquez, B. E. Turk, and R. J. Shaw. 2008. AMPK phosphorylation of raptor mediates a metabolic checkpoint. *Mol Cell* 30(2):214–226.

Halbsgut, N., K. Linnemannstöns, L. I. Zimmermann, and A. Wodarz. 2011. Apical-basal polarity in Drosophila neuroblasts is independent of vesicular trafficking. *Molecular Biology of the Cell* 22(22):4373–4379.

Hara, K., Y. Maruki, X. Long, K.-i. Yoshino, N. Oshiro, S. Hidayat, C. Tokunaga, and J. Avruch, *et al.* 2002. Raptor, a binding partner of target of rapamycin (TOR), mediates TOR action. *Cell* 110(2):177–189.

Hardie, D. G., and D. R. Alessi. 2013. LKB1 and AMPK and the cancer-metabolism link - ten years after. *BMC Biol* 11:36.

Harris, T. J. C. 2012. Adherens junction assembly and function in the Drosophila embryo. *Int Rev Cell Mol Biol* 293:45–83.

Harris, T. J. C., and M. Peifer. 2004. Adherens junction-dependent and -independent steps in the establishment of epithelial cell polarity in Drosophila. *J Cell Biol* 167(1):135–147.

Harris, T. J. C., and M. Peifer. 2005. The positioning and segregation of apical cues during epithelial polarity establishment in Drosophila. *J Cell Biol* 170(5):813–823.

Hawley, S. A., J. Boudeau, J. L. Reid, K. J. Mustard, L. Udd, T. P. Mäkelä, D. R. Alessi, and D. G. Hardie. 2003. Complexes between the LKB1 tumor suppressor, STRAD alpha/beta and MO25 alpha/beta are upstream kinases in the AMP-activated protein kinase cascade. *J Biol* 2(4):28.

Hawley, S. A., M. Davison, A. Woods, S. P. Davies, R. K. Beri, D. Carling, and D. G. Hardie. 1996. Characterization of the AMP-activated Protein Kinase Kinase from Rat Liver and

Identification of Threonine 172 as the Major Site at Which It Phosphorylates AMP-activated Protein Kinase. *J Biol Chem* 271(44):27879–27887.

Hearle, N., V. Schumacher, F. H. Menko, S. Olschwang, L. A. Boardman, J. J. P. Gille, J. J. Keller, and A. M. Westerman, *et al.* 2006. Frequency and spectrum of cancers in the Peutz-Jeghers syndrome. *Clin Cancer Res* 12(10):3209–3215.

Hemminki, A., D. Markie, I. Tomlinson, E. Avizienyte, S. Roth, A. Loukola, G. Bignell, and W. Warren, *et al.* 1998. A serine/threonine kinase gene defective in Peutz-Jeghers syndrome. *Nature* 391(6663):184–187.

Henkels, K. M., G. P. Boivin, E. S. Dudley, S. J. Berberich, and J. Gomez-Cambronero. 2013. Phospholipase D (PLD) drives cell invasion, tumor growth and metastasis in a human breast cancer xenograph model. *Oncogene* 32(49):5551–5562.

Henkels, K. M., S. Short, H.-J. Peng, M. Di Fulvio, and J. Gomez-Cambronero. 2009. PLD2 has both enzymatic and cell proliferation-inducing capabilities, that are differentially regulated by phosphorylation and dephosphorylation. *Biochem Biophys Res Commun* 389(2):224–228.

Henrique, D., and F. Schweisguth. 2003. Cell polarity: The ups and downs of the Par6/aPKC complex. *Curr Opin Genet Dev* 13(4):341–350.

Hirano, Y., S. Yoshinaga, R. Takeya, N. N. Suzuki, M. Horiuchi, M. Kohjima, H. Sumimoto, and F. Inagaki. 2005. Structure of a cell polarity regulator, a complex between atypical PKC and Par6 PB1 domains. *J Biol Chem* 280(10):9653–9661.

Hirose, T., Y. Izumi, Y. Nagashima, Y. Tamai-Nagai, H. Kurihara, T. Sakai, Y. Suzuki, and T. Yamanaka, *et al.* 2002. Involvement of ASIP/PAR-3 in the promotion of epithelial tight junction formation. *J Cell Sci* 115(Pt 12):2485–2495.

Hirose, T., M. Karasawa, Y. Sugitani, M. Fujisawa, K. Akimoto, S. Ohno, and T. Noda. 2006. PAR3 is essential for cyst-mediated epicardial development by establishing apical cortical domains. *Development* 133(7):1389–1398.

Homem, C. C. F., and J. A. Knoblich. 2012. Drosophila neuroblasts: A model for stem cell biology. *Development* 139(23):4297–4310.

Horikoshi, Y., S. Hamada, S. Ohno, and S. Suetsugu. 2011. Phosphoinositide binding by par-3 involved in par-3 localization. *Cell Struct Funct* 36(1):97–102.

Horikoshi, Y., A. Suzuki, T. Yamanaka, K. Sasaki, K. Mizuno, H. Sawada, S. Yonemura, and S. Ohno. 2009. Interaction between PAR-3 and the aPKC-PAR-6 complex is indispensable for apical domain development of epithelial cells. *J Cell Sci* 122(Pt 10):1595–1606.

Hou, X., S. Xu, K. A. Maitland-Toolan, K. Sato, B. Jiang, Y. Ido, F. Lan, and K. Walsh, *et al.* 2008. SIRT1 regulates hepatocyte lipid metabolism through activating AMP-activated protein kinase. *J Biol Chem* 283(29):20015–20026.

Houde, V. P., M. S. Ritorto, R. Gourlay, J. Varghese, P. Davies, N. Shpiro, K. Sakamoto, and D. R. Alessi. 2014. Investigation of LKB1 Ser431 phosphorylation and Cys433 farnesylation using mouse knockin analysis reveals an unexpected role of prenylation in regulating AMPK activity. *Biochem J* 458(1):41–56.

Huo, Y., and I. G. Macara. 2014. The Par3-like polarity protein Par3L is essential for mammary stem cell maintenance. *Nat Cell Biol* 16(6):529–537.

Hurd, T. W., S. Fan, C. J. Liu, H. K. Kweon, K. Hakansson, and B. Margolis. 2003a. Phosphorylation-dependent binding of 14-3-3 to the polarity protein Par3 regulates cell polarity in mammalian epithelia. *Current Biology* 13(23):2082–2090.

Hurd, T. W., L. Gao, M. H. Roh, I. G. Macara, and B. Margolis. 2003b. Direct interaction of two polarity complexes implicated in epithelial tight junction assembly. *Nat Cell Biol* 5(2):137–142.

Hurov, J. B., J. L. Watkins, and H. Piwnica-Worms. 2004. Atypical PKC phosphorylates PAR-1 kinases to regulate localization and activity. *Curr Biol* 14(8):736–741.

Hutterer, A., J. Betschinger, M. Petronczki, and J. A. Knoblich. 2004. Sequential roles of Cdc42, Par-6, aPKC, and Lgl in the establishment of epithelial polarity during Drosophila embryogenesis. *Dev Cell* 6(6):845–854.

Iden, S., D. Rehder, B. August, A. Suzuki, K. Wolburg-Buchholz, H. Wolburg, S. Ohno, and J. Behrens, *et al.* 2006. A distinct PAR complex associates physically with VE-cadherin in vertebrate endothelial cells. *EMBO Rep* 7(12):1239–1246.

Inoki, K., Y. Li, T. Xu, and K.-L. Guan. 2003a. Rheb GTPase is a direct target of TSC2 GAP activity and regulates mTOR signaling. *Genes Dev* 17(15):1829–1834.

Inoki, K., T. Zhu, and K.-L. Guan. 2003b. TSC2 mediates cellular energy response to control cell growth and survival. *Cell* 115(5):577–590.

Insolera, R., S. Chen, and S.-H. Shi. 2011. Par proteins and neuronal polarity. *Dev Neurobiol* 71(6):483–494.

Itoh, M., H. Sasaki, M. Furuse, H. Ozaki, T. Kita, and S. Tsukita. 2001. Junctional adhesion molecule (JAM) binds to PAR-3: A possible mechanism for the recruitment of PAR-3 to tight junctions. *J Cell Biol* 154(3):491–497.

Izumi, Y., T. Hirose, Y. Tamai, S. Hirai, Y. Nagashima, T. Fujimoto, Y. Tabuse, and K. J. Kemphues, *et al.* 1998. An atypical PKC directly associates and colocalizes at the epithelial tight junction with ASIP, a mammalian homologue of Caenorhabditis elegans polarity protein PAR-3. *J Cell Biol* 143(1):95–106.

Jaleel, M., A. McBride, J. M. Lizcano, M. Deak, R. Toth, N. A. Morrice, and D. R. Alessi. 2005. Identification of the sucrose non-fermenting related kinase SNRK, as a novel LKB1 substrate. *FEBS Lett* 579(6):1417–1423.

James, S. R., C. P. Downes, R. Gigg, S. J. Grove, A. B. Holmes, and D. R. Alessi. 1996. Specific binding of the Akt-1 protein kinase to phosphatidylinositol 3,4,5-trisphosphate without subsequent activation. *Biochem J* 315 (Pt 3):709–713.

Jansen, M., J. P. ten Klooster, G. J. Offerhaus, and H. Clevers. 2009. LKB1 and AMPK family signaling: The intimate link between cell polarity and energy metabolism. *Physiol Rev* 89(3):777–798.

Jensen, D. R., C. Woytovich, M. Li, P. Duvnjak, M. S. Cassidy, R. O. Frederick, L. F. Bergeman, and F. C. Peterson, *et al.* 2010. Rapid, robotic, small-scale protein production for NMR screening and structure determination. *Protein Sci* 19(3):570–578.

Jishage, K.-i., J.-i. Nezu, Y. Kawase, T. Iwata, M. Watanabe, A. Miyoshi, A. Ose, and K. Habu, *et al.* 2002. Role of Lkb1, the causative gene of Peutz-Jegher's syndrome, in embryogenesis and polyposis. *Proc Natl Acad Sci U S A* 99(13):8903–8908.

Joberty, G., C. Petersen, L. Gao, and I. G. Macara. 2000. The cell-polarity protein Par6 links Par3 and atypical protein kinase C to Cdc42. *Nat Cell Biol* 2(8):531–539.

Jones, R. G., D. R. Plas, S. Kubek, M. Buzzai, J. Mu, Y. Xu, M. J. Birnbaum, and C. B. Thompson. 2005. AMP-activated protein kinase induces a p53-dependent metabolic checkpoint. *Mol Cell* 18(3):283–293.

Kabsch, W. 2010. XDS. *Acta Crystallogr D Biol Crystallogr* 66(Pt 2):125–132.

Karuman, P., O. Gozani, R. D. Odze, X. C. Zhou, H. Zhu, R. Shaw, T. P. Brien, and C. D. Bozzuto, *et al.* 2001a. The Peutz-Jegher gene product LKB1 is a mediator of p53-dependent cell death. *Mol Cell* 7(6):1307–1319.

Karuman, P., O. Gozani, R. D. Odze, X. C. Zhou, H. Zhu, R. Shaw, T. P. Brien, and C. D. Bozzuto, *et al.* 2001b. The Peutz-Jegher Gene Product LKB1 Is a Mediator of p53-Dependent Cell Death. *Mol Cell* 7(6):1307–1319.

Kemphues, K. J., J. R. Priess, D. G. Morton, and N. S. Cheng. 1988. Identification of genes required for cytoplasmic localization in early C. elegans embryos. *Cell* 52(3):311–320.

Kempkens, O., E. Médina, G. Fernandez-Ballester, S. Ozüyaman, A. Le Bivic, L. Serrano, and E. Knust. 2006. Computer modelling in combination with in vitro studies reveals similar binding affinities of Drosophila Crumbs for the PDZ domains of Stardust and DmPar-6. *Eur J Cell Biol* 85(8):753–767.

Kim, C. A., M. L. Phillips, W. Kim, M. Gingery, H. H. Tran, M. A. Robinson, S. Faham, and J. U. Bowie. 2001. Polymerization of the SAM domain of TEL in leukemogenesis and transcriptional repression. *EMBO J* 20(15):4173–4182.

Kim, D.-H., D. D. Sarbassov, S. M. Ali, J. E. King, R. R. Latek, H. Erdjument-Bromage, P. Tempst, and D. M. Sabatini. 2002. mTOR interacts with raptor to form a nutrient-sensitive complex that signals to the cell growth machinery. *Cell* 110(2):163–175.

Kimura, N., C. Tokunaga, S. Dalal, C. Richardson, K.-i. Yoshino, K. Hara, B. E. Kemp, and L. A. Witters, *et al.* 2003. A possible linkage between AMP-activated protein kinase (AMPK) and mammalian target of rapamycin (mTOR) signalling pathway. *Genes Cells* 8(1):65–79.

Klippel, A., W. M. Kavanaugh, D. Pot, and L. T. Williams. 1997. A specific product of phosphatidylinositol 3-kinase directly activates the protein kinase Akt through its pleckstrin homology domain. *Mol Cell Biol* 17(1):338–344.

Knoblich, J. A. 2008. Mechanisms of asymmetric stem cell division. *Cell* 132(4):583–597.

Koch, L., S. Feicht, R. Sun, A. Sen, and M. P. Krahn. 2016. Domain-specific functions of Stardust in Drosophila embryonic development. *R Soc Open Sci* 3(11):160776.

Konen, J., S. Wilkinson, B. Lee, H. Fu, W. Zhou, Y. Jiang, and A. I. Marcus. 2016. LKB1 kinase-dependent and -independent defects disrupt polarity and adhesion signaling to drive collagen remodeling during invasion. *Molecular Biology of the Cell* 27(7):1069–1084.

Krahn, M. P., J. Bückers, L. Kastrup, and A. Wodarz. 2010a. Formation of a Bazooka-Stardust complex is essential for plasma membrane polarity in epithelia. *J Cell Biol* 190(5):751–760.

Krahn, M. P., D. Egger-Adam, and A. Wodarz. 2009. PP2A antagonizes phosphorylation of Bazooka by PAR-1 to control apical-basal polarity in dividing embryonic neuroblasts. *Dev Cell* 16(6):901–908.

Krahn, M. P., D. R. Klopfenstein, N. Fischer, and A. Wodarz. 2010b. Membrane targeting of Bazooka/PAR-3 is mediated by direct binding to phosphoinositide lipids. *Curr Biol* 20(7):636–642.

Krawchuk, D., S. Anani, N. Honma-Yamanaka, S. Polito, M. Shafik, and Y. Yamanaka. 2015. Loss of LKB1 leads to impaired epithelial integrity and cell extrusion in the early mouse embryo. *J Cell Sci* 128(5):1011–1022.

Kuchinke, U., F. Grawe, and E. Knust. 1998a. Control of spindle orientation in Drosophila by the Par-3-related PDZ-domain protein Bazooka. *Current Biology* 8(25):1357–1365.

Kuchinke, U., F. Grawe, and E. Knust. 1998b. Control of spindle orientation in Drosophila by the Par-3-related PDZ-domain protein Bazooka. *Current Biology* 8(25):1357–1365.

Lai, D., Y. Chen, F. Wang, L. Jiang, and C. Wei. 2012. LKB1 controls the pluripotent state of human embryonic stem cells. *Cell Reprogram* 14(2):164–170.

Lalli, G. 2009. RalA and the exocyst complex influence neuronal polarity through PAR-3 and aPKC. *J Cell Sci* 122(Pt 10):1499–1506.

LaLonde, M. M., H. Janssens, E. Rosenbaum, S.-Y. Choi, J. P. Gergen, N. J. Colley, W. S. Stark, and M. A. Frohman. 2005. Regulation of phototransduction responsiveness and retinal degeneration by a phospholipase D-generated signaling lipid. *J Cell Biol* 169(3):471–479.

Lan, F., J. M. Cacicedo, N. Ruderman, and Y. Ido. 2008. SIRT1 modulation of the acetylation status, cytosolic localization, and activity of LKB1. Possible role in AMP-activated protein kinase activation. *J Biol Chem* 283(41):27628–27635.

Laprise, P., K. M. Lau, K. P. Harris, N. F. Silva-Gagliardi, S. M. Paul, S. Beronja, G. J. Beitel, and C. J. McGlade, *et al.* 2009. Yurt, Coracle, Neurexin IV and the Na(+),K(+)-ATPase form a novel group of epithelial polarity proteins. *Nature* 459(7250):1141–1145.

Larkin, M. A., G. Blackshields, N. P. Brown, R. Chenna, P. A. McGettigan, H. McWilliam, F. Valentin, and I. M. Wallace, *et al.* 2007. Clustal W and Clustal X version 2.0. *Bioinformatics* 23(21):2947–2948.

Latorre, I. J., M. H. Roh, K. K. Frese, R. S. Weiss, B. Margolis, and R. T. Javier. 2005. Viral oncoprotein-induced mislocalization of select PDZ proteins disrupts tight junctions and causes polarity defects in epithelial cells. *J Cell Sci* 118(Pt 18):4283–4293.

Lee, J. H., H. Koh, M. Kim, Y. Kim, S. Y. Lee, R. E. Karess, S.-H. Lee, and M. Shong, *et al.* 2007. Energy-dependent regulation of cell structure by AMP-activated protein kinase. *Nature* 447(7147):1017–1020.

Lee, J. H., H. Koh, M. Kim, J. Park, S. Y. Lee, S. Lee, and J. Chung. 2006. JNK pathway mediates apoptotic cell death induced by tumor suppressor LKB1 in Drosophila. *Cell Death Differ* 13(7):1110–1122.

Lee, S.-W., C.-F. Li, G. Jin, Z. Cai, F. Han, C.-H. Chan, W.-L. Yang, and B.-K. Li, *et al.* 2015a. Skp2-dependent ubiquitination and activation of LKB1 is essential for cancer cell survival under energy stress. *Mol Cell* 57(6):1022–1033.

Lee, W., M. Tonelli, and J. L. Markley. 2015b. NMRFAM-SPARKY: Enhanced software for biomolecular NMR spectroscopy. *Bioinformatics* 31(8):1325–1327.

Lemmers, C., D. Michel, L. Lane-Guermonprez, M.-H. Delgrossi, E. Médina, J.-P. Arsanto, and A. Le Bivic. 2004. CRB3 binds directly to Par6 and regulates the morphogenesis of

the tight junctions in mammalian epithelial cells. *Molecular Biology of the Cell* 15(3):1324–1333.

Li, B., H. Kim, M. Beers, and K. Kemphues. 2010a. Different domains of C. elegans PAR-3 are required at different times in development. *Dev Biol* 344(2):745–757.

Li, J., H. Kim, D. G. Aceto, J. Hung, S. Aono, and K. J. Kemphues. 2010b. Binding to PKC-3, but not to PAR-3 or to a conventional PDZ domain ligand, is required for PAR-6 function in C. elegans. *Dev Biol* 340(1):88–98.

Li, T., D. Liu, X. Lei, and Q. Jiang. 2017. Par3L enhances colorectal cancer cell survival by inhibiting Lkb1/AMPK signaling pathway. *Biochem Biophys Res Commun* 482(4):1037–1041.

Limatola, C., D. Schaap, W. H. Moolenaar, and W. J. van Blitterswijk. 1994. Phosphatidic acid activation of protein kinase C-zeta overexpressed in COS cells: Comparison with other protein kinase C isotypes and other acidic lipids. *Biochem J* 304 (Pt 3):1001–1008.

Lin, D., A. S. Edwards, J. P. Fawcett, G. Mbamalu, J. D. Scott, and T. Pawson. 2000. A mammalian PAR-3-PAR-6 complex implicated in Cdc42/Rac1 and aPKC signalling and cell polarity. *Nat Cell Biol* 2(8):540–547.

Lin, D., G. D. Gish, Z. Songyang, and T. Pawson. 1999. The carboxyl terminus of B class ephrins constitutes a PDZ domain binding motif. *J Biol Chem* 274(6):3726–3733.

Liu, L., F.-M. Siu, C.-M. Che, A. Xu, and Y. Wang. 2012a. Akt blocks the tumor suppressor activity of LKB1 by promoting phosphorylation-dependent nuclear retention through 14-3-3 proteins. *Am J Transl Res* 4(2):175–186.

Liu, W., K. B. Monahan, A. D. Pfefferle, T. Shimamura, J. Sorrentino, K. T. Chan, D. W. Roadcap, and D. W. Ollila, *et al.* 2012b. LKB1/STK11 inactivation leads to expansion of a prometastatic tumor subpopulation in melanoma. *Cancer Cell* 21(6):751–764.

Liu, Z., X. Dai, H. Zhu, M. Zhang, and M.-H. Zou. 2015. Lipopolysaccharides Promote S-Nitrosylation and Proteasomal Degradation of Liver Kinase B1 (LKB1) in Macrophages in Vivo. *J Biol Chem* 290(31):19011–19017.

Lizcano, J. M., O. Göransson, R. Toth, M. Deak, N. A. Morrice, J. Boudeau, S. A. Hawley, and L. Udd, *et al.* 2004. LKB1 is a master kinase that activates 13 kinases of the AMPK subfamily, including MARK/PAR-1. *EMBO J* 23(4):833–843.

MacMicking, J. D., C. Nathan, G. Hom, N. Chartrain, D. S. Fletcher, M. Trumbauer, K. Stevens, and Q.-w. Xie, *et al.* 1995. Altered responses to bacterial infection and endotoxic shock in mice lacking inducible nitric oxide synthase. *Cell* 81(4):641–650.

Mali, V. R., and S. S. Palaniyandi. 2014. Regulation and therapeutic strategies of 4-hydroxy-2-nonenal metabolism in heart disease. *Free Radic Res* 48(3):251–263.

Martin, S. G., and D. St Johnston. 2003. A role for Drosophila LKB1 in anterior-posterior axis formation and epithelial polarity. *Nature* 421(6921):379–384.

Martin-Belmonte, F., A. Gassama, A. Datta, W. Yu, U. Rescher, V. Gerke, and K. Mostov. 2007. PTEN-mediated apical segregation of phosphoinositides controls epithelial morphogenesis through Cdc42. *Cell* 128(2):383–397.

Matsumoto, S., R. Iwakawa, K. Takahashi, T. Kohno, Y. Nakanishi, Y. Matsuno, K. Suzuki, and M. Nakamoto, *et al.* 2007. Prevalence and specificity of LKB1 genetic alterations in lung cancers. *Oncogene* 26(40):5911–5918.

McCaffrey, L. M., J. Montalbano, C. Mihai, and I. G. Macara. 2012. Loss of the Par3 polarity protein promotes breast tumorigenesis and metastasis. *Cancer Cell* 22(5):601–614.

McCoy, A. J., R. W. Grosse-Kunstleve, P. D. Adams, M. D. Winn, L. C. Storoni, and R. J. Read. 2007. Phaser crystallographic software. *J Appl Crystallogr* 40(Pt 4):658–674.

McKinley, R. F. A., C. G. Yu, and T. J. C. Harris. 2012. Assembly of Bazooka polarity landmarks through a multifaceted membrane-association mechanism. *J Cell Sci* 125(Pt 5):1177–1190.

McTaggart, S. J. 2006. Isoprenylated proteins. *Cell Mol Life Sci* 63(3):255–267.

Mehenni, H., C. Gehrig, J. Nezu, A. Oku, M. Shimane, C. Rossier, N. Guex, and J. L. Blouin, *et al.* 1998. Loss of LKB1 kinase activity in Peutz-Jeghers syndrome, and evidence for allelic and locus heterogeneity. *Am J Hum Genet* 63(6):1641–1650.

Menon, S., and B. D. Manning. 2008. Common corruption of the mTOR signaling network in human tumors. *Oncogene* 27 Suppl 2:S43-51.

Miyoshi, H., M. Nakau, T.-o. Ishikawa, M. F. Seldin, M. Oshima, and M. M. Taketo. 2002. Gastrointestinal hamartomatous polyposis in Lkb1 heterozygous knockout mice. *Cancer Res* 62(8):2261–2266.

Mizuno, K., A. Suzuki, T. Hirose, K. Kitamura, K. Kutsuzawa, M. Futaki, Y. Amano, and S. Ohno. 2003. Self-association of PAR-3-mediated by the conserved N-terminal domain contributes to the development of epithelial tight junctions. *J Biol Chem* 278(33):31240–31250.

Mohseni, M., J. Sun, A. Lau, S. Curtis, J. Goldsmith, V. L. Fox, C. Wei, and M. Frazier, *et al.* 2014. A genetic screen identifies an LKB1-MARK signalling axis controlling the Hippo-YAP pathway. *Nat Cell Biol* 16(1):108–117.

Morais Cabral, J. H., C. Petosa, M. J. Sutcliffe, S. Raza, O. Byron, F. Poy, S. M. Marfatia, and A. H. Chishti, *et al.* 1996. Crystal structure of a PDZ domain. *Nature* 382(6592):649–652.

Morais-de-Sá, E., V. Mirouse, and D. St Johnston. 2010. aPKC phosphorylation of Bazooka defines the apical/lateral border in Drosophila epithelial cells. *Cell* 141(3):509–523.

Morton, J. P., N. B. Jamieson, S. A. Karim, D. Athineos, R. A. Ridgway, C. Nixon, C. J. McKay, and R. Carter, *et al.* 2010. LKB1 haploinsufficiency cooperates with Kras to promote pancreatic cancer through suppression of p21-dependent growth arrest. *Gastroenterology* 139(2):586-97, 597.e1-6.

Mukhopadhyay, S., M. Saqcena, A. Chatterjee, A. Garcia, M. A. Frias, and D. A. Foster. 2015. Reciprocal regulation of AMP-activated protein kinase and phospholipase D. *J Biol Chem* 290(11):6986–6993.

Nagai-Tamai, Y., K. Mizuno, T. Hirose, A. Suzuki, and S. Ohno. 2002. Regulated protein-protein interaction between aPKC and PAR-3 plays an essential role in the polarization of epithelial cells. *Genes Cells* 7(11):1161–1171.

Nagalingam, A., J. L. Arbiser, M. Y. Bonner, N. K. Saxena, and D. Sharma. 2012. Honokiol activates AMP-activated protein kinase in breast cancer cells via an LKB1-dependent pathway and inhibits breast carcinogenesis. *Breast Cancer Res* 14(1):R35.

Nakada, D., T. L. Saunders, and S. J. Morrison. 2010. Lkb1 regulates cell cycle and energy metabolism in haematopoietic stem cells. *Nature* 468(7324):653–658.

Nakano, A., and S. Takashima. 2012. LKB1 and AMP-activated protein kinase: Regulators of cell polarity. *Genes Cells* 17(9):737–747.

Nakayama, M., A. Nakayama, M. van Lessen, H. Yamamoto, S. Hoffmann, H. C. A. Drexler, N. Itoh, and T. Hirose, *et al.* 2013. Spatial regulation of VEGF receptor endocytosis in angiogenesis. *Nat Cell Biol* 15(3):249–260.

Nam, S.-C., and K.-W. Choi. 2003. Interaction of Par-6 and Crumbs complexes is essential for photoreceptor morphogenesis in Drosophila. *Development* 130(18):4363–4372.

Nelson, W. J. 2003. Adaptation of core mechanisms to generate cell polarity. *Nature* 422(6933):766–774.

Nezu, J., A. Oku, and M. Shimane. 1999. Loss of cytoplasmic retention ability of mutant LKB1 found in Peutz-Jeghers syndrome patients. *Biochem Biophys Res Commun* 261(3):750–755.

Noda, Y., M. Kohjima, T. Izaki, K. Ota, S. Yoshinaga, F. Inagaki, T. Ito, and H. Sumimoto. 2003. Molecular recognition in dimerization between PB1 domains. *J Biol Chem* 278(44):43516–43524.

Noda, Y., R. Takeya, S. Ohno, S. Naito, T. Ito, and H. Sumimoto. 2001. Human homologues of the Caenorhabditis elegans cell polarity protein PAR6 as an adaptor that links the small GTPases Rac and Cdc42 to atypical protein kinase C. *Genes Cells* 6(2):107–119.

Nony, P., H. Gaude, M. Rossel, L. Fournier, J.-P. Rouault, and M. Billaud. 2003. Stability of the Peutz-Jeghers syndrome kinase LKB1 requires its binding to the molecular chaperones Hsp90/Cdc37. *Oncogene* 22(57):9165–9175.

Ohno, S. 2001. Intercellular junctions and cellular polarity: The PAR-aPKC complex, a conserved core cassette playing fundamental roles in cell polarity. *Curr Opin Cell Biol* 13(5):641–648.

Pawelczyk, T., and A. Matecki. 1999. Phospholipase C-delta3 binds with high specificity to phosphatidylinositol 4,5-bisphosphate and phosphatidic acid in bilayer membranes. *Eur J Biochem* 262(2):291–298.

Pawson, T., and P. Nash. 2003. Assembly of cell regulatory systems through protein interaction domains. *Science* 300(5618):445–452.

Penkert, R. R., H. M. DiVittorio, and K. E. Prehoda. 2004. Internal recognition through PDZ domain plasticity in the Par-6-Pals1 complex. *Nat Struct Mol Biol* 11(11):1122–1127.

Petronczki, M., and J. A. Knoblich. 2001. DmPAR-6 directs epithelial polarity and asymmetric cell division of neuroblasts in Drosophila. *Nat Cell Biol* 3(1):43–49.

Pocha, S. M., and E. Knust. 2013. Complexities of Crumbs function and regulation in tissue morphogenesis. *Curr Biol* 23(7):R289-93.

Price, N. L., A. P. Gomes, A. J. Y. Ling, F. V. Duarte, A. Martin-Montalvo, B. J. North, B. Agarwal, and L. Ye, *et al.* 2012. SIRT1 is required for AMPK activation and the beneficial effects of resveratrol on mitochondrial function. *Cell Metab* 15(5):675–690.

Raghu, P., M. Manifava, J. Coadwell, and N. T. Ktistakis. 2009. Emerging findings from studies of phospholipase D in model organisms (and a short update on phosphatidic acid effectors). *Biochim Biophys Acta* 1791(9):889–897.

Ramel, D., F. Lagarrigue, V. Pons, J. Mounier, S. Dupuis-Coronas, G. Chicanne, P. J. Sansonetti, and F. Gaits-Iacovoni, *et al.* 2011. Shigella flexneri infection generates the

lipid PI5P to alter endocytosis and prevent termination of EGFR signaling. *Sci Signal* 4(191):ra61.

Ritho, J., S. T. Arold, and E. T. H. Yeh. 2015. A Critical SUMO1 Modification of LKB1 Regulates AMPK Activity during Energy Stress. *Cell Rep* 12(5):734–742.

Rizzo, M. A., K. Shome, C. Vasudevan, D. B. Stolz, T. C. Sung, M. A. Frohman, S. C. Watkins, and G. Romero. 1999. Phospholipase D and its product, phosphatidic acid, mediate agonist-dependent raf-1 translocation to the plasma membrane and the activation of the mitogen-activated protein kinase pathway. *J Biol Chem* 274(2):1131–1139.

Rolls, M. M., R. Albertson, H.-P. Shih, C.-Y. Lee, and C. Q. Doe. 2003. Drosophila aPKC regulates cell polarity and cell proliferation in neuroblasts and epithelia. *J Cell Biol* 163(5):1089–1098.

Rowan, A., V. Bataille, R. MacKie, E. Healy, D. Bicknell, W. Bodmer, and I. Tomlinson. 1999. Somatic mutations in the Peutz-Jeghers (LKB1/STKII) gene in sporadic malignant melanomas. *J Invest Dermatol* 112(4):509–511.

Saito, M., M. Iwadate, M. Higashimoto, K. Ono, Y. Takebayashi, and S. Takenoshita. 2007. Expression of phospholipase D2 in human colorectal carcinoma. *Oncol Rep* 18(5):1329–1334.

Salinas-Saavedra, M., T. Q. Stephenson, C. W. Dunn, and M. Q. Martindale. 2015. Par system components are asymmetrically localized in ectodermal epithelia, but not during early development in the sea anemone Nematostella vectensis. *Evodevo* 6:20.

Sanchez-Cespedes, M., P. Parrella, M. Esteller, S. Nomoto, B. Trink, J. M. Engles, W. H. Westra, and J. G. Herman, *et al.* 2002. Inactivation of LKB1/STK11 is a common event in adenocarcinomas of the lung. *Cancer Res* 62(13):3659–3662.

Sapkota, G. P., J. Boudeau, M. Deak, A. Kieloch, N. Morrice, and D. R. Alessi. 2002a. Identification and characterization of four novel phosphorylation sites (Ser31, Ser325, Thr336 and Thr366) on LKB1/STK11, the protein kinase mutated in Peutz-Jeghers cancer syndrome. *Biochem. J.* 362(Pt 2):481–490.

Sapkota, G. P., M. Deak, A. Kieloch, N. Morrice, A. A. Goodarzi, C. Smythe, Y. Shiloh, and S. P. Lees-Miller, *et al.* 2002b. Ionizing radiation induces ataxia telangiectasia mutated kinase (ATM)-mediated phosphorylation of LKB1/STK11 at Thr-366. *Biochem. J.* 368(Pt 2):507–516.

Sapkota, G. P., A. Kieloch, J. M. Lizcano, S. Lain, J. S. Arthur, M. R. Williams, N. Morrice, and M. Deak, *et al.* 2001. Phosphorylation of the protein kinase mutated in Peutz-Jeghers cancer syndrome, LKB1/STK11, at Ser431 by p90(RSK) and cAMP-dependent protein kinase, but not its farnesylation at Cys(433), is essential for LKB1 to suppress cell vrowth. *J Biol Chem* 276(22):19469–19482.

Sarkes, D., and L. E. Rameh. 2010. A novel HPLC-based approach makes possible the spatial characterization of cellular PtdIns5P and other phosphoinositides. *Biochem J* 428(3):375–384.

Sato, T., T. Hongu, M. Sakamoto, Y. Funakoshi, and Y. Kanaho. 2013. Molecular mechanisms of N-formyl-methionyl-leucyl-phenylalanine-induced superoxide generation and degranulation in mouse neutrophils: Phospholipase D is dispensable. *Mol Cell Biol* 33(1):136–145.

Schaur, R. 2003. Basic aspects of the biochemical reactivity of 4-hydroxynonenal. *Molecular Aspects of Medicine* 24(4-5):149–159.

Schindelin, J., I. Arganda-Carreras, E. Frise, V. Kaynig, M. Longair, T. Pietzsch, S. Preibisch, and C. Rueden, *et al.* 2012. Fiji: An open-source platform for biological-image analysis. *Nat Methods* 9(7):676–682.

Schober, M., M. Schaefer, and J. A. Knoblich. 1999. Bazooka recruits Inscuteable to orient asymmetric cell divisions in Drosophila neuroblasts. *Nature* 402(6761):548–551.

Schwamborn, J. C., and A. W. Püschel. 2004. The sequential activity of the GTPases Rap1B and Cdc42 determines neuronal polarity. *Nat Neurosci* 7(9):923–929.

Scott, J. W., S. A. Hawley, K. A. Green, M. Anis, G. Stewart, G. A. Scullion, D. G. Norman, and D. G. Hardie. 2004. CBS domains form energy-sensing modules whose binding of adenosine ligands is disrupted by disease mutations. *J. Clin. Invest.* 113(2):274–284.

Sebbagh, M., M.-J. Santoni, B. Hall, J.-P. Borg, and M. A. Schwartz. 2009. Regulation of LKB1/STRAD localization and function by E-cadherin. *Curr Biol* 19(1):37–42.

Sen, A., Z. Nagy-Zsvér-Vadas, and M. P. Krahn. 2012. Drosophila PATJ supports adherens junction stability by modulating Myosin light chain activity. *J Cell Biol* 199(4):685–698.

Sen, A., R. Sun, and M. P. Krahn. 2015. Localization and Function of Pals1-associated Tight Junction Protein in Drosophila Is Regulated by Two Distinct Apical Complexes. *J Biol Chem* 290(21):13224–13233.

Sengupta, S., A. Nagalingam, N. Muniraj, M. Y. Bonner, P. Mistriotis, A. Afthinos, P. Kuppusamy, and D. Lanoue, *et al.* 2017. Activation of tumor suppressor LKB1 by honokiol abrogates cancer stem-like phenotype in breast cancer via inhibition of oncogenic Stat3. *Oncogene*.

Seo, M. S., J. H. Kim, H. J. Kim, K. C. Chang, and S. W. Park. 2015. Honokiol activates the LKB1-AMPK signaling pathway and attenuates the lipid accumulation in hepatocytes. *Toxicol Appl Pharmacol* 284(2):113–124.

Shackelford, D. B., E. Abt, L. Gerken, D. S. Vasquez, A. Seki, M. Leblanc, L. Wei, and M. C. Fishbein, *et al.* 2013. LKB1 inactivation dictates therapeutic response of non-small cell lung cancer to the metabolism drug phenformin. *Cancer Cell* 23(2):143–158.

Shackelford, D. B., and R. J. Shaw. 2009. The LKB1-AMPK pathway: Metabolism and growth control in tumour suppression. *Nat Rev Cancer* 9(8):563–575.

Shackelford, D. B., D. S. Vasquez, J. Corbeil, S. Wu, M. Leblanc, C.-L. Wu, D. R. Vera, and R. J. Shaw. 2009. mTOR and HIF-1alpha-mediated tumor metabolism in an LKB1 mouse model of Peutz-Jeghers syndrome. *Proc Natl Acad Sci U S A* 106(27):11137–11142.

Shahab, J., M. D. Tiwari, M. Honemann-Capito, M. P. Krahn, and A. Wodarz. 2015. Bazooka/PAR3 is dispensable for polarity in Drosophila follicular epithelial cells. *Biol Open* 4(4):528–541.

Shaw, R. J., N. Bardeesy, B. D. Manning, L. Lopez, M. Kosmatka, R. A. DePinho, and L. C. Cantley. 2004a. The LKB1 tumor suppressor negatively regulates mTOR signaling. *Cancer Cell* 6(1):91–99.

Shaw, R. J., M. Kosmatka, N. Bardeesy, R. L. Hurley, L. A. Witters, R. A. DePinho, and L. C. Cantley. 2004b. The tumor suppressor LKB1 kinase directly activates AMP-activated kinase and regulates apoptosis in response to energy stress. *Proc Natl Acad Sci U S A* 101(10):3329–3335.

Shaw, R. J., K. A. Lamia, D. Vasquez, S.-H. Koo, N. Bardeesy, R. A. DePinho, M. Montminy, and L. C. Cantley. 2005. The kinase LKB1 mediates glucose homeostasis in liver and therapeutic effects of metformin. *Science* 310(5754):1642–1646.

Shelly, M., L. Cancedda, S. Heilshorn, G. Sumbre, and M.-M. Poo. 2007. LKB1/STRAD promotes axon initiation during neuronal polarization. *Cell* 129(3):565–577.

Shen, Y.-A. A., Y. Chen, D. Q. Dao, S. R. Mayoral, L. Wu, D. Meijer, E. M. Ullian, and J. R. Chan, *et al.* 2014. Phosphorylation of LKB1/Par-4 establishes Schwann cell polarity to initiate and control myelin extent. *Nat Commun* 5:4991.

Shen, Z., X.-F. Wen, F. Lan, Z.-Z. Shen, and Z.-M. Shao. 2002. The tumor suppressor gene LKB1 is associated with prognosis in human breast carcinoma. *Clin Cancer Res* 8(7):2085–2090.

Shi, M., Y. Zheng, A. Garcia, L. Xu, and D. A. Foster. 2007. Phospholipase D provides a survival signal in human cancer cells with activated H-Ras or K-Ras. *Cancer Lett* 258(2):268–275.

Shi, S.-H., L. Y. Jan, and Y.-N. Jan. 2003. Hippocampal neuronal polarity specified by spatially localized mPar3/mPar6 and PI 3-kinase activity. *Cell* 112(1):63–75.

Smith, D. P., J. Spicer, A. Smith, S. Swift, and A. Ashworth. 1999a. The mouse Peutz-Jeghers syndrome gene Lkb1 encodes a nuclear protein kinase. *Hum Mol Genet* 8(8):1479–1485.

Smith, D. P., J. Spicer, A. Smith, S. Swift, and A. Ashworth. 1999b. The Mouse Peutz-Jeghers Syndrome Gene Lkbl Encodes a Nuclear Protein Kinase. *Hum Mol Genet* 8(8):1479–1485.

Song, P., Z. Xie, Y. Wu, J. Xu, Y. Dong, and M.-H. Zou. 2008. Protein kinase Czeta-dependent LKB1 serine 428 phosphorylation increases LKB1 nucleus export and apoptosis in endothelial cells. *J Biol Chem* 283(18):12446–12455.

Songyang, Z., A. S. Fanning, C. Fu, J. Xu, S. M. Marfatia, A. H. Chishti, A. Crompton, and A. C. Chan, *et al.* 1997. Recognition of unique carboxyl-terminal motifs by distinct PDZ domains. *Science* 275(5296):73–77.

Soriano, E. V., M. E. Ivanova, G. Fletcher, P. Riou, P. P. Knowles, K. Barnouin, A. Purkiss, and B. Kostelecky, *et al.* 2016. aPKC Inhibition by Par3 CR3 Flanking Regions Controls Substrate Access and Underpins Apical-Junctional Polarization. *Dev Cell* 38(4):384–398.

Sotillos, S., M. T. Díaz-Meco, E. Caminero, J. Moscat, and S. Campuzano. 2004. DaPKC-dependent phosphorylation of Crumbs is required for epithelial cell polarity in Drosophila. *J Cell Biol* 166(4):549–557.

Stace, C. L., and N. T. Ktistakis. 2006. Phosphatidic acid- and phosphatidylserine-binding proteins. *Biochim Biophys Acta* 1761(8):913–926.

Stiffler, M. A., J. R. Chen, V. P. Grantcharova, Y. Lei, D. Fuchs, J. E. Allen, L. A. Zaslavskaia, and G. MacBeath. 2007. PDZ domain binding selectivity is optimized across the mouse proteome. *Science* 317(5836):364–369.

Suzuki, A., K. Akimoto, and S. Ohno. 2003. Protein kinase C lambda/iota (PKClambda/iota): A PKC isotype essential for the development of multicellular organisms. *J Biochem* 133(1):9–16.

Suzuki, A., and S. Ohno. 2006. The PAR-aPKC system: Lessons in polarity. *J Cell Sci* 119(Pt 6):979–987.

Suzuki, A., T. Yamanaka, T. Hirose, N. Manabe, K. Mizuno, M. Shimizu, K. Akimoto, and Y. Izumi, *et al.* 2001. Atypical protein kinase C is involved in the evolutionarily conserved par protein complex and plays a critical role in establishing epithelia-specific junctional structures. *J Cell Biol* 152(6):1183–1196.

Takekuni, K., W. Ikeda, T. Fujito, K. Morimoto, M. Takeuchi, M. Monden, and Y. Takai. 2003. Direct binding of cell polarity protein PAR-3 to cell-cell adhesion molecule nectin at neuroepithelial cells of developing mouse. *J Biol Chem* 278(8):5497–5500.

Tanwar, P. S., G. Mohapatra, S. Chiang, D. A. Engler, L. Zhang, T. Kaneko-Tarui, Y. Ohguchi, and M. J. Birrer, *et al.* 2014. Loss of LKB1 and PTEN tumor suppressor genes in the ovarian surface epithelium induces papillary serous ovarian cancer. *Carcinogenesis* 35(3):546–553.

Tee, A. R., B. D. Manning, P. P. Roux, L. C. Cantley, and J. Blenis. 2003. Tuberous Sclerosis Complex Gene Products, Tuberin and Hamartin, Control mTOR Signaling by Acting as a GTPase-Activating Protein Complex toward Rheb. *Current Biology* 13(15):1259–1268.

Tepass, U. 2012. The apical polarity protein network in Drosophila epithelial cells: Regulation of polarity, junctions, morphogenesis, cell growth, and survival. *Annu Rev Cell Dev Biol* 28:655–685.

Tiainen, M., A. Ylikorkala, and T. P. Mäkelä. 1999. Growth suppression by Lkb1 is mediated by a G(1) cell cycle arrest. *Proc Natl Acad Sci U S A* 96(16):9248–9251.

Tortelote, G. G., R. R. Reis, F. de Almeida Mendes, and J. G. Abreu. 2017. Complexity of the Wnt/β‐catenin pathway: Searching for an activation model. *Cell Signal*.

Toschi, A., E. Lee, L. Xu, A. Garcia, N. Gadir, and D. A. Foster. 2009. Regulation of mTORC1 and mTORC2 complex assembly by phosphatidic acid: Competition with rapamycin. *Mol Cell Biol* 29(6):1411–1420.

Towler, M. C., S. Fogarty, S. A. Hawley, D. A. Pan, D. M. A. Martin, N. A. Morrice, A. McCarthy, and M. N. Galardo, *et al.* 2008. A novel short splice variant of the tumour suppressor LKB1 is required for spermiogenesis. *Biochem J* 416(1):1–14.

Trojan, J., A. Brieger, J. Raedle, M. Esteller, and S. Zeuzem. 2000. 5'-CpG island methylation of the LKB1/STK11 promoter and allelic loss at chromosome 19p13.3 in sporadic colorectal cancer. *Gut* 47(2):272–276.

Tsunoda, S., J. Sierralta, Y. Sun, R. Bodner, E. Suzuki, A. Becker, M. Socolich, and C. S. Zuker. 1997. A multivalent PDZ-domain protein assembles signalling complexes in a G-protein-coupled cascade. *Nature* 388(6639):243–249.

Tyler, R. C., F. C. Peterson, and B. F. Volkman. 2010. Distal interactions within the par3-VE-cadherin complex. *Biochemistry* 49(5):951–957.

Vaahtomeri, K., and T. P. Mäkelä. 2011. Molecular mechanisms of tumor suppression by LKB1. *FEBS Lett* 585(7):944–951.

van der Velden, Y. U., L. Wang, J. Zevenhoven, E. van Rooijen, M. van Lohuizen, R. H. Giles, H. Clevers, and A.-P. G. Haramis. 2011. The serine-threonine kinase LKB1 is essential for survival under energetic stress in zebrafish. *Proc Natl Acad Sci U S A* 108(11):4358–4363.

Várnai, P., and T. Balla. 1998. Visualization of phosphoinositides that bind pleckstrin homology domains: Calcium- and agonist-induced dynamic changes and relationship to myo-3Hinositol-labeled phosphoinositide pools. *J Cell Biol* 143(2):501–510.

Veleva-Rotse, B. O., J. L. Smart, A. F. Baas, B. Edmonds, Z.-m. Zhao, A. Brown, L. R. Klug, and K. Hansen, *et al.* 2014. STRAD pseudokinases regulate axogenesis and LKB1 stability. *Neural Dev* 9:5.

Vogelmann, R., and W. J. Nelson. 2004. Fractionation of the Epithelial Apical Junctional Complex: Reassessment of Protein Distributions in Different Substructures. *Molecular Biology of the Cell* 16(2):701–716.

Walther, R. F., F. Nunes de Almeida, E. Vlassaks, J. J. Burden, and F. Pichaud. 2016. Pak4 Is Required during Epithelial Polarity Remodeling through Regulating AJ Stability and Bazooka Retention at the ZA. *Cell Rep* 15(1):45–53.

Wang, J.-W., Y. Imai, and B. Lu. 2007. Activation of PAR-1 kinase and stimulation of tau phosphorylation by diverse signals require the tumor suppressor protein LKB1. *J Neurosci* 27(3):574–581.

Wang, Q., T. W. Hurd, and B. Margolis. 2004. Tight junction protein Par6 interacts with an evolutionarily conserved region in the amino terminus of PALS1/stardust. *J Biol Chem* 279(29):30715–30721.

Wasserscheid, I., U. Thomas, and E. Knust. 2007. Isoform-specific interaction of Flamingo/Starry Night with excess Bazooka affects planar cell polarity in the Drosophila wing. *Dev Dyn* 236(4):1064–1071.

Watts, J. L., B. Etemad-Moghadam, S. Guo, L. Boyd, B. W. Draper, C. C. Mello, J. R. Priess, and K. J. Kemphues. 1996. par-6, a gene involved in the establishment of asymmetry in early C. elegans embryos, mediates the asymmetric localization of PAR-3. *Development* 122(10):3133–3140.

Watts, J. L., D. G. Morton, J. Bestman, and K. J. Kemphues. 2000. The C. elegans par-4 gene encodes a putative serine-threonine kinase required for establishing embryonic asymmetry. *Development* 127(7):1467–1475.

Waudby, C. A., A. Ramos, L. D. Cabrita, and J. Christodoulou. 2016. Two-Dimensional NMR Lineshape Analysis. *Sci Rep* 6:24826.

Wei, S.-Y., L. M. Escudero, F. Yu, L.-H. Chang, L.-Y. Chen, Y.-H. Ho, C.-M. Lin, and C.-S. Chou, *et al.* 2005. Echinoid is a component of adherens junctions that cooperates with DE-Cadherin to mediate cell adhesion. *Dev Cell* 8(4):493–504.

Whitney, D. S., F. C. Peterson, A. W. Kittell, J. M. Egner, K. E. Prehoda, and B. F. Volkman. 2016. Binding of Crumbs to the Par-6 CRIB-PDZ Module Is Regulated by Cdc42. *Biochemistry* 55(10):1455–1461.

Wiedemann, U., P. Boisguerin, R. Leben, D. Leitner, G. Krause, K. Moelling, R. Volkmer-Engert, and H. Oschkinat. 2004. Quantification of PDZ domain specificity, prediction of ligand affinity and rational design of super-binding peptides. *J Mol Biol* 343(3):703–718.

Wieschaus, E., and C. Nusslein-Volhard. 1986. Looking at embryos. In Roberts, D. B. (ed.): "Drosophila: A Practical Approach.". *Oxford: IRL Press*:199–227.

Wiesner, S., and R. Sprangers. 2015. Methyl groups as NMR probes for biomolecular interactions. *Curr Opin Struct Biol* 35:60–67.

Wilkinson, S., Y. Hou, J. T. Zoine, J. Saltz, C. Zhang, Z. Chen, L. A. D. Cooper, and A. I. Marcus. 2017. Coordinated cell motility is regulated by a combination of LKB1 farnesylation and kinase activity. *Sci Rep* 7:40929.

Williamson, M. P. 2013. Using chemical shift perturbation to characterise ligand binding. *Prog Nucl Magn Reson Spectrosc* 73:1–16.

Winder, W. W., and D. G. Hardie. 1996. Inactivation of acetyl-CoA carboxylase and activation of AMP-activated protein kinase in muscle during exercise. *Am J Physiol* 270(2 Pt 1):E299-304.

Wingo, S. N., T. D. Gallardo, E. A. Akbay, M.-C. Liang, C. M. Contreras, T. Boren, T. Shimamura, and D. S. Miller, *et al.* 2009. Somatic LKB1 mutations promote cervical cancer progression. *PLoS ONE* 4(4):e5137.

Wirtz-Peitz, F., T. Nishimura, and J. A. Knoblich. 2008. Linking cell cycle to asymmetric division: Aurora-A phosphorylates the Par complex to regulate Numb localization. *Cell* 135(1):161–173.

Wodarz, A. 2002. Establishing cell polarity in development. *Nat Cell Biol* 4(2):E39-44.

Wodarz, A. 2005. Molecular control of cell polarity and asymmetric cell division in Drosophila neuroblasts. *Curr Opin Cell Biol* 17(5):475–481.

Wodarz, A., A. Ramrath, A. Grimm, and E. Knust. 2000a. Drosophila atypical protein kinase C associates with Bazooka and controls polarity of epithelia and neuroblasts. *J Cell Biol* 150(6):1361–1374.

Wodarz, A., A. Ramrath, A. Grimm, and E. Knust. 2000b. Drosophila Atypical Protein Kinase C Associates with Bazooka and Controls Polarity of Epithelia and Neuroblasts. *J Cell Biol* 150(6):1361–1374.

Wodarz, A., A. Ramrath, U. Kuchinke, and E. Knust. 1999. Bazooka provides an apical cue for Inscuteable localization in Drosophila neuroblasts. *Nature* 402(6761):544–547.

Woods, A., S. R. Johnstone, K. Dickerson, F. C. Leiper, L. G. D. Fryer, D. Neumann, U. Schlattner, and T. Wallimann, *et al.* 2003. LKB1 is the upstream kinase in the AMP-activated protein kinase cascade. *Current Biology* 13(22):2004–2008.

Wu, H., W. Feng, J. Chen, L.-N. Chan, S. Huang, and M. Zhang. 2007. PDZ domains of Par-3 as potential phosphoinositide signaling integrators. *Mol Cell* 28(5):886–898.

Xie, Z., Y. Dong, R. Scholz, D. Neumann, and M.-H. Zou. 2008. Phosphorylation of LKB1 at serine 428 by protein kinase C-zeta is required for metformin-enhanced activation of the AMP-activated protein kinase in endothelial cells. *Circulation* 117(7):952–962.

Xie, Z., Y. Dong, J. Zhang, R. Scholz, D. Neumann, and M.-H. Zou. 2009. Identification of the serine 307 of LKB1 as a novel phosphorylation site essential for its nucleocytoplasmic transport and endothelial cell angiogenesis. *Mol Cell Biol* 29(13):3582–3596.

Xie, Z., Y. Dong, M. Zhang, M.-Z. Cui, R. A. Cohen, U. Riek, D. Neumann, and U. Schlattner, *et al.* 2006. Activation of protein kinase C zeta by peroxynitrite regulates LKB1-dependent AMP-activated protein kinase in cultured endothelial cells. *J Biol Chem* 281(10):6366–6375.

Yamanaka, T., Y. Horikoshi, N. Izumi, A. Suzuki, K. Mizuno, and S. Ohno. 2006. Lgl mediates apical domain disassembly by suppressing the PAR-3-aPKC-PAR-6 complex to orient apical membrane polarity. *J Cell Sci* 119(Pt 10):2107–2118.

Yamanaka, T., Y. Horikoshi, Y. Sugiyama, C. Ishiyama, A. Suzuki, T. Hirose, A. Iwamatsu, and A. Shinohara, *et al.* 2003. Mammalian Lgl forms a protein complex with PAR-6 and aPKC independently of PAR-3 to regulate epithelial cell polarity. *Curr Biol* 13(9):734–743.

Yamanaka, T., Y. Horikoshi, A. Suzuki, Y. Sugiyama, K. Kitamura, R. Maniwa, Y. Nagai, and A. Yamashita, *et al.* 2001. PAR-6 regulates aPKC activity in a novel way and mediates cell-cell contact-induced formation of the epithelial junctional complex. *Genes Cells* 6(8):721–731.

Yang, R., E. Kong, J. Jin, A. Hergovich, and A. W. Püschel. 2014. Rassf5 and Ndr kinases regulate neuronal polarity through Par3 phosphorylation in a novel pathway. *J Cell Sci* 127(Pt 16):3463–3476.

Yang, W.-L., X. Zhang, and H.-K. Lin. 2010. Emerging role of Lys-63 ubiquitination in protein kinase and phosphatase activation and cancer development. *Oncogene* 29(32):4493–4503.

Ylikorkala, A., E. Avizienyte, I. P. Tomlinson, M. Tiainen, S. Roth, A. Loukola, A. Hemminki, and M. Johansson, *et al.* 1999. Mutations and impaired function of LKB1 in familial and non-familial Peutz-Jeghers syndrome and a sporadic testicular cancer. *Hum Mol Genet* 8(1):45–51.

Ylikorkala, A., D. J. Rossi, N. Korsisaari, K. Luukko, K. Alitalo, M. Henkemeyer, and T. P. Mäkelä. 2001. Vascular abnormalities and deregulation of VEGF in Lkb1-deficient mice. *Science* 293(5533):1323–1326.

Yoon, M.-S., C. L. Rosenberger, C. Wu, N. Truong, J. V. Sweedler, and J. Chen. 2015. Rapid mitogenic regulation of the mTORC1 inhibitor, DEPTOR, by phosphatidic acid. *Mol Cell* 58(3):549–556.

Yu, C. G., and T. J. C. Harris. 2012. Interactions between the PDZ domains of Bazooka (Par-3) and phosphatidic acid: In vitro characterization and role in epithelial development. *Molecular Biology of the Cell* 23(18):3743–3753.

Zeng, P.-Y., and S. L. Berger. 2006. LKB1 is recruited to the p21/WAF1 promoter by p53 to mediate transcriptional activation. *Cancer Res* 66(22):10701–10708.

Zeqiraj, E., B. M. Filippi, M. Deak, D. R. Alessi, and D. M. F. van Aalten. 2009. Structure of the LKB1-STRAD-MO25 complex reveals an allosteric mechanism of kinase activation. *Science* 326(5960):1707–1711.

Zhang, C.-S., S. A. Hawley, Y. Zong, M. Li, Z. Wang, A. Gray, T. Ma, and J. Cui, *et al.* 2017a. Fructose-1,6-bisphosphate and aldolase mediate glucose sensing by AMPK. *Nature* 548(7665):112–116.

Zhang, C.-S., B. Jiang, M. Li, M. Zhu, Y. Peng, Y.-L. Zhang, Y.-Q. Wu, and T. Y. Li, *et al.* 2014. The lysosomal v-ATPase-Ragulator complex is a common activator for AMPK and mTORC1, acting as a switch between catabolism and anabolism. *Cell Metab* 20(3):526–540.

Zhang, W., X. Li, G. Song, and D. Luo. 2017b. Prognostic significance of LKB1 promoter methylation in cutaneous malignant melanoma. *Oncol Lett* 14(2):2075–2080.

Zhang, Y., W. Wang, J. Chen, K. Zhang, F. Gao, B. Gao, S. Zhang, and M. Dong, *et al.* 2013a. Structural insights into the intrinsic self-assembly of Par-3 N-terminal domain. *Structure* 21(6):997–1006.

Zhang, Y.-L., H. Guo, C.-S. Zhang, S.-Y. Lin, Z. Yin, Y. Peng, H. Luo, and Y. Shi, *et al.* 2013b. AMP as a low-energy charge signal autonomously initiates assembly of AXIN-AMPK-LKB1 complex for AMPK activation. *Cell Metab* 18(4):546–555.

Zheng, B., J. H. Jeong, J. M. Asara, Y.-Y. Yuan, S. R. Granter, L. Chin, and L. C. Cantley. 2009. Oncogenic B-RAF negatively regulates the tumor suppressor LKB1 to promote melanoma cell proliferation. *Mol Cell* 33(2):237–247.

Zheng, Y., V. Rodrik, A. Toschi, M. Shi, L. Hui, Y. Shen, and D. A. Foster. 2006. Phospholipase D couples survival and migration signals in stress response of human cancer cells. *J Biol Chem* 281(23):15862–15868.

Zhong, W., and W. Chia. 2008. Neurogenesis and asymmetric cell division. *Curr Opin Neurobiol* 18(1):4–11.

Zhu, H., C. M. Moriasi, M. Zhang, Y. Zhao, and M.-H. Zou. 2013. Phosphorylation of serine 399 in LKB1 protein short form by protein kinase Cζ is required for its nucleocytoplasmic transport and consequent AMP-activated protein kinase (AMPK) activation. *J Biol Chem* 288(23):16495–16505.

Zu, Y., L. Liu, M. Y. K. Lee, C. Xu, Y. Liang, R. Y. Man, P. M. Vanhoutte, and Y. Wang. 2010. SIRT1 promotes proliferation and prevents senescence through targeting LKB1 in primary porcine aortic endothelial cells. *Circ Res* 106(8):1384–1393.